Exploration of microbial systems as biocatalysts for conversion of syngas to bio-based chemicals

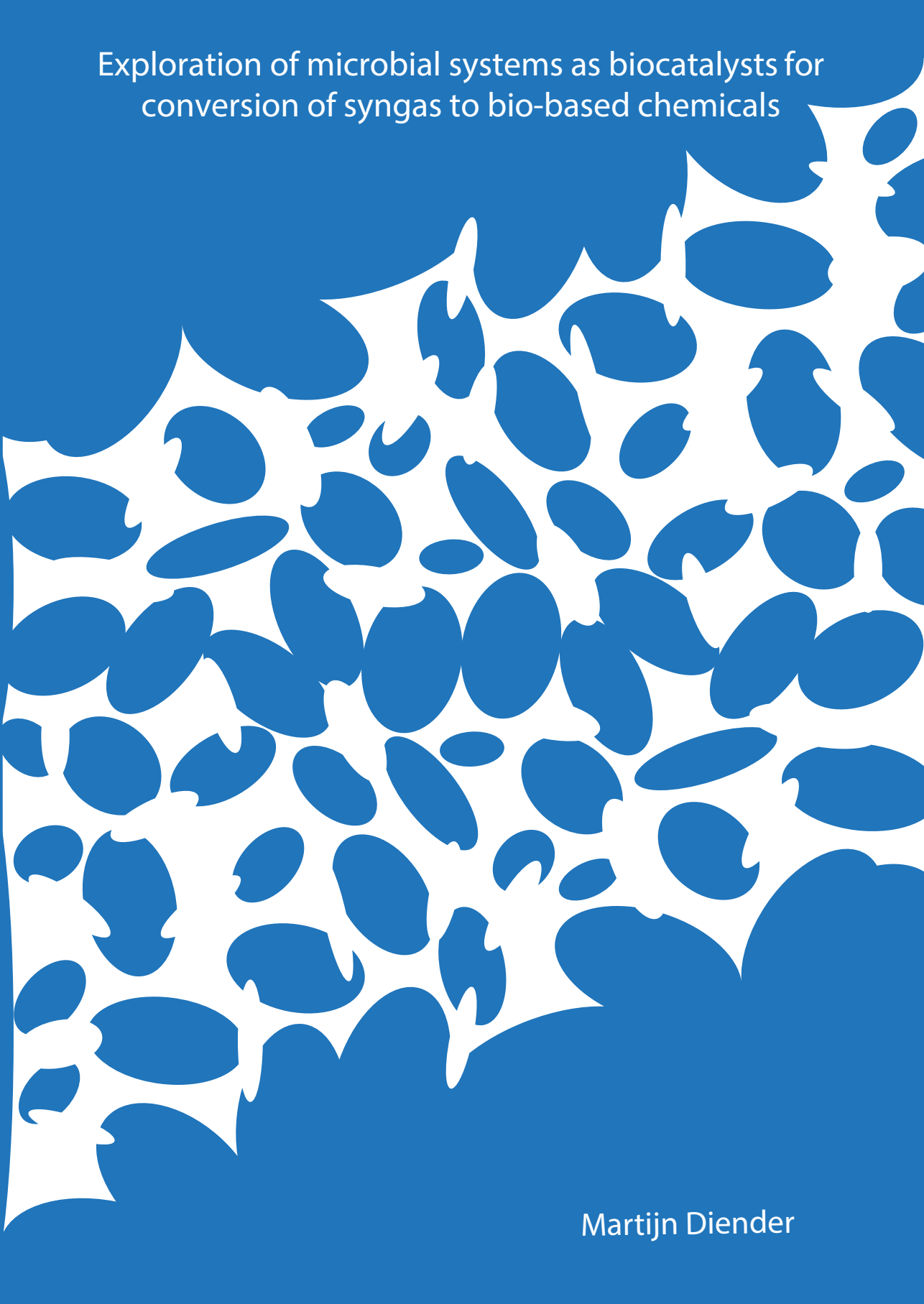

Martijn Diender

Propositions

1. Synthetic communities offer better perspectives to optimize gas fermentation processes than pure- or complex undefined-mixed culture approaches.
   (this thesis)

2. The ability to convert a broad spectrum of wastes by syngas fermentation will eventually be more important than the cost, rate or yield of the overall process.
   (this thesis)

3. With the increasing use of ~omics and computational techniques, our microbial physiological knowledge is becoming increasingly based on assumptions.

4. Mathematics is always correct.

5. Work performed by robots should be taxed in order to keep human labour competitive.

6. With the integration of the internet in our society, education should focus less on knowledge transfer and more on development of analytical skills.

7. One learns most by explaining to another.

Propositions belonging to the thesis entitled:

"Exploration of microbial systems as biocatalysts for conversion of synthesis gas to bio-based chemicals"

Martijn Diender

Wageningen, 8 February 2019

Exploration of microbial systems as biocatalysts for conversion of synthesis gas to bio-based chemicals

Martijn Diender

Thesis committee

Promotor
Prof. Dr A.J.M. Stams
Personal chair at the Laboratory of Microbiology
Wageningen University & Research

Co-promotor
Dr D.Z. Machado de Sousa
Associate professor, Laboratory of Microbiology
Wageningen University & Research

Other members
Prof. Dr A.J.H. Janssen, Wageningen University & Research
Prof. Dr R.K. Thauer, Max Planck Institute for Terrestrial Microbiology, Germany
Prof. Dr W. Verstraete, Ghent University, Belgium
Dr A.M. Lopez Contreras, Wageningen University & Research

This research was conducted under the auspices of the Graduate School for Socio-Economic and Natural Sciences of the Environment (SENSE).

Exploration of microbial systems as biocatalysts for conversion of synthesis gas to bio-based chemicals

Martijn Diender

Thesis

submitted in fulfilment of the requirements for the degree of doctor
at Wageningen University
by the authority of the Rector Magnificus,
Prof. Dr A.P.J. Mol,
in presence of the
Thesis Committee appointed by the Academic Board
to be defended in public
on Friday 8 February 2019
at 4 p.m. in the Aula.

Martijn Diender

Exploration of microbial systems as biocatalysts for conversion of synthesis gas to bio-based chemicals,

204 pages.

PhD thesis, Wageningen University, Wageningen, NL (2019)

With references, with summaries in English and Dutch

DOI: https://doi.org/10.18174/466065

ISBN: 978-94-6343-391-4

First step to tackle any problem: 'Stay calm'

-A.H. Diender

Table of contents

Chapter 1. Introduction and thesis outline 11

Chapter 2. Pathways and bioenergetics of carbon monoxide fermentation 23

Chapter 3. Proteomics analysis of the hydrogen and carbon monoxide metabolism of *Methanothermobacter marburgensis* 51

Chapter 4. High rate biomethanation of carbon monoxide-rich gases via a thermophilic synthetic co-culture 71

Chapter 5. Production of medium-chain fatty acids and higher alcohols by a synthetic co-culture grown on carbon monoxide or syngas 89

Chapter 6. *Clostridium kluyveri* drives carboxydotrophic growth of *Clostridium autoethanogenum* to ethanol production 109

Chapter 7. A flexible alcohol metabolism in *Clostridium autoethanogenum* allows additional energy conservation. 131

Chapter 8. General discussion 153

Appendices 171

References 172
English Summary 189
Dutch Summary 192
Co-author affiliations 195
List of publications 196
Acknowledgements 197
About the Author 201
SENSE Diploma 202

Chapter 1

General introduction and thesis outline

Syngas fermentation for the sustainable production of chemicals and fuels

Our planet is currently dealing with a rapid increase in world population with a consequent increase in the demand for fuels and chemicals. To answer this increasing demand, and ensure a viable environment for future generations, production processes need to become more sustainable (IPCC, 2014). Currently, many industrial processes are driven by fossil sources, causing environmental damage and contributing to global warming due to the exhaust of greenhouse gases. One of the ways to create a more sustainable economy is to make it circular, enabling the reuse of waste as a resource for the production of new commodities. Bio-based technologies, that use microorganisms to produce commodity chemicals and fuels, offer great potential, but are often limited to utilizing materials with easy accessible sugar content (e.g. starchy biomass) (Naik et al., 2010). However, production of such biomass often competes with food and feed supply, making the sustainability of this process questionable (Naik et al., 2010). For this reason, processes utilizing ligno-cellulosic, non-food biomass are preferred. However, this type of biomass is more recalcitrant and requires intensive pre-treatment (e.g. steam explosion, enzymatic treatment) in order to release the sugar content for fermentation (Naik et al., 2010). Weight percentage of the highly recalcitrant lignin content in woody biomass was estimated on average at about 25%, while in agricultural biomass this might even be 30% (Vassilev et al., 2012). Therefore, in case of optimal conversion of all non-lignin content this will still result in significant losses of the initial substrate, decreasing the yield of the overall process and resulting in generation of additional waste streams. This limits the scope of starting materials that bio-based technologies can utilize and leaves many other types of abundant waste (e.g. municipal wastes) unutilized. Currently, wastes that cannot be processed are burned or buried, contributing to environmental pollution and exhaust of greenhouse gases (Wiedinmyer et al., 2014). An alternative to the fermentation of sugar is gas fermentation (figure 1). In gas fermentation, CO_2 is used by microorganisms as carbon source while utilizing an external electron source (e.g. H_2, CO) to generate added-value products.

Gas fermentation processes can be fed with different gases originating from distinct sources, such as off-gases from industry (Molitor et al., 2016) and from the gasification of carbonaceous materials (Daniell et al., 2016; Drzyzga et al., 2015). In addition, electrochemical systems can be used for the reduction of H_2O/CO_2 streams to form H_2 and CO rich gases (Dubois and Dubois, 2009; Furler et al., 2012; Redissi and Bouallou, 2013). Gasification followed by syngas fermentation allows for the recovery of carbon from recalcitrant wastes, such as municipal waste,

lignocellulose and plastics. Gasification is performed at high temperature (>700 °C) and at low oxygen:biomass ratio. This results in the partial oxidation of the carbonaceous materials and the formation of a gaseous mix consisting mainly of CO, H_2 and CO_2 (synthesis gas or syngas) (Heidenreich and Foscolo, 2015). Syngas can be used as a substrate for microbial fermentation processes where H_2 and CO will act as electron donor while CO and CO_2 acts as carbon source. One of the main challenges with syngas as substrate is the toxicity of CO towards the microbial catalyst. Thus, suitable carboxydotrophic strains (i.e. strains able to thrive on CO) need to be employed in the fermentation process to make it run efficiently. Presence of CO does however also allow for the production of more reduced compounds (such as 2,3-butanediol or alcohols) compared to H_2/CO_2 feed gas (Diender et al., 2015, **Chapter 2**; Oelgeschläger and Rother, 2008). Fermentation of gaseous substrates, with main focus on synthesis gas fermentation, is a way to generate chemicals and fuels from a wide spectrum of wastes and is the main topic of this thesis.

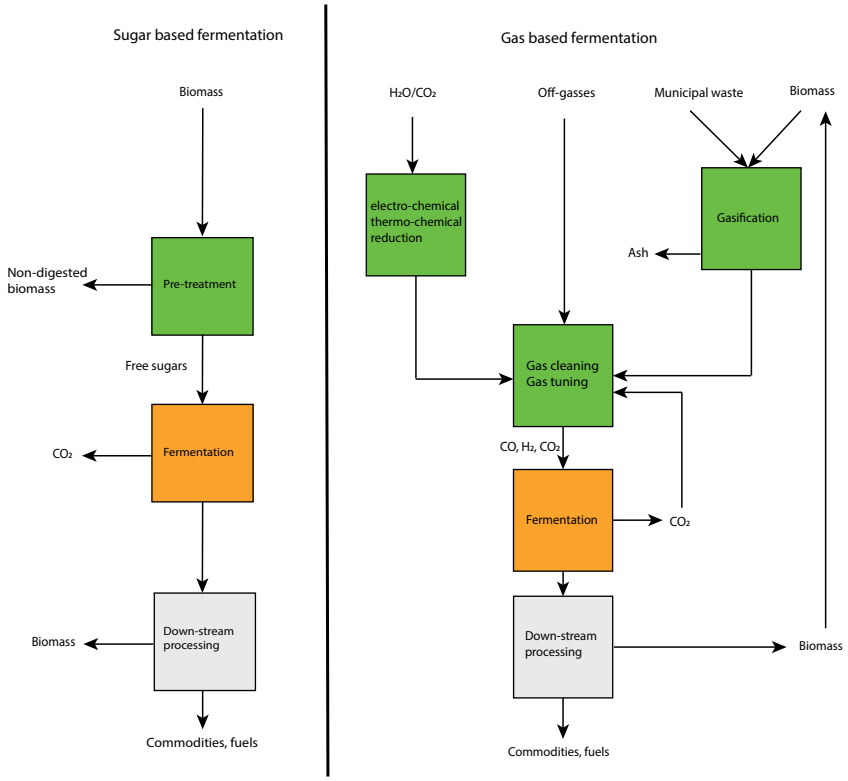

Figure 1. Simplified scheme of sugar based fermentation (left) vs. gas based fermentation (right). Colours indicate either pre-fermentation processing (green), microbial fermentation (orange) or down-stream processing (grey).

Microbial syngas fermentation and its (current) limitations

During fermentation of syngas, the CO and H_2 are oxidized and the released electrons are used to reduce CO_2. Microbes suitable for fermentation of syngas are mainly acetogens, hydrogenogens and methanogens. In all known cases the organisms involved in utilization of CO/H_2 for fermentation processes are strict anaerobes. However, besides these fermentation types of metabolism, also respiratory metabolism can be involved in conversion of syngas (e.g. coupled to sulfate or oxygen reduction) (Diender et al., 2015, **Chapter 2**; Oelgeschläger and Rother, 2008). From an industrial perspective, acetogens are interesting due to their native end products: acetate and ethanol. Additionally, natural products from syngas conversion by acetogens are in some cases longer acids and alcohols (e.g. butyrate, butanol), lactic acid or 2,3-butanediol (Bengelsdorf et al., 2013; Köpke et al., 2011b, 2014; Phillips et al., 2015). The two most studied acetogens for the conversion of syngas are *Clostridum autoethanogenum* (Abrini et al., 1994) and *Clostridium ljungdahlii* (Tanner et al., 1993). However, many other strains are capable of utilizing syngas as substrate, which is further highlighted in **Chapter 2**.

Syngas fermentation has several advantages over sugar based fermentation, such as the possibility of using a broad spectrum of starting materials and the ability to fix CO_2 in case additional H_2 or electricity is supplied (figure 1). However, there are some technological challenges that need to be solved, both from the biological and process engineering perspective. As the process utilizes a gaseous substrate, the gas transfer rate from gas to liquid is a key factor, requiring a different process design than sugar based fermentation processes (Asimakopoulos et al., 2018). One of the challenges from the view of the biocatalyst is diversifying the end-product portfolio of syngas fermentation, allowing production of other products than the natural products of the applied strains. This is challenging due to the energetic limitations of the syngas metabolism (Molitor et al., 2017), and more insight is required into the physiology of the syngas fermenting strains to stimulate further developments. With quick developments in the genetic engineering of gas fermenting strains, in-depth study of the biological catalysts becomes possible (Humphreys and Minton, 2018). Recently, several successful genetic engineering attempts have been reported in the model strains *C. autoethanogenum* and *C. ljungdahlii* (Huang et al., 2016; Liew et al., 2017), allowing for knockout studies of genes such as alcohol dehydrogenase (adhE) and acetaldehyde oxidoreductase (aor). These developments will eventually contribute to the further understanding of syngas metabolism and the applicability of the biocatalysts.

Fundamentals of the syngas fermentation metabolism: the Wood-Ljungdahl pathway

The pathway that plays a central role in syngas fermentation is the Wood-Ljungdahl pathway (WLP) (figure 2). All syngas fermentation types of metabolism utilize the WLP for either assimilatory purpose or for energy conservation. The WLP is proposed to be one of the first ancient metabolisms to have occurred (Fuchs, 2010; Nitschke and Russell, 2013). This theory is exemplified by experimental results showing that all reactions in the WLP occur abiotically on zero-valent transition metals surfaces in simulated 'early earth' conditions (Varma et al., 2018). The WLP consists of two branches; the methyl-branch and the carbonyl-branch (figure 2), where in total 8 reducing equivalents are invested to generate acetyl-CoA. In assimilatory metabolism, acetyl-CoA can be utilized to form cell metabolites for biomass build-up. Acetyl-CoA can also be processed further to acetate resulting in conservation of ATP via substrate level phosphorylation. The WLP is ATP neutral when it comes to ATP generation via solely substrate level phosphorylation, as one ATP is formed during acetate formation, but another ATP needs to be invested to convert formate to formyl-tetrahydrofolate (figure 2). For a long time it was unclear how the WLP could result in net energy conservation, while simultaneously maintaining a stoichiometrically balanced redox metabolism. With the discovery of electron bifurcating enzyme complexes the functioning of the WLP was further elucidated (Buckel and Thauer, 2013). Bifurcation processes allow for generation of reduced low potential electron carriers (e.g. ferredoxin) from less strong reduced redox intermediates (e.g. NADH/NADPH or H_2), providing flexibility to the cell to optimally distribute redox equivalents over its metabolism. Additionally, essential for understanding the energy conserving role of the WLP was the discovery of the cation-translocating functions of the RnF-complex, exporting either sodium or protons, driven by ferredoxin oxidation coupled to NADH reduction (Müller et al., 2008). The chemiosmotic gradient generated by pumping of cations across the membrane allows for subsequent generation of ATP via ATPases. Due to this mechanism, the WLP is one of the pathways with the lowest ATP investment requirement to obtain acetyl-CoA via CO_2 fixation (Claassens et al., 2016). Therefore, compared to other CO_2-fixating processes, few to no additional energy conserving processes are required to drive the CO_2 fixation process, allowing for efficient use of electron donor. Not all organisms use the WLP for catabolism: methanogens and hydrogenogens conserve energy via methanogenesis and hydrogenogenesis respectively, and use the WLP for biomass assimilatory purposes. Interestingly, while the WLP is similar in different microorganisms, different redox carriers, co-factors and combinations of

bifurcating enzymes can be employed (**Chapter 2**). This is an additional challenge in understanding microorganisms employing the WLP.

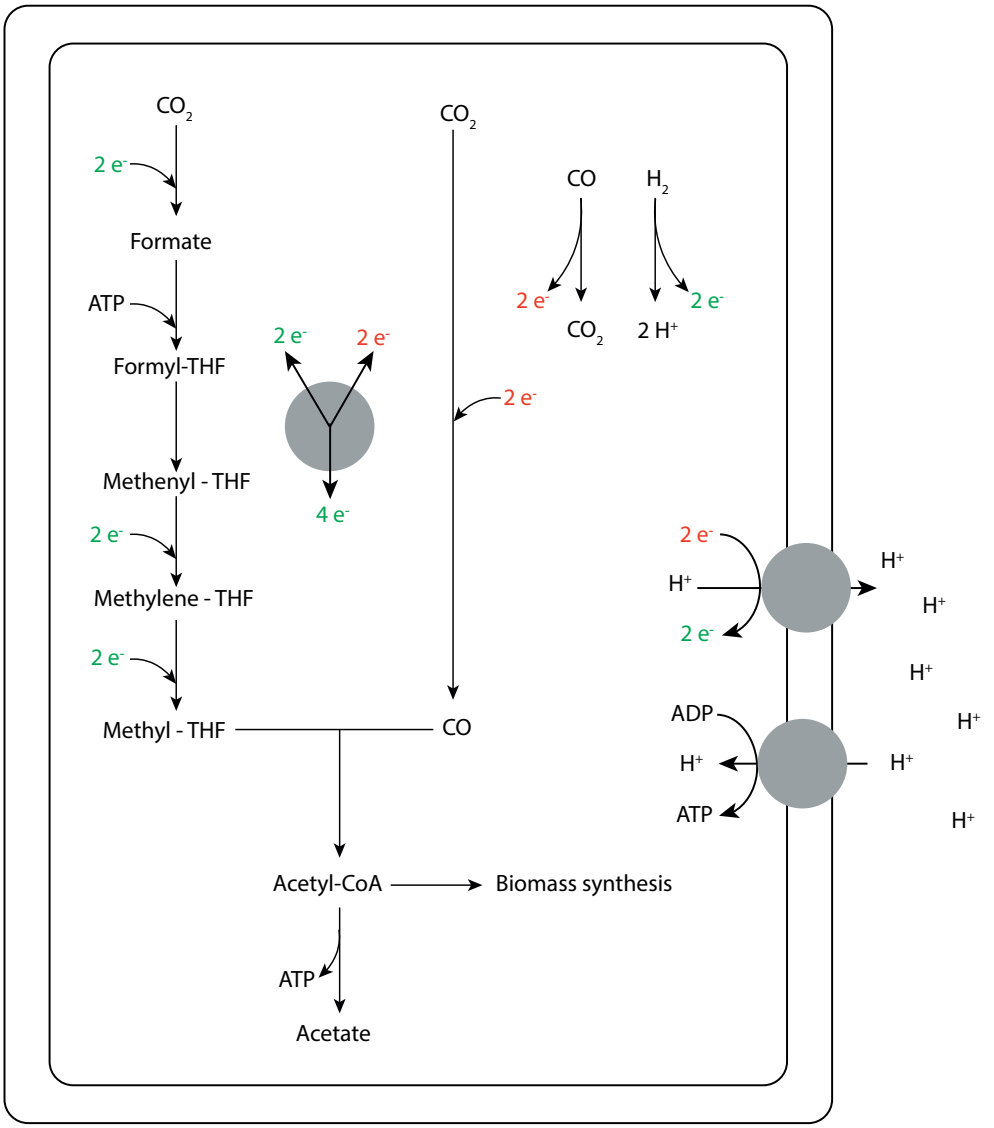

Figure 2. A simplified general representation of the Wood-Ljungdahl pathway and associated bifurcation and ion-translocating enzymes. Electrons are either depicted as ferredoxin (red) or as less strong reduced equivalents such as NAD(P)H (green). Both protons or sodium ions can be pumped out of the cytoplasm (in the figure only protons are depicted).

Processes for gas fermentation; natural vs. synthetic mixed cultures

Like any biotechnological process, gas fermentation processes can be performed in different ways using either mixed- or pure cultures. Undefined mixed cultures are usually preferred in large open systems (e.g. waste water treatment, anaerobic digestion), due to the robustness of a mixed community in the non-sterile system. One of the main goals of these systems is to treat the waste stream, minimizing impact on the environment when the stream is disposed. These systems can be used to produce commodity chemicals or fuels as an additional product (e.g. polyhydroxyalkanoates or methane). However, production of a single end-product in high concentrations via such processes is challenging, due to complex interactions in the culture, often resulting in a mixed spectrum of products. Pure cultures, on the other hand, are easier to control and steer towards a single end-product. Employment of pure cultures additionally allows for implementing genetic modifications (GM) to enhance production or yield of the desired end products. Introducing such GM strains in open undefined mixed cultures might result in loss of the strain due to competition with other microbes in the community and the GM strain cannot be easily retained within the system.

Syngas can be added as supplement feed in anaerobic digestion during treatment of organic waste streams to increase product yield (Jing et al., 2017; Rao et al., 2018). However, such mixed communities fed with syngas have been found to mainly produce methane or acetate as end products, with in some cases minor amounts of longer volatile fatty acids (VFAs) or alcohols (Redl et al., 2017). In pure cultures of gas fermenters, such as *C. autoethanogenum* or *C. ljungdahlii*, mainly acetate and ethanol are found as end-products, but also 2,3-butanediol or lactate are produced in minor amounts (Bengelsdorf et al., 2013). Overall the yield of specific products is higher in pure culture fermentations compared to mixed-culture processes, but the current scope of feasible end-products by pure cultures is still limited to mainly acetate and ethanol. Improvements on the yields and scope of products can be made via genetic engineering or by applying specific cultivation strategies. It has been shown that it is possible to increase ethanol production from syngas via genetic engineering approaches (Liew et al., 2017). Production of non-native products from syngas has, so far, not been reported. Exploration of the pathways of ‘interesting’ products, for example 2,3-butanediol production in *C. autoethanogenum*, has been done via genetics studies (Köpke et al., 2014). Multiple cultivation approaches have been tested to overcome the relatively low yields and limited product spectrum of syngas fermentation. In order to increase yield of ethanol from syngas fermentation,

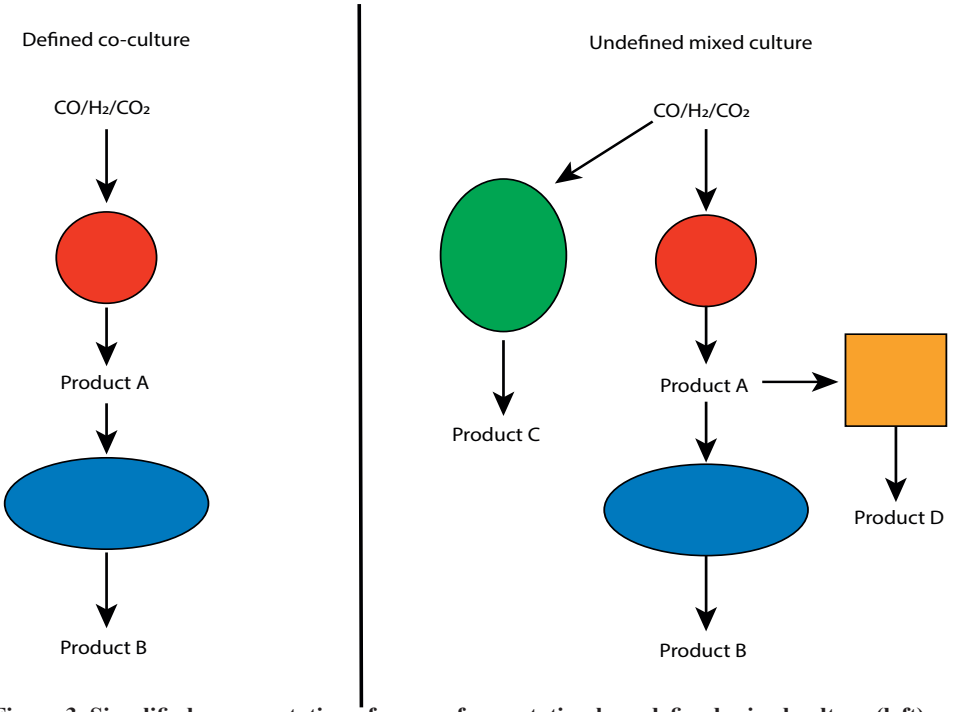

Figure 3. Simplified representation of syngas fermentation by a defined mixed culture (left) and an undefined mixed culture (right). Coloured shapes represent microorganisms, arrows represent the conversions made by those organisms.

two-stage fermentation was applied where under pH 6 conditions acetate was formed, to be subsequently converted to ethanol under more acidic conditions (Richter et al., 2013). A similar two-stage approach was used to expand the scope of syngas fermentation to produce longer chain acids such as butyrate and caproate (Gildemyn et al., 2017; Vasudevan et al., 2014). Production of the dicarboxylic acid malate was performed via sequential fermentation of the acetogen *C. ljungdahlii* and the fungus *Aspergillus oryzae*, utilizing the acetate from syngas fermentation to support the fungal growth (Oswald et al., 2016).

A relatively unexplored approach in syngas fermentation is the application of defined mixed communities of microbes in a single vessel. In this way a food web is established allowing subsequent microbes to form products with higher yield and purity compared to undefined mixed cultures (figure 3). Additionally, products can be synthesized that are inefficiently or not produced by single strains. Defined mixed cultures can be more easily controlled compared to undefined mixed cultures, but are less robust due to their limited diversity. Additionally, while not extensively tested yet, a sterile system is likely required to allow for successful operation of these

defined mixed cultures. However, defined mixed cultures might be specific enough to establish themselves in the system and minimize competition with contaminants. **Chapter 3** and **Chapter 4** describe proof of concept studies of such synthetic mixed cultures and their production potential. Similar to pure cultures, genetic modifications can be introduced to defined mixed cultures as competition for similar roles in the community is lower or even absent (figure 3).

Conclusions

Overall syngas fermentation holds potential to become a solid technology able to convert recalcitrant waste streams into chemicals and fuels. Before such a technology can be implemented, further understanding of the cultivation techniques, physiology and genetics of the bio-catalysts is required. Therefore, the physiology of syngas fermentation biocatalysts and synthetic co-cultivation strategies for enhancing productivity and broadening the product scope were studied in this thesis.

Thesis outline

Carbon monoxide is one of the main components of syngas and is relatively poorly studied as substrate compared to other microbial substrates, such as soluble sugars and polysaccharides. However, information on carbon monoxide metabolism and enzymology is available from research performed in the 80s and 90s of the last century. **Chapter 2** addresses this research in the light of the three main categories of physiology found in CO fermenting microbes: hydrogenogenesis, methanogenesis and acetogenesis. These three processes are interesting for application in either syngas cleaning or production of chemicals and fuels. Next to background information provided in **Chapter 2**, all three processes are studied in the other thesis chapters.

Relatively little is known about the carbon monoxide metabolism of methanogens. In **Chapter 3** we identify *Methanothermobacter marburgensis* as a strain capable of growing methanogenically on CO as sole substrate. However, due to toxicity and potentially redox stress, the strain grows poorly on CO as substrate (like most other methanogens). Therefore, CO-containing gas streams are not easily converted to methane at a high rate. Methane can however be interesting as end-product of gas fermentation due to its properties as stable gaseous fuel, and might be desired to be produced from syngas or off-gas streams. In **Chapter 4** we explore the potential of a co-culture of *Carboxydothermus hydrogenoformans* and *Methanothermobacter thermoautotrophicus* to convert CO containing gases to methane rich off-gas. This co-culture approach showed to be an efficient way to produce high methane content gas and can potentially compete with the other technologies converting CO containing gases to methane.

The co-cultivation strategy was also applied to achieve efficient chain-elongation from CO or syngas as substrate. **Chapter 5** shows a proof of concept of this using a combined culture of *Clostridium autoethanogenum* and *Clostridium kluyveri* forming a food chain utilizing CO, and forming C4 and C6 volatile fatty acids and alcohols as final end products. In **Chapter 6** the metabolic interactions and control of the co-culture are further explored. Chemostat cultivation is used to study the culture on both gene regulation level via transcriptomics, and metabolic level by assessing carbon flow through the system. This shows that ethanol production by *C. autoethanogenum* is significantly stimulated when grown in co-culture with *C. kluyveri*, which led to a remarkable increase of the product yield on the gaseous substrate.

Observations during the co-cultivation studies suggested that the alcohol metabolism of *C. autoethanogenum* is flexible and can operate in both alcohol producing and oxidizing direction. This has resulted in a separate study on the control of the alcohol metabolism of *C. autoethanogenum*. This is described in **Chapter 7**, with focus on the alcohol oxidation properties of the strain during gas fermentation. This information can be used in both monocultures of *C. autoethanogenum* aiming to produce ethanol or can be used to control and steer synthetic co-cultures. Additionally, it was observed that during exposure to increased CO concentrations in the liquid, *C. autoethanogenum* conserves more energy per acetate formed, which we hypothesize to be the result of cycling of acetate, via acetaldehyde and acetyl-CoA back to acetate, resulting in CO-driven ATP conservation.

Current developments in the field of syngas fermentation from both a fundamental and applied perspective are discussed in **Chapter 8**. Here three main topics are addressed: future potential of gas fermentation technology, future potential of synthetic co-cultivation and recent developments in the fundamental physiology of syngas fermenting microbes.

Chapter 2

Pathways and bioenergetics of anaerobic carbon monoxide fermentation

Authors: Martijn Diender, Alfons J.M. Stams & Diana Z. Sousa

Chapter has been published as:

Diender, M., Stams, A. J. M., and Sousa, D. Z. (2015). Pathways and bioenergetics of anaerobic carbon monoxide fermentation. Front. Microbiol. 6. Doi:10.3389/fmicb.2015.01275.

Abstract

Carbon monoxide can act as a substrate for different modes of fermentative anaerobic metabolism. The trait of utilizing CO is spread among a diverse group of microorganisms, including members of bacteria as well as archaea. Over the last decade this metabolism has gained interest due to the potential of converting CO-rich gas, such as synthesis gas, into bio-based products. Three main types of fermentative CO metabolism can be distinguished: hydrogenogenesis, methanogenesis and acetogenesis, generating hydrogen, methane and acetate, respectively. Here, we review the current knowledge on these three variants of microbial CO metabolism with an emphasis on the potential enzymatic routes and bio-energetics involved.

Introduction

Carbon monoxide is a tasteless, odourless gas, best known for its toxic characteristics. It is part of the global carbon cycle, is involved in assimilatory and dissimilatory pathways of numerous microorganisms and was found to act as a signal molecule in mammals (Ryter and Otterbein, 2004). Additionally, it is speculated to be an important substrate for early life on earth (Miyakawa et al., 2002). CO is chemically formed during oxygen limited combustion of carbon materials, and can be biologically generated via cellular metabolism (Eikmanns et al., 1985; Ryter and Otterbein, 2004) or enzymatic degradation of heme (Chin and Otterbein, 2009). A large part of naturally generated CO is assumed to be formed via photochemical reactions (Weinstock and Niki, 1972). Other sources contributing to the atmospheric CO level are: volcanic activity, forest fires, and over the last two centuries industrial activity. Cumulative, these activities result in the production of approximately 2.6 petagram (Pg) CO per year (Khalil and Rasmussen, 1990).

Due to the foreseen depletion of fossil energy sources and consideration on environmental impact of current chemical industry, alternative sustainable technologies are being developed. A bio-based economy is considered one of the sustainable solutions for the growing resource depletion, and has potential to replace petroleum industries in the future. However, the hydrolysis of non-food-competing, ligno-cellulosic biomass limits the application of bio-based technologies, leaving a significant amount of the initial substrate unused (Hamelinck et al., 2005). Gasification of the carbohydrate material, forming syngas, is a potential way of gaining access to all material of the original source, mainly in the form of CO, H_2 and CO_2. A large spectrum of carbon sources can fuel this technology, from coal, tar and gas to ligno-cellulosic biomass, all kinds of municipal waste, and digester sludge. As syngas mainly consists of CO, H_2 and CO_2, autotrophic, CO-tolerant microorganisms are required as biocatalysts for fermentation of this gas. Numerous microorganisms have shown to utilize CO as a substrate, producing organic compounds such as acetate, ethanol, 2,3-butanediol and butyrate (Dürre and Eikmanns, 2015; Latif et al.,

2014; Tiquia-Arashiro, 2014). In addition, methanogenesis and hydrogenogenesis using syngas as a substrate could have large implications for biofuel production. Even though production of interesting chemicals from syngas is possible, the exact metabolism of syngas conversion is not fully understood. This limits the optimization of potential production strains and, thus, the development of bio-based production processes. Different aspects of biological conversion of CO and syngas have been reviewed in the past decade (Bengelsdorf et al., 2013; Dürre and Eikmanns, 2015; Henstra et al., 2007b; Latif et al., 2014; Oelgeschläger and Rother, 2008; Sokolova and Lebedinsky, 2013). However, a large part of these reviews focus on industrially relevant species and their application potential, while only few address fundamental aspects.

Two types of CO metabolism can be distinguished: respiratory and fermentative (table 1), the former involving an exogenous electron acceptor, whereas the latter utilizes internally generated intermediates as electron acceptor. A relatively well studied example of respiratory CO metabolism is CO oxidation coupled to oxygen reduction (Meyer et al., 1986; Meyer and Schlegel, 1983). Other, less characterized, electron acceptors that have been identified for carboxydotrophic growth are sulphate (Parshina et al. 2010; Parshina et al. 2005), anthroquinone disulfonate (AQDS) (Henstra and Stams, 2004), fumarate (Henstra and Stams, 2004) and ferrihydrite (Slobodkin et al., 2006). The main focus of this review is on fermentative CO metabolism, distinguishing hydrogenogenesis, acetogenesis and methanogenesis with a special emphasis on the potential enzymatic routes and bio-energetics involved. Classifying hydrogenogenesis as a fermentative process is debatable because protons can be considered exogenous acceptors. However, as protons are present in any microbial environment and are generated from the substrate water during hydrogenogenesis, hydrogenogenic metabolism is considered here as fermentative.

General microbial CO metabolism

Both aerobic and anaerobic CO metabolism process the CO molecule via the enzyme: carbon monoxide dehydrogenase (CODH). Here, we only consider the anaerobic CODHs, which differ from the aerobic CODHs by structure and the presence of nickel-iron clusters in their active centres (Jeoung et al., 2014). About 6% of all known microbial genomes contain at least one [Ni-Fe] CODH gene sequence, out of which 43% contain at least two, suggesting a more widespread anaerobic CO-utilizing capability than assumed before (Techtmann et al., 2012). It has been shown that CODH genes cluster according to function, instead of clustering by phylogeny, suggesting horizontal gene transfer events have led to the establishment of the CODH gene in the different microbial genomes (Techtmann et al., 2012). CODHs from different organisms have been purified and characterized, including the ones from three relatively well studied anaerobic carboxydotrophic organisms: *Rhodospirillum*

rubrum (Drennan et al., 2001), *Carboxydothermus hydrogenoformans* (Setlichny et al., 1991) and *Moorella thermoacetica* (Darnault et al., 2003; Doukov, 2002). All the structures of these anaerobic CODHs contain iron-sulfur centres (Dobbek et al., 2001; Hu et al., 1996). Additionally, these CODHs contain nickel as a cofactor, for binding and coordinating CO in the active site (Dobbek et al., 2001; Drennan et al., 2001). Other divalent metals were found in the active centre of anaerobic CODHs, however only the nickel containing enzymes were observed to be active in CO conversion (Darnault et al., 2003). CODH can be mono- or bifunctional, both enabling the organism to utilize CO for the energy metabolism. The bifunctional CODH is associated with an acetyl-CoA synthase (ACS), and additionally has a role in carbon fixation, catalysing the condensation of CO, CoA-SH and a methyl-group into acetyl-CoA. The bacterial CODH and ACS are connected via a hydrophobic tunnel (Lindahl, 2002; Maynard and Lindahl, 1999; Seravalli and Ragsdale, 2008), preventing CO from being a toxic intermediate in the metabolism of the cell (Doukov, 2002).

The redox potential of the CO/CO_2 pair (E_0' = -520 mV), is lower than that of H_2/H^+ (E_0' = -414 mV), which has significant implications for the metabolism. While a metabolism driven by hydrogen requires bifurcation mechanisms to reduce ferredoxin (E_0' = -400 mV) (Buckel and Thauer, 2013), CO can solely drive this reaction. However, the more negative redox potential of CO poses a challenge for the redox balance of the organism. Therefore, efficient cofactor re-oxidizing pathways are required to avoid the cell from becoming completely reduced. Additionally, hydrogenases are considered to be a weak point in CO metabolism, as hydrogen metabolism is often observed to be rapidly inactivated upon CO exposure (Bertsch and Müller, 2015a; Daniels et al., 1977; Genthner and Bryant, 1982; Perec et al., 1962). However, [Ni-Fe]-hydrogenases were found to be less sensitive to CO than [Fe-Fe] or iron-only hydrogenases (Adams, 1990b; De Lacey et al., 2007). Some microorganismes possess [Ni-Fe] hydrogenases that are highly tolerant to CO, such as *Rhodospirillum rubrum* (Fox et al., 1996b) and *Pyrococcus furiosus* (Adams, 1990a). CO is known to strongly bind to metals via a process called back bonding, which is also considered to be the mechanism of toxicity (Jeoung et al., 2014).

CO driven hydrogenogenic metabolism

Coupling CO oxidation to proton reduction is, conceptually seen, one of the simplest mechanisms of biological energy conservation. This reaction, also known as the water-gas shift reaction, results in the formation of hydrogen and CO_2 (table 1). The reaction was found to be completed by three enzymes: CODH, an electron transfer protein and an energy converting hydrogenase (EcH). CO is oxidized via the CODH complex, and electrons are transferred to a “ferredoxin-like” electron carrier. Oxidation of this

electron carrier can be coupled to proton reduction via an EcH complex, producing hydrogen and simultaneously generating an ion motive force (Hedderich and Forzi, 2006). Besides being involved in hydrogenogenic metabolism, EcH enzymes also play a role in sugar fermentation (Sapra et al., 2003) and methanogenesis (Thauer et al., 2010). Several microorganisms which hydrogenogenically metabolize CO have been isolated; most of them are thermophiles (table 2). Two microorganisms conserving energy via the water-gas shift reaction have been rather well studied, the mesophilic *Rhodospirillum rubrum* (Kerby et al., 1995) and the thermophilic *Carboxydothermus hydrogenoformans* (Svetlichny et al., 1991).

R. rubrum, Rubirivivax gelatinosa and *Rhodopseudomonas palustris* are photosynthetic bacteria and the only known mesophiles capable of efficiently conserving energy from the water-gas shift reaction (table 2). In *R. rubrum* the CO-dependent metabolism is regulated via a heme-protein, which acts as CO sensor (CooA) and controls transcription of the enzymatic machinery required for CO dependent growth (Roberts et al., 2001). The genes controlled by CooA in *R. rubrum* are arranged in two gene clusters: cooFSCTJ and cooMKLXUH. The first gene cluster codes for the active CODH (cooS), electron carrier (cooF) and a nickel inserting complex (cooCTJ) (Kerby et al., 1997), whereas the latter codes for a six subunit EcH complex. The CODH structure of *R. rubrum* has been resolved to 2.8Å, and is similar to the CODH of anaerobes such as *C. hydrogenoformans* and *M. thermoacetica* (Dobbek et al., 2001; Drennan et al., 2001). Electrons from CO oxidation are transferred to an iron-sulfur protein (CooF), which shuttles the electrons to the EcH complex. The CooF complex is tightly associated with the CODH, and was shown to be reduced upon CO exposure (Ensign and Ludden, 1991). Other electron carriers, such as other native ferredoxins from *R. rubrum*, were ineffective in mediating electron transfer from CODH to the hydrogenase (Ensign

Table 1. Reaction equations and their standard Gibbs free energy (ΔG^0) for several modes of carboxydotrophic growth.

Metabolism		Reaction	$\Delta G^{0'}$ (kJ)
Fermentative			
	Hydrogenogenic	$CO + H_2O \rightarrow CO_2 + H_2$	-20
	Methanogenic	$4\ CO + 2\ H_2O \rightarrow CH_4 + 3\ CO_2$	-210
	Acetogenic	$4\ CO + 2\ H_2O \rightarrow CH_3COO^- + H^+ + 2\ CO_2$	-174
	Solventogenic (ethanol)	$6\ CO + 3\ H_2O \rightarrow C_2H_5OH + 4\ CO_2$	-224
Respiratory			
	Oxygen	$2\ CO + O_2 \rightarrow 2\ CO_2$	-514
	Sulphate	$4\ CO + SO_4^{2-} + H^+ \rightarrow 4\ CO_2 + HS^-$	-231

and Ludden, 1991). This suggests that the CooF subunit is highly specific for electron transfer from CODH to the hydrogenase. Not only is the *R. rubrum* CODH efficient in converting CO to CO_2, also its CO-induced hydrogenase is well adapted to CO dependent growth (Bonam et al., 1989). The EcH of *R. rubrum* consists of 6 subunits, of which two subunits, CooH and CooL, are similar to the ones found in some [Ni-Fe] hydrogenases. In addition, all six subunits show high similarity with complex I NADH:oxidoreductases, which are involved in proton translocation coupled to NADH oxidation (Fox et al., 1996b, 1996a). During activity assays, the EcH is found to function optimally in presence of CODH:CooF, which is theorised to promote forming and maintaining a stable complex (Singer et al., 2006). The CO-induced hydrogenase of *R. rubrum* is highly CO tolerant, and only shows signs of inhibition above 60% CO in the headspace (Fox et al., 1996a).

Despite the seemingly efficient water-gas shift metabolism in *R. rubrum*, autotrophic growth on solely CO as a carbon source is very slow (Dashekvicz and Uffen, 1979). *R. rubrum* requires small amounts of yeast extract and acetate as a carbon source to grow efficiently. *R. gelatinosus* and *R. palustris* exhibit a similar hydrogenogenic CO metabolism as *R. rubrum*. However, in contrast to *R. rubrum*, these bacteria were able to perform the water-gas shift reaction and grow on CO as a sole carbon source, but merely in presence of light (Jung et al., 1999; Maness et al., 2005). Growth was significantly slowed down for *R. gelatinosus* in the dark, which was not assessed for *R. palustris*. The growth rate of *R. gelatinosus* increased significantly after addition of malate as a carbon source (Maness et al., 2005). So, despite efficient energy conservation via the water-gas shift reaction, as shown in the presence of organic carbon sources, autotrophic growth seems very energy intensive for these phototrophic bacteria. The relatively slow growth on CO as a sole carbon source is likely due to the use of the energy demanding Calvin-cycle, which can be considered the main carbon-fixation mechanism in these phototrophic bacteria. All three isolated mesophilic, hydrogenogenic carboxydotrophs are phototrophs. However, it is unclear why the trait of hydrogenogenic CO-utilization among mesophiles is exclusive to this group.

Among thermophilic hydrogenogens, *C. hydrogenoformans* is one of the best studied. This bacterium was first thought to only grow fermentatively on CO or pyruvate as substrate, but was later shown to be capable of respiratory growth with CO as well (Henstra and Stams, 2004). With five different CODHs encoded in its genome, it is one of the few organisms known to have multiple CODH types, which is likely related to its exceptional growth capabilities on CO (Wu et al., 2005). *C. hydrogenoformans* uses a CODH-CooF-EcH complex, which is highly similar to the system found in *R. rubrum* (Soboh et al., 2002). In contrast to the mentioned mesophilic phototrophs, *C. hydrogenoformans* is capable of efficient autotrophic

growth, using solely CO as energy and carbon source. This characteristic might be assigned to the presence of the Wood-Ljungdahl pathway, which in contrast to the Calvin-cycle is not as energy demanding. Additionally, a turnover rate of 31000 s^{-1} was found for the CODHII of *C. hydrogenoformans* (Svetlichnyi et al., 2001), allowing for fast generation of reduction equivalents and thus a quick energy metabolism. Upon increased hydrogen and carbon dioxide pressure, acetate is produced from CO by *C. hydrogenoformans*. This suggests acetogenic use of the Wood-Ljungdahl pathway could act as a backup for its hydrogenogenic metabolism (Henstra and Stams, 2011). *C. hydrogenoformans* and related thermophilic species are suggested to fulfil an important role in the volcanic environments they originate from, ensuring CO concentrations are kept below toxic levels, making life of other non-CO tolerant organisms possible (Techtmann et al., 2009). Furthermore, it seems horizontal gene transfer events have played an important role in the establishment of CO-driven hydrogenogenic metabolism in these environments (Sant'Anna et al., 2015; Techtmann et al., 2012).

When assessing the distribution of isolated hydrogenogenic carboxydotrophic microorganisms (table 2), thermophilic isolates seem to be more prevalent than mesophilic ones, which contrasts with the solubility of gaseous substrates at elevated temperatures. Temperature increase has two effects on dissolved gases: decreased gas solubility and increased gas diffusion rates. In a hydrogenogenic metabolism the microorganisms use a gaseous substrate, subsequently producing a gaseous product. The thermodynamics of this metabolism thus relies on the concentration of two gases, which is indirectly related to the diffusion rate of these gases. The apparent Km values for the exchange reaction of the CODH in *R. rubrum*, *C. hydrogenoformans*, and the acetogen *M. thermoacetica*, are in the order of 0.032, 0.018 and 0.01 mM, respectively (Jeon et al., 2005; Raybuck et al., 1988; Seravalli and Ragsdale, 2008; Svetlitchnyi et al., 2001). The maximal solubility of CO in water is approximately 1.6 to 0.38 mM, in the range of 273 to 353 K, respectively. Assuming a Km of 0.03 mM and applying simple Michaelis-Menten kinetics, the associated CODH reaction rate at these CO concentrations goes from 98 to 93% of Vmax (figure 1). This suggests that carboxydotrophic microorganisms are not significantly limited by the maximal solubility of CO at elevated temperatures. The CO diffusion coefficient, an indication of the diffusion rate of the gas, is 2.0 * 10-5 cm2/s in water at 298 K. Compared to 298 K, the estimated diffusion constant at 333 K is two times larger and three times larger at 353 K (approximated by the Stokes-Einstein equation, using the dynamic viscosity of water, figure 1).

Table 2. Isolated micro-organisms capable of conserving energy from the water-gas shift reaction. Not determined parameters are marked N.D.

Species	Origin	Temperature optimum, ºC	Carboxydotrophic generation time, hr	References
Mesophilic bacteria				
Rhodospirillum rubrum	various environments	30	5 (dark, acetate)	(Kerby et al., 1995)
Rubirivivax gelatinosa	lake sediment	34	6.7 (dark, trypticase), 10 (light, autotrophically) 1.5 (light, malate)	(Maness et al., 2005; Uffen, 1976)
Rhodopseudomonas palustris	anaerobic wastewater sludge digester	30	2 (light, autotrophically)	(Jung et al., 1999)
Thermophilic bacteria				
Caldanaerobacter subterraneus subsp. pacificus	submarine hot vent, Okinawa Trough	70	7.1	(Fardeau, 2004; Sokolova et al., 2001)
Carboxydocella sporoproducens	hot spring, Karymskoe Lake	60	1	(Slepova et al., 2006)
Carboxydocella thermoautotrophica	terrestrial hot vent, Kamchatka Peninsula	58	1.1	(Sokolova et al., 2002)
Carboxydothermus hydrogenoformans	freshwater hydrothermal spring, Kunashir Island	70	2	(Svetlichny et al., 1991)
Carboxydothermus islandicus	hot spring, Hveragerdi	65	2	(Novikov et al., 2011)
Carboxydothermus pertinax	Volcanic acidic hot spring, Kyushu Island	65	1.5	(Yoneda et al., 2012)
Carboxydothermus siderophilus	hot spring, Kamchatka Peninsula	65	9.3	(Slepova et al., 2009)
Dictyoglomus carboxydivorans	hot spring, Kamchatka Peninsula	75	60	(Kochetkova et al., 2011)
Moorella stamsii	digester sludge	65	N.D.	(Alves et al., 2013)
Thermincola carboxydiphila	hot spring, Lake Baikal	55	1.3	(Sokolova et al., 2005)
Thermincola ferriacetica	hydrothermal spring, Kunashir Island	60	N.D.	(Zavarzina et al., 2007)
Thermincola potens	thermophilic microbial fuel cell	55	N.D.	(Byrne-Bailey et al., 2010)
Thermolithobacter carboxydivorans	mud and water, Calcite Spring	73	1.3	(Sokolova et al., 2007)
Thermosinus carboxydivorans	hot spring, Norris Basin	60	1.15	(Sokolova et al., 2004a)
Thermoanaerobacter thermohydrosulfuricus subsp. carboxydovorans	geothermal spring, Turkey	70	N.D.	(Balk et al., 2009)
Desulfotomaculum carboxydivorans	paper mill wastewater sludge	55	N.D.	(Parshina et al., 2005)
Thermophilic Archaea				
Thermococcus onnurineus	deep-sea hydrothermal vent	80	5	(Bae et al., 2006, 2012)
Thermococcus AM4	hydrothermal vent	82	5	(Sokolova et al., 2004b)
Thermofilum carboxyditrophus	Kamchatka hot springs	90	N.D.	(Kochetkova et al., 2011)

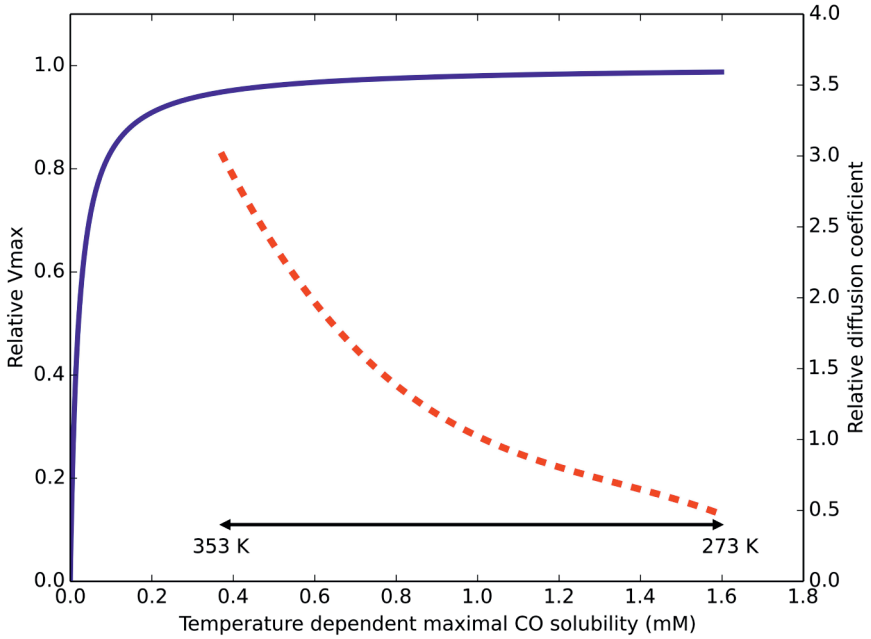

Figure 1. Temperature effect on parameters for CO driven hydrogenogenic growth.
Estimated relative Vmax of a CO dehydrogenase (CODH), displayed by the blue continuous line, assuming Michaelis-Menten kinetics (Km = 0.03 mM) based on maximal solubilized CO. The approximated ratio of the diffusion constant for any dissolved gas (at atmospheric pressure) in water compared to its diffusion constant at 298 K is displayed by the red dashed line. The physiologically relevant temperature range is displayed by the double headed black arrow. The displayed temperature scale is not linear due to the non-linear relation between temperature and CO solubility.

This suggests that at increased temperatures, CO is more rapidly supplied to the microorganisms. Via the same mechanism, the temperature indirectly affects the degree of accumulation of hydrogen in the near vicinity of the microorganism, allowing two times faster removal of H_2 at 333 K, and three times at 353 K. This suggests thermophilic hydrogenogenic metabolism suffers less from hydrogen accumulation to thermodynamically unfavourable levels when compared to mesophilic conditions. Therefore, we hypothesise that CO driven hydrogenogenic metabolism is more favourable at higher temperatures when compared to lower temperatures, giving rise to the currently observed temperature distribution of carboxydotrophic hydrogenogenic isolates (table 2). If this potential advantage also translates into an increased energy yield, and thus a higher growth rate with increasing temperatures is unclear as numerous factors influence the growth rate.

CO driven acetogenesis and related metabolisms

Formation of acetate from CO was first reported in 1982 (Lynd et al., 1982). Since then many acetogens have been discovered to utilize CO, both homo-acetogenic organisms (i.e. generating solely acetate) and mixed-product acetogenic organisms (i.e. generating a mixture of end-products) (table 3). Large differences can be observed between the growth rates and yields of CO-grown acetogens, indicating differences in their ways of energy conservation and pathways utilized (table 3). The Wood-Ljungdahl pathway is the central metabolism for acetogenic growth (Ragsdale and Pierce, 2008). In contrast to the Calvin-cycle, the reductive TCA-cycle or the 3-hydroxypropionate cycle, the Wood-Ljungdahl pathway can be used to conserve energy. The Wood-Ljungdahl pathway consists of two branches, which in total require 8 reduction equivalents and one ATP to form acetyl-CoA from two CO_2. During formation of acetate the ATP investment is regained by substrate level phosphorylation, but no net ATP is gained, thus requiring an ion motive force to conserve net energy. Complex I related RnF complexes have been identified as the cation extruding mechanism in many acetogens, linking ferredoxin oxidation to NAD reduction, simultaneously forming either a sodium or proton gradient (Biegel et al., 2011). Upon consumption of this gradient, ATP is formed from ADP and phosphate via an ATPase (Müller, 2003). The availability of ferredoxin can thus be considered the driving force of energy generation in the autotrophic acetogenic metabolism. It is assumed that in hydrogenotrophic acetogens electron-bifurcating hydrogenases are required to generate reduced ferredoxin (Buckel and Thauer, 2013; Poehlein et al., 2012). As CO can directly reduce ferredoxin, these bifurcating systems seem redundant during CO-driven growth, but might be utilized to correctly distribute reduction equivalents over the metabolism. Four steps in the Wood-Ljungdahl pathway require input of electrons for fixation of two CO_2. The type of cofactors utilized in each of these steps differs per enzyme and per microorganism, making it impossible to propose a general metabolism for acetogenic CO metabolism. This distinct use of cofactors can explain part of the differences observed in yield and growth rate of different acetogens (table 3). Recently, the energy metabolism for autotrophic growth on H_2/CO_2 for *A. woodii*, *M. thermoacetica* and *C. ljungdahlii* was reviewed (Schuchmann and Müller, 2014). Here, we assess and compare the CO metabolism of these three species, which are the current model organisms for acetogenic metabolism.

Moorella thermoacetica is one of the best studied homo-acetogenic bacteria able to utilize CO. This organism differs from other acetogenic strains in the sense that it does not possess an RnF complex, leaving the mechanism of cation transport unknown (Pierce et al., 2008). Either an EcH complex or cytochromes are proposed to perform the build-up of an ion motive force. Several cytochromes have been found

in Moorella species that are potentially active in proton transport (Gottwald et al., 1975). However, the role of these electron carrier proteins in acetogenic metabolism has never been experimentally shown. Additionally, a role of these cytochromes in respiratory metabolism is likely to exist, as growth with nitrate and nitrite was shown to be possible (Drake and Daniel, 2004). An EcH complex is coded for in the genome of *M. thermoacetica* (Huang et al., 2012), making cation export via this enzyme a possibility. Based on presence of an EcH complex, an energy metabolism for growth on H_2/CO_2 has been proposed for *M. thermoacetica* (Schuchmann and Müller, 2014). The plausible metabolism is based on the assumption that methylenetetrahydrofolate reductase, responsible for the exergonic reduction of methylenetetrahydrofolate to methyltetrahydrofolate, is somehow coupled to energy conservation. As all enzymes of the Wood-Ljungdahl pathway are considered soluble, none of these is expected to be involved in generation of an ion motive force. Crude membrane extraction methods were thought to be the cause of finding all the enzymes in the soluble fraction, and more gentle extraction methods confirmed membrane attachment of methylenetetrahydrofolate reductase (Hugenholtz and Ljungdahl, 1989). Also in the acetogen *Blautia producta*, methylenetetrahydrofolate reductase was found to be loosely attached to the cellular membrane, supporting a potential role in energy conservation (Wohlfarth et al., 1990). Further experimental evidence for a direct role of this enzyme in energy conservation has never been found though. A recent theory is that the methylenetetrahydrofolate reductase has bifurcation activity, coupling the oxidation of two NADH molecules to the reduction of ferredoxin and methylenetetrahydrofolate (Huang et al., 2012). The hypothesis for a bifurcating function of this enzyme in *M. thermoacetica* is supported by the following arguments: i) the enzyme was found to be associated with subunits similar to F420 non-reducing hydrogenases, also found in archaea for bifurcational reduction of CoM-CoB (Huang et al., 2012), ii) in several acetogens the complex was found to contain flavin (Clark and Ljungdahl, 1986; Wohlfarth et al., 1990), which is thought to be essential for bifurcation of the electrons over the two acceptors (Buckel and Thauer, 2013; Herrmann et al., 2008; Kaster et al., 2011; Nitschke and Russell, 2012; Thauer et al., 2008). The flavin is theorised to donate one electron to a high potential acceptor, leaving the flavin at a “red hot” flavosemiquinone state, capable of reducing a low potential acceptor (Buckel and Thauer, 2013). This can be repeated for another two electrons, obtaining two fully reduced products. In case of methylenetetrahydrofolate reductase, the high potential acceptor would be methylenetetrahydrofolate (E_0’ = -200 mV) whereas ferredoxin (E_0’= -400 mV) would be the low potential acceptor. Assuming a bifurcating function of methylenetetrahydrofolate reductase and a proton translocation ratio of 1:1 per hydrogen formed by the EcH complex, the energy yield of H_2/CO_2 grown *M. thermoacetica* was suggested to be 0.5 ATP per acetate formed

Table 3. Properties of CO grown acetogenic microorganisms. Parameters measured in medium containing complex additives like yeast extract or rumen fluid are indicated as undefined medium (UM). Parameters measured in medium of which the exact composition is known are indicated as defined medium (DM). SLP: substrate level phosphorylation. Not determined parameters are marked N.D, whereas not applicable parameters are indicated N.A.

Organism	Energy conservation: mechanism (cation)	Minimal generation time reported, hr		Biomass yield, g_{Cells}/mol		References
		CO	H_2	CO	H_2	
Mixed fermenters						
Clostridium ljungdahlii	RnF (H^+)	12[A] (DM) 3.8 (UM)	22[A] (DM)	1.38 (DM) 8.4[C] (UM)	0.37 (DM)	(Cotter et al., 2009; Köpke et al., 2011a; Phillips et al., 1994; Tanner et al., 1993; Younesi et al., 2005)
Clostridium autoethanogenum	RnF (H^+)	4 (UM)	N.D.	N.D.	N.D.	(Abrini et al., 1994; Cotter et al., 2009; Köpke et al., 2011a)
Clostridium formicoaceticum	RnF (N.D.)	7 (UM)	No growth	N.D.	N.A.	(Lux and Drake, 1992)
Clostridium ragsdalei	RnF (N.D.)	4 (UM)	N.D.	N.D.	N.D.	(Köpke et al., 2011a; Kundiyana et al., 2011)
Clostridium scatologenes	RnF (N.D.)	11.6 (UM)	17.3 (UM)	N.D.	N.D.	(Liou, 2005)
Clostridium drakei	RnF (N.D.)	5.8 (UM)	3.5 (UM)	N.D.	N.D.	(Kusel et al., 2000; Liou, 2005)
Clostridium carboxidivorans	RnF (H+)	4.3 (UM)	5.8 (UM)	0.25	N.D.	(Liou, 2005; Rajagopalan et al., 2002)
Alkalibaculum bacchi	RnF (N.D.)	5.8 (UM)	N.D.	0.8-2 (UM)	N.D.	(Allen et al., 2010; Liu et al., 2012a)
Butyribacterium methylotrophicum	RnF (N.D.)	13.9[A] (UM)	9 (UM)	3 (UM)	1.7 (UM)	(Heiskanen et al., 2007; Lynd et al., 1982; Lynd and Zeikus, 1983)
Eubacterium limosum	RnF (Na^+)	7 (UM)	~20[B] (UM)	3.38 (UM)	0.84 (UM)	(Genthner and Bryant, 1982, 1987; Jeong et al., 2015)
Oxobacter pfennigii	RnF (N.D.)	13.9[A] (UM)	No growth	2.50 (UM)	N.A.	(Krumholz and Bryant, 1985)
Homo-acetogenic						
Moorella thermoautotrophica	EcH/ Cytochromes (H^+)	7 (UM), 9 (DM)	33 (DM)	3.34 (UM) 2.53 (DM)	0.82 (DM)	(Collins et al., 1994; Savage et al., 1987; Savage and Drake, 1986)
Moorella thermoacetica	EcH/ Cytochromes (H^+)	9 (DM)	16 (DM)	1.28 (UM)	0.46 (UM)	(Collins et al., 1994; Daniel et al., 1990; Pierce et al., 2008)
Acetobacterium Woodii	RnF (Na^+)	13[D] (UM), 5.5[A] (UM + formate)	6.2[A] (UM)	N.D.	1.05[C] (DM)	(Balch et al., 1977; Bertsch and Müller, 2015b; Genthner and Bryant, 1987; Hess et al., 2013; Tschech and Pfennig, 1984)
Blautia producta	RnF (Na^+)	1.5 (UM)	5 (UM)	2.13[C] (UM)	0.65[C] (UM)	(Geerligs et al., 1989; Lorowitz and Bryant, 1984)
Clostridium aceticum	RnF (N.D.)	~10[B] (UM)	20 (UM)	N.D.	N.D.	(Braun et al., 1981; Sim et al., 2007)
Acetogenic Archaea						
Archeoglobus fulgidus	SLP	~10	N.A.	N.D.	N.A.	(Henstra et al., 2007a)
Methanosarcina acetivorans	SLP, RnF(Na^+)	~20	N.A.	2.5	N.A.	(Rother and Metcalf, 2004)

[A] Duplication time is recalculated from a given specific growth rate (μ) assuming: $2 = e^{\mu t}$

[B] Duplication time is estimated from a given graph, as numbers were not mentioned.

[C] Yield was recalculated from g protein/mol CO to g_{Cells}/mol CO, making the assumption proteins makes up 60% of the dry weight (Krumholz and Bryant, 1985).

[D] *A. woodii* was shown to not grow on CO as a sole carbon source, generation time displayed was measured in rich medium likely containing substrates for co-fermentation.

(Schuchmann and Müller, 2014). Applying a model using similar assumptions, the metabolism on CO is expected to yield 1.5 ATP per acetate formed (figure 2). The suggested three times increase in energy yield matches with the increased observed growth yield of *M. thermoacetica* with CO (table 3). The same yield increase is observed in the related organism *M. thermoautotrophica*, which is thought to exhibit a similar metabolism (table 3).

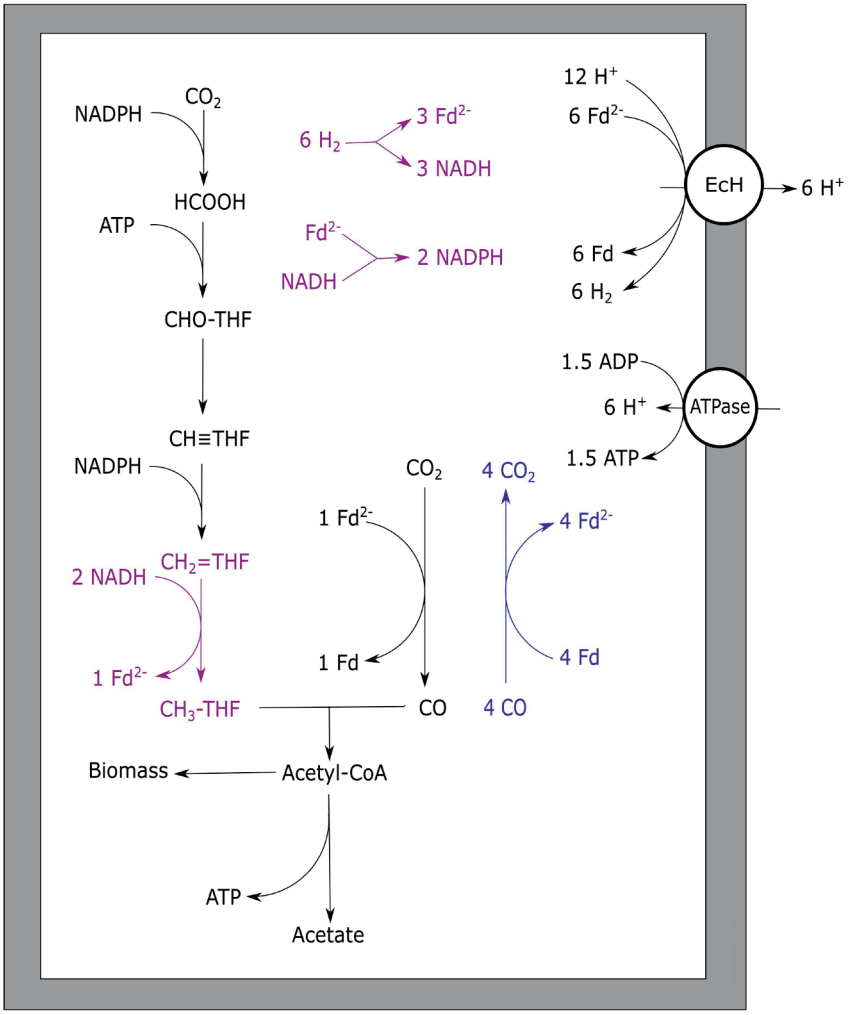

Figure 2. Carbon monoxide metabolism of *M. thermoacetica*. Stoichiometric conversion of CO to acetate by *M. thermoacetica* is disaplayed. Reactions marked blue indicate CO oxidizing activity by CODH, bifurcating reactions are marked purple. The EcH is assumed to transport one proton per hydrogen formed whereas the ATPase is assumed to generate one ATP per four protons translocated. EcH, energy converting hydrogenase; ATPase, ATP synthase; Fd, ferredoxin; THF, tetrahydrofolate.

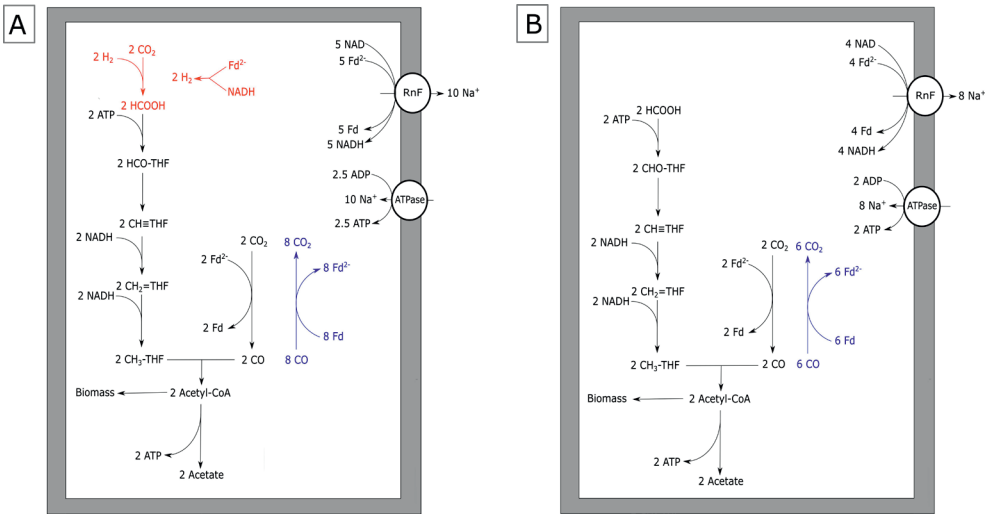

Figure 3. Carbon monoxide metabolism of *A. woodii*. Acetogenic CO metabolism of *A. woodii* is displayed. A) The proposed theoretical pathway and energetic yield of CO conversion to acetate. Pathways prone to CO inhibition are shown in red. B) Proposed metabolism and energetic yield of acetogenic metabolism driven by CO co-fermented with formate. Reactions marked blue indicate CO oxidizing activity by CODH. The RnF complex is assumed to transport two sodium ions per Fd oxidized whereas the ATPase is assumed to generate one ATP per four sodium ion translocated. Rnf, RnF complex; ATPase, ATP synthase; Fd, ferredoxin; THF, tetrahydrofolate.

Initially, the acetogen *Acetobacterium woodii* was reported to grow homoacetogenically on CO as a sole energy source (Genthner and Bryant, 1987). However, recently it was shown that the organism can only utilize CO in co-fermentation with either hydrogen or formate (Bertsch and Müller, 2015a). Additionally, *A. woodii* was shown to produce ethanol when the pressure of CO in the headspace was over 25 kPa (Bertsch and Müller, 2015a). These contradictory observations might be explained by the rich undefined medium used in the initial study, which makes it possible that the organism has co-fermented CO with other substrates, such as formate (Bertsch and Müller, 2015a). This is further supported by findings of the initial study that it was not possible to grow *A. woodii* with solely CO on defined medium (Genthner and Bryant, 1987). For *A. woodii*, a metabolism on H_2/CO_2 was proposed based on genomic data (Poehlein et al., 2012), and was later adapted suggesting a gain of ~0.3 ATP per acetate formed (Schuchmann and Müller, 2014). *A. woodii* is suggested to contain a non-bifurcating methylenetetrahydrofolate reductase, using only NADH to form methyltetrahydrofolate (Schuchmann and Müller, 2014). Growth on H_2/

CO_2 for *A. woodii* was reported with a generation time of approximately 6 hours. Presence of increasing levels of CO negatively affected the growth rates on H_2/CO_2, and became almost fully inhibited above 15 kPa CO (Bertsch and Müller, 2015a). *A. woodii* efficiently co-fermented CO (25 kPa) with formate at a generation time of approximately 5.5 h. Levels up to 50 kPa CO stimulated growth when co-fermenting formate, however higher CO pressures caused a decrease in growth rate. Growth remained possible up to a maximally tested pressure of 100 kPa CO (Bertsch and Müller, 2015a). The inhibitory effect of CO on the *A. woodii* metabolism is suggested to be related to its formate dehydrogenase (Bertsch and Müller, 2015a), which is associated with a [Fe-Fe] hydrogenase (Schuchmann and Müller, 2013). Additionally, bifurcational [Fe-Fe] hydrogenases present in *A. woodii* can be a bottleneck in utilisation of CO (figure 3A). In the presence of formate, CO-inhibited enzymes are expected not to be required, facilitating the use of CO as a substrate (figure 3B).

Unlike *M. thermoacetica*, which contains an EcH, RnF-utilizing acetogens cannot directly couple ferredoxin oxidation to proton reduction. Therefore, to prevent a completely reduced state of the cell, RnF-containing acetogens need to stoichiometrically couple CO oxidation to the Wood-Ljungdahl pathway. When compared to hydrogenotrophic acetogenesis, acetogenic growth on CO often leads to the formation of additional alcohols, hydrogen or fatty acids. These by-products are likely formed due to the more strongly reduced environment created by CO. An example is the CO metabolism of *E. limosum*, which produced solely acetate when grown on H_2/CO_2, but generates a mixture of acetate and butyrate when grown on CO (Jeong et al., 2015). The best studied pathway for maintaining redox balance during acetogenic growth on CO is solventogenesis. The model organism for this type of fermentation is *Clostridium ljungdahlii*, which is known for its fast growth rate and solventogenic production characteristics on CO (Köpke et al., 2010). In contrast to *A. woodii* and *M. thermoacetica*, the enzymes from the Wood-Ljungdahl pathway in *C. ljungdahlii* have not been purified and tested for cofactor specificity. Therefore, the proposed metabolism of *C. ljungdahlii* on H_2/CO_2 was partly based on genomic data (Schuchmann and Müller, 2014). The proposed metabolism on H_2 is to yield a minimum of 0.13 ATP per acetate formed, and can go up to 0.63 ATP per acetate, depending on which cofactors are utilized in each of the steps. Based on the assumptions of the minimal H_2 metabolism, a model for CO driven acetogenic growth can be proposed for *C. ljungdahlii*, and related bacteria (figure 4). The model shows a yield of about 1.125 ATP per acetate formed (figure 4), which is further reduced when formation of side products is taken into account. Despite the fact that the energy yield per acetate formed is less as proposed for *M. thermoacetica*, the generation time of *C. ljungdahlii* is shorter. Two mechanisms might contribute to this

enhanced growth rate: a bifurcational formate dehydrogenase, and the up-regulation of re-oxidizing reactions. A related bacterium, *Clostridium autoethanogenum*, was found to highly express a formate dehydrogenase associated with a [Fe-Fe]-bifurcating hydrogenase. This formate dehydrogenase is suggested to use one mole of NADPH and one mole of ferredoxin to reduce two moles of CO_2 to formate (Wang et al., 2013). Despite the sensitivity of [Fe-Fe]-hydrogenases to CO, levels in the cell are assumed to be kept low enough for the hydrogenase to function. The utilization of both NADPH and ferredoxin results in re-oxidation of these two important cofactors, and prevents over-reduction of the cell. However, loss of ferredoxin in re-oxidizing reactions reduces its capacity to act as a driving force for cation export via the RnF complex, lowering the energy yield of the overall metabolism. *C. ljungdahlii* codes for a similar formate dehydrogenase complex in its genome, and might thus utilize a similar system during growth on CO. Additionally, solventogenic reactions play a role in maintaining redox balance. Ethanol production in *C. ljungdahlii* occurs via two pathways: a direct or an indirect pathway (Köpke et al., 2010, 2011a). The direct pathway forms ethanol via acetaldehyde directly from acetyl-CoA, utilizing an acetaldehyde/alcohol dehydrogenase complex. This pathway is expected to largely reduce the overall energy yield as no ATP is generated via acetate formation. The indirect pathway does not omit the ADP phosphorylation step, maintaining the energy conservation via acetate synthesis. Acetate is theorised to subsequently be reduced with ferredoxin to acetaldehyde via an aldehyde oxidoreductase. This enzyme was shown to be expressed in CO grown *C. ljungdahlii*, and its expression is stimulated by the addition of external acids (Xie et al., 2015). Ethanol is subsequently formed from acetaldehyde via an alcohol dehydrogenase, utilizing additional reducing equivalents such as NADH or NADPH (Köpke et al., 2010). Energy conservation linked to ethanol formation from H_2/CO_2 in *C. autoethanogenum* is also expected to run via this indirect pathway (Mock et al., 2015). Additionally, a similar pathway could be responsible for conversion of different carboxylic acids into alcohols, as observed in mixed cultures exposed to syngas (Liu et al., 2014a).

As the suggested energy yield per acetate formed from CO for *C. ljungdahlii* is 1.125 ATP (figure 4), 0.125 ATP is generated up to acetyl-CoA formation. This suggests net energy can be yielded by this organism from any product formed from acetyl-CoA which does not require further investment of ATP. This could include compounds such as C4-carboxylic acids, lactate, fatty acids and a variety of alcohols, which are considered interesting end products of bio-based processes (Dürre and Eikmanns, 2015).

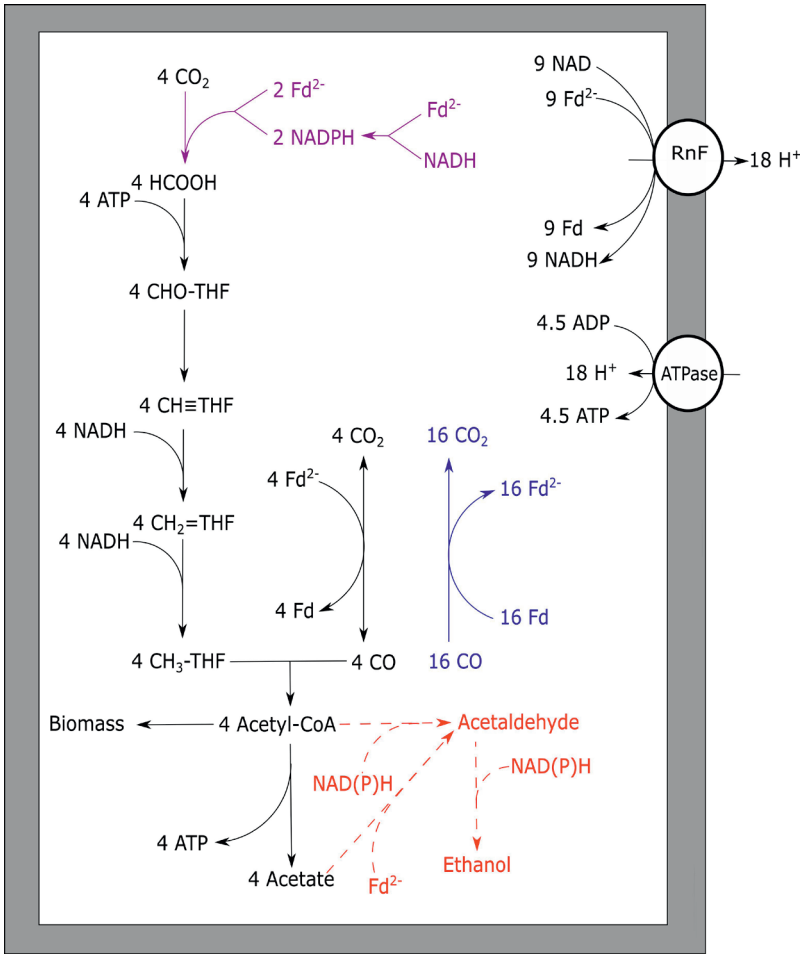

Figure 4. Carbon monoxide metabolism of *C. ljungdahlii.* Stoichiometric conversion of CO to acetate for *C. ljungdahlii* is displayed. The pathways of ethanol formation are indicated by the dotted line in red, and are not taken into account for the energy yield displayed. Reactions marked blue indicate CO oxidizing activity by CODH, bifurcating reactions are marked purple. The RnF complex is assumed to transport two protons per Fd oxidized whereas the ATPase is assumed to generate one ATP per four protons translocated. Rnf, RnF complex; ATPase, ATP synthase; Fd, ferredoxin; THF, tetrahydrofolate.

Carboxydotrophic methanogenic metabolism

Methane can be formed anaerobically from different substrates, such as H_2/CO_2, formate, methanol, acetate or methylamines. The physiology and bioenergetics of different types of methanogenic metabolism have been reviewed before (Thauer et al., 2008). CO is a less studied substrate of methanogenesis, and was first reported in 1931 (Fischer et al., 1931). It has thereafter been shown to be utilized in the

Table 4. Methanogenic archaea capable of metabolizing CO. Not determined parameters are marked N.D.

Species	Native physiology	Experimental procedure used	Inhibitory levels[A]	Products from CO	Generation time on CO, hr	References
Mesophilic						
Methanobrevibacter arboriphilicus	Hydrogenotrophic	Enzyme assay	N.D.	N.D.	N.D.	(Hammel et al., 1984)
Methanosarcina acetivorans C2A	Aceticlastic	Cultivation/Enzyme assay	>150 kPa	Methane, acetate, formate	~20	(Oelgeschläger and Rother, 2009; Rother and Metcalf, 2004)
Methanosarcina barkeri	Aceticlastic	Cultivation/Enzyme assay	>100 kPa	Hydrogen, Methane	~65	(Bott et al., 1986; O'Brien et al., 1984)
Methanobacterium formicicum	Hydrogenotrophic	Cultivation	N.D.	N.D.	No growth	(Kluyver and Schnellen, 1947)
Methanosaeta concillii	Aceticlastic	Enzyme assay	N.D.	N.D.	No growth	(Jetten et al., 1989)
Thermophilic						
Methanothermobacter thermoautotrophicus	Hydrogenotrophic	Cultivation/Enzyme assay	50 kPa	Methane, hydrogen	~200	(Daniels et al., 1977; Wasserfallen et al., 2000)
Methanosarcina thermophila	Aceticlastic	Cultivation	>2 kPa	Hydrogen, Methane	N.D.	(Zinder and Anguish, 1992)
Methanothrix sp. Strain CALS-1	Aceticlastic	Cultivation	<2 kPa	Methane	No growth	(Zinder and Anguish, 1992)
Archaeoglobus fulgidus[B]	Sulphate reducer	Cultivation	>136 kPa	Acetate, formate	~10	(Henstra et al., 2007a)

[A] Forward arrows (>) indicate inhibitory levels have not been reached, numbers displayed are the maximal level tested. Reverse arrows (<) indicate the tested level was the highest tested and the inhibitory concentration lies below this level.

[B] *A. fulgidus* is not capable of generating methane, but is displayed here due to its capacity to generate acetate and formate from CO, like *M. acetivorans*.

metabolism of several methanogenic strains (table 4). Methanogenic growth on CO as sole substrate appears not to be very efficient, as only three species have been reported to grow while producing methane: *Methanobacterium thermoautotrophicus, Methanosarcina acetivorans* and *Methanosarcina barkeri*. To gain insight in CO utilization by different groups of methanogens, two main types of methanogenic metabolism are of interest: hydrogenotrophic and aceticlastic methanogenesis. CO is an intermediate in both types of methanogenic metabolism: playing a role in anabolism or catabolism of acetyl-CoA. It is therefore not surprising that genes coding for CODH in methanogens are mainly located in the genome as neighbour of an ACS (Techtmann et al., 2012). Some methanogens do however possess more than one CODH, which are not all associated with an ACS complex. Examples are *Methanothermobacter marburgensis* and *Methanococcus jannaschii*. *M. jannaschii* has a CODH which is in located the same operon as a hydrogenase, suggesting that hydrogenogenic carboxydotrophic metabolism is possible. However, many methanogenic strains have never been tested for utilization of CO as a substrate, and their growth potential on CO is therefore unknown. Unlike in many bacteria, the routes for electron transfer from CODH to the rest of the metabolism are not well established for archaea. In general, "ferredoxin-like" proteins are proposed as the acceptor molecules for CODH complexes. This is confirmed for some methanogens, such as *Methanosarcina thermophila* (Abbanat and Ferry, 1991; Terlesky and Ferry, 1988) and *Methanosarcina barkeri* (Fischer and Thauer, 1990), which require ferredoxin to perform CO-dependent reactions. However, cell-free extract of *M. thermoautotrophicus* exhibited F420-reducing activity in presence of CO, while ferredoxin of *Clostridium pasteurianum* was not reduced (Daniels et al., 1977). F420 was also observed to be reduced by purified CODH from *Methanosaeta concilii*, indicating potential ability of this enzyme to reduce this cofactor (Jetten et al., 1989). However, ferredoxin was not tested as acceptor for the CODH complex of *M. concilii*, and thus cannot be excluded as acceptor. When assuming E = -500 mV for ferredoxin under physiological conditions (Buckel and Thauer, 2013), it can be expected that ferredoxin is an ideal acceptor for electrons from CO (E_0 = -520 mV). Transfer of electrons to F420 (E_0 = -380 mV) would result in additional energy loss, and would require bifurcation processes to generate reduced ferredoxin. Ferredoxins have in general been shown to be interchangeable over long phylogenetic ranges, as indicated by the similar characteristics of plant and bacterial ferredoxins (Tagawa and Arnon, 1968). However, ferredoxin from spinach did not form a complex with the CODH of *M. thermoacetica* and was not reduced by this bacterial CODH (Drake et al., 1980; Shanmugasundaram and Wood, 1992). Additionally, the observation that the CODH from *R. rubrum* could only effectively donate electrons to the tightly associated CooF complex (Ensign and Ludden, 1991), suggests not all ferredoxins are

efficient in receiving in electrons from a CODH complex. Therefore, the observation that some archaeal CODHs do not transfer electrons to non-native ferredoxin might be related to a difference in characteristics, such as structure and location of the special nickel-iron-sulphur clusters present in the CODH and the possibly different mid-point redox potentials of the ferredoxin.

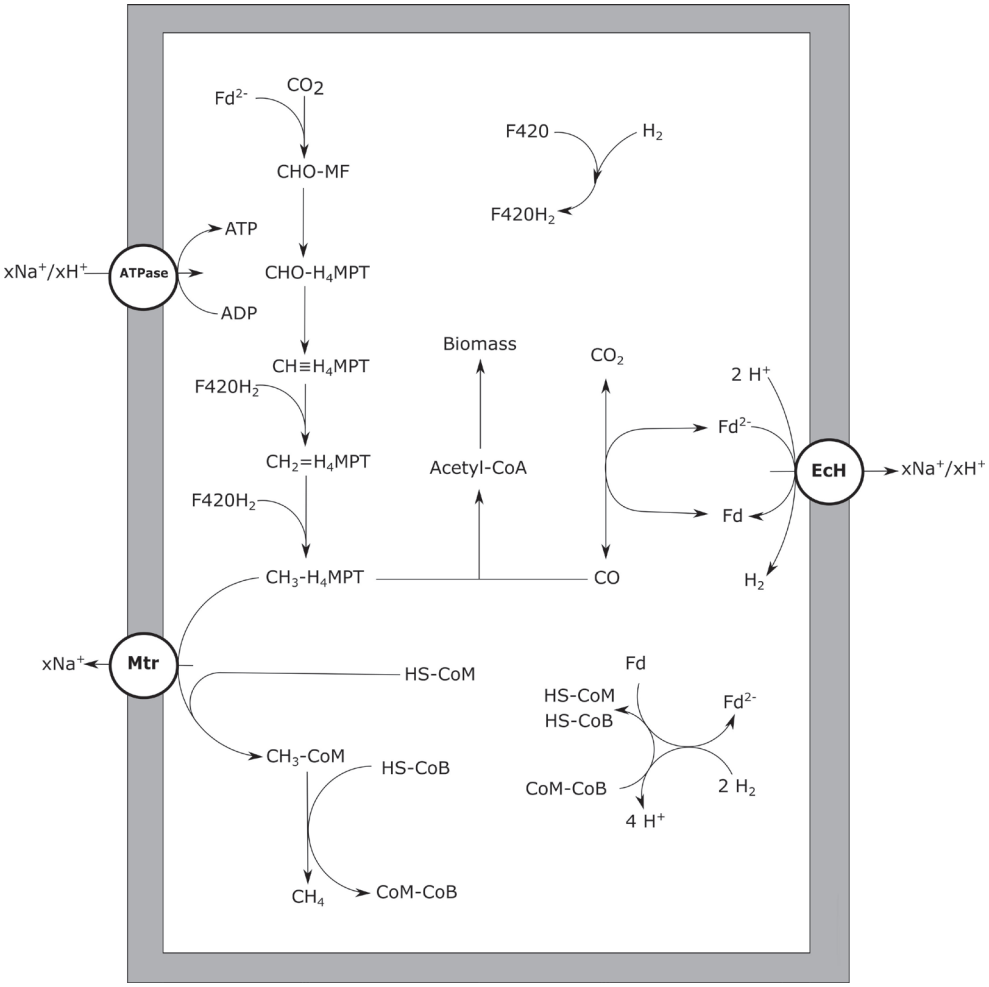

Figure 5. Carbon monoxide metabolism of hydrogenotrophic methanogens. CO driven methanogenesis with hydrogen as an intermediate is displayed. xH^+ or xNa^+ indicate translocation of an undefined number of protons or sodium ions respectively. Reactions are not displayed stoichiometrically. EcH, energy converting hydrogenase; Mtr, methyl-H4MPT:HS-CoM methyltransferase; ATPase, ATP synthase; Fd, ferredoxin; MF, methanofuran; H4MPT, tetrahydromethanopterin; HS-CoM, coenzyme M; HS-CoB, coenzyme B.

In autotrophic, hydrogen-utilizing methanogens, CO is an intermediate of the anabolic reductive acetyl-CoA pathway, a pathway functionally similar to the Wood-Ljungdahl pathway in bacteria (Berg et al., 2010). The archaeal CODH required for growth is a nickel-dependent enzyme, just as observed in bacteria (Hammel et al., 1984). For CO to be utilized as energy source by methanogens, a CODH has to be present that can function in the CO oxidizing direction, and suitable cofactors for electron transfer to the methanogenic metabolism should be available. Thermophilic *Methanothermobacter thermoautotrophicus* is capable of growing on CO, but slowly; at CO pressures up to 50 kPa at a rate of 1% compared to its growth rate on H_2/CO_2 (Daniels et al., 1977). The genome of *M. thermoautotrophicus* (Smith et al., 1997) codes for a single CODH enzyme with ACS as a neighbouring gene, which are used for anabolism during growth on hydrogen (Stupperich et al., 1983). Growing *M. thermoautotrophicus* on CO as sole electron donor, results in methane formation and small amounts of H_2, suggesting hydrogen is an intermediate or side product of the metabolism. In hydrogenotrophic methanogens an EcH is present, which is involved in the reduction of ferredoxin with H_2, driven by a proton gradient (Thauer et al., 2010). Generation of reduced ferredoxin by CODH allows for the reverse reaction to take place, generating a proton gradient. This additionally results in the formation of hydrogen, which subsequently can be used for reduction of CO_2 to methane (figure 5). Metabolic activity using CO, with H_2 as intermediate, is also observed in *Methanosarcina barkeri* (Fischer and Thauer, 1990) and *Methanosarcina thermophila* (Terlesky and Ferry, 1988; Zinder and Anguish, 1992). Experiments with cell extracts and washed cells of *M. thermophila* show increased hydrogenogenic activity upon exposure to CO (Zinder and Anguish, 1992). When growing *M. thermophila* on acetate, hydrogen production was detected besides methane formation, suggesting coupling of CO oxidation to proton reduction (Terlesky and Ferry, 1988). *M. barkeri* also has the capability of oxidizing CO coupled to formation of hydrogen, resulting in the formation of a proton gradient (Bott and Thauer, 1989). Upon addition of methanogenic inhibitors, cell suspensions of *M. barkeri* were still capable of utilizing CO, producing hydrogen and additionally resulting in formation of ATP (Bott et al., 1986). If a hydrogenogenic metabolism can sustain growth in *M. barkeri* is unclear. Without methanogenic inhibitors, the formed hydrogen is further oxidized to form methane, allowing for growth (O'Brien et al., 1984). Judging from the carboxydotrophic generation time of *M. barkeri* (~65h) and *M. thermoautotrophicus* (~200h), the methanogenic metabolism on CO is not very efficient. For both strains, hydrogen accumulation is observed during methanogenic carboxydotrophic growth (Daniels et al., 1977; O'Brien et al., 1984). This suggests hydrogenases, required for the formation of methane from the intermediately formed hydrogen, are inhibited by CO. The involved hydrogenases, such as the heterodisulfide

reductase-associated hydrogenase and the F420-reducing hydrogenase, are of the [Ni-Fe] type (Thauer et al., 2010) and can be expected to be relatively resistant, but not insensitive, to CO (De Lacey et al., 2007). Additionally, *M. thermoautotrophicus* contains an iron-dependent methylenetetrahydromethanopterin dehydrogenase, which is involved in the conversion of methenyltetrahydromethanopterin to methylenetetrahydromethanopterin directly using hydrogen as a donor (Zirngibl et al., 1990). This hydrogenase is found in several hydrogenotrophic methanogens, and is mainly expressed under nickel-deprived conditions (Afting et al., 1998, 2000). The enzyme is susceptible to CO (Lyon et al., 2004) and is therefore a potential target for inhibition during carboxydotrophic growth. Despite the indication that hydrogenases are a limiting factor for carboxydotrophic methanogenesis, inhibition of other enzymes by CO cannot be ruled out as only limited information is available on the mechanisms of CO toxicity in methanogens.

During aceticlastic methanogenesis, CO is an intermediate originating from the splitting of acetyl-CoA by the CODH/ACS complex (Grahame, 2003). Subsequently, CODH is used to further oxidize CO and provide electrons for reduction of the methyl-group to methane. Methanogenic bioreactors fed with acetate accumulated CO to levels up to 0.25Pa, likely resulting from its role as intermediate in aceticlastic methanogenesis (Hickey and Switzenbaum, 1990). Obligate aceticlastic methanogens such as Methanothrix sp. strain CALS-1, were observed to accumulate CO to low partial pressures while metabolizing acetate (Zinder and Anguish, 1992). Upon addition of low amounts of CO, it was consumed till equilibrium levels of 0.16 Pa. Addition of CO to levels of 2 kPa caused inhibition of growth on acetate. Obligate aceticlastic methanogens are devoid of hydrogenases (Deppenmeier et al., 1996; Smith and Ingram-Smith, 2007). This makes it unlikely that inhibition of hydrogenases results in CO toxicity for these methanogens. However, in contrast to EcH containing methanogens, the electrons released from CO oxidation cannot be coupled to proton reduction, requiring other pathways to re-oxidize formed reduction equivalents. The methyl-branch of the reductive acetyl-CoA pathway could theoretically fulfil this role, as the genes are present in the genome of aceticlastic Methanosaeta/Methanothrix species (Zhu et al., 2012). All of these organisms however, lack the ability to grow on H_2/CO_2 or formate (Thauer et al., 2008), suggesting no activity of this pathway in the CO_2-reducing direction. The genes of the methyl-branch coded for in these species are phylogenetically similar to genes present in methylotrophic methanogens, which use this branch in the oxidative direction, in order to generate reduction equivalents for biosynthesis (Zhu et al., 2012). This is further supported by C13 labelling studies in *Methanosaeta harundinacea* which confirms activity in the oxidizing but not in the reducing direction (Zhu et al., 2012). This suggests the methyl-branch of the reductive acetyl-CoA pathway in aceticlastic methanogens is not optimal for re-

oxidation of reduced cofactors, as is suggested for hydrogenotrophic methanogens (figure 5). When exposed to elevated levels of CO this could result in an over-reduced state of the cell, making it difficult for obligate aceticlastic methanogens to utilize it as a substrate.

The only methanogen which appears to deal quite well with CO is *Methanosarcina acetivorans*, which was initially isolated from marine sediments (Sowers et al., 1984). In addition to methane, acetate and formate were observed to be the main end products from CO (Rother and Metcalf, 2004). Additionally, *M. acetivorans* was found to produce methylated-thiols from CO (Oelgeschläger and Rother, 2009). The *M. acetivorans* genome codes for two isoforms of CODH/ACS, Cdh1 and Cdh2, which are both considered to be functional in acetyl-CoA anabolism and catabolism (Matschiavelli et al., 2012). The expression levels of the two isoforms are theorised to be regulated on transcriptional and posttranscriptional level by a CdhA subunit (CdhA3), which is suggested to act as a CO sensor (Matschiavelli et al., 2012). In addition to the CODH/ACS complex, two monofunctional CODH, CooS1F and CooS2, were found to assist in removal of the CO at high CO partial pressures (Rother et al., 2007). For *M. acetivorans* no hydrogen formation is observed during growth on CO, which is supported by the fact that it is devoid of any significant hydrogen metabolism (Sowers et al., 1984). Despite the inability of *M. acetivorans* to grow on H_2/CO_2, its genome codes for homologs of the methyl-branch of the reductive acetyl-CoA pathway (Galagan et al., 2002). Proteomic analysis shows that these genes are more abundantly expressed during CO-dependent growth when compared to growth on acetate or methanol (Lessner et al., 2006). This suggests that, in contrast to what is proposed for Methanosaeta/Methanotrix species, *M. acetivorans* uses the methyl-branch of the reductive acetyl-CoA pathway to regenerate its reduction equivalents. However, due to its lack of hydrogenases it is unclear how the organism couples oxidation of CO to reduction of F420, which is required to operate this pathway. *M. acetivorans* was shown to express a sodium dependent "RnF-like" complex when metabolizing acetate (Li et al., 2007; Schlegel et al., 2012). It is speculated that this RnF complex couples ferredoxin oxidation to reduction of methanophenazine, subsequently passing on the electrons to the heterodisulfide reductase (Hdr) complex, involved in HS-CoM/HS-CoB regeneration (Li et al., 2007) (figure 6). Proteomic data of *M. acetivorans* show that in cells grown on CO the F420-oxidizing:Fpo complex is relatively more abundant, which suggests a role in CO metabolism (Lessner et al., 2006). This protein complex possibly operates in combination with the RnF complex, to catalyse ferredoxin-dependent F420 reduction (Lessner et al., 2006) (figure 6). An alternative for coupling ferredoxin oxidation to F420 reduction is via a subunit from the Fpo complex which partly resides in the cytoplasm: FpoF. This subunit was found to catalyse ferredoxin:F420 reduction in EcH knockout mutants

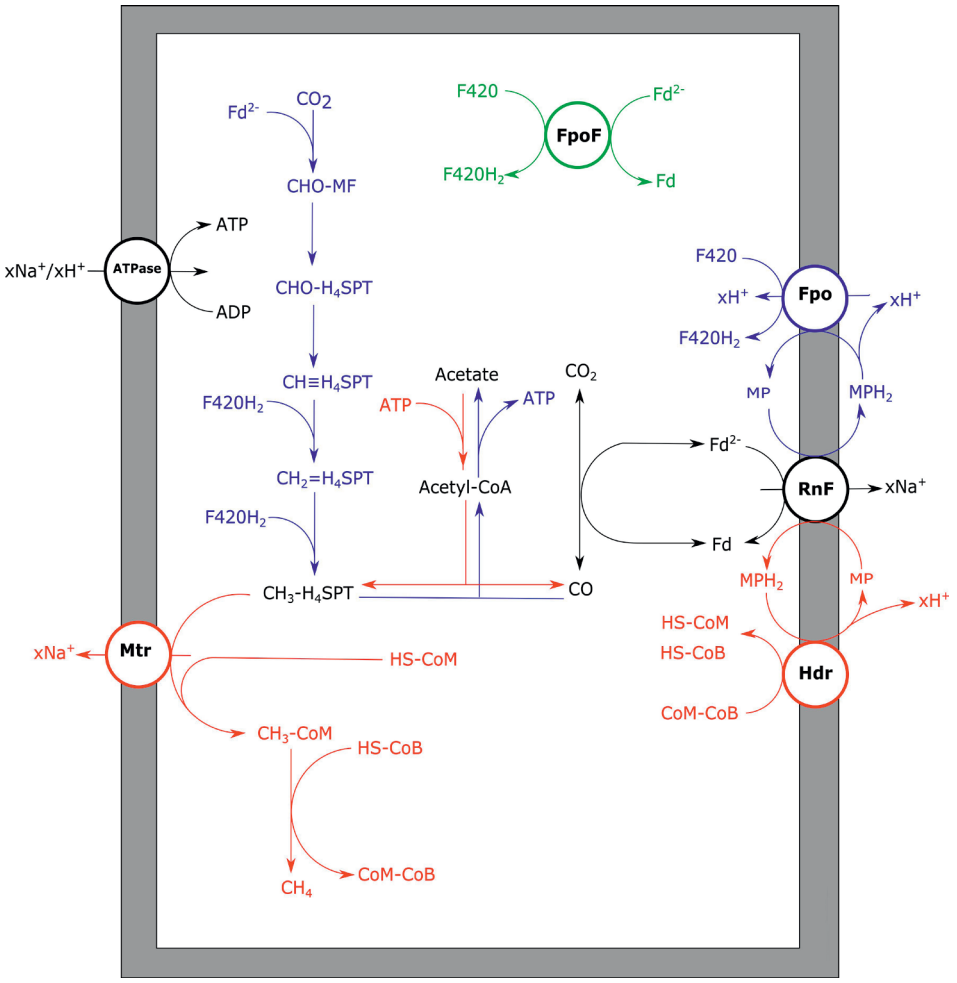

Figure 6. Aceticlastic and carboxydotrophic metabolism of *M. acetivorans*. Aceticlastic methanogenic pathway proposed for *M. acetivorans* (red) and carboxydotrophic pathway proposed for *M. acetivorans* (blue). For carboxydotrophic growth either RnF/Fpo (blue) or FpoF (green) are proposed to generate reduced F420 from ferredoxin. xH^+ or xNa^+ indicate translocation of an undefined number of protons or sodium ions respectively. RnF, RnF-like complex; ATPase, ATP synthase; Mtr, methyl-H4SPT:HS-CoM methyltransferase; Fpo, F420 dehydrogenase complex; FpoF, F420 dehydrogenase subunit F; Hdr, heterodisulfide reductase; Fd, ferredoxin; MF, methanofuran; H4SPT, tetrahydrosarcinapterin; HS-CoM, coenzyme M; HS-CoB, coenzyme B

of *Methanosarcina mazei*, whereas knockout mutants of the FpoF subunit did not show this activity (Welte and Deppenmeier, 2011). Despite the lack of genes coding for formate dehydrogenases in the genome of *M. activorans* (Galagan et al., 2002), formate is produced in addition to acetate and methane during carboxydotrophic growth. Formate is suggested to originate from activity of formyl-methanofuran dehydrogenase and is theorized to act as a redox exhaust of the cell during CO driven growth (Matschiavelli and Rother, 2015).

M. acetivorans is not the only archaeon producing acetate and formate from CO, as also the hyperthermophilic, sulphate-reducing *Archaeoglobus fulgidus* generates these products during carboxydotrophic growth in absence of sulphate. In *A. fulgidus* however, both the RnF and EcH complexes are not coded for in the genome (Hocking et al., 2014). A FpoF homolog, FqoF, is encoded for in the genome of *A. fulgidus* (Brüggemann et al., 2000), which could take part in the coupling of ferredoxin oxidation to F420 reduction. The absence of an EcH complex poses also a question for the redox balance of the organism, as hydrogen cannot be used as a redox exhaust. It is possible that formate is formed in a similar way as theorized for *M. acetivorans,* but it can also be formed via F420-dependent formate dehydrogenases, allowing favourable redox balance during growth.

Comparison and application of fermentative carboxydotrophic metabolism

Comparing the three main variants of fermentative CO metabolism, it is obvious that similar sets of enzymes and pathways are used. Hydrogenogenic microorganisms seem to be the most efficient CO-utilizers due to their relatively simple and "redox-closed" energy metabolism. This allows the water-gas shift mechanism to operate at a rate independent of the rest of the metabolism, minimizing metabolic stress. To maximize the energetic yield on CO, a methanogenic or acetogenic microorganism would first have to perform hydrogenogenesis, conserving energy via an EcH complex, subsequently gaining energy from the use of hydrogen for methanogenesis or acetogenesis. Hydrogenotrophic methanogens and acetogens like *M. thermoacetica* seem to make use of this strategy, maximizing the ATP yield per CO utilized. However, despite these optimized energy yields, these organisms have no outstanding growth performance on CO. This is likely related to the CO sensitivity of hydrogenases, essential for this type of metabolism. Acetogens which employ RnF complexes, seem less prone to inhibition by CO, but need to couple CO oxidation stoichiometrically to the Wood-Ljungdahl pathway in order to prevent an over-reduced state of the cell. In relatively fast growing acetogenic bacteria, this is prevented by utilizing alternative pathways to re-oxidize cofactors faster. Loss of "energy-rich" reduction equivalents in these re-oxidizing reactions lowers the overall energy yield of the cell. However, this is expected to allow for better maintenance of redox balance, resulting in reduced stress for the overall metabolism. Still net energy

is assumed to be conserved by CO-utilizing acetogens, such as *C. ljungdahlii*, during acetyl-CoA formation. This suggests a large and diverse range of products can be formed from carboxydotrophic metabolism, making it interesting for future research and bio-based applications.

Chapter 3

Proteomic analysis of the hydrogen and carbon monoxide metabolism of *Methanothermobacter marburgensis*

Authors: Martijn Diender, Ricardo Pereira, Hans J.C.T. Wessels, Alfons J.M. Stams & Diana Z. Sousa

Chapter has been published as:

Diender, M., Pereira, R., Wessels, H. J. C. T., Stams, A. J. M., and Sousa, D. Z. (2016). Proteomic Analysis of the Hydrogen and Carbon Monoxide Metabolism of *Methanothermobacter marburgensis*. Front. Microbiol. 7. doi:10.3389/fmicb.2016.01049.

Abstract

Hydrogenotrophic methanogenic archaea are efficient H_2 utilizers, but only a few are known to be able to utilize CO. *Methanothermobacter thermoautotrophicus* is one of the hydrogenotrophic methanogens able to grow on CO, albeit about 100 times slower than on H_2 + CO_2. In this study we show that the hydrogenotrophic methanogen *Methanothermobacter marburgensis*, is able to perform methanogenic growth on H_2/CO_2/CO and on CO as a sole substrate. To gain further insight in its carboxydotrophic metabolism, the proteome of *M. marburgensis,* grown on H_2/CO_2 and H_2/CO_2/CO, was analysed. Cultures grown with H_2/CO_2/CO showed relative higher abundance of enzymes involved in the reductive acetyl-CoA pathway and proteins involved in redox metabolism. The data suggest that the strong reducing capacity of CO negatively affects hydrogenotrophic methanogenesis, making growth on CO as a sole substrate difficult for this type of methanogens. *M. marburgensis* appears to partly deal with this by upregulating co-factor regenerating reactions and activating additional pathways allowing for formation of other products, like acetate.

Introduction

Methanogenesis from hydrogen, acetate, methanol or methanethiols is a relatively well-studied process (Thauer et al., 2008). In 1931, CO was shown to potentially act as a substrate for methanogens in mixed cultures (Fischer et al., 1931), but knowledge of carboxydotrophic methanogenesis is still rather limited. Gaining insight in CO-driven methanogenesis is not only of interest from a fundamental point of view, but also from an applied scope. The rapid development of syngas technology makes it cheaper to convert any carbon rich source into a gaseous mixture, consisting mainly of CO, H_2 and CO_2 (syngas). Syngas-driven carboxydotrophic methanogenesis can be considered as an alternative to biogas production via anaerobic digestion. About 10-25% of the biomass consists of lignin, which is difficult to degrade biologically and can even prevent degradation of easily degradable biopolymers such as hemicellulose (Daniell et al., 2012; Jönsson and Martín, 2016). Additionally, biomass-derived biogas contains a fraction of 25-45% CO_2 (de Mes et al., 2003) and needs to be subsequently upgraded to bio-methane before injection in the gas grid is possible. Via the syngas route a higher substrate conversion yield can be achieved, and by increasing the H_2 content of the gas substrate a CO_2-free end product can be obtained in one process step.

Carbon monoxide appears to be a difficult substrate for methanogens, and only three methanogens have been shown to utilize it for growth: *Methanothermobacter thermoautotrophicus* (Daniels et al., 1977), *Methanosarina barkeri* (Bott et al., 1986; O'Brien et al., 1984) and *Methanosarcina acetivorans* (Rother and Metcalf, 2004). Carboxydotrophic growth of *M. thermoautotrophicus* is possible with CO as a sole

carbon source up to pressures of 50 kPa. Doubling times reported for CO-grown *M. thermoautotrophicus* are about 200 hours, which is about a 100 times slower than with H_2/CO_2 (Daniels et al., 1977). *M. barkeri* was observed to utilize 100 kPa CO, but also at a relatively slow doubling time (about 65 hours) compared to growth on other substrates (O'Brien et al., 1984). *Methanosarcina acetivorans* can withstand higher CO partial pressures (>150 kPa) and grows on CO with a doubling time of about 20 hours. However, it shifts its methanogenic metabolism towards formation of acetate and formate with increasing CO pressures (Rother and Metcalf, 2004). Detailed research has been performed on the CO metabolism of *M. acetivorans* (Lessner et al., 2006; Matschiavelli et al., 2012; Rother et al., 2007; Rother and Metcalf, 2004), providing more insight in the enzymes involved in carboxydotrophic metabolism of this aceticlastic methanogen. Currently, *M. thermoautotrophicus* is the only hydrogenotrophic methanogen known that can grow on CO as a substrate, and there is limited knowledge on the carboxydotrophic metabolism of hydrogenotrophic methanogens in general. Carboxydotrophic methanogenesis is expected to be operated in a similar way as hydrogenotrophic metabolism (Daniels et al., 1977;Diender et al., 2015, **Chapter 2**). Electrons derived from the oxidation of CO or H_2 are used to reduce CO_2 to methyl-tetrahydromethanopterin (methyl-H4MPT). This key-intermediate can subsequently be converted into either methane, for energy generation, or assimilated via acetyl-CoA, for biomass production.

In this study we aimed to assess the CO-metabolism of *Methanothermobacter marburgensis*. *M. marburgensis* has a highly similar CODH sequence to that of *M. thermoautotrophicus* (93% identity). Additionally, it was shown that the methyl-coenzyme M reductase (MCR) of *M. marburgensis* was activated 15 times faster by CO than by H_2 (Zhou et al., 2013). Here we show that *M. marburgensis* can grow methanogenically on CO and we assessed its carboxydotrophic metabolism via physiological analysis and proteomics. Additionally, we evaluated the limitations of this type of metabolism, which is theorised to be related to hydrogenase inhibition or redox-stress (Diender et al., 2015, **Chapter 2**).

Material and methods

Strains and cultivation

Strains *M. thermoautotrophicus* (DSM 1053) and *M. marburgensis* (DSM 2133) were obtained from the German Collection of Microorganisms and Cell Cultures (DSMZ) (Braunschweig, Germany). Strains were initially cultivated at 65 °C on recommended Methanobacterium medium (DSM-119) using anaerobic cultivation procedures. After growth was confirmed, the strains were adapted to growth in a carbonate-phosphate buffered medium with the following composition per liter: 0.4 g KH_2PO_4, 0.53 g K_2HPO_2* 2 H_2O, 0.3 g NH_4Cl, 0.3 g NaCl, 0.1 g $MgCl_2$*6 H_2O, 0.5

g yeast extract, and 0.5 mg resazurin. Medium was supplemented, per liter, with 61.8 µg H_3BO_3, 61.25 µg $MnCl_2$, 943.5 µg $FeCl_2$, 64.5 µg $CoCl_2$, 12.86 µg $NiCl_2$, 67.7 µg $ZnCl_2$, 13.35 µg $CuCl_2$, 17.3 µg Na_2SeO_3, 29.4 µg Na_2WO_4 and 20.5 µg Na_2MoO_4. Medium was prepared, boiled and cooled under a continuous nitrogen flow. Bottles (120 ml total volume, 50 ml liquid) were filled with medium and instantly capped with rubber stopper and aluminium cap. The gas phase was exchanged with either 80:20 N_2/CO_2 or 80:20 H_2/CO_2, resulting in a final pressure of 170 kPa. When necessary, the headspace was further fine-tuned by addition of CO, keeping final pressure at 170 kPa. The bottles were autoclaved and stored at room temperature till further use. Before inoculation medium was supplied with the following volumes of stock solutions: 1% of 11 g $CaCl_2$*2 H_2O per liter, 1% of a vitamin solution containing per liter: biotin 20 mg, nicotinamid 200 mg, p-aminobenzoic acid 100 mg, thiamin 200 mg, panthotenic acid 100 mg, pyridoxamine 500 mg, cyanocobalamine 100 mg, riboflavine 100 mg. The medium was reduced by introducing a 5% volume of a stock solution containing 4.8 g Na_2S * x H_2O (x = 7-9) and 80 g NaHCO3 per liter. Unless stated otherwise, bottles were inoculated with an exponentially growing culture in a 1:50 ratio (v/v).

Analytical procedures

Headspace composition was determined by gas chromatography using a GC-2014 (Shimadzu, Kyoto, Japan) equipped with a thermal conductivity detector. H_2, CH_4 and CO were measured with a Molsieve 13X column, 2 m long and an inner diameter of 3mm. Argon was used as carrier gas at a flow rate of 50 ml/min. Injector, column and detector temperatures were set to 80, 60 and 130°C, respectively. CO_2 was measured separately in a CP Poraplot column of 25 m x 0.53 mm, with a stationary phase film thickness of 20 µm, employing helium as carrier gas at a flow rate of 15 ml/min. Injector, column and detector temperatures were set to 60, 34 and 130°C, respectively. The detection limits for H_2, CO, CO_2 and CH_4 were 20, 250, 20 and 80 Pa, respectively.

Liquid phase composition was analysed via high pressure liquid chromatography equipped with a MetaCarb 67H column (Agilent Technologies, Santa Clara, CA). The column was operated at a temperature of 45 °C with a flow rate of 0.8 ml/min using 0.01 N H_2SO_4 as eluent. Detection of acetate was done using an RI and UV detector. Concentrations of 0.5 mM could be accurately determined and lower levels are referred to as trace amounts.

Cell free extract preparation and measuring CO-oxidation activity

Cells of *M. marburgensis* were grown on either 80:20 H_2/CO_2 or 60:20:20 H_2/CO_2/CO. Biological triplicates were prepared for each condition. Cells were harvested at end log-phase in an anaerobic tent, where the broth was centrifuged at 13000 g for

10 minutes. Supernatant was discarded and the pellets were dissolved in 1 ml 50 mM Tris-HCl, pH 8. Cells were disrupted using a VC-40 sonicator (Sonics materials, CT, USA) using 5 cycles of 30 seconds sonication, at a power input of 20 W, followed by 30 seconds rest at 0 °C. Cell free extract (CFE) was put in 5 ml glass vials and capped with rubber stoppers inside the anaerobic tent. Subsequently, the headspace of these vials was exchanged to 1.5 bar N_2 to remove traces of H_2.

CO-oxidation activity of the CFE was determined as follows: glass cuvettes (2 ml total volume) were closed with a rubber stopper and flushed three times by using 5 ml N_2 or CO. Subsequently, 1 ml assay buffer (50 mM MOPS, pH 7, 20mM methyl viologen (MV) and 2 mM DTT) was added to the cuvette and reduced with 1 µl of 100 mM dethionite. The cuvette was put into a pre-heated U-2010 spectrophotometer (Hitachi, Tokyo, Japan) and was left to heat up to 60 °C. Absorption of MV was measured at 578 nm. The initial extinction was set to a value between 0.2 and 0.6. After obtaining a stable baseline, 50 or 25 µl cell free extract (CFE) was added to the cuvette, initiating the reaction. Each separate biological sample was assessed for CO-oxidizing activity and endogenous activity (using N_2 instead of CO). The initial activity of CO-oxidation after CFE addition was taken, and corrected for the initial slope of the endogenous activity. In order to confirm that CO was the electron donor, cuvettes were prepared with N_2 headspace and CFE was added. After seizure of endogenous activity 0.3 ml CO was added to the sample as initiation trigger. Each biological sample was at least analysed in duplicate using either 50 µl or 25 µl CFE. An extinction coefficient 9.7 mM^{-1} cm^{-1} (Bonam and Ludden, 1987) was used for MV at 578 nm. Protein concentration in the CFE was determined by using Roti-Nanoquant protein quantitation assay (CarlRoth, Karlsruhe, Germany), according to manufacturer instructions.

Sample preparation for proteomics

Duplicate cultures of *M. marburgensis* grown in two conditions, 80:20 H_2/CO_2 and 60:20:20 $H_2/CO_2/CO$, were harvested in late exponential phase by centrifugation (cultivation was performed in 1 liter anaerobic bottles containing 500 ml medium). Prior to centrifugation cultures were quickly cooled down on ice and kept at 4°C for 30 minutes to decrease cell activity. Cell pellets were resuspended in TE buffer (10 mM Tris-HCl, pH 7.5; 1 mM EDTA) containing 1 mM phenylmethanesulfonylfluoride, and passed through a French pressure cell operated at 138 MPa. Proteins were stabilized by addition of 8 M of urea in a proportion of 1:1 and samples were concentrated using a 3.5 kDa MWCO filter. Final protein concentration in samples obtained for LC-MS/MS analysis were assessed using Qubit® Protein Assay Kit in a Qubit® 2.0 Fluorometer (Life technologies). Samples were subjected to in-solution tryptic digestion as described elsewhere (Wessels et al., 2011).

LC-MS/MS data acquisition

Protein samples obtained from the two sets of biological duplicates were analysed in duplicate using C18 reversed phase liquid chromatography with online tandem mass spectrometry (LC-MS/MS). Measurements were performed using a nanoflow ultra-high pressure liquid chromatograph (nano-Advance; Bruker Daltonics) coupled online to an orthogonal quadrupole time-of-flight mass spectrometer (maXis 4G ETD, otofControl v3.4 build 14; Bruker Daltonics) via an axial desolvation vacuum assisted electrospray ionization source (Captive sprayer; Bruker Daltonics). Five microliters of tryptic digest were loaded onto the trapping column (Acclaim PepMap 100, 75µm x 2 cm, nanoViper, 3µm 100Å C18 particles; Thermo Scientific) using 0.1% FA at a flow rate of 9000 nl/min for 3 minutes at room temperature. Next, peptides were separated on a C18 reversed phase 15 cm length x 75 µm internal diameter analytical column (Acclaim PepMap RSLC, 75µm x 15 cm, nanoViper, 2µm 100Å C18 particles; Thermo scientific) at 40 °C using a linear gradient of 3-35% ACN 0.1% FA in 120 minutes at a flow rate of 600 nl/min. The mass spectrometer was operated in positive ion mode and was tuned for optimal ion transmission in the range of m/z 300-1400. Electrospray ionization conditions were 3 l/min 180 °C N_2 drying gas, 1400V capillary voltage and 0.4 Bar N_2 for gas phase supercharging (nanobooster) using acetonitrile as dopant. Parameters for optimal ion transmission were funnel RF: 400Vpp, multipole RF: 400 Vpp, quadrupole ion energy: 5.0 eV, quadrupole low mass: 300 m/z, collision cell energy: 9.0 eV, collision cell RF: 3500 Vpp, ion cooler transfer time: 64 µs, ion cooler RF: 250 Vpp, pre-pule storage: 22 µs. Data dependent acquisition of MS/MS spectra (AutoMSn) was performed using a 3 second duty cycle at 2 Hz acquisition rate for full MS spectra and a variable number of MS/MS experiments at precursor intensity scaled spectra rate (3Hz MS/MS spectra rate at 2000 counts, 20Hz MS/MS spectra rate @ 100.000 counts). Precursor ions within the range of 400-1400 m/z with charge state $z = 2^+$ or higher (preferred charge state range of $z = 2^+$ to $z = 4^+$) were selected for MS/MS analysis with active exclusion enabled (excluded after 1 spectrum, released after 0.5min, reconsidered precursor if current intensity/previous intensity >= 4, smart exclusion disabled). Spectra were saved as line spectra only and were calculated from profile spectra as the sum of intensities across a mass spectral peak (5 counts absolute threshold, peak summation width 7 points).

Proteomics analysis

Protein identification and relative quantitation was performed using the MaxQuant software (v.1.5.0.0) (Cox and Mann, 2008) using the build-in Andromeda database search algorithm. Extracted MS/MS spectra were searched against the SWISS-PROT *Methanothermobacter marburgensis* protein sequence database. Amino acid sequences of known contaminant proteins (e.g. skin and hair proteins, Trypsin,

LysC) were added to the database. The following settings were used for peptide and protein identification: carbamidomethyl (Cys) as fixed modification, oxidation (Met) and deamidation (NQ) as variable modifications, predefined MS and MS/MS settings for TOF instruments, minimal peptide length 6 amino acids and a maximum allowed false discovery rate of 1% at both the peptide and protein level. Label free quantitation (LFQ) was performed with the match between runs and re-quantify options using at least 2 razor + unique peptides. Retention time alignment was performed with a time alignment window of 20 minutes and a retention time match window of 0.5 minutes. Label-free quantitation (LFQ) values were used for subsequent data analysis. Proteins quantified in at least 3 out of 4 measurements for either growth condition were analyzed by student T-tests to identify differentially expressed proteins with $p < 0.05$. The mass spectrometry proteomics data have been deposited to the ProteomeXchange Consortium via the PRIDE (Vizcaíno et al., 2016) partner repository with the dataset identifier PXD003661.

Results

Carboxydotrophic growth of M. thermoautotrophicus and M. marburgensis

Both, *M. thermoautotrophicus* and *M. marburgensis* were capable of growing methanogenically on $H_2/CO_2/CO$ or CO as a sole substrate. When assessing the production profiles on $H_2/CO_2/CO$, it appears that both strains co-utilize H_2 and CO (figure 1). For both strains H_2 utilization becomes slower with exposure to higher CO pressures. The maximal H_2 consumption rate of *M. marburgensis* dropped from 1.3 $mmol/l_{liquid}/h$ to 0.43 $mmol/l_{liquid}/h$ when increasing the CO pressure from 0 to 70 kPa. Similarly M. *thermoautotrophicus* decreased its maximal H_2 consumption rate from 0.55 $mmol/l_{liquid}/h$ to 0.19 $mmol/l_{liquid}/h$ when increasing the CO pressure from 0 to 70 kPa. *M. marburgensis* could be grown on CO as a sole substrate up to 50 kPa (data not shown), which is similar to the value found for *M. thermoautotrophicus* (Daniels et al., 1977).

M. marburgensis appears to utilize carbon monoxide more easily as it depletes 34 kPa CO within 120 hours, while *M. thermoautotrophicus* uses this substrate significantly slower (figure 1). This suggests that *M. marburgensis* can be better adapted to carboxydotrophic growth than *M. thermoautotrophicus*. It was attempted to adapt both strains to cultivation on purely CO by repeatedly transferring them in presence of solely CO as electron donor. The initial lag phase of *M. marburgensis* growing solely on 34 kPa CO was ~500 h, but in the two subsequent transfers the lag phase for CO conversion decreased to ~100 h (figure 2). CO consumption and methane production rates between these transfers did not change significantly (figure 2). Cultures transferred back to H_2/CO_2 quickly lost this adaptation to CO and showed again a longer lag phase when incubated with CO alone. Nevertheless, a re-

adaptation of these cultures to CO was possible. Growth of *M. thermoautotrophicus* on $H_2/CO_2/CO$ or CO as the sole substrate could not be improved via subsequent transfers, nor could the lag phase be decreased. Due to this inefficient growth of *M. thermoautotrophicus* in presence of CO it was decided to perform further analysis and proteomics solely with *M. marburgensis*.

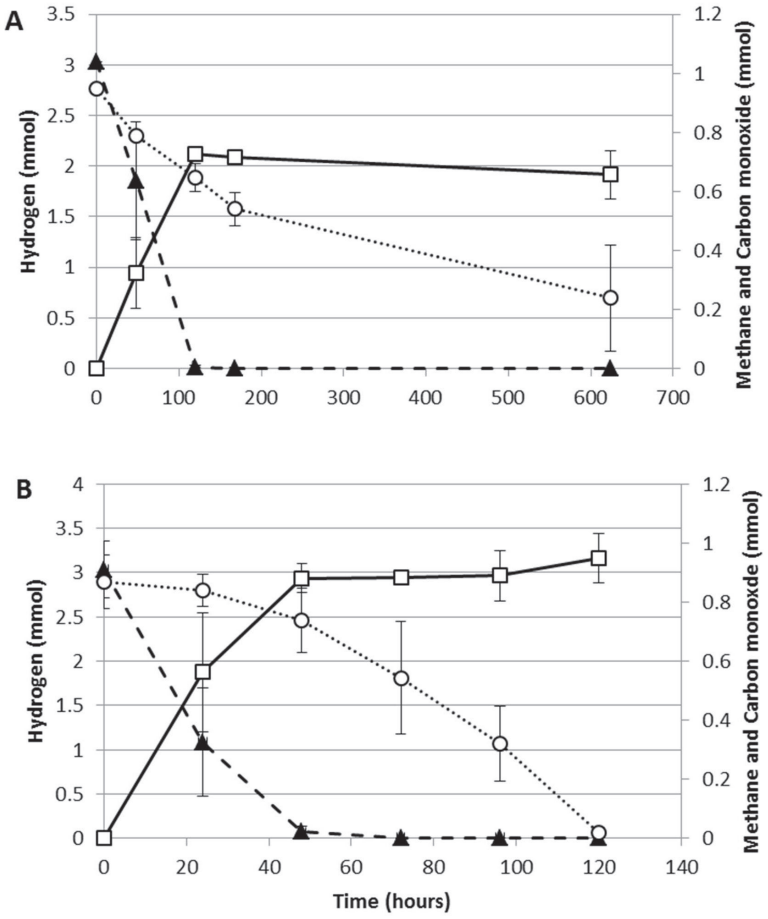

Figure 1. Production profile of hydrogenotrophic methanogens growing on $H_2/CO_2/CO$. A) production profile of *M. thermoautotrophicus* B) production profile of *M. marburgensis*. Hydrogen: solid black triangles, Methane: open black squares, Carbon monoxide: open black circles. Gas is represented as total amount of mmol present in the bottle headspace. Error bars display maximal and minimal amounts over duplicate experiments.

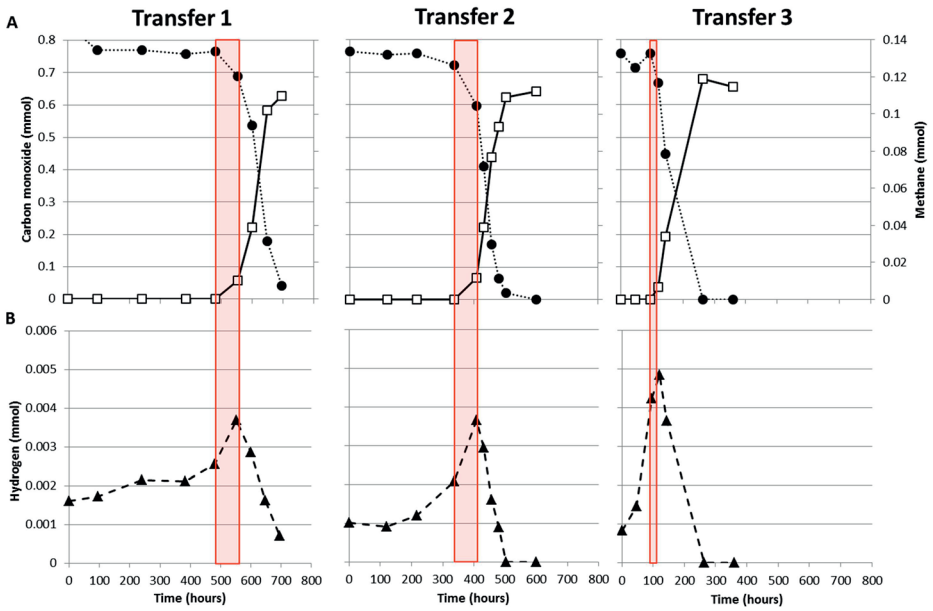

Figure 2. Adaptation of *M. marburgensis* to carboxydotrophic growth. A) consumption of CO (black solid circles) and production of methane (open squares). B) H_2 production and consumption profile during growth on CO. Red planes indicate the timeframe where methanogenesis is initiated. Gas is represented as total amount of mmol present in the bottle headspace.

In all cultures of *M. marburgensis* growing on CO as a sole substrate, H_2 is observed to accumulate in the headspace before the onset of methanogenesis (figure 2). Upon initiation of carboxydotrophic methanogenesis, H_2 is co-utilized. At the end of cultivation, not all the CO is converted to methane as approximately 1 mol methane is formed per 6 mol CO consumed (figure 2), suggesting formation of other products. Acetate formation was observed in incubations of *M. marburgensis* grown in presence of CO, which ranged from 2-4 mM at the end of cultivation.

Assessing the *M. marburgensis* CO oxidizing activity in the CFE of $H_2/CO_2/CO$ grown cells resulted in a specific MV reducing activity of 2.74 ± 0.3 µmol MV min^{-1} mg $protein^{-1}$ after correction for endogenous activity. H_2/CO_2 grown cells showed a specific MV reducing activity of 2.06 ± 0.13 µmol MV min^{-1} mg $protein^{-1}$ after correction for endogenous activity, which is about 1.3 times lower than in the condition with CO. Additionally, the CFE of H_2/CO_2 grown cells showed no endogenous activity, while cells grown on $H_2/CO_2/CO$ showed an average initial endogenous activity of 0.6 µmol MV min^{-1} mg $protein^{-1}$. This endogenous activity decayed over time, completely seizing after ~150 seconds. Addition of CO, after

seizure of endogenous activity, resulted again in reduction of MV in all samples.

Comparative proteomics of *M. marburgensis*

Comparative proteomic analysis was performed on *M. marburgensis* incubated with 80:20 H_2/CO_2 or 60:20:20 $H_2/CO_2/CO$. In the proteomics analysis 5845 peptides from 831 non-redundant proteins were identified (False discovery rate (FDR) ≤ 1%, average absolute mass error: 1.14 ± 1.76 ppm) of which 590 proteins were quantified using at least 2 razor + unique peptides in ≥ 3 measurements of either growth condition. Both the technical and biological reproducibility was very good based on median LFQ standard deviations of 6.9% and 18.4%, respectively. In total, 203 proteins were found to be differentially abundant between the two growth conditions (student T-test $p < 0.05$, median LFQ standard deviation: 14.8%). All the proteins required for hydrogenotrophic methanogenesis and the reductive acetyl-CoA pathway could be detected in both the H_2/CO_2 and $H_2/CO_2/CO$-grown cultures (figure 3). In presence of CO, several subunits of carbon monoxide dehydrogenase (CODH) and acetyl-CoA synthase (ACS) were more abundant. Several enzymes in the methyl-branch of the acetyl-CoA pathway were found to be increased in abundance in the presence of CO (table 1): mainly the formylmethanofuran dehydrogenase, methyl-coenzyme M reductase-I and the F420 dependent methylene-H4MPT dehydrogenase. Additionally, a higher abundance of the subunit H of the tetrahydromethanopterin S-methyltransferase was detected with CO as substrate. Other subunits of this complex were not significantly overproduced, and levels of subunit B and G were even lowered. Also, a predicted acetyl-CoA synthetase, theorised to be involved in acetate metabolism, was found to be more abundant.

Polyferredoxin, belonging to the energy conserving hydrogenase (EcH), was more abundant in the presence of CO, but other subunits of this EcH were not clearly differentially present. Other hydrogenase related proteins, such as the HypE protein, involved in hydrogenase maturation, and subunits of the F420-reducing hydrogenase were also found to be more abundant in cultures grown with CO in the headspace. In presence of CO, several proteins related to redox stress were found in higher numbers: F420 oxidase, superoxide dismutase, superoxide reductase and F390 synthethase (table S1). In addition to redox stress proteins, a predicted universal stress protein was found to be more abundant. Also a decrease in 30S and 50S ribosomal proteins was observed in presence of CO. Tuning down of ribosomal RNA and ribosomal proteins, is often observed as a response to different types of stress in *Escherichia coli* (Wagner, 2001), but also in other microorganisms this is observed (Abee and Wouters, 1999; van de Guchte et al., 2002). The decrease in ribosomal proteins in *M. marburgensis* in presence of CO could thus potentially be an additional indication of stress.

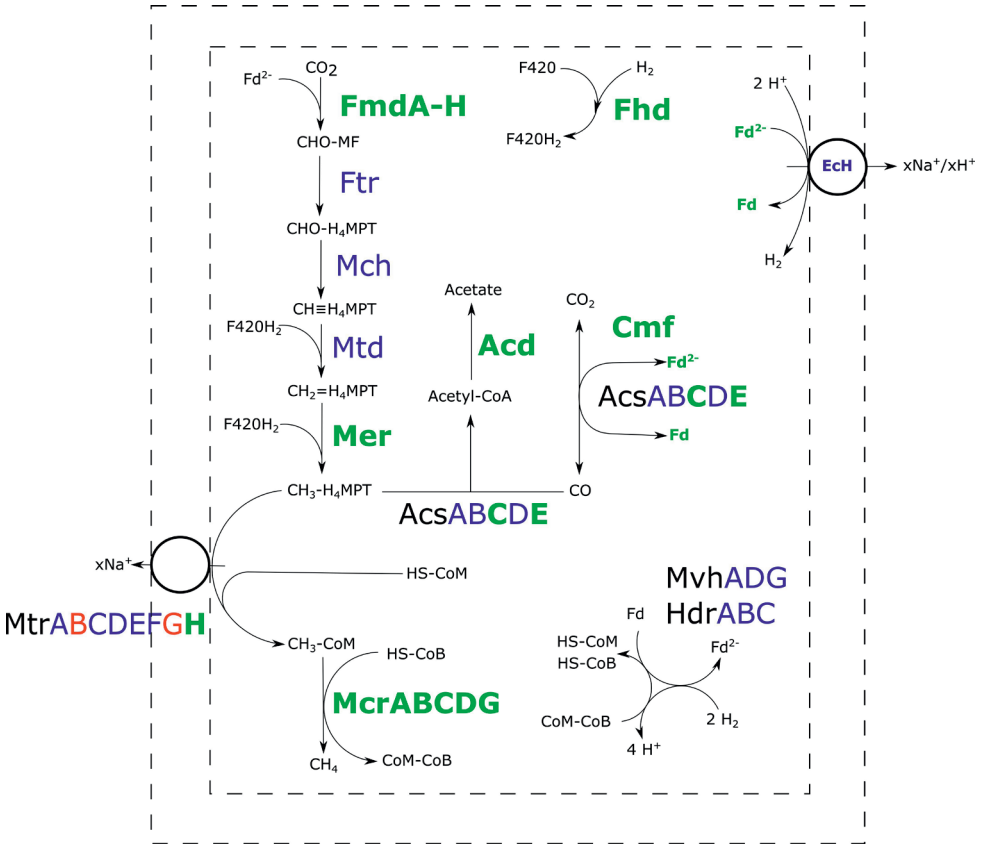

Figure 3. Comparative proteomic analysis of methanogenic metabolism of *M. marburgensis* grown on $H_2/CO_2/CO$ or H_2/CO_2. Relative abundance of proteins of carboxydotrophic growth compared to hydrogenotrophic growth is shown. Proteins highlighted green are found more abundantly present, proteins highlighted blue are not significantly changed in abundance and proteins highlighted in red are found to be less abundant in presence of CO ($p < 0.05$). Fmd, formyl-methanofuran dehydrogenase; Ftr, Tetramethanopterin Formyl-transferase; Mch, methenyltetramethanopterin cyclohydrolase; Mtd, methylene-H4MPT dehydrogenase; Mer, Methylene-H4MPT reductase; Acs, Acetyl-CoA synthase; Acd, Acetyl-CoA synthetase; Cmf, CODH maturation factor; Mvh/Hdr, F420-non-reducing hydrogenase / heterodisulfide reductase; Mtr, tetrahydromethanopterin S-methyltransferase; Mcr, methyl-coenzyme M reductase; EcH, Energy conserving hydrogenase; Fhd, F420 dehydrogenase; H4MPT, tetrahydromethanopterin; MF, methanofuran.

Table 1. Highlighted set of more abundant proteins of *M. marburgensis* grown on $H_2/CO_2/CO$ vs. H_2/CO_2. A cutoff value of $p < 0.05$ was used to assess if proteins were more abundantly present. The complete proteomics dataset can be found in supplementary I.

Protein		Relative abundance ($H_2/CO_2/CO$ vs. H_2/CO_2)	p-value
Methanogenesis related proteins			
	Tungsten formylmethanofuran dehydrogenase (subunit A)	2.13	2.54E-03
	Tungsten formylmethanofuran dehydrogenase (subunit B)	3.16	6.15E-04
	Tungsten formylmethanofuran dehydrogenase (subunit C)	1.7	7.50E-03
	Tungsten formylmethanofuran dehydrogenase (subunit D)	2.36	8.02E-03
	Tungsten Formylmethanofuran dehydrogenase (subunit F)	1.48	1.95E-02
	Tungsten formylmethanofuran dehydrogenase (subunit G)	2.4	1.68E-02
	F420-dependent methylene-H4MPT dehydrogenase	1.68	6.39E-03
	Methyl-coenzyme M reductase component A2-like protein	2.06	3.84E-04
	Methyl-coenzyme M reductase I subunit alpha	1.97	1.34E-03
	Methyl-coenzyme M reductase I subunit beta	1.63	6.65E-05
	Methyl-coenzyme M reductase I subunit gamma	1.8	1.51E-03
	Methyl-coenzyme M reductase I operon protein D	9.63	8.67E-05
	Methyl-coenzyme M reductase I operon protein C	unique to $H_2/CO_2/CO$	2.76E-02
	Tetrahydromethanopterin S-methyltransferase subunit H	1.83	2.55E-02
CODH/ACS related proteins			
	Acetyl-CoA synthase, subunit gamma	1.76	4.86E-02
	Acetyl-CoA synthase, subunit epsilon	4.62	1.15E-02
	Carbon monoxide dehydrogenase, iron sulfur subunit	3.48	1.12E-02
	CO dehydrogenase maturation factor	unique to $H_2/CO_2/CO$	2.61E-02
Acetate related genes			
	Predicted acetyl-coenzyme A synthetase	3.11	1.79E-02

Discussion

When growing on hydrogen, hydrogenotrophic methanogens generate methyl-H4MPT required in the final part of methanogenesis (Thauer et al., 2008). In addition, they can assimilate acetyl-CoA from methyl-H4MPT for biosynthetic purposes, by using the acetyl-CoA synthase (ACS). This requires CODH activity to reduce CO_2 to CO, which is subsequently condensed with methyl-H4MPT and CoA-SH to form acetyl-CoA. For methanogens, the CODH complex is in almost all cases associated with an ACS complex (Techtmann et al., 2012), suggesting it mainly plays a role in the assimilatory metabolism.

CODH/ACS related metabolism

The slight, but significant, increase in CO-oxidation activity observed in the CFE of $H_2/CO_2/CO$ grown cultures compared to the CFE of H_2/CO_2 grown cells suggests that more CO-oxidizing enzymes are present. This is in accordance with the higher abundance of several CODH/ACS related proteins when *M. marburgensis* is grown in the presence of CO: the epsilon and gamma subunit of the main complex, the CODH maturation protein and a CODH related ferredoxin. Two CODH-related operons can be found in the genome of *M. marburgensis* (cdh1 and cdh2) (Liesegang et al., 2010). The cdh2 operon codes for all the five subunits of a CODH/ACS, a CODH-like maturation factor and a CODH-related ferredoxin. Detection of the complete CODH/ACS complex under both of the tested conditions suggests that it is at least involved in assimilatory metabolism. Higher abundance of several CODH subunits, the CODH maturation factor and the CODH-related ferredoxin in the $H_2/CO_2/CO$ condition could indicate that the complex is also involved in CO-oxidation, allowing transfer of electrons to other co-factors/proteins. Such an observation is also made in *M. acetivorans* of which the genome contains two CODH/ACS operons (cdh1 and cdh2). Higher abundance of these CODH/ACS complexes was observed during proteomic analysis comparing CO-grown to acetate- or methanol-grown cultures. This suggests an important role for the CODH/ACS complex in CO-oxidation (Lessner et al., 2006; Rother et al., 2007). It has been shown later on that both Cdh isoforms of *M. acetivorans* are functional CODH/ACS complexes and that one isoform is sufficient for catabolic and anabolic functions (Matschiavelli et al., 2012). It is therefore likely that the CODH/ACS complex of *M. marburgensis* plays a main role in CO-oxidation.

The cdh1 operon of *M. marburgensis* contains the sequence of one pseudo annotated CODH alpha subunit and a sequence coding for a HycB-like, ferredoxin-related, protein. The presence of the HycB gene next to the CODH sequence could indicate that this protein is involved in CO-oxidation. However, its function remains unclear as this protein is not detected in the H_2/CO_2 nor the $H_2/CO_2/CO$ condition. The genome of *M. acetivorans* contains three other CODH sequences in addition to

the two CODH/ACS operons: two monofunctional CODH related genes (cooS1F and cooS2) and one operon containing solely the alpha subunit of the CODH/ACS complex (cdhA3). Knockout studies showed that the two monofunctional CODHs are not essential for CO utilization, as CO was still utilized as a substrate in the knockout strains (Rother et al., 2007). These monofunctional CODHs were observed to have a function at elevated CO pressures as detoxification mechanism. The CdhA3 protein is suggested to play a role in CO sensing and is apparently not directly involved in CO oxidation (Matschiavelli et al., 2012). The Cdh1 of *M. marburgensis* was not detected in the conditions tested here, and thus no conclusions can be drawn on its function. However, as the CO concentrations used in this study are relatively low, it is possible this protein is involved in CO-detoxification at higher CO pressures, similar to the observation in *M. acetivorans*. However, a different role or non-functionality of this protein cannot be ruled out.

Methyl-branch related proteins

In addition to CODH/ACS related proteins, several enzymes involved in the methyl-branch of the reductive acetyl-CoA pathway were more abundant in cultures grown on $H_2/CO_2/CO$. In particular, formylmethanofuran dehydrogenase, acting in the formation of formylmethanofuran from CO_2, and the F420-dependent methylene-H4MPT dehydrogenase, involved in generation of methyl-H4MPT from methylene-H4MPT, are significantly more abundant in incubations with CO (table 1, figure 3). Both proteins play a role in re-oxidation of co-factors, and their higher abundance might assist in countering the redox pressure of CO. Other proteins involved in the methyl-branch stay similar in abundance compared to incubations with H_2/CO_2 (figure 3).

The higher abundance of several enzymes in the methyl-branch in $H_2/CO_2/CO$ grown *M. marburgensis* is expected to result in an increased flow through the pathway and thus requires upregulation of subsequent pathways. This might explain the 'switching-on' of the acetate formation pathway and the increased production of enzymes involved in the final steps of methanogenesis (figure 3). The observed acetate formation by *M. marburgensis* in presence of CO is supported by the finding of higher abundance of a predicted acetyl-coenzyme A synthetase (E.C. 6.2.1.1), theorised to be involved in acetate production and consumption. Proteomics data of *M. marburgensis* grown on $H_2/CO_2/CO$ shows higher abundance of all subunits of methyl-coenzyme M reductase. Additionally, the H-subunit of tetrahydromethanopterin methyl-transferase is found to be more abundant. Studies on the H-subunit in *M. thermoautotrophicus* shows it catalyses the conversion of cob(I)alamin with CH3-H4MPT to methylcob(III) alamin, but lacks conversion activity of methylcob(III)alamin to methyl-CoM in absence of the rest of the complex (Hippler and Thauer, 1999). Other subunits of this complex are unchanged or even lowered in abundance in presence of CO (figure

3). The membrane associated nature of this protein complex might have hindered accurate quantification, making it difficult to assess the relative abundance of the different subunits between the two conditions. This hinders the assessment of the role of the complex as a whole in the carboxydotrophic methanogenic metabolism of *M. marburgensis*.

Comparing the proteomics results obtained here with results reported for *M. acetivorans* is difficult as the native aceticlastic metabolism of *M. acetivorans* is different from the hydrogenotrophic metabolism of *M. marburgensis*. *M. acetivorans* cannot be grown on hydrogen and comparative proteomic studies with CO have been performed using acetate and methanol as alternative substrates (Lessner et al., 2006; Rother et al., 2007). A detailed comparison between the carboxydotrophic metabolism of *M. acetivorans* and *M. marburgensis* would therefore not be accurate.

Limitations in hydrogenotrophic carboxydotrophic methanogenic metabolism

Carbon monoxide affects metalloproteins by interacting with their active-centres via back-bonding (Jeoung et al., 2014). Hydrogenases are considered CO-sensitive enzymes and H_2 metabolism of several microbial strains is inhibited by CO (Bertsch and Müller, 2015a; Daniels et al., 1977; Genthner and Bryant, 1982). However, [Ni-Fe]-hydrogenases are considered more robust and more resistant to CO-inhibition (Adams, 1990b; De Lacey et al., 2007). Hydrogenases involved in methanogenesis are in general [Ni-Fe]-hydrogenases, except for the iron-only hydrogenase present in *M. thermoautotrophicus*, replacing the methylene-H4MPT dehydrogenase in nickel deprived conditions (Afting et al., 1998, 2000). Higher CO-pressures seem to inhibit the metabolism of both *M. thermoautotrophicus* and *M. marburgensis*, as can be seen from the slowing down in H_2 consumption rate. However, the ability of both strains to co-utilize H_2 and CO suggests hydrogenase inhibition is not the only mechanism of toxicity in these hydrogenotrophic methanogens.

CO has a low redox-potential (E_0' = -520 mV), which can be seen as a major difficulty for the methanogens. Generation of ferredoxin by hydrogenotrophic methanogens is in general done via reverse proton transport via the EcH or a bifurcation reaction performed by a F420-non-reducing hydrogenase (Buckel and Thauer, 2013). The low redox potential of CO does however allow for direct reduction of ferredoxin via CODH, making reduced ferredoxin more accessible in the cell. This lowers the Fd_{ox}/Fd_{red} ratio in the cell, lowering the electron potential of the ferredoxin couple. Judging from proteomics data, several redox response systems are activated. However, many of these, such as the superoxide dismutase and F420-oxidase, are normally a response to oxidised compounds (e.g. oxygen), which is the opposite of the more reduced environment created by CO. It might be that these genes respond to redox stress in general or are regulated by universal stress proteins. Additionally,

the F390-synthetase, involved in redox sensing was found to be more abundant. In *M. thermoautotrophicus*, this system was found to react on changes in redox potential, regulating the expression of MCR-I, F420-dependant MDH and the F420-reducing hydrogenase (Vermeij et al., 1997). The CFE of $H_2/CO_2/CO$ grown cells showed more endogenous activity when compared to H_2/CO_2 grown cells. This could indicate more reducing equivalents are present in the cells grown in presence of CO. The overall increase in abundance of proteins involved in redox stress and co-factor regeneration, and the higher endogenous reducing activity suggest that *M. marburgensis* cells exposed to CO are subjected to changes in redox balance.

When grown solely on CO, *M. marburgensis* shows production of H_2 from the moment incubation is started (figure 2). Methanogenesis is not started instantly, and CO appears to be solely used for H_2 production. Methanogenesis initiates only after H_2 has accumulated in the headspace (figure 2 and figure 4) and, from that point on, quickly co-utilizing H_2 and CO. These data suggest that a minimal amount of H_2 is required to operate the carboxydotrophic methanogenic metabolism. We theorise this is related to the properties of the bifurcating F420-non-reducing hydrogenase required to regenerate CoM-SH and CoB-SH. Feasibility of the overall bifurcating reaction was estimated by calculating the potential difference between the two separate reactions catalysed (Eq. 1 & 2). The following assumptions were made during calculation: I) pH is assumed to be 7 and temperature 338 K, II) the ferredoxin couple is assumed to have a standard electron potential of -500 mV under physiological conditions (Thauer et al., 2008), but is assumed to approach the electron potential of the CO/CO_2 couple at the respective partial pressures (assessed via Nernst equation). Similarly the electron potential of H_2 is assumed to be similar to its partial pressure, III) the CoM-CoB couple is assumed to have an electron potential of -140 mV, and IV) the bifurcation reaction is considered feasible if the sum in potential of reaction 1 and 2 has a negative value.

$$H_2 + Fd \rightarrow 2\,H^+ + Fd^{2-} \qquad \Delta E_0' = +\,86\ mV \qquad (1)$$

$$CoM\text{-}CoB + H_2 \rightarrow CoM\text{-}SH + CoB\text{-}SH \qquad \Delta E_0' = -\,274\ mV \qquad (2)$$

H_2 has to drive the reduction of both CoM-CoB and ferredoxin in the reaction catalysed by the F420-non-reducing hydrogenase. However, as the electron potential of ferredoxin is expected to be lowered in presence of CO, and H_2 is almost absent in the cultures, the overall reaction becomes less exergonic. When assessing the difference between the two separate reactions, it is observed that the overall reaction is not favoured under the starting conditions of incubation (figure 4, dotted lines). Under these conditions the CoM-SH and CoB-SH cannot be replenished, potentially blocking methanogenesis. As more H_2 is generated, via the EcH complex, the reaction becomes more favourable, eventually allowing to start methanogenesis

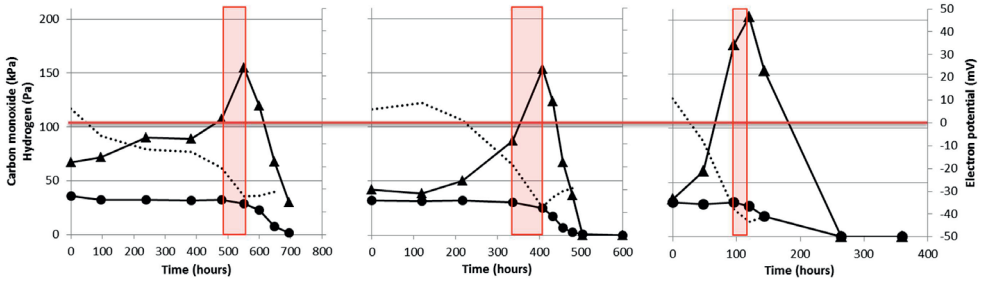

Figure 4. Thermodynamic analysis of the reaction catalysed by the F420-non-reducing hydrogenase in *M. marburgensis*. The used dataset is the same as the one displayed in figure 2. H_2 pressure in Pa is given by the black triangles and the carbon monoxide pressure in kPa is given by the black circles. The estimated difference between the two reactions catalysed by the bifurcating F420-non-reducing hydrogenase is indicated by the dotted black line. Red boxes indicate the phase where methanogenesis is initiated. The last time point is not assessed as the gases had reached a pressure which could not be determined accurately.

(figure 4). Inhibition of hydrogenases or an irreversible reduced state of the cell at higher CO pressures could prevent H_2 production and consumption, preventing the methanogenic metabolism from starting. The proposed limitation of the F420-non-reducing hydrogenase might explain why hydrogenotrophic methanogens as *M. marburgensis* and *M. thermoautotrophicus* can only utilize CO as a sole substrate up to 50 kPa, whereas *M barkeri* and *M. acetivorans*, which do not employ a bifurcating F420-non-reducing hydrogenase (Thauer et al., 2008), can perform carboxydotrophic growth using >100 kPa and >150 kPa CO, respectively. The CO metabolism of hydrogenotrophic methanogens is thus potentially limited by their F420-non-reducing hydrogenase, and this would explain the observation that their efficiency of carboxydotrophic growth is strongly connected to the availability of hydrogen.

Conclusion

The hydrogenotrophic methanogen *M. marburgensis*, was found to grow methanogenically on $H_2/CO_2/CO$ or CO alone. CO could be used as a sole substrate up to 50 kPa and its consumption was stimulated in the presence of hydrogen. Proteomic analysis indicates higher abundance of CODH/ACS related proteins and enzymes of the methyl-branch in presence of CO. Most of the abundant proteins in cultures grown in the presence of CO are involved in redox reactions, potentially required to counter the strong reducing capacity of CO. Additionally, the pathway

towards acetate production was found upregulated, which explains formation of small amounts of acetate as an end-product in presence of CO. The ability to utilize H_2 in the presence of CO suggests that hydrogenase inhibition is not the main mechanism of toxicity in hydrogenotrophic methanogens. The requirement of small amounts of hydrogen, before methanogenesis with CO could start, suggests that this is an essential intermediate in the methanogenic metabolism. The F420-non-reducing bifurcating hydrogenase is a likely candidate for CO inhibition as low H_2 pressures potentially can cause this reaction to become unfavourable, blocking the methanogenic metabolism.

Supplementary material I can be found online at:

https://www.frontiersin.org/article/10.3389/fmicb.2016.01049

Chapter 4
High rate biomethanation of carbon monoxide rich gases via a thermophilic synthetic co-culture

Authors: Martijn Diender, Philipp S. Uhl, Johannes H. Bitter, Alfons J.M. Stams and Diana Z. Sousa

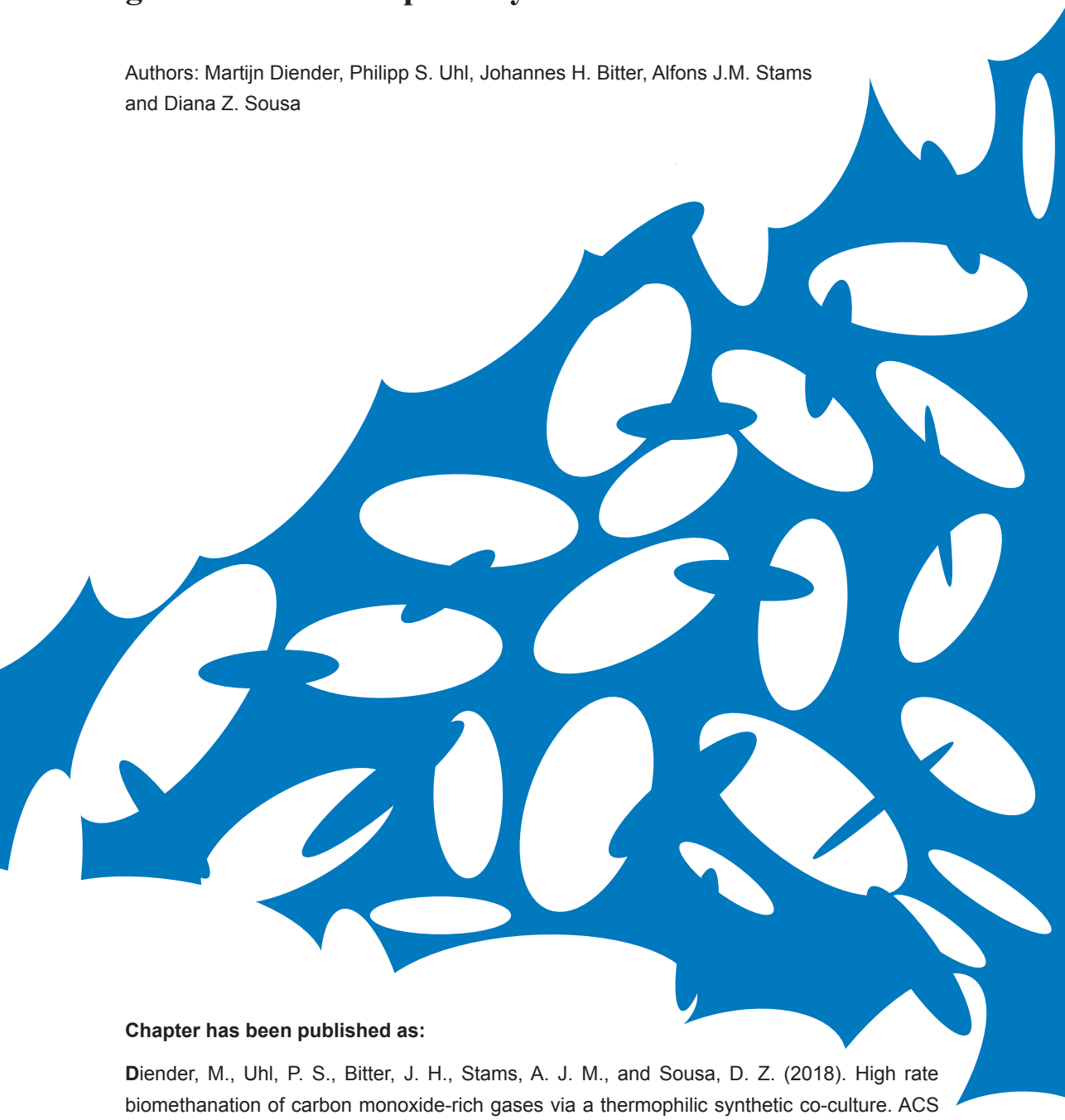

Chapter has been published as:

Diender, M., Uhl, P. S., Bitter, J. H., Stams, A. J. M., and Sousa, D. Z. (2018). High rate biomethanation of carbon monoxide-rich gases via a thermophilic synthetic co-culture. ACS Sustain. chem. eng. 6, 2169–2176. doi:10.1021/acssuschemeng.7b03601.

Abstract

Carbon monoxide-fermenting microorganisms can be used for the production of a wide range of commodity chemicals and fuels from syngas (generated by gasification of e.g. wastes or biomass) or industrial off-gases (e.g. from steel industry). Microorganisms are normally more resistant to contaminants in the gas (e.g. hydrogen sulfide) than chemical catalysts, less expensive and self-regenerating. However, some carboxydotrophs are sensitive to high concentrations of CO, resulting in low growth rates and productivities. We hypothesize that cultivation of synthetic co-cultures can be used to improve overall rates of CO bioconversion. As case study a thermophilic microbial co-culture, consisting of *Carboxydothermus hydrogenoformans* and *Methanothermobacter thermoautotrophicus* was constructed to study the effect of co-cultivation on conversion of CO-rich gases to methane. In contrast to the methanogenic monoculture, the co-culture was able to efficiently utilize CO or mixtures of H_2/CO/CO_2 to produce methane at high efficiency and high rates. In CSTR-bioreactors operated in continuous mode, the co-culture converted artificial syngas (66.6% H_2: 33.3% CO) to an outflow gas with a methane content of 72%, approaching the 75% theoretical maximum. CO conversion efficiencies of 93% and volumetric production rates of 4 $m^3_{methane}/m^3_{liquid}$/day were achieved. This case shows that microbial co-cultivation can result in a significant improvement of gas-fermentation of CO-rich gases.

Introduction

Bio-based technologies are quickly upcoming to take part in the closing of carbon- and other waste streams in our society. However, many of these bio-based technologies cannot deal with recalcitrant substrates, such as lignified biomass or municipal waste. Conversion of such carbon-wastes via gasification technology yields synthesis gas (syngas), a mixture of mainly CO, H_2 and CO_2, giving opportunity to access the full carbon spectrum of the initial material via gas fermentation. Alternative sources interesting for gas fermentation are off-gases from industry (e.g. steel mills) and syngas generated via high temperature co-electrolysis (HTCE), reforming steam and CO_2 into syngas (Stoots et al., 2009). HTCE can also be operated with solely sunlight as energy source, deriving syngas from inorganic sources (Frost et al., 2010). Making use of microbial gas fermentation processes, waste streams can be converted via a uniform substrate into fuels and commodity chemicals. Companies, such as Lanzatech, establish large scale production systems to generate bio-based products from CO-rich, steel mill waste gases, showing the application potential of gas fermentation technology (LanzaTech; Köpke et al., 2011a).

Carbon monoxide is one of the main components in untreated syngas, and is known as an odourless, colourless and toxic gas. Despite its toxicity, it can act as a natural

substrate for anaerobic microorganisms, driving acetogenic, hydrogenogenic and methanogenic metabolisms (Diender et al., 2015b, **Chapter 2**). Its low reduction potential (E_0' = -520 mV) makes it a strong electron donor, and theoretically allows for higher energy conservation compared to hydrogen oxidation (E_0' = -414 mV). However, generally methanogens grow poorly on CO. This can also be deduced from the fact that only four methanogens have been shown to grow on CO as a sole substrate: *Methanosarcina acetivorans* (Rother and Metcalf, 2004), *Methanothermobacter thermoautotrophicus* (Daniels et al., 1977), *Methanothermobacter marburgensis* (Diender et al. 2016, **Chapter 3**) and *Methanosarcina barkeri* (Daniels et al., 1977). The hydrogenotrophic methanogens *M. thermoautotrophicus* and *M. marburgensis* both showed CO conversion to methane but preferred H_2/CO_2 over CO (Diender et al. 2016, **Chapter 3**). These poor CO utilization capabilities are likely related to the excess reducing equivalents in the cytoplasm of the cell (Diender et al. 2016, **Chapter 3**).

Co-cultivation of microbes can be used to improve the growth of microorganisms and generate a different product spectrum. This can either be via product removal, generating a thermodynamic advantage for one or both strains, or via excretion of useful secondary metabolites to support growth. Co-culture engineering can be used to tune and optimize the production system for specific products, significantly improving the production potential (Santala et al., 2014). For CO fermentation, co-cultivation was shown as one of the approaches to expand the product spectrum towards chain elongated products and alcohols (Diender et al., 2016b, **Chapter 5**; Richter et al., 2016a). In these co-cultures the partner strain accepted products from the CO-fermenter, allowing for production of caproate and hexanol. Such products are rarely formed in mono- or undefined mixed cultures grown on syngas and, when formed, their production rates and final product concentrations are low (Diender et al., 2016b, **Chapter 5**).

This study aimed to overcome the poor methanogenic potential of CO containing gases by co-cultivating *M. thermoautotrophicus*, a relatively well studied hydrogenotrophic methanogen, with *Carboxydothermus hydrogenoformans* (Svetlichny et al., 1991), a carboxydotrophic hydrogenogen. Hydrogenogens are highly efficient CO utilizers, rapidly converting the CO to H_2 via the water-gas shift reaction. At standard conditions the energy yield of this reaction is rather low ($\Delta G^{0'}$ = -20 kJ), but this gets more negative with increasing temperature. Doubling times of hydrogenogens in general are rather short (1-2 hours) indicating a high rate, low energy yielding metabolism (Diender et al., 2015b, **Chapter 2**; Oelgeschläger and Rother, 2008). The organisms selected for this study are thermophiles with a growth optimum around 65 °C, allowing for increased reaction kinetics and increase in the transfer rate of gas during operation. A downside of the thermophilic conditions is

the lower saturation level of gases at higher temperatures. But, as gas transfer rate is usually the limiting factor, the system is likely not much affected by the maximal gas saturation levels (Diender et al., 2015b, **Chapter 2**).

We hypothesize that methanogenesis from CO-rich gases is more efficient by the co-culture when compared to the mono-culture, due to the removal of CO by the hydrogenogen, lifting the toxic effects on the methanogen while simultaneously providing substrate in the form of H_2/CO_2. In contrast to an open mixed culture approach the defined co-culture is expected to have better product specificities, higher production rates and have a more robust production profile.

Material and Methods

Strains and cultivation

Strains *M. thermoautotrophicus ΔH* (DSM-1053) and *C. hydrogenoformans* Z-2901 (DSM-6008) were ordered from the DSMZ strain collection (Braunschweig, Germany). Strains were initially cultivated at 65 °C in medium recommended by the provider, using anaerobic cultivation procedures. After growth was confirmed, the strains were transferred to a carbonate-phosphate buffered medium with the following composition per liter: 0.4 g KH_2PO_4, 0.53 g K_2HPO_4*2 H_2O, 0.3 g NH_4Cl, 0.3 g NaCl, 0.1 g $MgCl_2$*6 H_2O, 0.5 g yeast extract and 0.5 mg resazurin. Medium was supplemented, per liter, with 61.8 µg H_3BO_3, 61.25 µg $MnCl_2$, 943.5 µg $FeCl_2$, 64.5 µg $CoCl_2$, 12.86 µg $NiCl_2$, 67.7 µg $ZnCl_2$, 13.35 µg $CuCl_2$, 17.3 µg Na_2SeO_3, 29.4 µg Na_2WO_4 and 20.5 µg Na_2MoO_4. Medium was prepared, boiled and subsequently cooled under a continuous nitrogen flow. Bottles (120 ml total volume) were filled with 50 ml medium and instantly capped with rubber stopper and aluminium cap. The gas phase was exchanged with 80:20 H_2:CO_2 in the case of *M. thermoautotrophicus* and 80:20 N_2/CO_2 in the case of *C. hydrogenoformans*, resulting in a final pressure of 170 kPa. The headspace was further tuned by partial removal of gas and introduction of additional CO, H_2 or CO_2. The bottles were autoclaved and stored at room temperature till further use. Before inoculation, medium was augmented with the following volumes of stock solutions: 1% of 11 g $CaCl_2$*2 H_2O per liter, 1% of a vitamin solution containing per liter: biotin 20 mg, nicotinamide 200 mg, p-aminobenzoic acid 100 mg, thiamin 200 mg, panthotenic acid 100 mg, pyridoxamine 500 mg, cyanocobalamine 100 mg, riboflavine 100 mg. The medium was reduced by introducing a 5% volume of a stock solution containing 4.8 g Na_2S * 7-9 H_2O and 80 g $NaHCO_3$ per liter. Unless stated otherwise, bottles were inoculated with an exponentially growing culture in a 1:50 ratio (v/v).

Co-culture establishment and characterization

Pure cultures of *M. thermoautotrophicus* and *C. hydrogenoformans* were pre-grown

on H_2/CO_2 and CO as substrate, respectively. During exponential growth phase of both cultures, cross inoculation was performed, establishing co-culture conditions. CO was added at 60 kPa partial pressure after cross-inoculation. Co-cultures were transferred at least every 5 days to keep them active. Subsequent co-cultures were kept under a headspace of approximately 47/40/13 $H_2/CO/CO_2$ ratio. The effect of headspace composition on co-culture performance was assessed by varying the H_2:CO composition between 1:0 / 2:1 / 1:2. Co-cultures were regularly inspected by microscopy to verify the presence of the two microorganisms.

Bioreactor operation

Cultivation in both batch and continuous, was performed in a 1.5 liter bioreactor (Applikon, Delft, the Netherlands). Hydrogen and CO were supplied using mass flow controllers (Brooks Instruments BV, Ede, the Netherlands). Medium used in the bioreactors was similar as that described above, except the addition of carbonate or CO_2 was omitted. The liquid volume in the reactor was set to 750 ml for both batch and continuous experiments. Stirring was performed by two rushton stirrers on a single shaft, stirrers were placed at 33% and 66% of the liquid height. The pH was controlled using 3 M KOH and 33% acetic acid solutions. Gas outflow rates were determined using a bubble counter. After sterilization, reactors were connected to the control tower, initiating temperature (65 °C) and pH (7.2) control. Reactors were flushed for 3 hours with N_2 at a rate of 20 ml/min, to create anaerobic conditions. Right before inoculation the N_2 flow was changed for a CO/H_2 flow. Additionally, salts, vitamins, yeast extract, and H_2S were introduced in the reactor in the same ratio as described above. When the redox potential of the medium was lowered to a value below -300 mV, the reactor was inoculated with the co-culture (5% inoculum, v/v); establishment of the co-culture in the bioreactor was visually monitored by microscopy. For continuous operation a peristaltic pump (Masterflex, Gelsenkirchen, Germany) was used, and a HRT of 1.5 days was applied. Sterile medium was supplied from 10 L medium vessels continuously sparged with nitrogen (5 l/h) during the experiment to ensure anaerobic conditions of the inflow medium. All mentions of gas-volumes in supply or production rates throughout the text are considered to be at 1 atm pressure and 298 K.

Analytical procedures

For gas analysis, gas samples of 0.2 ml were taken by syringe and analysed in a Compact GC 4.0 (Global Analyser Solutions, Breda, The Netherlands). CO, CH_4 and H^2 were measured using a molsieve 5A column operated at 100 °C coupled to a Carboxen 1010 pre-column. CO_2 was measured using a Rt-Q-BOND column operated at 80 ºC. Detection was in all cases done via a thermal conductivity detector.

Liquid phase composition was analysed with a high pressure liquid chromatograph

equipped with a MetaCarb 67H column (Agilent Technologies, Santa Clara, CA). The column was operated at a temperature of 45 °C with a flow rate of 0.8 ml/min. Detection was done via a RI and UV detector. H_2SO_4 (0.01 N) was used as eluent. In all cases, samples of 0.5 ml were taken and immediately centrifuged at 13000g. Subsequently 0.4 ml supernatant was added to 0.6 ml 10 mM DMSO in 0.1 N H_2SO_4 solution. Concentrations below 0.3 mM could not accurately be quantified and are referred to as trace amounts.

Dry weight of the biomass was determined from 4 ml fresh sample. Samples were centrifuged at 13000 rpm for 2 min. In order to remove salts and other medium components, the pellet was washed with deionized water, centrifuged and subsequently re-suspended in 1 ml deionized water. The suspended biomass was dried on a pre-weighed aluminium container at 120 °C for at least 3h, after which the dry weight was determined.

Results & Discussion

Pure cultures of *C. hydrogenoformans* and *M. thermoautotrophicus* were tested for growth on CO. *C. hydrogenoformans* utilized the provided 60 kPa CO substrate within 30 hours, producing H_2 and CO_2 as the main end products. *M. thermoautotrophicus* could be grown on H_2/CO_2 in presence and absence of CO, but CO was utilized only slowly. It becomes clear that hydrogen is relatively quickly utilized in presence of CO (within 100 hours), but only a fraction of the CO itself is consumed over 500 hours (figure 1). This is in accordance with what has been reported earlier for this strain (Diender et al. 2016, **Chapter 3**; Daniels et al. 1977). Growth on CO as a sole substrate was not tested here for *M. thermoautotrophicus*, but has been reported to be almost 100 times slower than growth on H_2/CO_2 (Daniels et al., 1977).

Co-cultivation significantly increases methane production rate and efficiency from CO

Co-cultivation of *C. hydrogenoformans* and *M. thermoautotrophicus* resulted in rapid conversion of a $H_2/CO_2/CO$ mixture (figure 2 A – B) or pure CO (figure 2 C) to methane. The co-culture was able to utilize 60 kPa CO in approximately 24 hours, whereas *M. thermoautotrophicus* monocultures needed over 500 hours to utilize less than this amount of CO (figure 1).

After 20 hours of incubation, traces of acetate, in the range of 0.5 to 1.5 mM, were found in the co-culture incubations as additional end-products. This is likely due to the acetogenic potential of *C. hydrogenoformans* (Henstra and Stams, 2011). From the tested conditions it becomes clear that relatively high CO pressures, up to the maximum tested pressure of 150 kPa, can be utilized by this co-culture to produce methane and CO_2. When grown solely on CO as a substrate, a clear distinction can be

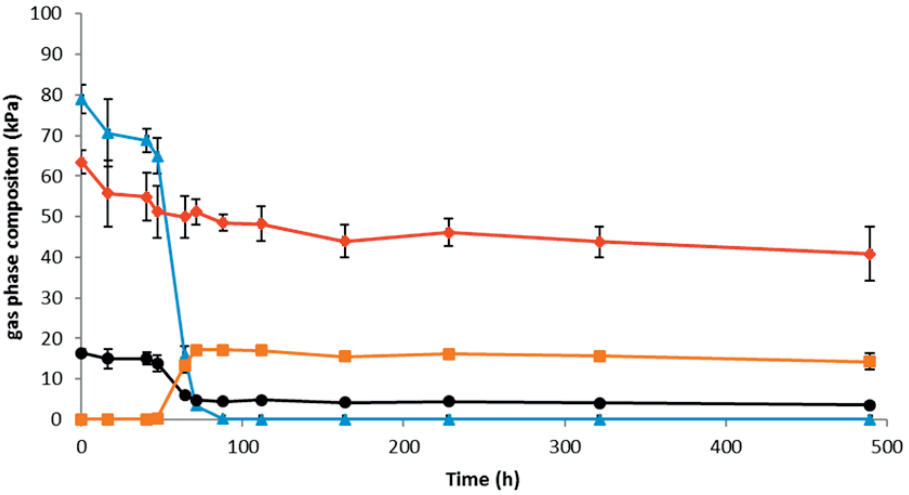

Figure 1. Growth of *M. thermoautotrophicus* on a CO:H_2:CO_2 mixture. Substrate product spectrum of *M. thermoautotrophicus* grown on a mixture containing CO, H_2 and CO_2. Standard deviations are shown over triplicate bottle experiments. CO, red diamonds; H_2, blue triangles, CO_2 black circles, CH_4, orange squares.

made between the phases where *C. hydrogenoformans* and *M. thermoautotrophicus* are metabolically active. However, within 48 hours all substrate was converted to methane and CO_2. Shifting the initial headspace composition to contain relatively more hydrogen (1:2 CO/H_2) decreases the time required for conversion to 24 hours. Additionally, the higher H_2 content decreases the amount of CO_2 released. It is hypothesized that both strains profit from the co-cultivation: *C. hydrogenoformans* removes toxic CO and is capable of producing H_2, CO_2 and acetate, supporting the growth of the methanogen. The methanogen is capable of rapidly removing hydrogen and CO_2 from the environment, creating thermodynamically more favourable conditions for *C. hydrogenoformans* to grow. Such interactions are also expected to occur in the natural habitat of these organisms, where hydrogenogens are suggested to cleanse the environment of CO for other organisms to grow (Techtmann et al., 2009).

Several reactions take place in the co-culture (Eq. 1-3). As *M. thermoautotrophicus* utilizes CO inefficiently compared to *C. hydrogenoformans*, we assume a neglectable amount of CO is directly converted to methane. As can be seen from reaction 3, in the ideal situation (CO:H_2 = 1:3), the overall stoichiometry is CO_2 neutral and can yield solely methane and water as end-product. Additionally, this poses an interesting scenario as no protons are produced or consumed in the overall reaction, requiring minimal addition of acid or base during the process.

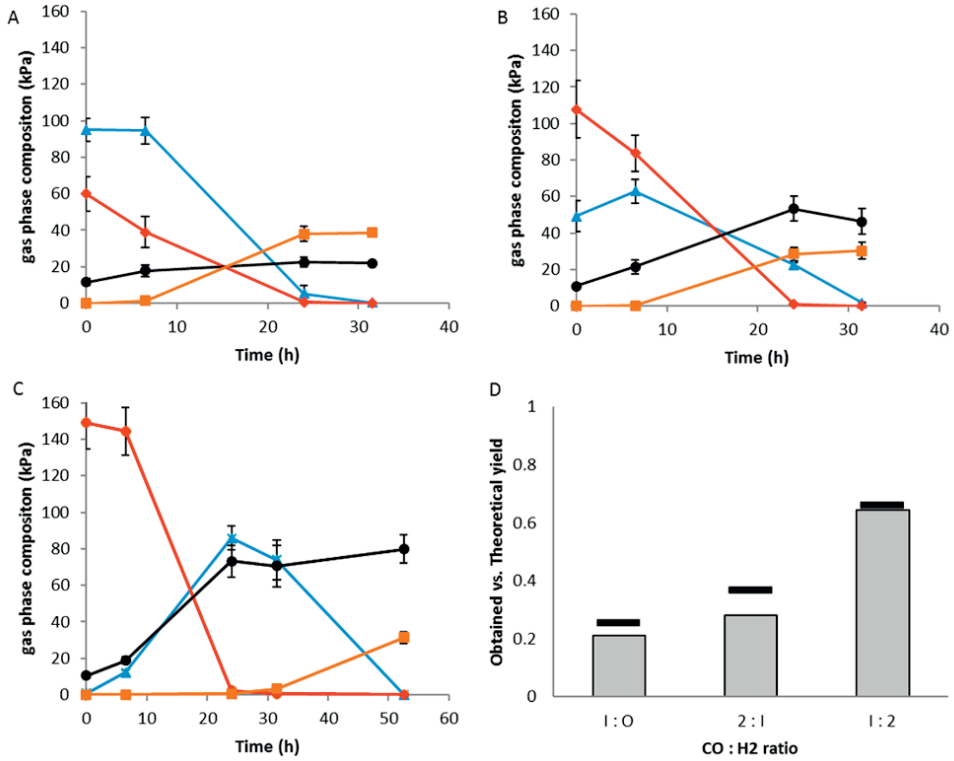

Figure 2. Methanogenic co-culture converting different headspace compositions to methane. A). 1:2 CO:H_2 mixture ,B). 2:1 CO:H_2 ,C). 1:0 CO:H_2 mixture. Standard deviations are shown over triplicate bottle experiments. CO, red diamonds; H_2, blue triangles, CO_2 black circles, CH_4, orange squares. D). Methane yield per CO consumed under different initial CO:H_2 compositions. Horizontal bars above the graphs display the theoretical yield based on initial gas content in the bottles.

$$CO + H_2O \rightarrow CO_2 + H_2 \quad (1)$$

$$4\ H_2 + CO_2 \rightarrow CH_4 + 2\ H_2O \quad (2)$$

$$CO + 3\ H_2 \rightarrow CH_4 + H_2O \quad (3)$$

The methane production yields per CO consumed (figure 2 D) approximate the theoretical values in each of the conditions, showing that most CO is eventually converted to methane and that there is minor conversion to other side products. When using open mixed cultures for biomethanation of syngas, side products such as acetate, propionate and ethanol are produced, lowering the overall efficiency of the system (Guiot et al., 2011; Navarro et al., 2016). In studies with immobilized methanogenic mixed cultures on charcoal, CO was largely converted to methane (~50%), however methanogenesis was partly inhibited by CO and formation of acetate/formate as by-products was observed (Schwede et al., 2017).

High methane content gas production in batch bioreactors

The methane production capacity of the co-culture was further tested by cultivation in a gas fed CSTR. Different reactor parameters were tested to assess their effect on co-culture functioning. Initial reactor runs were performed with 100 rpm stirring, resulting only in a methane content of 2% in the outflow gas at a rate of 0.150 $m^3_{methane}/m^3_{liquid}$/day. Increasing the stirring speed from 100 to 400 rpm resulted in an increase of average H_2 consumption efficiency from ~20% to ~80%, whereas average CO consumption efficiency increased from ~20% to ~60% (Supporting information S1.A) and average relative methane production efficiency increased from ~3% to ~40% (Supporting information S1.B). The increase in stirring rate increases the gas mass transfer, making it more accessible to the microbes. Runs with stirring speeds up to 400 rpm resulted in a system generating a headspace with peak concentrations up to 77% CH_4, with 13% H_2 and 5% CO and CO_2. Increasing the stirring above 400 rpm resulted in a drop in methanogenic activity, potentially due to high shear stress, or CO accumulation in the liquid due to a high transfer rate. This inhibition could not be reversed by lowering the stirring speed. When applying batch conditions with 400 rpm stirring speed, the culture could be maintained for about 10 days without any addition of new medium while continuously converting the inflow gas to mainly methane. After ~10 days, production rates declined which was likely due to depletion of nutrients.

Continuous production of methane enriched gas

During continuous operation the co-culture maintained biomass concentrations of approximately 0.5 g l^{-1}. Consumption of CO at high rates, indicating activity of *C. hydrogenoformans*, and methane production, indicating activity of *M. thermoautotrophicus*, showed that none of the two organisms washed out during the whole run. This was confirmed by visual inspection of the co-culture: two distinct phenotypes, corresponding to *C. hydrogenoformans* and *M. thermoautotrophicus*, could be observed throughout bioreactor operation.

During the first phase of continuous operation hydrogen inflow was set to 5 ml min^{-1} while CO inflow was set to 2 ml min^{-1}. Under these conditions, average outflow gas was composed of 70% methane and a fraction of 14% H_2, 8% CO_2 and 8% CO (figure 3, day 6 - 12). As not all hydrogen was used under these conditions, hydrogen gas flow was not further increased. Based on mass balance calculations, introduced CO was removed with 90% efficiency whereas introduced hydrogen was removed with 93% efficiency. Hydrogen was almost completely converted to methane (~90%).

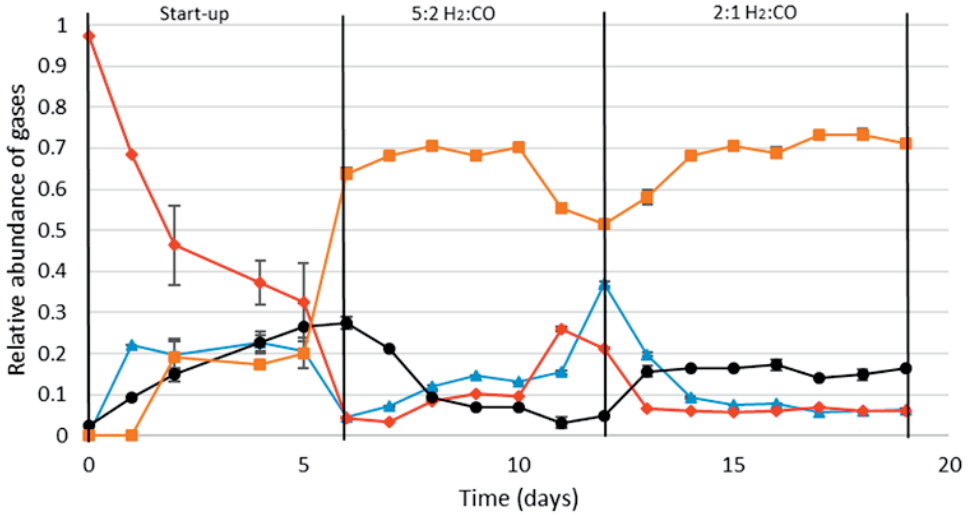

Figure 3. Relative outflow gas composition of the co-culture in a continuous bioreactor. Relative gas composition in the reactor is shown. Total pressure in the system was 1 atmosphere. Average values and standard deviations shown are calculated from triplicate measurements. Day 0-6: start-up phase in which CO and H_2 flow and stirring were ramped up. Day 6-12: operation was performed with 2 ml/min CO and 5 ml/min H_2. Day 12-19: operation was performed with 2 ml/min CO and 4 ml/min H_2. CO, red diamonds; H_2, blue triangles, CO_2 black circles, CH_4, orange squares.

Volumetric methane production rates reached an average value of 3.5 $L_{methane}/L_{liquid}$/day (figure 4, day 6-12). A steady state could however not be obtained with these operation conditions as can be seen from the instability in production rates during this phase (figure 4). The increased CO content in the gas phase of the reactor, together with a drop in methane production, during the period from day 6 to day 12 suggests that the culture cannot deal properly with the provided conditions. During this phase cyclic patterns appeared for the redox potential, alternating between -500 and -600 mV. The issue was solved by lowering the hydrogen inflow rate to 4 ml min^{-1}, and covering the reactor from light. The instability might be related to the sensitivity of *M. thermoautotrophicus* to light, which has been observed earlier (Olson et al., 1991). The reactor was able to reach a more stable state (day 12-19) after covering the reactor from light, and lowering the hydrogen flow to 4 ml min^{-1}, resulting in a CO:H_2 ratio of 1:2. Redox was no longer going down to -600 mV and stabilized around -500 mV. CO levels in the outflow were decreased further to 4%, and the overall production rates increased to 4 $m^3_{methane}/m^3_{liquid}$/day (figure 4). For reverse membrane reactors, rates of about 0.2 $m^3_{methane}/m^3_{liquid}$/day were reported (Westman et al., 2016; Youngsukkasem et al., 2015), which is significantly lower than rates

reported here for the non-biomass retaining co-culture system. Average methane outflow content in the co-culture reactor system during steady operation was around 72% (figure 3, day 14 - 19), close to the theoretical maximum of 75% at this inflow gas composition.

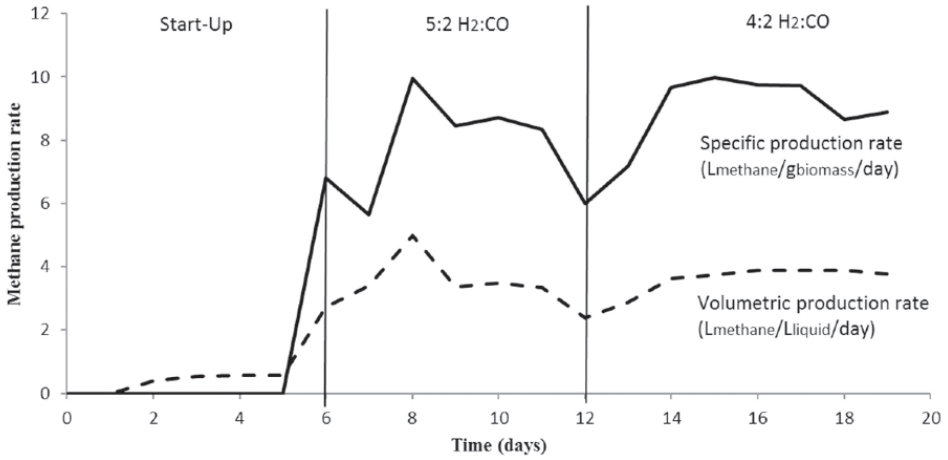

Figure 4. Volumetric and specific production rates of methane by the co-culture in a continuous bioreactor. Solid line represent specific methane production rates in $L_{methane}/g_{biomass}$/day. Dashed line represent volumetric methane production rates in $L_{methane}/L_{liquid}$/day.

A CO conversion efficiency of 93% was achieved under these conditions and 97% of the inflowing hydrogen was converted. Similarly as in the bottle experiments, small amounts of acetate were produced in the reactor. After correction for the acetate externally added to the system for pH control, average production rates of 13 ± 1.4 mmol/l/day (day 6-12) and 7 ± 0.99 mmol/l/day (day 13 – 19) were observed, which is 8 and 4% of the total product spectrum in those conditions, respectively. This amount of acetate produced is relatively low compared to mixed culture fermentations for biomethanation of syngas, where CO is for a larger fraction (up to 50%) converted into other products (Navarro et al., 2016; Schwede et al., 2017). The observed gas composition could accurately be modelled by calculating the metabolic fluxes through the system using the obtained efficiencies and gas inflow ratios (figure 5).

Despite the high efficiency of the co-culture, other gases (mainly CO_2) are still in the outflow gas. This can potentially be explained by either of the following two factors, or both: i) not enough electron donor is available to convert all CO_2, ii) a four times decrease in gas phase volume due to formation of methane from hydrogen and CO, causing the gases to be retained in the system for a longer time. Despite the high

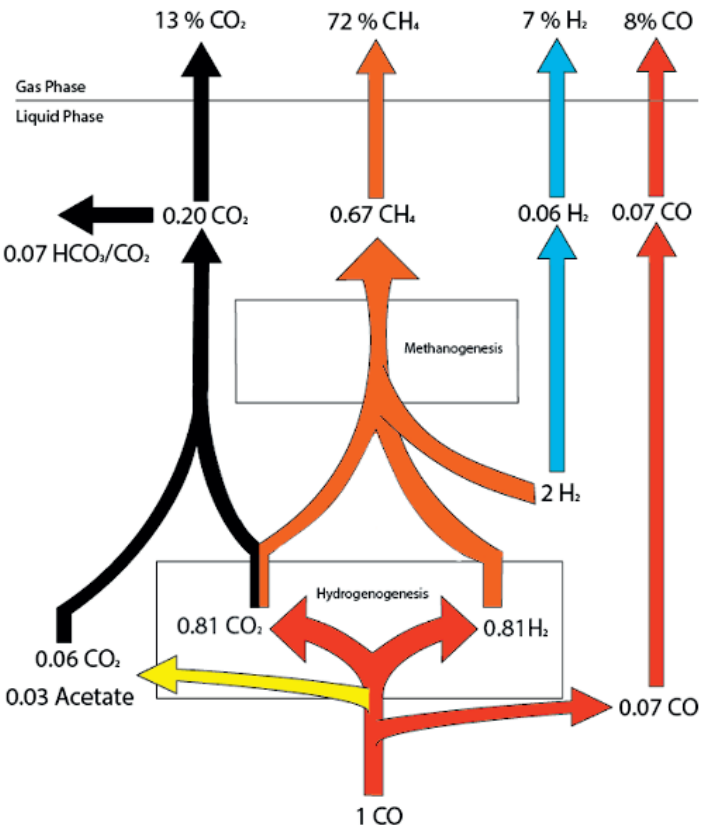

Figure 5. Schematic overview of the production routes of the methanogenic co-culture. Schematic representation of the metabolite flow in a continuous bioreactor operated with a methanogenic co-culture system. Acetate production is assumed to take place directly from CO only, by the hydrogenogen. In contrast to CO, H_2 and CH_4, CO_2 is also removed in significant amounts via the liquid outflow (HCO_3/CO_2). Calculation were performed using pH 7.2.

methane content in the outflow gas, the gas is still not optimal for introduction into the gas grid. Mainly the leftover percentage of CO is a problem and further removal is desired. Batch bottle experiments show no traces of CO after incubation and suggest the gas can be completely purified from CO by the co-culture. Additionally, the system needs to be further adapted to be able to deal with 3:1 inflow ratios of H_2:CO, and might be achieved by increasing the HRT of the system to retain more biomass, co-culture optimization, medium improvement or using a different reactor setup, such as gas-lift. Overall, the work performed here shows that a continuous system can maintain the methanogenic co-culture, efficiently producing methane at a high rate from a CO rich gas.

Application perspectives of syngas bio-methanation

One can discuss the feasibility of utilization of methane versus bio-hydrogen, or alcohols as fuels. Hydrogen is considered a clean fuel, as solely water is produced when combusted. Additionally, hydrogen (142 MJ/kg) has a higher energy density per mass as methane (55.5 MJ/kg). However, as with other biofuels, bio-hydrogen production from renewable biomass or waste indirectly generates CO_2, and is at best CO_2 neutral. Therefore, hydrogen production from non-carbon generated electricity, such as solar power, is 'cleaner' from a CO_2 emission perspective. Additionally, a pure-hydrogen mixture is a difficult fuel to store and to transport (Dunn, 2002), and cannot be used in the current natural gas infrastructure. Methane gas on the other hand can be transported, stored and used in the current infrastructure, and can be blended with natural gas (Thrän et al., 2014). Liquid fuels, such as ethanol and butanol, do not have to be compressed before use, which is an advantage over gaseous fuels. However, in contrast to gaseous fuels, alcohols need to be extracted from the aqueous broth, reducing the overall efficiency of the process. Also, the heating value of methane per mass is almost two times higher than that of ethanol (29.7 MJ/kg) and 1.5 times that of butanol (36.7 MJ/kg). Therefore, methane-containing fuels still have the potential to be widely applied in industry in the future, and are expected to be good replacements for fossil transportation and jet fuels (Adlunger et al., 2016; Edwards et al., 2004) .

Conventional processes for biogas production from biomass are often limited by the poor degradation potential of its lignocellulosic fraction (table 1), losing a large fraction of the initial energy stored and resulting in an overall chemical efficiency between 20 and 40% (McKendry, 2002). Extensive pre-treatment methods, such as thermal pressure hydrolysis or enzyme addition, have to be applied to access the bulk part of the biomass efficiently (Weiland, 2010). The final biogas composition can contain large fractions of CO_2, thus requiring the gas to be cleaned or upgraded before injection into the gas grid is possible. Cleaning and upgrading of biogas can be done in various ways, such as CO_2 fixation by hydrogenotrophic methanogens or using CO_2-fixing phototrophs (Muñoz et al., 2015). However, upgrading of biogas can often not be carried out in the anaerobic digester, and thus requires additional process steps to obtain an applicable gas. Despite biogas upgrading being possible, conversion of tough substrates such as lignin or the utilization of more recalcitrant wastes via anaerobic digestion remains difficult.

The biological conversion of syngas as described here requires gasification as the main pre-treatment step (table 1). Interestingly, not only biomass can be fed to gasifiers, but other poor-quality carbon-containing streams, e.g. municipal waste, excess sludge, can also be supplied as a starting source. The feasibility of production of methane from renewable syngas is debatable as methane is a relatively low value

Table 1. Overview of different processes capable of converting renewable biomass to methane gas

	Anaerobic digestion	**Syngas bio-methanation**	**Syngas methanation**
Pre-treatment	Mechanical, Chemical, Biological	Gasification	Gasification
Conversion mechanism	Saccharolysis, acidogenesis, methanogenesis	Hydrogenogenesis, methanogenesis	Chemical methanation
Catalyst	Biological (undefined mixed culture)	Biological (defined (co)-culture)	Metal catalysts (e.g. nickel)
Disadvantages	Low substrate conversion efficiency High CO_2 content in outlet (up to 50%) Relatively low production rates	Low production rates compared to chemical conversion Outlet gas not completely free of CO_2, CO and H_2	Sensitive to different syngas compositions Sensitive to syngas impurities Relatively expensive catalysts Outlet gas not completely free of CO_2, CO and H_2
Advantages	Relatively robust and cheap process Can convert dilute organic wastes (e.g. organic rich wastewater)	Cheap, self-replicating catalysts Good production rate for a biological system High methane content in a single step. Robust for different syngas compositions Tolerance to syngas pollutants	High production rates High methane content in a single step
Gas composition	CH_4, CO_2	CH_4, H_2, CO_2, CO	CH_4, H_2, CO_2, CO
Chemical efficiency[1]	20-40% (McKendry, 2002)	N.D.	50-70% (wood to SNG) (Duret et al., 2005; van der Meijden et al., 2010)

[1]Energy of the product compared to the energy content of the original feedstock.

In contrast to biomethanation, the chemical methanation process requires an obligate gas composition with a H_2:CO ratio of 3 or higher in order to produce methane efficiently (Kopyscinski et al., 2010). Renewable syngas composition can vary widely based on the starting material used, and additionally often contain high amounts of impurities. Strong gas purification and fine-tuning are thus required to operate the chemical process. The strong exergonic nature of the methanation reaction generates heat, which can be reused in the chemical process to generate steam. The biological methanation does not generate high potential heat streams, but does also not require steam in order to perform the methanation process. Additionally, heat originating from the gasification process might be used in biomass drying, closing part of the energy loop. Also, depending on the heat generation of the microbial system, heating of the reactor might be required as it is operated at thermophilic temperatures. Total energy requirement of the bioreactor on large scale depends on its type and exact size, making it difficult to currently state anything on this or its economic feasibility compared to the chemical process. The biological process described here uses a self-replicating catalyst, making growth medium the main requirement to sustain the bio-catalysts. Additionally, the biological catalyst is expected to be less prone to inhibition by sulphur compounds, and might even use those as growth supplements, and thus is expected to require less stringent syngas purification before application (Daniell et al., 2012). The chemical process has a higher production rate compared to the biological process, but the robustness of the biological system is advantageous. Additionally, the study here is a proof of concept and does not yet involve major process optimizations. The bio-methanation of syngas can likely be improved further in terms of production rates and efficiency, by factors such as medium optimization, reactor configuration and biomass retention. Also tests with different co-culture combinations or defined mixed cultures might improve the overall culture performance.

Conclusion

This study shows that by using a defined co-culture of *C. hydrogenoformans* and *M. thermoautotrophicus* it is possible to convert CO-rich gases to methane at high efficiency and high rate in a conventional CSTR bioreactor without gas recycling. In contrast to anaerobic digestion of biomass, this syngas route utilises the full carbon spectrum of the initial material, can process recalcitrant carbon wastes and can generate a gas with a high content of methane in a single process step. Compared to chemical methanation of syngas, the biological processes are relatively slow. However, the robustness of the biological catalysts compared to the relatively expensive metal catalysts is an advantage. Further research is required to assess the (economic) feasibility of a biological syngas methanation system, which in the future might be used as an addition to or alternative for current methane production processes.

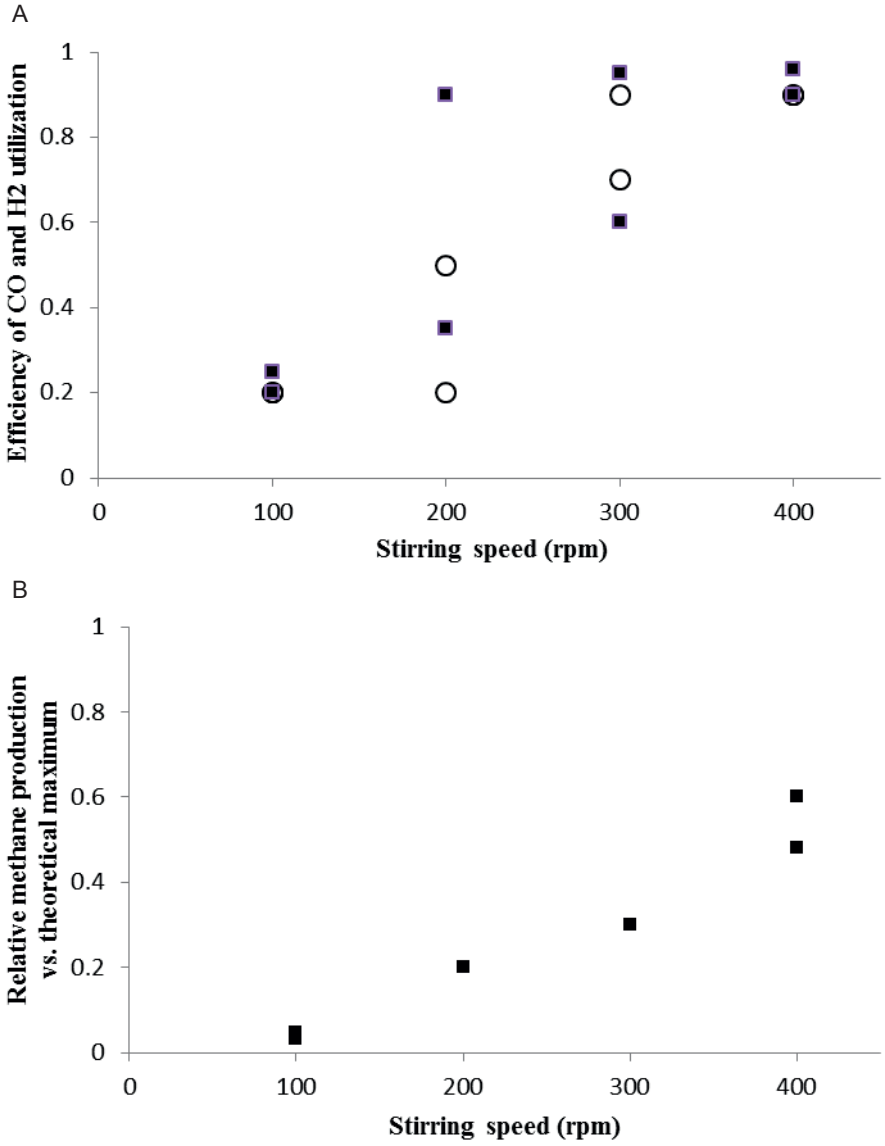

Supporting information S1. Methane production rate of the methanogenic co-culture in batch bioreactors at different stirring speeds. A) efficiency of CO and H_2 utilization vs. stirring speed. B) Relative methane production expressed as fraction of the theoretical maximum.

Chapter 5

Production of medium-chain fatty acids and higher alcohols by a synthetic co-culture grown on carbon monoxide or syngas

Authors: Martijn Diender, Alfons J.M. Stams and Diana Z. Sousa

Chapter has been published as:

Diender, M., Stams, A. J. M., and Sousa, D. Z. (2016b). Production of medium-chain fatty acids and higher alcohols by a synthetic co-culture grown on carbon monoxide or syngas. Biotechnol. Biofuels 9. doi:10.1186/s13068-016-0495-0.

Abstract

Background: Synthesis gas, a mixture of CO, H_2 and CO_2, is a promising renewable feedstock for bio-based production of organic chemicals. Production of medium-chain fatty acids can be performed via chain elongation, utilizing acetate and ethanol as main substrates. Acetate and ethanol are main products of syngas fermentation by acetogens. Therefore, syngas can be indirectly used as a substrate for the chain elongation process.

Results: Here we report the establishment of a synthetic co-culture consisting of *Clostridium autoethanogenum* and *Clostridium kluyveri*. Together, these bacteria are capable of converting CO and syngas to a mixture of C4 and C6 fatty acids and their respective alcohols. The co-culture is able to grow using solely CO or syngas as a substrate, and presence of acetate significantly stimulated production rates. The co-culture produced butyrate and caproate at a rate of 8.5 ± 1.1 mmol/l/day and 2.5 ± 0.63 mmol/l/day, respectively. Butanol and hexanol were produced at a rate of 3.5 ± 0.69 and 2.0 ± 0.46 mmol/l/day, respectively. The pH was found to be a major factor during cultivation, influencing the growth performance of the separate strains and caproate toxicity.

Conclusion: This co-culture poses an alternative way to produce medium-chain fatty acids and higher alcohols from carbon monoxide or syngas and the process can be regarded as an integration of syngas fermentation and chain elongation in one growth vessel.

Introduction

Over the last decade, synthesis gas (syngas) fermentation has gained attention because of its potential to convert a large variety of waste materials to bio-based chemicals (Dürre and Eikmanns, 2015). Additionally, it is possible to convert pure CO_2 and water into syngas via high temperature co-electrolysis, which can be supplied with electricity and heat derived solely from solar power (Frost et al., 2010).

Syngas fermentation to acetate and ethanol is relatively well studied, and the array of possible products is rapidly expanding (Latif et al., 2014). Bio-based production of medium-chain fatty acids (MCFA), such as butyrate and caproate, is of potential interest because they can serve as commodity chemicals. Additionally, their respective alcohols - butanol and hexanol - could serve as potential biofuels. Butyrate has been shown to be produced naturally from CO by *Eubacterium limosum* (Jeong et al., 2015) and *Butyribacterium methylotrophicum* (Worden et al., 1989). Additionally, a pure culture of *Clostridium carboxydivorans* formed butyrate and caproate from CO after medium optimization (Phillips et al., 2015). Production of higher alcohols from syngas has been reported for genetically engineered clostridia (Berzin et al., 2013;

Köpke et al., 2010), mixed-cultures fed with butyrate, caproate and syngas (Liu et al., 2014a, 2014b), and several pure cultures of carboxydotrophic bacteria (Fernández-Naveira et al., 2016; Perez et al., 2013; Ramió-Pujol et al., 2015). Genetic engineering is one of the approaches to enhance strain production capabilities because most of the wild type strains have low production rates and yields. For clostridia, the most anticipated syngas biocatalysts, genetic systems are being quickly developed (Cho et al., 2015). However, despite recent developments, options to perform metabolic engineering in carboxydrotrophs are still rather limited.

Here we report the use of a synthetic co-culture of *Clostridium autoethanogenum* (DSM 10061) and *Clostridium kluyveri* (DSM 555) to convert CO or syngas into MCFA and their respective alcohols. *C. autoethanogenum* is one of the model organisms for syngas metabolism and is known for its excellent properties to convert CO or syngas to ethanol and acetate (table 1) (Abrini et al., 1994). *C. kluyveri* is found in ruminal environments (Weimer and Stevenson, 2012), and was reported to stimulate production of MCFA in the rumen (Weimer et al., 2015). It also represents a major fraction of microorganisms in systems performing chain elongation (Zhang et al., 2013). *C. kluyveri* is well known for its reversed β-oxidation metabolism, converting short chain fatty acids with ethanol into MCFA and hydrogen (table 1). We hypothesize that a co-culture approach might become an upcoming route to produce MCFA from syngas. Besides, it could also serve as a model and provide insight in how the carboxylate platform, operated with mixed cultures, performs using syngas as electron donor.

Table 1. Summary of reactions performed by *C. autoethanogenum* and *C. kluyveri*. Xn displays a saturated carbon chain of length n. Reaction stoichiometry of butyrate and caproate formation might differ based on the concentrations of substrates available.

	Product	Reaction
Clostridium autoethanogenum	Acetate	$4\ CO + 2\ H_2O \rightarrow CH_3COO^- + H^+ + 2\ CO_2$
	Ethanol	$6\ CO + 3\ H_2O \rightarrow C_2H_5OH + 4\ CO_2$
	Alcohols indirect	$2\ CO + H_2O + X_n\text{-}COOH + H^+ \rightarrow X_n\text{-}CH_2OH + 2\ CO_2$
Clostridium kluyveri	Butyrate	$6\ C_2H_5OH + 4\ CH_3COO^- \rightarrow 5\ C_3H_7COO^- + H^+ + 3\ H_2O + 2\ H_2$
	Caproate	$6\ C_2H_5OH + 5\ C_3H_7COO^- \rightarrow 5\ C_5H_{11}COO^- + CH_3COO^- + H^+ + 3\ H_2O + 2\ H_2$

Material and Methods

Microorganisms and cultivation

Clostridium autoethanogenum (DSM 10061) and *Clostridium kluyveri* (DSM 555) were purchased from the DSMZ strain collection (Braunschweig, Germany). *C. autoethanogenum* and *C. kluyveri* were initially cultivated in DSM-640 and DSM-

52 medium, respectively. For co-cultivation a new medium was designed containing (per liter of medium): 0.9 g NH_4CL, 0.9 g NaCl, 0.2 g $MgSO_4$ * 7 H_2O, 0.75 g KH_2PO_4, 1.94 g K_2HPO_4 * 3 H_2O, 0.02 g $CaCl_2$ and 0.5 mg resazurin. The medium was supplemented with the following trace-elements (per liter of medium): 1.5 mg $FeCl_2$ * 4 H_2O, 0.025 mg $FeCl_3$ * 6 H_2O, 0.070 mg $ZnCl_2$, 0.1 mg MnCl * 4 H_2O, 0.006 mg H_3BO_3, 0.190 mg $CoCl_2$ * 6 H_2O, 0.002 mg $CuCl_2$ * 2 H_2O, 0.024 mg $NiCl_2$ * 6 H_2O and 0.056 mg Na_2MoO_4 * 2 H_2O, 0.0035 mg, Na_2SeO_3 and 0.2 mg Na_2WO_4. The medium was boiled and cooled on ice under N_2 flow, after which 0.75 g L-cysteine was added per liter of medium as reducing agent. Unless stated otherwise the pH was set to 6 using NaOH and HCl. Reduced medium was dispensed, under continuous N_2 flow, into bottles that were immediately capped with rubber stoppers and aluminium caps. The headspace was filled with the desired gas (e.g., CO, H_2/CO_2) to a final pressure ranging from 100 to 150 kPa, depending on the experiment. Bottles were autoclaved immediately after preparation. Before inoculation, the medium was further supplemented with a vitamin solution in a 1:50 dilution, containing per liter: 1 mg biotin, 10 mg nicotinamid, 5 mg p-aminobenzoic acid, 10 mg thiamin, 5 mg panthothenic acid, 25 mg pyridoxamine, 5 mg cyanocobalamine and 5 mg riboflavine. Yeast extract, trypticase peptone, ethanol and acetate were added from sterile stock solutions. Initial incubations for co-cultivation were done at an amount of 1 g yeast extract and 1 g peptone per liter of medium. Subsequent transfers and characterization experiments were performed in presence of 0.5 g/l yeast extract and in absence of peptone. Unless stated otherwise cultivation was done non-shaking at 37 °C. Unless stated otherwise, pure cultures were incubated as follows: *C. kluyveri* was grown with 90 mM ethanol and 80 mM acetate in presence of 10 kPa CO_2 and *C. autoethanogenum* was grown with 130 kPa CO as sole substrate.

Co-culture experiments

Initial co-culture experiments were performed in 250 ml bottles with 70 ml liquid phase. *C. autoethanogenum* and *C. kluyveri* were transferred from actively growing cultures in exponential phase to the designed medium. Pre-cultures of *C. autoethanogenum* were incubated at 150 rpm shaking in presence of 80 mM acetate under a headspace of 100 kPa CO and 50 kPa H2. Pre-cultures of *C. kluyveri* were grown non-shaking in absence of CO. After detection of growth in both pure cultures, 35 ml of each culture was inoculated into the other culture, initiating the co-cultivation. Immediately after initiation of co-cultivation, the headspace of the CO and H_2 containing bottles was re-pressurized with CO and H_2. In bottles initially containing no CO or H_2, 50 kPa CO was added. The bottles were further incubated non-shaking at 37 °C. After detection of growth of both organisms in the co-cultures via liquid and gas profile analysis and microscopic observation, 0.5 ml of the co-cultures was transferred to new 250 ml bottles containing 70 ml medium with 80

mM acetate and a 130 kPa CO. The co-culture was further maintained under these conditions, requiring transfer every 14 days.

All characterization tests were performed using 120 ml bottles containing 35 ml liquid. For tests requiring acetate, butyrate or caproate, stock solutions were used which were made anaerobic via N_2 flushing and set at pH 6 using NaOH and HCl. In case of re-addition of CO during the experiment, 4 cycles of flushing with pure CO were applied, using a 0.22 μm filter to keep the gas flow sterile. When assessing the effect of shaking conditions, 150 rpm shaking was applied in all cases. For characterizing the production profile in presence of excessive amounts of CO, bottles with 1140 ml total volume were used, containing 100 ml medium and a 110 kPa CO headspace. Culture inoculation was done in 1:100 ratio with an actively growing co-culture. The bottles were initially incubated non-shaking and shaking was applied after ethanol-limited butyrate production became apparent. Product and substrate profiles were in all cases assessed using HPLC and GC.

Analytical techniques

Liquid phase composition was analysed via high pressure liquid chromatography equipped with a MetaCarb 67H column (Agilent Technologies, Santa Clara, CA). The column was operated at a temperature of 45 °C with a flow rate of 0.8 ml/min. Detection was done via a RI and UV detector. 0.01 N H_2SO_4 was used as eluent. In all cases, samples of 0.5 ml were taken and immediately centrifuged at 13000 g. Subsequently 0.4 ml supernatant was added to 0.6 ml 10 mM DMSO in 0.1 N H_2SO_4. Concentrations below 0.3 mM could not accurately be quantified and are further referred to as trace amounts.

For gas analysis, gas samples of 0.2 ml were taken with a 1 ml syringe and analyzed in a Compact GC 4.0 (Global Analyser Solutions, The Netherlands). CO and H_2 were measured using a molsieve 5A column operated at 100 °C coupled to a Carboxen 1010 pre-column. CO_2 was measured using a Rt-Q-BOND column operated at 80 ºC. Detection was in all cases done via a thermal conductivity detector.

Model fitting and production rate estimation

Production rates of the co-culture were estimated by nonlinear data fitting to a modified Gompertz model (Eq.1) (Zwietering et al., 1990). To estimate the net production rates, the derivative of the modified Gompertz model was used (Eq.2), in which A represents the maximal concentration of product reached (mM), V_m indicates the maximal volumetric production rate (mmol/l/day) and γ is a representation of the lag time before production occurs (days). Standard errors of the determined parameters were translated to standard errors of the production rate via error propagation.

$$f(t) = Ae^{-e^{\frac{V_m e}{A}(\gamma - t)+1}} \quad (1)$$

$$f'(t) = eV_m e^{-e^{\frac{V_m e}{A}(\gamma - t)+1}} e^{\frac{V_m e}{A}(\gamma - t)+1} \quad (2)$$

Results

C. autoethanogenum and *C. kluyveri* both grew efficiently in the designed medium. *C. autoethanogenum* grown on CO/H_2 formed acetate and ethanol, and chain elongated products were not formed (figure 1A). Pure cultures of *C. kluyveri* utilized ethanol and acetate as substrate, forming butyrate, caproate and hydrogen as end-products. Introduction of 50 kPa CO in pure cultures of *C. kluyveri* inhibited its activity (figure 1B). Some chain elongated products accumulated, but consumption of acetate and ethanol halted before they were depleted. Upon initiation of co-

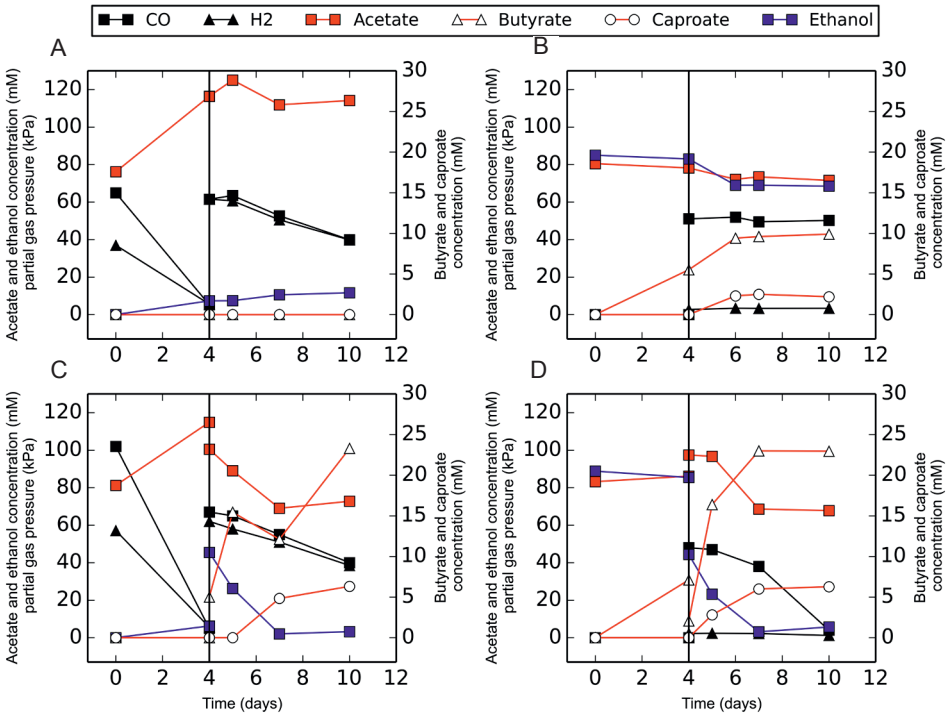

Figure 1. Co-culture establishment. (A) Production profile of *C. autoethanogenum* grown with CO and H_2, the headspace was refilled with H_2/CO at t = 4. (B) Production profile of *C. kluyveri*, at t = 4, 50 kPa CO was introduced to the culture. (C) A pure culture of *C. autoethanogenum* mixed in a 1:1 ratio with a pure culture of *C. kluyveri* at t = 4. (D) A pure culture of *C. kluyveri* mixed in a 1:1 ratio with a pure culture of *C. autoethanogenum* at t = 4. The legend is representative for all displayed graphs. Solid and open circle symbols represent left and right y-axis, respectively.

cultivation by adding both monocultures together in 1:1 ratio, carboxydotrophic and chain elongating activity was observed (figure 1 C/D). Trace amounts of butanol and hexanol were detected in the co-culture, while these compounds were not observed in any of the monocultures incubated with CO, acetate and ethanol. Co-cultures could be maintained and transferred stably by incubating non-shaking under CO or CO/H_2 headspace in presence of 80 mM acetate (figure 2). The co-culture was capable of growing efficiently with 0.5 g/l yeast extract. Lower concentrations of yeast extract had a strong negative effect on the production rates, and significantly increased the lag phase. Studies have shown that it is possible to grow both Clostridium strains in absence of yeast extract after an adaptation period (Bornstein and Barker, 1948; Martin et al., 2016). However, as the main focus of this study was on establishing co-cultivation, it was chosen to keep the yeast extract at 0.5 g/l to ensure non-stringent growth conditions for both organisms. A pH range from 7 to 4 was tested to assess the co-culture tolerance, yielding a functional co-culture between a pH of 6.5 and 5.5. The production profile was similar within this pH range, and thus a pH of 6 was selected for subsequent incubations.

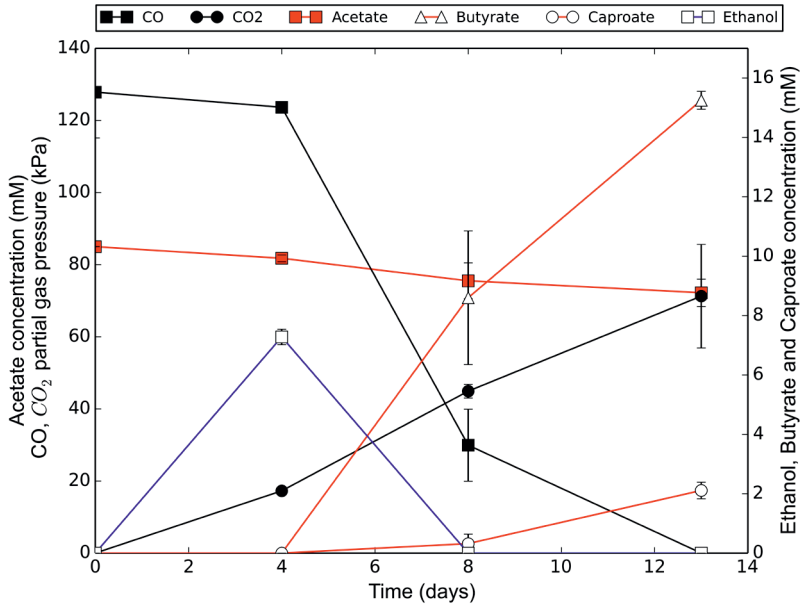

Figure 2. Standard production profile of the co-culture in non-shaking conditions. On all data series a standard deviation is displayed over duplicate experiments. Solid and open circle symbols represent left and right y-axis, respectively.

Effect of organic acid concentrations

Increasing initial acetate concentration in the medium, from 0 to 80 mM, resulted in a significant increase in butyrate production (figure 3). Co-cultures incubated without initial addition of acetate did grow, but were significantly slower and showed a lower butyrate yield after consuming the full CO headspace. Caproate production was not affected by the initial acetate levels. The effect of different initial butyrate concentrations was tested in a range of 0-45 mM, of which the highest concentration is triple the amount reached under the standard incubation conditions (figure 2). No toxicity effects on the co-culture were observed in this range. However, butanol production was observed with increasing butyrate concentrations, reaching levels up to 6 mM when 45 mM butyrate was initially present. Initial caproate concentrations ranging from 0 to 35 mM were tested. Increasing caproate concentrations resulted in a longer lag phase, suggesting toxicity effects. Co-cultures incubated with initial caproate concentrations above 12 mM did not grow after 16 days of incubation, whereas controls initiated growth within the first four days of incubation. In cultures with 12 mM caproate, hexanol reached concentrations of 2.5 mM at the end of cultivation. Additionally, monocultures of C. autoethanogenum incubated with CO in presence of initial butyrate or caproate formed butanol or hexanol, respectively.

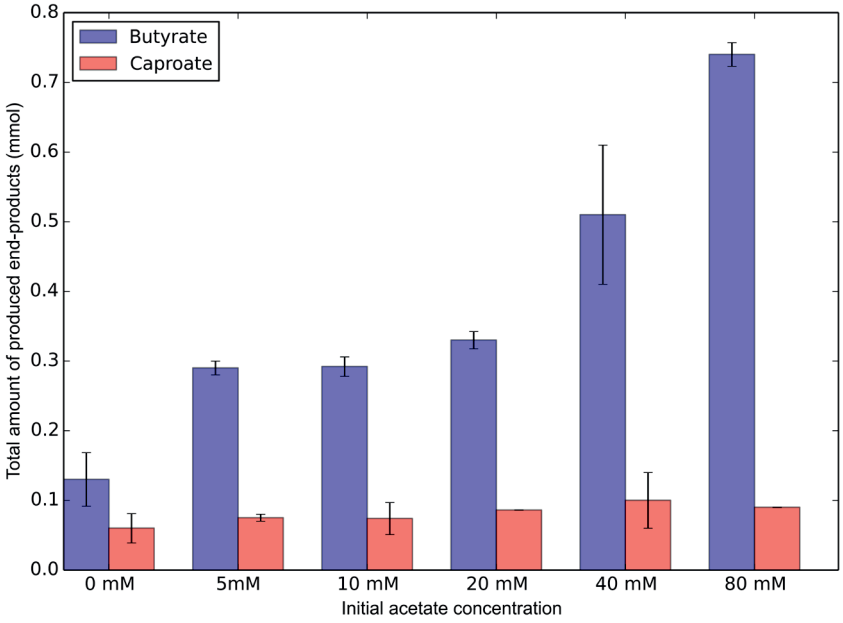

Figure 3. Effect of initial acetate concentration on the production of MCFAs. Data displayed is representative for 13 days after incubation using 130 kPa CO as a substrate. At the end of cultivation CO was depleted in all cultures. On all graphs a standard deviation is displayed over duplicate experiments.

Effect of gas composition

To assess if syngas could be a potential donor for the co-culture, the effect of different H_2/CO ratios was tested under non-shaking conditions (figure 4). Hydrogen and CO were co-utilized and resulted in similar end-products as from CO alone. Incubations with 80:20 H_2/CO_2 sustained the co-culture (figure 4d), producing butyrate, but no caproate. Additionally, production rates and end-concentrations were lower when compared with incubations with H_2/CO. Co-cultures under a H_2/CO_2 headspace utilized both gases, and after CO_2 depletion consumption of H_2 stopped. Cultures with a higher CO/H_2 ratio produced relatively more chain elongated products, compared to cultures containing relatively less CO (figure 4e). Additionally, cultures with higher CO/H_2 ratio utilized more acetate per mole of gas consumed (figure 4f).

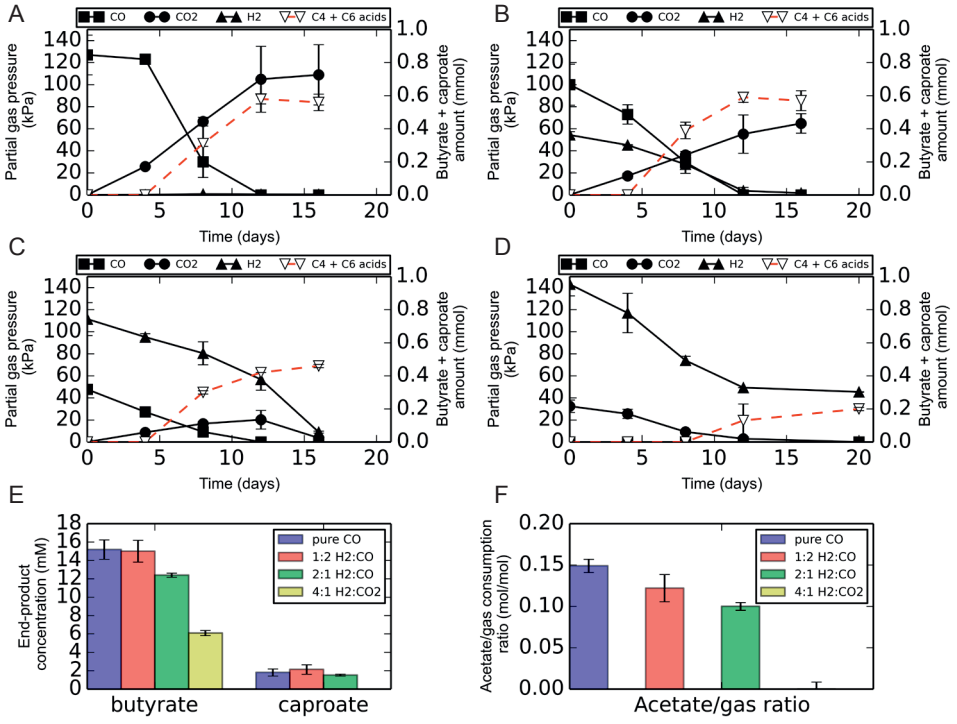

Figure 4. The effect of H_2:CO ratio on the production profile of the co-culture. (A) Pure CO headspace. (B) 1:2 ratio of H_2/CO (C) 2:1 ratio of H_2:CO. (D) H_2/CO_2 headspace. (E) Product concentrations at the end of incubation. (F) Mole of acetate consumed per mole of gas (H_2 + CO) consumed. On all graphs a standard deviation is displayed over duplicate experiments. Solid and open circle symbols represent left and right y-axis, respectively.

Enhancing productivity of the co-culture

Co-cultures put under shaking conditions initially produced ethanol and acetate, but did not show butyrate and caproate formation (figure 5a). Instead, these incubations converted ethanol back to acetate upon reaching low CO pressures in the headspace. Cultivation with a CO-pressure maintained above 50 kPa during shaking cultivation resulted in less oxidation of ethanol back to acetate (figure 5b). The fact that no MCFA were produced indicates that *C. kluyveri* activity is inhibited. Re-oxidation of ethanol to acetate at the end of the experiment is likely performed by the metabolically active *C. autoethanogenum*. Initiating co-cultivation under non-shaking conditions, followed by transfer to shaking conditions after butyrate production was detected, resulted in a functional co-culture (figure 5c).

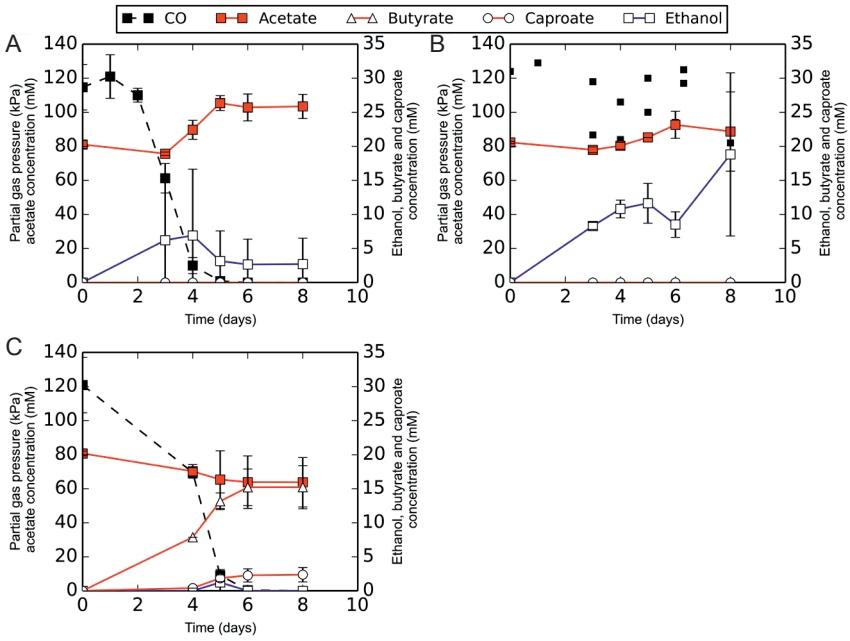

Figure 5. Effect of shaking and CO pressure on the co-culture. (A) production profile under shaking conditions. (B) production profile with maintained CO pressure (>50 kPa), under shaking conditions. (C) production profile after initial non-shaking incubation and subsequent transfer to shaking conditions (after t = 4). On all data series a standard deviation is displayed over duplicate experiments. Solid and open circle symbols represent left and right y-axis, respectively.

Production potential of the co-culture under CO-excess and shaking conditions was tested. During the non-shaking phase of incubation, mainly butyrate and caproate were produced (figure 6 A, B, C). Upon applying shaking conditions, production of these products further increased and additionally production of butanol and hexanol was observed. MCFAs or alcohols with a length longer than C6 were not detected.

After two days of shaking, the pH of the culture had increased from 6.0 to 7.2. After this point, CO-consumption rates declined and production rates dropped. Eventually, production stopped before CO had been depleted. In order to assess the production rates of the co-culture, the data was fitted to a modified Gompertz-equation (Zwietering et al., 1990). As butyrate can act as acceptor molecule in caproate formation and both acids are precursors for their respective alcohols, their total production is masked by the production of other compounds as displayed by Eq. 3 and 4. The estimated total product concentrations were fitted to the model (figure 6D, table 2). The derivative of the obtained Gompertz equation (Eq. 2) was used to estimate the total volumetric production rates of each of the compounds in time (figure 6E). The net volumetric production rate was approximated by compensating the total volumetric production rate for the volumetric production rate of subsequent products (figure 6F).

$$[\text{butyrate}]_{\text{total}} = [\text{butyrate}]_{\text{observed}} + [\text{caproate}]_{\text{observed}} + [\text{butanol}]_{\text{observed}} + [\text{hexanol}]_{\text{observed}} \quad (3)$$

$$[\text{caproate}]_{\text{total}} = [\text{caproate}]_{\text{observed}} + [\text{hexanol}]_{\text{observed}} \quad (4)$$

The maximal production rate for butyrate is approximately 8.5 ± S.E 1.1 mmol/l/day. Caproate reaches a maximal net production rate of 2.5 ± S.E 0.63 mmol/l/day. Butanol and hexanol are the last to be formed at maximal production rates of 3.5 ± S.E 0.69 and 2.0 ± S.E 0.46 mmol/l/day, respectively.

Table 2. Gompertz model parameter estimates for the produced products, A (maximal concentration reached), Vm (maximal volumetric production rate) and γ (lag phase) represent the parameters displayed in Eq 1 and 2. Standard errors are indicated in brackets.

	Butyrate	Caproate	Butanol	Hexanol
A (mM)	25.8 (±0.24)	10.0 (±0.25)	5.73 (±0.12)	4.01 (±0.16)
Vm (mmol/L/day)	10.4 (±0.80)	2.86 (±0.31)	3.47 (±0.69)	1.98 (±0.46)
γ (days)	2.99 (±0.11)	3.69 (±0.19)	4.28 (±0.18)	4.95 (±0.26)

Discussion

The co-culture of *C. autoethanogenum* and *C. kluyveri* is capable of converting CO or syngas to a mixture of C4 and C6 fatty acids and their respective alcohols. Monocultures of *C. kluyveri* are unable to utilize CO and its metabolism is even inhibited by it. Nonetheless, activity of *C. kluyveri* is observed in the co-culture in presence of 130 kPa CO. *C. autoethanogenum* likely facilitates growth of *C. kluyveri*, by removing CO from the liquid. This is analogous to the theorized role of thermophilic carboxydotrophs in volcanic environments, creating a niche for non-CO-tolerant organisms (Techtmann et al., 2009). This additionally explains the inability

of the co-culture to grow instantly in shaking conditions. Low biomass levels at the start combined with increased CO mass transfer under shaking conditions, cause inhibition of *C. kluyveri*, resulting in growth of *C. autoethanogenum* only (figure 5). Cultivation under non-shaking conditions allows both organisms to initiate growth, eventually allowing shaking conditions.

Effect of environmental factors on co-culture functionality

Ethanol is the driving compound for chain elongation, making it a key intermediate in the co-culture. Its production is observed at the start of cultivation, but concentrations quickly decrease to levels below the detection limit when butyrate and caproate were formed (figure 2, 6B). This suggests that ethanol production is the limiting factor for

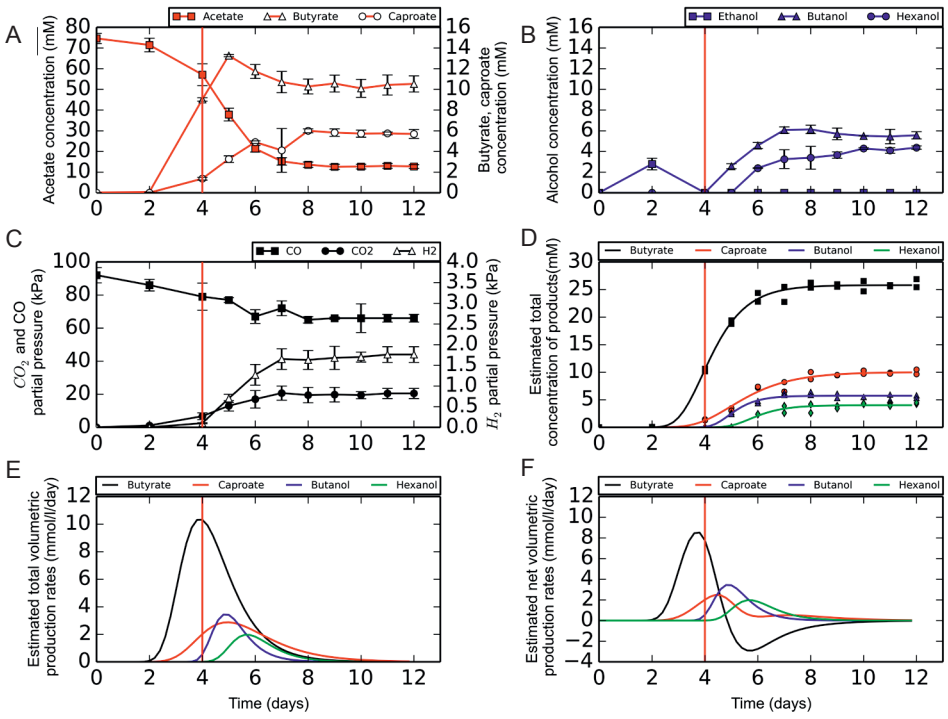

Figure 6. Co-cultivation under excess CO conditions. Shaking was applied after 4 days (red vertical line). (A) Acid concentration profile. (B) Alcohol concentration profile. (C) Partial gas pressures of CO, CO_2 and H_2. (D) Estimated total concentration of products formed, approximated by a Gompertz equation. (E) Total estimated volumetric production rates displayed as the derivative of the Gompertz equation. (F) Estimated net volumetric production rates after compensation of product formation and consumption according to Eq. 3 and Eq. 4. Solid and open circle symbols represent left and right y-axis, respectively.

chain elongation. Several environmental factors were expected to increase ethanol production of the carboxydotrophic strain. Two of these factors are lowering of pH and decreasing concentration of yeast extract (Abubackar et al., 2012). However, we observed no clear differences in production within the tested range of viable pH and yeast extract concentrations of the co-culture.

Ethanol production in acetogenic carboxydotrophs can occur directly via acetyl-CoA or indirectly via acetate (Köpke et al., 2010, 2011a). When *Clostridium ljungdahlii* is grown on CO it expresses an aldehyde oxidoreductase (AOR), required for the indirect ethanol production pathway. Upon addition of external acids, AORs were found more abundantly expressed, indicating upregulation of the indirect alcohol production pathways (Xie et al., 2015). In the co-culture we observed increased butyrate production upon addition of acetate (figure 3), which indirectly indicates that ethanol production is stimulated. Similarly, the presence of butyrate or caproate, stimulated the production of their respective alcohols. This suggests that, as observed in pure cultures of *C. ljungdahlii* (Perez et al., 2013; Xie et al., 2015), alcohol production in this co-culture is stimulated by the presence of their respective acids. This could be a stress response to the presence of relatively more acids in the undissociated form, which can be considered toxic, stimulating conversion to their respective alcohols. Additionally, the acids could act as an electron sink, to counter the strong reducing pressure of CO, which would explain the formation of relatively more alcohols in the shaking cultures (figure 6b). Presence of high concentrations of acetate thus serves a double purpose: i) substrate for chain elongation and ii) stimulation of the formation of ethanol. The co-culture was functional in absence of acetate, indicating that the synthetic community can sustain itself on purely CO as a substrate. However, production rates under these conditions were significantly lower.

When incubating instantly under shaking conditions, the oxidation of ethanol to acetate was observed when CO became depleted (figure 5a). As no chain elongation activity is observed, *C. autoethanogenum* appears responsible for the ethanol oxidizing activity, potentially utilizing it as an alternative electron donor to produce acetate. Such a metabolism was observed for the acetogen *Acetobacterium woodii*, utilizing ethanol for production of acetate (Bertsch et al., 2016). Oxidation of ethanol to acetate by *C. autoethanogenum* was partly suppressed under maintained CO pressure (figure 5B). The maintained CO pressure potentially causes the cells to be more reduced, forcing the reaction towards production of ethanol to maintain proper redox balance.

When applying syngas technology, all the gas is preferably converted to soluble products, leaving no CO_2 in the exhaust gas. Presence of hydrogen in the headspace

allows for additional fixation of CO_2, which makes hydrogen an interesting component to completely remove CO without CO_2 exhaust. Under the tested conditions, a 2:1 ratio of H_2:CO appears to be close to optimal as almost all the gaseous compounds are converted to soluble products after depletion of electron donor, releasing no net CO_2 (figure 4c). However, the amount of chain elongated products formed is slightly decreased under these conditions as larger amounts of H_2 appear to be required to obtain similar results as with CO (figure 4e). This might be related to the lower redox potential of CO (E_0' = -520 mV) compared to hydrogen (E_0' = -414 mV). This allows for production of relatively more reduced products such as ethanol (Bertsch and Müller, 2015a; Diender et al., 2015, **Chapter 2**; Hurst and Lewis, 2010), which can subsequently be used as substrate for chain elongation. At lower CO/H_2 ratios, formation of ethanol is expected to be less favourable, resulting in relatively more acetate formation. This is supported by the lowered net amount of acetate consumed per mole of gas used (figure 4f).

Co-culture limitations

In cultures incubated under shaking conditions with excess CO, more acetate is consumed than is required for chain-elongation (figure 6, table 1). This suggests that acetate is mainly converted to ethanol. This is supported by the observation that a major part of the oxidized CO can be found back as CO_2 (figure 6c), indicating that CO mainly acts as an electron donor for the reduction of acetate to ethanol (table 1). This rapid conversion of acetate to ethanol and the production of higher alcohols from the generated medium-chain fatty acids (figure 6b), likely caused the observed pH increase from 6.0 to 7.2. *C. autoethanogenum* was reported to grow in a pH range of 4.5 to 6.5 with an optimum of 6 (Abrini et al., 1994). *C. kluyveri* was reported to grow within a pH range of 6.0 to 7.5 with an optimum of 6.8 (Barker and Taha, 1941). The pH reached during co-cultivation exceeds 6.5 and thus likely causes inhibition of *C. autoethanogenum*. Resulting in a decrease in activity of the co-culture before CO was depleted. Additionally, the pH of the medium also affects the amount of chain-elongated products that can be accumulated. Caproate toxicity is a general problem in chain elongation processes and is strongly pH dependent, as the toxicity effect is caused by the undissociated form (Steinbusch et al., 2011). A mixed culture bioreactor, fed with ethanol effluent from a syngas reactor, tolerated 3 mM caproate at pH 5.4. The undissociated fraction at this pH is 22%, which equals 0.66 mM (Vasudevan et al., 2014). Reactors operated at a higher pH or reactors with continuous removal of caproate allowed a higher accumulation and higher production rates, respectively (Agler et al., 2011; Grootscholten et al., 2013). *C. kluyveri* strain 3231B was found to accumulate caproate to levels of 110 mM at pH 6.8 (Weimer and Stevenson, 2012), which translates into an undissociated fraction of 1.3 mM. The co-culture of *C. kluyveri* and *C. autoethanogenum*, at pH 6, tolerated 12 mM caproate.

Under these conditions 7% is in undissociated form (approx. 0.88 mM), which is in the same order of magnitude of the numbers reported for other cultures.

Growth performance of the individual strains and chain elongated product toxicity are thus both strongly affected by pH. More acidic environments stimulate growth of *C. autoethanogenum*, but inhibit *C. kluyveri* and promote toxicity of caproate. A higher pH allows for higher caproate concentrations but inhibits *C. autoethanogenum*. Therefore, controlling pH between 5.5 and 6.5 appears essential for maintaining a well-performing co-culture.

Co-culture assessment and comparison

Based on the pure culture incubations, *C. autoethanogenum* produces ethanol and acetate from CO. *C. kluyveri* is not able to utilize CO. Butyrate and caproate are not observed to be generated by *C. autoethanogenum* in pure culture containing CO, ethanol, acetate or a combination of the substrates. Production of these MCFAs can thus solely be assigned to *C. kluyveri*. Pure culture incubation of *C. autoethanogenum* with CO and butyrate or caproate resulted in butanol and hexanol production. Production of these alcohols was never observed in any of the tested pure cultures of *C. kluyveri*. Hydrogen can be formed by both members of the co-culture, but appears to be only utilized by *C. autoethanogenum*. Taking these factors into account, a model system with solely CO as an input, generating butyrate, caproate, butanol and hexanol as the end products can be proposed (figure 7).

Only few reports describe microbial systems producing MCFAs and/or higher alcohols from carbon monoxide or syngas. Mixed cultures in a H_2/CO_2 fed membrane bioreactor, dominated by Clostridium species, produced fatty acids up to C8 length (Zhang et al., 2013). However, this system lacked CO in the inflow-gas, which is a major component in non-pre-treated syngas. The lower redox pressure of H_2/CO_2 compared to CO-containing syngas might be a main reason for the relatively low production rates and absence of longer chain alcohols reported in the previous system (table 3). *Clostridium carboxydivorans* is one of the organisms known to be capable of producing chain elongated acids and their respective alcohols from CO in pure culture (table 3). Production rates of the alcohols by *C. carboxydivorans* appear to increase at sub-optimal growth temperatures (Ramió-Pujol et al., 2015). The co-culture described here, currently has production rates comparable to the pure cultures of *C. carboxydivorans* (table 3). However, the functioning of the co-culture is not fully explored and several parameters can still be optimized, such as pH control, medium composition and gas composition/mass transfer. Therefore, we expect the production potential of the co-culture can be increased, potentially becoming interesting for syngas based applications.

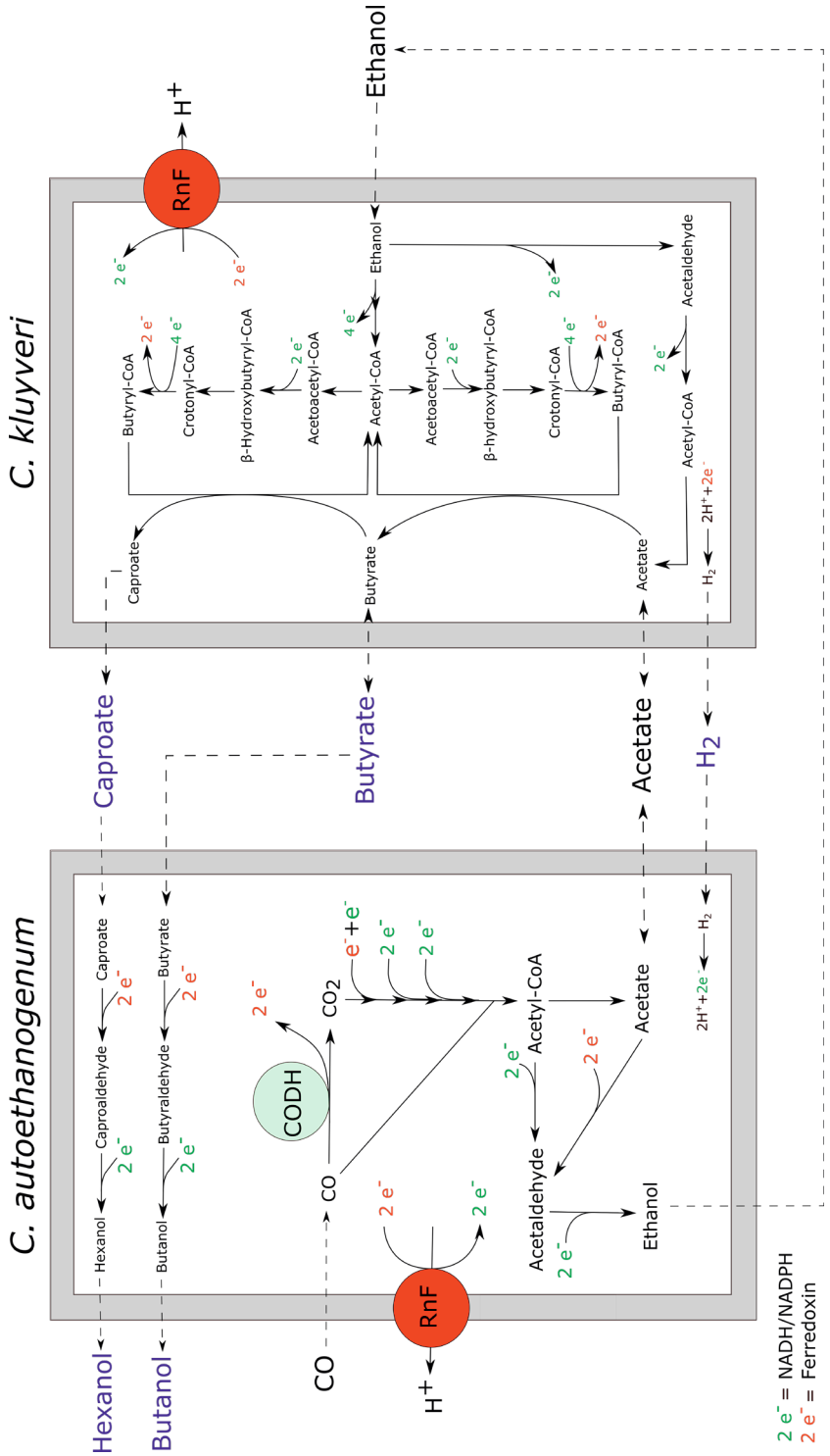

Figure 7. Schematic representation of the co-culture of *C. autoethanogenum* and *C. kluyveri*. Reaction stoichiometry and ATP yield for each of the cells are not displayed. Conversion of butyrate to butyraldehyde and caproate to caproaldehyde are assumed to proceed via an aldehyde oxidoreductase, as is observed for acetate to acetaldehyde formation. CODH: Carbon monoxide dehydrogenase, RnF: ferredoxin-NAD:oxidoreductase

Table 3. Maximal (M) and average (A) production rates (mmol/l/day) of the co-culture compared with pure- and mixed cultures generating similar end-products. Zero or negative rates are indicated N.A., not determined rates are indicates N.D.

	acetate	butyrate	caproate	ethanol	butanol	hexanol	Substrate	reference
Co-culture (M)	N.A.	8.5	2.5	N.A.	3.5	2.0	Acetate + CO	This study
Co-culture (A)[a]	N.A.	4.2	0.7	N.A.	1.4	0.9	Acetate + CO	This study
Clostridium carboxydivorans (A)[b]	0.8	0.25	0.2	3.0	1.0	0.6	$CO + H_2$	[6]
Clostridium carboxydivorans P7 (M)[c]	47	6.3	4.6	8.1	2.7	2.1	$CO + H_2$	[11]
Clostridium carboxydivorans P7 (A)[c]	2.3	0.89	0.48	1.57	0.53	0.25	$CO + H_2$	[11]
Clostridium carboxydivorans(M)[d]	N.A.	N.A.	N.D.	16.7	4.5	N.D.	CO	[12]
Mixed culture on H_2/CO_2[e]	3.25	0.65	0.26	N.D.	N.D.	N.D.	$H_2 + CO_2$	[17]

[a] Average production rates in this study were calculated over the production stage with net rates above 0.05 mmol/l/day, in this way the lag phase and inhibited phase, in which there is no significant production, are neglected.

[b] Rates were recalculated from given concentrations assuming a production phase of 360h. The data displayed represents the culture labelled as –Cu/+10 x Mo.

[c] Rates reported were originally in mmol/$g_{protein}$/hour and were here recalculated to the maximal and average volumetric production rates using the maximal and average value for the protein concentration and specific production rate reported, respectively. Data shown is taken from the culture growing at 25 °C in exponential phase.

[d] Rates were recalculated from given specific production rates in (g/$g_{biomass}$/hour). A value 0.2 g/l biomass was used for performing the recalculation.

[e] Rates were recalculated from given volumetric production rates in (mmol-C/l/day). Data displayed here represent the maximal reported production rates in different phases of the cultivation.

Conclusion

The synthetic co-culture of *C. autoethanogenum* and *C. kluyveri* is able to convert carbon monoxide and syngas to a mixture of medium-chain fatty acids and their respective alcohols. Despite the toxic effect of CO on *C. kluyveri,* chain elongation activity was found in the co-culture, indicating that CO toxicity is relieved by the presence of a carboxydotrophic organism. The culture grows without addition of ethanol and acetate, but presence of acetate significantly stimulated production. The co-culture was limited by the quickly increasing pH as a result of solventogenic reactions. Additionally, caproate concentration can be an inhibitory factor, of which the toxicity effect is a trade-off between pH and concentration. Overall this co-culture is a proof-of-principle that the carboxylate and syngas platform can be integrated in one growth vessel, and could become a promising way to enhance production of MCFAs and their respective alcohols from syngas.

Chapter 6

Clostridium kluyveri drives carboxydotrophic growth of *Clostridium autoethanogenum* to ethanol production

Authors: Martijn Diender, Ivette Parera Olm, Jasper J. Koehorst, Marten Gelderloos,

Peter J. Schaap, Alfons J.M. Stams & Diana Z. Sousa

Abstract

Syngas fermentation gets increased attention due to its potential to convert recalcitrant wastes and industrial off-gases to fuels and commodity chemicals. Applying synthetic microbial communities can be used to enhance the performance of fermentation and broaden the product spectrum. A co-culture of *Clostridium autoethanogenum*, a carboxydotroph, and *Clostridium kluyveri*, performing reverse β-oxidation, was previously shown to convert CO or syngas ($CO+H_2$) to butyrate and caproate. Here, we describe how the co-culture can be optimized. Monocultures of *C. autoethanogenum* grown in a CO-fed chemostat produced acetate and traces of ethanol, shuttling >99% of the electrons to acetate. During co-cultivation with *C. kluyveri* 30-40% of the electrons were shuttled to ethanol, indicating that *C. kluyveri* strongly affects the metabolism of *C. autoethanogenum*. Comparison of transcriptome data of *C. autoethanogenum* in mono- and co-culture showed that the central carbon and energy metabolism of *C. autoethanogenum* remained unaltered. Further experiments indicated that continuous removal of ethanol by *C. kluyveri* keeps production of ethanol thermodynamically more favourable than acetate production. This mechanism results in higher substrates to product efficiencies and can be exploited to enhance product concentration and yield.

Introduction

With the substantially increasing size of the world population and the pressure this puts on the environment, demand for sustainable technologies is increasing. One route that can play a role in the development of more sustainable production of chemicals from a broad spectrum of substrates is thermal gasification and subsequent syngas fermentation. The potential of this route to utilize recalcitrant and low biodegradable carbon waste streams (e.g. lignin, municipal waste) and off-gases from industry (e.g. steel mill waste) gives it great prospect within a circular economy (Clomburg et al., 2017; Dürre and Eikmanns, 2015; Molitor et al., 2016).

In the last years efforts were made to improve the syngas biocatalysts and expand the scope of products. This includes development of genetic tools for acetogenic clostridia (Huang et al., 2016; Liew et al., 2017; Woolston et al., 2018), bioreactor development (Asimakopoulos et al., 2018) and study of the physiology of the syngas biocatalysts (Bertsch and Müller, 2015a; Diender et al., 2015, **Chapter 2**; Richter et al., 2016b). Additionally, there is increasing attention for alternative cultivation strategies, such as applying defined and undefined mixed cultures (Diender et al., 2016b, **Chapter 5**; He et al., 2018; Liu et al., 2014b; Richter et al., 2016a). Using co-cultivation strategies allows to alter the product spectrum of syngas fermentation (Diender et al., 2016b, Chapter 5; Richter et al., 2016a). Understanding the type of interactions that take place in these co-cultures is essential for engineering and

improving these cultures for better performance.

A defined co-culture of *C. autoethanogenum* and *C. kluyveri*, growing solely on CO, formed medium chain fatty acids butyrate and caproate (table 1) and their respective alcohols butanol and hexanol (Diender et al., 2016b, **Chapter 5**). The co-culture was stable during subsequent culture transfers in batch and continuous culture. It remained unclear how the strains influence each other during growth and how product formation can be optimized. Here, we studied the response of C. autoethanogenum to environmental changes induced by C. kluyveri via transcriptomics and chemostat cultivation.

Table 1. Main reactions performed by the individual co-culture members

	C. autoethanogenum
Acetate	$4\ CO + 2\ H_2O \rightarrow CH_3COOH + 2\ CO_2$
Ethanol	$6\ CO + 3\ H_2O \rightarrow C_2H_5OH + 4\ CO_2$
Acetate to ethanol	$2\ CO + H_2O + CH_3COOH \rightarrow C_2H_5OH + 2\ CO_2$
	C. kluyveri
Butyrate	$6\ C_2H_5OH + 4\ CH_3COOH \rightarrow 5\ C_3H_7COOH + 4\ H_2O + 2\ H_2$
Caproate	$6\ C_2H_5OH + 5\ C_3H_7COOH \rightarrow 5\ C_5H_{11}COOH + CH_3COOH + 4\ H_2O + 2\ H_2$

Material and methods

Strains and cultivation

Clostridium autoethanogenum (DSM 10061) and *Clostridium kluyveri* (DSM 555) were obtained from the DSMZ strain collection (Braunschweig, Germany). Both strains were initially cultivated according to supplier instructions. Unless stated otherwise, experiments were conducted in medium containing (per liter of medium): 0.9 g NH_4CL, 0.9 g NaCl, 0.2 g $MgSO_4$ * $7H_2O$, 0.75 g KH_2PO_4, 1.94 g K_2HPO_4 * 3 H_2O, 0.02 g $CaCl_2$ and 0.5 mg resazurin. The medium was supplemented with the following trace-elements (per liter of medium): 1.5 mg $FeCl_2$ * 4 H_2O, 0.025 mg $FeCl_3$ * 6 H_2O, 0.070 mg $ZnCl_2$, 0.1 mg MnCl * 4 H_2O, 0.006 mg H_3BO_3, 0.190 mg $CoCl_2$ * 6 H_2O, 0.002 mg $CuCl_2$ * 2 H_2O, 0.024 mg $NiCl_2$ * 6 H_2O and 0.056 mg Na_2MoO_4 * 2 H_2O, 0.0035 mg, Na_2SeO_3 and 0.2 mg Na_2WO_4. The medium was boiled and cooled on ice under N_2 flow, after which 0.75 g L-cysteine was added per liter of medium as reducing agent. The pH was set to 6 using 1 M NaOH and 1 M HCl. Medium was dispensed under N2 flow, into glass serum bottles that were immediately capped with rubber stoppers and aluminium caps. The headspace was filled with the desired gas, to a final pressure ranging from of 150 kPa. Bottles were autoclaved immediately after preparation. Before inoculation, the medium was further supplemented with a vitamin solution in a 1:50 dilution, containing per liter: 1 mg biotin, 10 mg nicotinamid, 5 mg p-aminobenzoic acid, 10 mg thiamin, 5 mg panthothenic acid, 25 mg pyridoxamine, 5 mg cyanocobalamine and 5 mg riboflavin.

Other additives, such as: yeast extract (0.5 g/l), ethanol and acetate were added from sterile stock solutions. Unless stated otherwise, batch bottle cultivation was done at 37 °C while shaking at 150 rpm.

Bioreactor operation

Cultivation in bioreactors operated in continuous setting was performed in 1.5 liter (total volume) bioreactors (Applikon, Delft, the Netherlands). Gases CO, H_2 or N_2 were supplied using mass flow controllers (Brooks Instruments BV, Ede, the Netherlands). The liquid volume in the reactor was set to 750 or 1000 ml. Stirring was performed by two rushton stirrers on a single shaft, stirrers were placed at 33% and 66% of the liquid height. The pH was controlled using 3 M KOH. Gas outflow rates were determined using a bubble counter.

After sterilization, reactors were connected to the control tower, initiating temperature (37 °C) and pH control (for all experiments 6.2). Prior to inoculation, reactors were flushed for 3 hours with N_2 at a rate of 20 ml/min, to create anaerobic conditions. Vitamins, yeast extract, and L-Cysteine were introduced in the reactor in the same concentration as described for bottle cultivation. Before inoculation the gas flow was switched to the desired gas feed. After reduction of the medium below -300 mV the reactor was inoculated with the culture in a 1:20 ratio. For continuous operation a peristaltic pump (Masterflex, Gelsenkirchen, Germany) was used, applying a HRT of 1.5 or 2 days. The medium tank contained fully prepared medium and was acidified using 30 ml 37% HCl per 10 L medium to ensure sterile conditions of the inflowing medium. In experiments where acetate was provided in the inflow, 25, 50 or 90 mM acetic acid was added to the medium. The medium vessel was continuously sparged with nitrogen (5 L/h) to ensure anaerobic conditions of the inflow medium. All mentions of gas-volumes in supply or production rates throughout the text are considered to be at 1 atm pressure and 298 K. In case of co-cultivation, an exponentially growing *C. kluyveri* culture was inoculated on top of *C. autoethanogenum* in a 1:20 total volume ratio.

Analytical techniques

Liquid phase composition was analysed via high pressure liquid chromatography equipped with a MetaCarb 67H column (Agilent Technologies, Santa Clara, CA). The column was operated at a temperature of 45 °C with a flow rate of 0.9 ml/min. Detection was done via a RI and UV detector. 0.01 N H_2SO_4 was used as eluent. In all cases, samples of 0.5 ml were taken and immediately centrifuged at 13000g. Subsequently 0.4 ml supernatant was added to 0.6 ml 10 mM DMSO in 0.1 N H_2SO_4 solution. Concentrations below 0.1 mM could not be accurately be quantified and are further referred to as trace amounts.

In order to more accurately determine lower amounts of alcohols (<1 mM) samples

were analysed on GC-2010 (Shimazu, Tokio, Japan). The column (DB wax UI of 30m, 0.53µM diameter) was operated at a temperature gradient of 40 °C for 5 minutes, subsequently ramping to 200 °C over 5 minutes and remaining at the higher temperature for 5 minutes. Flame ionization detector was used to determine concentration.

For gas analysis, gas samples of 0.2 ml were taken using a 1 ml syringe and analysed in a Compact GC 4.0 (Global Analyser Solutions, The Netherlands). CO and H_2 were measured using a Molsieve 5A column operated at 100 °C coupled to a Carboxen 1010 pre-column. CO_2 was measured using a Rt-Q-BOND column operated at 80 ºC. Detection was in all cases done via a thermal conductivity detector.

Dry weight was determined by centrifuging a predetermined volume of culture broth (of at least 10 ml) and washing the pellet in ultrapure water two times. Cells were then dried at 120 °C in pre-weighed aluminium baskets, before re-weighing.

Iron levels were determined using a colorimetric method. Samples were centrifuged for 2 min 10000g to pellet the cells and supernatant used for subsequent analysis. Reagents used to determine iron concentration were: A: 10 mM ferrozine in 0.1 M ammonium acetate, B: 1.4 M hydroxylamine-HCl in 2 M HCl, C: 10 M ammonium acetate (pH 9.5). A 100 µl sample (or diluted sample) was mixed with 100 µl reagent A and 800 µl MilliQ water. Sample was mixed and measured at 562 nm to determine Fe(II) content. Fe(III) content was subsequently determined by adding 187.5 µl reagent B, mixing and leaving it for 20 minutes before addition of 62.5 µl of reagent C and measuring absorbance at 562 nm.

Transcriptomics

For transcriptomic analysis three, 25 ml samples were drawn from the chemostat operating in steady state. Samples were taken for 3 subsequent turnovers (under steady-state). Samples were collected in an anaerobic vials sealed with rubber stopper, containing 10 ml RNA later (ThermoFisher, Massachusetts, USA). After sampling, vials were instantly submerged in a slurry of dry-ice and ethanol causing instant freezing of the broth. Vials were stored at -80 °C till extraction.

After defrosting the samples on ice, RNA-extraction was performed. Cells were centrifuged at 4 °C in 50 ml Greigner tubes at 6000g for 15 minutes. Pellets were washed with 500 µl, 20mM TE-buffer (pH 7.2), centrifuged at 10000g (4 °C) and re-dissolved in 150 µl TE-buffer. Cell pre-treatment was done via Lysozyme incubation for 10 min at 20 °C. Cell lysis and RNase inactivation was done by addition of a mix containing 3 ul β-mercaptoethanol, 1µl proteinase-K and 150 µl of Gram positive lysis solution (Gram positive DNA extraction kit, Masterpure). Lysis was initiated by 10 min incubation at 60 °C, while vortexing every 5 minutes. After

incubation, the mix was quickly cooled on ice and proteins precipitated using the protein precipitation mix (Gram positive DNA extraction kit, Masterpure). Debris was removed via centrifugation at 4 °C 10000g. The sample was further cleaned and purified via the automated Maxwell LEV simply RNA extraction kit (Promega, Madison, USA), according to manufacturer's instructions. Quality of the RNA extracts was checked using Bio-Analyser (Agilent, Santa Clara, USA), according to manufacturer's instructions. RNA was collected in RNase free water and stored at -80 °C till further analysis. Depletion of rRNA and sequencing was performed by Novogene (Hong Kong, China) using HiSeq, paired-end reads.

Transcriptome data analysis

Genomes of Clostridium autoethanogenum DSM 10061 (GCA_000484505.1) and Clostridium kluyveri DSM 555 (GCA_000016505.1) were retrieved from the European Nucleotide Archive. Each genome was converted to Resource Description Framework (RDF) using SAPP (Koehorst et al., 2018). Gene expression levels were obtained via the Transcriptomics module using bowtie2. The reads were mapped to each genome independently and to the co-culture for the identification of cross-mapping and to obtain expression levels of the experimental configurations. Read counts were retrieved using SPARQL from the genome repository and converted into an expression matrix. Differential expression analysis was performed using DeSeq2 according to table 2.

Table 2. Comparative transcriptome analysis performed on *C. autoethanogenum*. All conditions contain only *C. autoethanogenum*, except for the co-culture case where also *C. kluyveri* is present.

	CO	co-culture	H_2/CO	H_2/CO/butyrate
CO	-	Supplementary I	Supplementary II	-
co-culture	-	-	-	-
H_2/CO	-	-	-	Supplementary III
H_2/CO/butyrate	-	-	-	-

Results

All experiments were performed in chemostats in order to control environmental conditions such as pH and growth rate, and to ensure stable medium composition. Gas consumption efficiency varied between 60 and 95%, depending on the conditions and is possibly explained by slight changes in reactor setup or differences in total gas feeding rate. Table 3 displays the four reactor runs, their main settings and experiments performed.

***C. autoethanogenum* alters product spectrum without altering transcription of its central carbon and energy metabolism during co-cultivation.**

The monoculture of *C. autoethanogenum* and co-culture of *C. autoethanogenum*

Table 3. Operating conditions of CO/syngas-fed bioreactors and identification of experiments performed of each run. All reactors were operated at pH 6.2 and were gas transfer limited.

Run nr.	CO inflow (mmol/l/d)	H_2 inflow (mmol/l/d)	Additional medium components	Strain	HRT (d)	Volume liquid (l)	CO consumption efficiency (%)	Experiment
1	155	0		CA	1.5	0.75	90	Transcriptome
	155	0		CA + CK	1.5	0.75	90	Transcriptome
2	155	77		CA	1.5	0.75	84	Transcriptome
	155	77	0-8 mM butyrate	CA	1.5	0.75	84	Transcriptome
3	116	0-93		CA	2	1	80-95	H_2 addition
	116	0-128		CA + CK	2	1	80-95	H_2 addition
4	155	0	0- 90 mM acetic acid	CA	1.5	0.75	60-70	Acetate addition
	155	0	0- 90 mM acetic acid	CA + CK	1.5	0.75	60-70	Acetate addition

HRT = hydraulic retention time

CA = *C. autoethanogenum*, CK = *C. kluyveri*

with *C. kluyveri* were fed with solely CO in a chemostat (table 3, run 1). Under the provided conditions *C. autoethanogenum* produced 54.7 ± 0.9 mM acetate and low amounts of ethanol (~0.2 mM) in steady state (figure 1, days 9-19). After inoculation of *C. kluyveri* and establishment of the co-culture, average product concentrations of butyrate and caproate were 5.5 ± 0.7 mM and 1.3 ± 0.3 mM, respectively (figure 1, days 30-37).

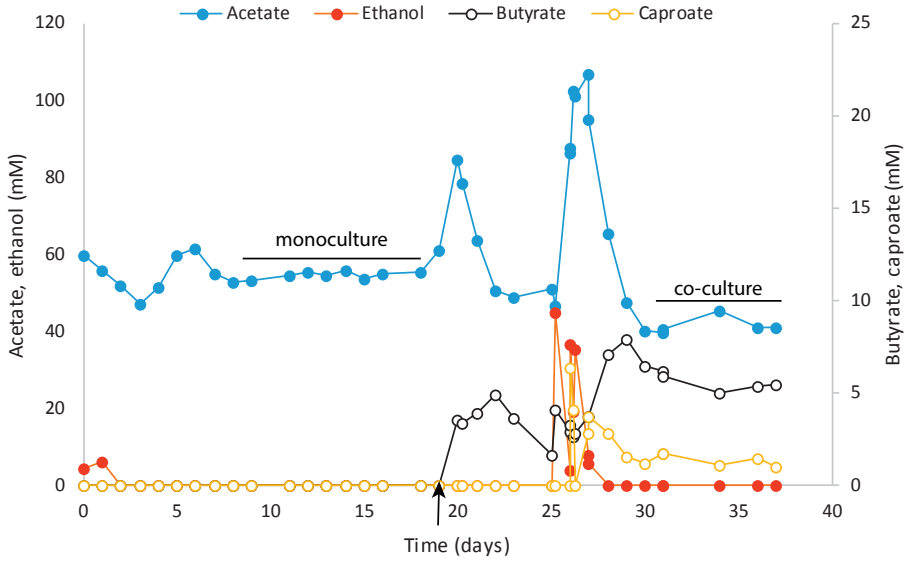

Figure 1. Monoculture vs. co-culture growth in chemostat (reactor run 1). Monoculture of *C. autoethanogenum* was grown from day 0-19, and co-cultivation initiated at day 19 (black arrow) and operated till day 37. Left and right axis are indicated using closed or open symbols respectively. The culture was spiked with ethanol at day 25 to temporarily boost *C. kluyveri* growth. Lines labelled 'monoculture' or 'co-culture' indicate the time frame where transcriptomics samples were taken (at least 3 samples in each condition).

In the co-culture, acetate levels stabilized at 41.7 ± 2 mM and ethanol was detected in trace amounts (<0.1 mM). Carbon monoxide consumption rates in both mono- and co-culture conditions were similar: 147 ± 0.3 mmol l^{-1} d^{-1} vs. 151 ± 1.2 mmol l^{-1} d^{-1}, respectively. Biomass levels during the mono- and co-culture steady state conditions were around 0.60 and 0.42 g/l respectively. When looking at electron distribution in the end products, the monoculture resulted in electrons mainly ending up in acetate, while in the co-culture 29% of the electrons end up in butyrate and 11% in caproate. Reverse calculating the acetate and ethanol production of *C. autoethanogenum* in the co-culture, assuming chain elongation took place according to table 1, the distribution of electrons in product of *C. autoethanogenum* is theoretically 70% into acetate and 30% into ethanol. This would correspond to 45 mM acetate and 7.4 mM ethanol product spectrum if no chain elongation had taken place. This observed

metabolic shift between the mono- and co-culture condition suggests that *C. kluyveri* pulls the metabolism of *C. autoethanogenum* towards solventogenesis. Organisms were not observed to aggregate or form macro-structures during co-cultivation, as confirmed by microscopic observation.

Comparative transcriptome analysis of the mono- and co-culture in steady state shows no major up or down regulation in the central energy and carbon metabolism of *C. autoethanogenum* (table 4, Supplementary material I). Genes of the Wood-Ljungdahl pathway are among the highest expressed in both the mono- and co-culture. When comparing to the co-culture condition, most of the genes present in the Wood-Ljungdahl pathway are significantly lower expressed ($p < 0.01$), but at a low fold change (table 4). Genes related to the alcohol metabolism in *C. autoethanogenum*, such as alcohol dehydrogenase (adhE, CAETHG 3747-3748) and acetaldehyde oxidoreductase (aor, CAETHG 0092, 0102) are not differentially expressed. Several other genes identified as alcohol dehydrogenases or acetaldehyde dehydrogenases are slightly downregulated in the co-culture condition (table 4). Expression of hydrogenases is not significantly affected by co-cultivation, as the majority of hydrogenases shows unaltered expression. Overall these results suggest that there are no large expression deviations in the central carbon and energy metabolism of *C. autoethanogenum* caused by the co-cultivation with *C. kluyveri*.

During co-cultivation a cassette of genes, CAETHG 2642 – 3064, is significantly upregulated 5-10 fold, coding for genes related to amino acid synthesis, pili/flagella formation/assembly and antibiotics production. Furthermore, the most striking changes in the *C. autoethanogenum* transcriptome were observed in the metal import related genes for iron and molybdenum. A relatively strong downregulation was observed for iron-transport related genes: feoA/B and several iron-chelate importers (table 4). Additionally, genes identified as molybdenum transporters were downregulated between 10 and 80-fold. Also increase in genes identified as ferric iron regulator (fur) transcription factors, reported to act as an iron import repressor (Braun and Killmann, 1999), are increasingly expressed in co-culture matching with the downregulation in expression for iron importers. Determining iron concentrations levels in the medium gave a concentration of 1.13 ± 0.24 μM in the monoculture compared to 1.76 ± 0.30 μM in the co-culture.

Additional hydrogen feeding triggers solventogenesis in *C. autoethanogenum*, but does not influence its general expression patterns

In order to assess the effect of main products of *C. kluyveri* (hydrogen and butyrate) on *C. autoethanogenum*, a monoculture of *C. autoethanogenum* was grown on 155 mmol l^{-1} d^{-1} CO and 77 mmol l^{-1} d^{-1} H_2 in presence or absence of 8 mM butyrate (table 3, run 2). Addition of hydrogen resulted in production of acetate (58 ± 0.8

Table 4. Highlights of significant changes ($p < 0.01$) in the comparative transcriptome of *C. autoethanogenum* in monoculture vs. *C. autoethanogenum in* co-culture with *C. kluyveri*.

	Locus tag	Gene	Fold change (up/down)
Wood-Ljungdahl pathway	CAETHG 2789-2799	Formate dehydrogenase (fdhA/hytA-E)	1 – 6 (↑)
	CAETHG 1618	Formate-THF ligase	1.4 (↓)
	CAETHG 1614 - 1615	methylene-THF reductase	1.9 (↓)
	CAETHG 1617	Methenyl-THF cyclohydrolase	1.4 (↓)
	CAETHG 1610-1611	CODH/ACS	1.5 – 2 (↓)
Alcohol metabolism	CAETHG 1813, 1841,	Alcohol dehydrogenase	2 - 3 (↓)
	CAETHG 1819, 1830	Acetaldehyde dehydrogenase	3 – 4 (↓)
Redox metabolism	CAETHG 1580	Nfn-complex	2 (↓)
	CAETHG 3003-3005	CODH	1.5-2.5 (↑)
	CAETHG 3840-3841	Hydrogenase	8-11 (↓)
Other	CAETHG 2642-3064	Host defence and assimilatory metabolism	5-10 (↑)
	CAETHG 0252-0254, 3479-3481	Iron transporters (feoA/B)	50-100 (↓)
	CAETHG 3827-3830, 0088-0092, 2677-2679	Iron transporters (iron-chelate)	5-10 (↓)
	CAETHG 0313-0315, 0671-0672, 3822-3825	molybdenum transporters	10-80 (↓)
	CAETHG 0018, 1463, 2706	Ferric uptake regulator (fur)	2-7 (↑)

mM) and ethanol (6.5 ± 0.5 mM) (supplementary IV). Compared to growth on only CO, by which almost all the electrons were used for acetogenesis (figure 1, day 9-19), feeding both CO and H_2 resulted in 85 % of the electrons in acetate and 15 % into ethanol. Experiments using a feed of solely CO at a rate similar to the combined H_2/CO feed rate (~232 mmol l^{-1} d^{-1}) resulted in solely acetate formation in steady state. When 8 mM butyrate was fed in addition to H_2 no additional changes were observed and consumption and production parameters did not significantly change compared to when no butyrate was added (supplementary IV).

Growth on CO:H_2 compared to growth on solely CO, does not result in large differences in Wood-Ljungdahl pathway expression (CAETHG 1608-1621) (supplementary II). Most of the genes were ~2 fold higher expressed in the condition with CO/H_2, except for the bifurcating formate dehydrogenase, which was not differently expressed. Interestingly, the CODH not related to ACS (CAETHG 3003-3005), was upregulated when H_2 was present (~10 fold). The alcohol metabolism does not show a uniform response as there was no clear up- or downregulation trend in acetaldehyde dehydrogenases, acetaldehyde oxidoreductases and alcohol dehydrogenases when exposed to CO/H_2. Also expression of hydrogenases appears not to change by presence of hydrogen, and even resulted in downregulation of some hydrogenases (CAETHG 3841). A block of genes (CAETHG 1705 – CAETHG 1912) related to assimilatory metabolism was slightly downregulated by ~3-6 fold. Overall this suggests a minor response to hydrogen addition on the expression level, with no major changes of the central energy or carbon metabolism. In the condition with butyrate, no further changes were observed in the transcriptome (supplementary III). Thus, both hydrogen or butyrate addition appear not to trigger any changes in transcriptomic changes explaining the ethanol producing behaviour, and are not similar to the response of C. autoethanogenum to the co-culture condition.

Hydrogen addition promotes chain elongation in co-culture via stimulation of *C. autoethanogenum* metabolism

Adding hydrogen in addition to CO stimulates the overall metabolism of *C. autoethanogenum*, and causes a shift towards solventogenesis. This suggests that hydrogen exchange between *C. kluyveri* and *C. autoethanogenum* could be a possible trigger for the observed metabolic shift during co-cultivation. In the co-culture grown on only CO, hydrogen was produced at a rate of 0.2 mmol l^{-1} d^{-1}. Predicted rates derived from chain elongation activity are in the range of 2 mmol l^{-1} d^{-1} suggesting that hydrogen produced by *C. kluyveri* was indeed consumed by *C. autoethanogenum*.

In order to test at which H_2 feed rates solventogenesis is triggered in *C. autoethanogenum*, a gradient of H_2 inflow with a steady CO background was created

in a chemostat (table 3: run 3). Hydrogen inflow rates from 0 to 93 mmol l^{-1} d^{-1} were tested in addition to 116 mmol l^{-1} d^{-1} CO. Hydrogen consumption was observed for all tested inflow concentrations, and was linearly correlated with the influx (figure 2a). The CO_2/CO ratio decreased linearly with increasing hydrogen inflow (figure 2c). Acetate formation increased gradually with increasing hydrogen influx and stimulation of solventogenesis was not observed at the tested influx rates below 46.6 mmol l^{-1} d^{-1} (table 5, figure 2a). At higher hydrogen inflow rates a stable ethanol production rate was observed in steady state conditions up to 3 mmol l^{-1} d^{-1} at a feed rate of 93 mmol l^{-1} d^{-1} of hydrogen. This is about 9% of the electrons in end products (figure 2c), not meeting the 30% observed in the co-culture solely fed with CO (figure 2d).

In order to test if hydrogen would enhance productivity and efficiency of the co-culture, a range of 0 to 128 mmol l^{-1} d^{-1} was fed to the co-culture. With increasing hydrogen inflow, chain elongation activity was stimulated compared to conditions where no hydrogen was added (table 5). When reverse calculating acetate and ethanol production rates, an increase in both acetogenic and solventogenic rate by *C. autoethanogenum* was observed (figure 2b). The electron distribution towards ethanol remained between 26 and 30% (figure 2d), which is similar to the co-culture growing solely on CO. This pattern was not observed when supplying excess of hydrogen (128 mmol l^{-1} d^{-1}), causing depletion of CO_2. This resulted in a rapid increase in solventogenic activity shuttling 45% of the electrons towards ethanol (figure 2d). This resulted in a background of 5.5 mM net ethanol formation, showing ethanol formation by *C. autoethanogenum* was no longer the limiting factor in the co-culture (table 5).

External acetate addition promotes ethanol as electron sink and enhances chain elongation in co-culture

The effect of acetate in steering the metabolism of *C. autoethanogenum* towards solventogenesis was tested; increasing acetate concentrations in a range of 0 to 60 mmol l^{-1} d^{-1} (table 3: run 4). Ethanol production rates went up from 0 to 0.75 mmol l^{-1} d^{-1} (figure 3). Despite that the activity of acetogenesis decreased from 27 ± 0.7 mmol l^{-1} d^{-1} to 20 ± 3 mmol l^{-1} d^{-1} at an acetate inflow of 60 mmol l^{-1} d^{-1}, the majority of electrons (~95 %) were still moving towards acetogenesis (figure 3c). Biomass levels decreased when more acetate was provided, illustrating the toxicity of acetic acid on *C. autoethanogenum* (table 5).

Supplying similar amounts of acetate to the co-culture resulted in an increase of chain elongated products up to 14 mM butyrate and 5.5 mM caproate, in steady-state (table 5). Reverse calculating the production rate of ethanol and acetate in these conditions, shows that the acetate production decreases and ethanol production

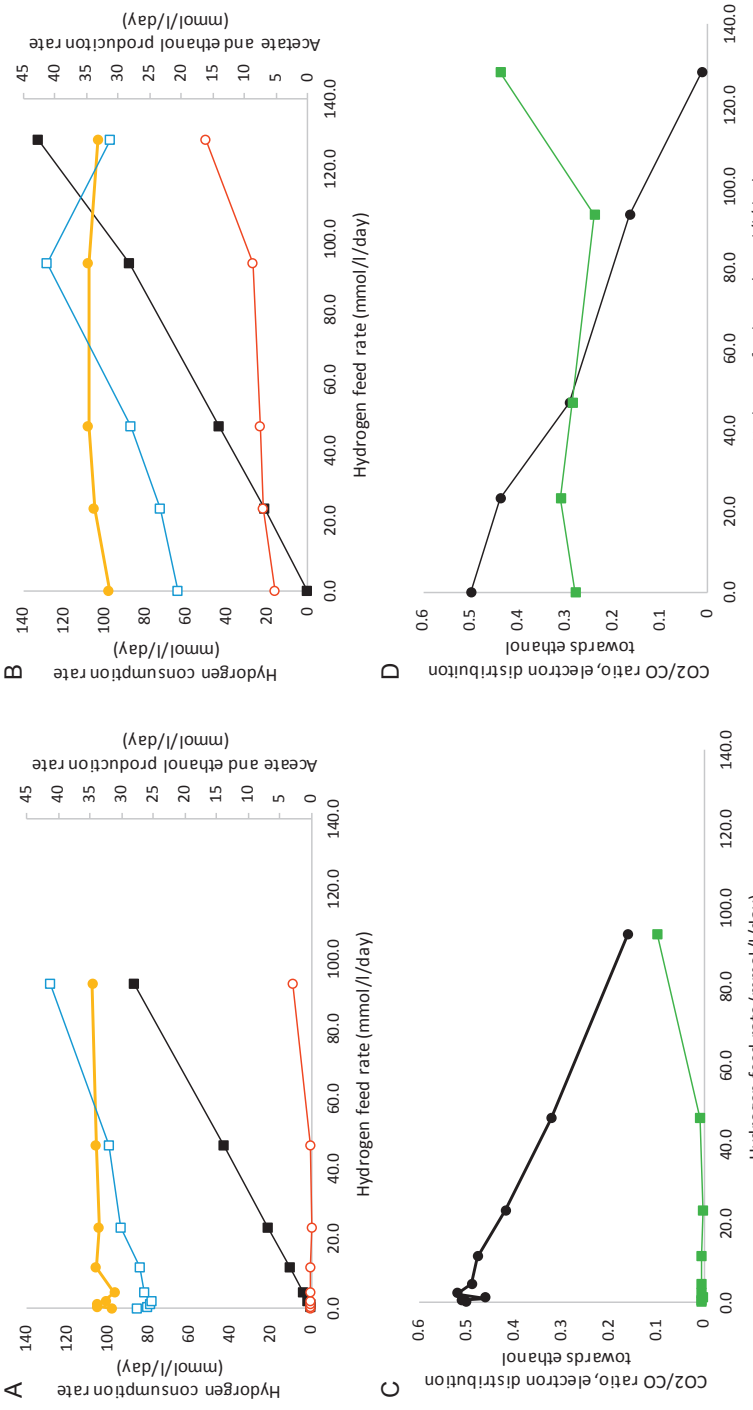

Figure 2. Physiological profile of *C. autoethanogenum* when grown on 116 mmol/l/day CO with increasing hydrogen feed in monoculture (A/C) or co-culture (B/D). In case of co-culture ethanol and acetate production, and the derived electron distribution are reverse calculated from observed chain elongation activity (table 5). Left and right axis are indicated using closed or open symbols respectively. A/B) Hydrogen consumption rate (black squares), CO consumption rate (yellow circles), acetate production (blue open squares) and ethanol production rate (red open circles). C/D: CO_2/CO ratio (black circles), electrons present in ethanol (green squares).

increases (figure 3b). At 60 mmol l^{-1} d^{-1} acetate inflow, *C. autoethanogenum* was fully solventogenic causing all CO derived electrons to be used for ethanol production (figure 3d). This contrasts with the 5% electrons in ethanol obtained in monoculture (figure 3c). All acetate produced by *C. autoethanogenum* was converted to ethanol, causing net conversion of externally supplied acetate to ethanol (table 1). In contrast to the monoculture, we observed no decrease in biomass when acetate is added to the co-culture, remaining stable around 0.2 g/l in all tested conditions (table 5).

Discussion

C. autoethanogenum and *C. kluyveri* can grow in a stable co-culture and produced chain elongated products from CO or syngas (Diender et al., 2016b, **Chapter 5**). In the chemostat experiments described here the total biomass levels of *C. autoethanogenum* and *C. kluyveri* were lower or similar to the ones with *C. autoethanogenum* alone. Thus, the *C. autoethanogenum* biomass is significantly lower in the co-culture compared to monoculture. As the metabolism of *C. autoethanogenum* appears to shift towards solventogenesis during co-cultivation, less energy is generated per CO consumed (Diender et al., 2015, **Chapter 2**), possibly explaining the lower biomass formation. Additionally, based on the observations in the transcriptome, a stress response of *C. autoethanogenum* to *C. kluyveri* appears to be initiated. Increase in transcription of anabolic pathways (e.g. amino acid synthesis) and host defence systems (e.g. sporulation, flagella/pili) increases upon co-cultivation, likely contributing to increased maintenance costs for *C. autoethanogenum* cells. Additionally, increased levels of chain elongated acids produced by *C. kluyveri* possibly resulted in increased maintenance costs due to their hydrophobic properties (Steinbusch et al., 2011). The lower biomass of *C. autoethanogenum* in the co-culture explains the downregulation of iron and molybdenum metal importers observed (10-100 fold). Less trace elements are required for biomass build-up, increasing their concentration in the medium. This is supported by the higher concentrations of iron found in the co-culture medium compared to the monoculture. Despite similar or lower total biomass levels, gas consumption efficiencies within the same chemostat runs using mono- or co-culture were similar (table 3). This suggests that the same gas consumption activity is performed by less biomass of *C. autoethanogenum*. We showed previously that *C. kluyveri* in monoculture is not using CO as substrate and even caused inhibition of its metabolism (Diender et al., 2016b, **Chapter 5**). Likely *C. autoethanogenum* continues to remove substrate till gas transfer limitation is reached, and despite lower biomass it is sufficient to achieve this.

For *C. kluyveri* to grow, substrate needs to be provided by *C. autoethanogenum*. As ethanol and acetate are products of *C. autoethanogenum* and are efficiently used by *C. kluyveri* (Thauer et al., 1968; Weimer and Stevenson, 2012), it is plausible that these are the intermediates in the co-culture. This is supported by the observation

Table 5. Steady state concentrations of fermentation products (mM) and cellular biomass ($g_{dry\ weight}$/L) in the mono- and co-culture during the hydrogen addition (mmol/l/day) and acetate supply (mmol/l/day) experiments.

	hydrogen feed rate	Acetate	Ethanol	Butyrate	Caproate	Biomass
mono	0	56.0	0.2			0.28
	23	61.0	0.2			0.22
	47	65.0	0.4			0.24
	93	83.0	6.0			0.3
co	0	35.5	<0.1	5.5	1.7	0.22
	23	39.5	<0.1	6.9	2.3	0.22
	47	48.5	<0.1	7.6	2.4	0.23
	93	73.2	<0.1	10.0	2.2	0.23
	128	48.0	5.5	12.6	7.1	0.23
	Acetate feed rate	Acetate	Ethanol	Butyrate	Caproate	Biomass
mono	0	40.7	0.20			0.15
	16	63.2	0.26			0.14
	33	81.1	0.55			0.09
	60	119.7	1.12			0.08
co	0	23.4	<0.1	5.3	1.8	0.13
	16	33.5	<0.1	7.7	4.0	0.15
	33	40.0	<0.1	10.1	5.0	0.14
	60	68.0	<0.1	14.0	5.5	0.14

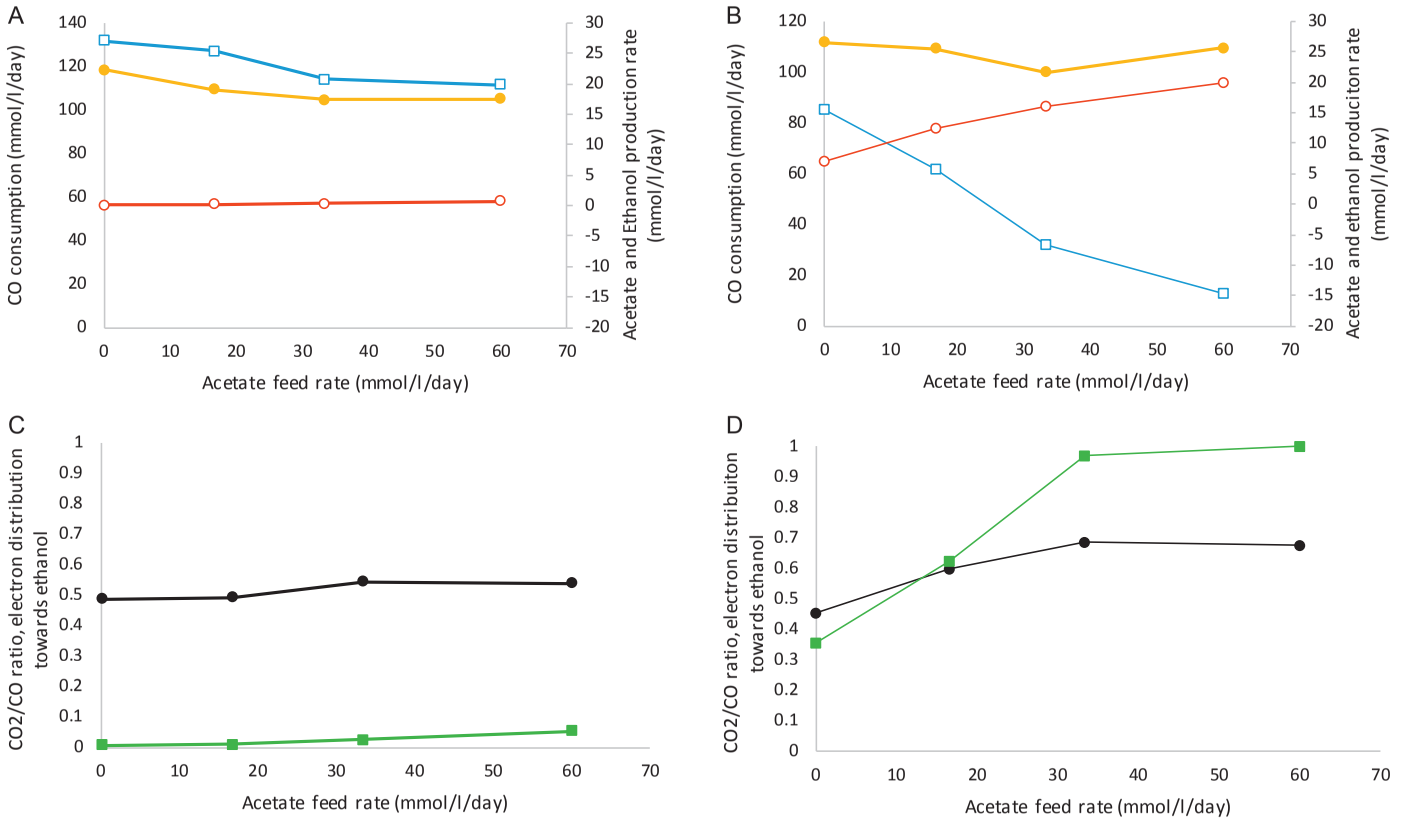

Figure 3. Physiological profile of *C. autoethanogenum* when grown on 155 mmol/l/day CO with increasing acetate feed in monoculture (A/C) or co-culture (B/D). In case of co-culture ethanol and acetate production, and the derived electron distribution are reverse calculated from observed chain elongation activity (table 5). Left and right axis are indicated using closed or open symbols respectively. A/B) CO consumption rate (yellow circles), acetate production (blue open squares) and ethanol production rate (red open circles). C/D: CO_2/CO ratio (black circles), electrons present in ethanol (green squares).

that ethanol levels remain lower (<0.1 mM) during co-cultivation compared to lowest values measured in monoculture (~0.2 mM) (table 5). The total production rates of chain elongated products do not match with the ethanol production rates in the *C. autoethanogenum* monoculture. This suggests that *C. kluyveri* is affecting the electron flow of *C. autoethanogenum* increasing the flux to the solventogenic metabolism. Several studies indicated that the solventogenic and acetogenic metabolism of gas fermenting acetogens is controlled by thermodynamics rather than by gene expression (Richter et al., 2016b; Valgepea et al., 2018). The ratio between acetate and ethanol formed is strongly influenced by environmental factors such as stirring regime, temperature and pH (Abubackar et al., 2015, 2016; Martin et al., 2016; Richter et al., 2013; Valgepea et al., 2018). Here we observe that co-cultivation has no significant effect on expression of the central carbon and energy metabolism of *C. autoethanogenum,* while observing large shifts in electron distribution in final end products, suggesting that the metabolic shift is not caused on expression level but on metabolic level. The main compounds that *C. kluyveri* provides during co-cultivation are butyrate, caproate and H_2, while removing mainly ethanol and acetate. Adding butyrate appears not to stimulate ethanol formation in *C. autoethanogenum*, suggesting that chain elongated products do not stimulate solventogenic metabolism in *C. autoethanogenum*. Hydrogen, when supplied in sufficient amounts (>46 mmol l^{-1} d^{-1}), steers the metabolism of *C. autoethanogenum* towards solventogenesis (figure 2). This is in line with earlier reports that hydrogen addition during CO fermentation resulted in more ethanol formation (Valgepea et al., 2018). Experiments performed here show that hydrogen is always consumed by *C. autoethanogenum*, even when small amounts are added (figure 2a). Relatively low amounts of H_2 are formed in the chain elongation process, ranging from an estimated 2 to 7 mmol l^{-1} d^{-1} in the experiments performed here. Measured hydrogen production rates by the co-culture are in the range of 0.2 mmol l^{-1} d^{-1}, indicating that part of the H_2 formed is consumed by *C. autoethanogenum*. However, as stimulation of solventogenesis is mainly observed at higher H_2 influx, the relatively small amount of H_2 produced by *C. kluyveri* is unlikely to drive the metabolic shift observed in the co-culture. Potential high local concentrations of hydrogen caused by *C. kluyveri* might have a stimulatory effect though, but due to the apparent homogeneous suspended growth, such local effects are not likely to occur.

If the *C. autoethanogenum* metabolism is regulated by thermodynamics it will shuttle electrons to the downstream pathways that are the most favourable electron sink. Such behaviour is observed here in the acetate stimulation experiment, where external acetate addition promotes ethanol formation while inhibiting acetogenesis in both mono- and co-culture (figure 3). By equating the formulas for Gibbs free energy of formation for acetate and ethanol formation, the concentration of ethanol can be

calculated where its production is still thermodynamically feasible (eq. 1-2). When grown solely on CO (eq. 1) the ethanol concentration at which ethanol production is still feasible depends linearly on acetate concentration and quadratically on the CO concentration in the liquid. An inverse quadratic relation with ethanol formation for CO_2 is found, indicating CO_2 depletion is beneficial for solventogenic activity. Feeding with a mixture of CO and H_2, assuming utilization ratio according to feed composition, a mix between CO and hydrogen metabolism will occur. Ethanol

$$C_{ethanol} = \frac{CO^2 \cdot C_{Acetic\ acid}}{{CO_2}^2} \cdot e^{\frac{\Delta G^0 acetogenesis - \Delta G^0 solventogenesis}{RT}} \quad (1)$$

$$C_{ethanol} = \frac{C_{Acetic\ acid} \cdot CO^{2-2x} \cdot {H_2}^{2x}}{{CO_2}^{2-2x}} \cdot e^{\frac{\Delta G^0 acetogenesis - \Delta G^0 solventogenesis}{RT}} \text{ where } x = \frac{CO}{CO+H_2} \quad (2)$$

concentrations can be estimated for CO:H_2 ratios between 1:0 and 1:1 using Eq. 2. As long as ethanol levels remain below the thermodynamic threshold concentration, it remains favourable to be produced. Steady state concentrations of acetate and ethanol in the monoculture were 38 and ~0.2 mM, respectively (table 5). These are thus the thermodynamic equilibria for acetogenesis and solventogenesis under the provided conditions. Under similar conditions, the co-culture generates acetate and ethanol concentrations of 23 and <0.1 mM, respectively (table 5). This low ethanol concentration, caused by continuous ethanol removal by *C. kluyveri*, potentially keeps reduction of acetate to ethanol favourable as electron sink. In monoculture of *C. autoethanogenum* the ethanol concentration will increase till the threshold is reached, whereas in co-culture a larger flux through ethanol becomes possible due to continuous removal (figure 4). When providing external acetate the thermodynamic ethanol threshold is elevated as is shown by higher ethanol concentrations in the monoculture, while simultaneously making acetogenesis more unfavourable (figure 3a, eq. 1), and causing increasingly more favourable conditions for solventogenesis over acetogenesis. *C. kluyveri* further enhances this by making ethanol a more favourable electron sink, eventually resulting in most electrons from CO to be used for ethanol production (figure 3d, figure 4). In contrast, hydrogen addition boosted overall chain-elongation activity in the co-culture, but did not result in a shift towards solventogenesis on top of the initial shift, remaining between 26 and 30 % electrons in ethanol (figure 2d). Where acetate addition inhibited acetogenesis, while stimulating solventogenesis (figure 3a), hydrogen addition stimulated both acetogenesis and solventogenesis (figure 2a). Ethanol removal by *C. kluyveri* enhances ethanol production, and removal of acetate for chain elongation also makes acetogenesis more favourable (figure 4). This likely is the cause for the absence of a shift towards ethanol production as observed in the acetate addition experiment. During excessive hydrogen feeding, however, a shift towards solventogenesis is

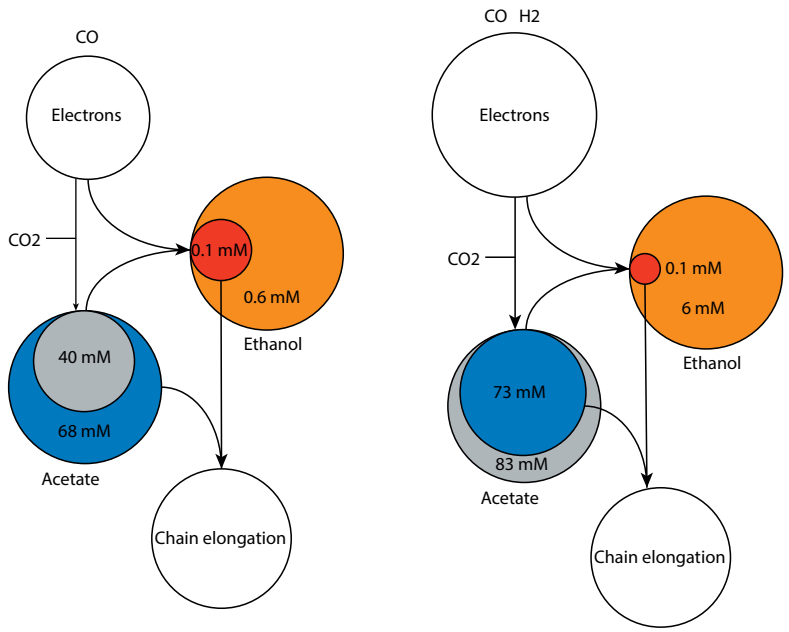

Figure 4. Quantitative model for the preferred pathways to deposit electrons in during acetate feeding (left) and hydrogen feeding (right). Blue and red spheres indicate the measured concentration of the compound in the co-culture whereas grey and orange spheres indicate the corresponding monoculture steady state concentrations. A smaller pool in co-culture suggests pathways towards this pool are facilitated while a larger pool in co-culture suggests pathways to be inhibited compared to monoculture conditions. Flux through the pathways is indicated via arrows.

observed, which is likely due to CO_2 limitation (figure 2b). The excess of hydrogen resulted in low CO_2 levels, limiting the potential of acetogenesis, and therefore favouring solventogenesis.

The observation that the metabolism of *C. autoethanogenum* can be strongly steered by changing the environmental concentrations of its end products poses an interesting concept for production potential of *C. autoethanogenum* and similar strains. Continuous ethanol removal from the fermentation broth by subsequent reactions can pull the metabolism of *C. autoethanogenum* towards solventogenesis, and can improve the yield of the process significantly. The finding that *C. autoethanogenum* produced solely ethanol in co-culture during the acetate stimulation experiment (figure 3d) is interesting as in monocultures of *C. autoethanogenum* the ratio of ethanol/acetate is usually <1 and is only in a few cases to be reported >1 (Valgepea et al., 2017, 2018) indicating ratios of ethanol/acetate are difficult to get above 1. Cases where this ratio is >1 are usually observed in the pH range 4-5 (Abubackar et al., 2012) and under relatively high gas feed rates (Abubackar et al., 2015). This is in

contrast to the 'high' 6.2 pH, low gas feed system presented here where we eventually achieve 100% solventogenic conditions for *C. autoethanogenum*. The interactions in this co-culture likely difficult to mimic in monoculture and therefore synthetic co-cultures might have potential to achieve higher substrate/product efficiencies as monocultures.

Conclusion

Co-cultivation of *C. autoethanogenum* and *C. kluyveri* results in a shift from acetogenesis to solventogenesis in *C. autoethanogenum*. No major changes were observed in the transcriptome related to central energy and carbon fixation metabolism of *C. autoethanogenum* and thus it is unlikely that these changes have resulted in the metabolic shift from acetate to ethanol production. The *C. autoethanogenum* pathways are regulated mainly on thermodynamic and less on expression level. In the co-culture, solventogenic activity of *C. autoethanogenum* could be further stimulated by addition of hydrogen or acetate, resulting in a stronger effect compared to the mono-culture conditions. This strongly suggests that removal of the ethanol by *C. kluyveri* enhances solventogenesis in *C. autoethanogenum*. Even a 100 % yield of ethanol of CO derived electrons is possible by C. autoethanogenum, but only when ethanol is continuously removed to levels below the thermodynamic threshold. Using this concept when constructing synthetic communities might be a valuable way to increase the efficiency of product formation from gaseous substrates.

Supplementary material I-III can be accessed via the archive of the Wageningen University Library: 4TU.Centre for Research data

Supplementary material IV

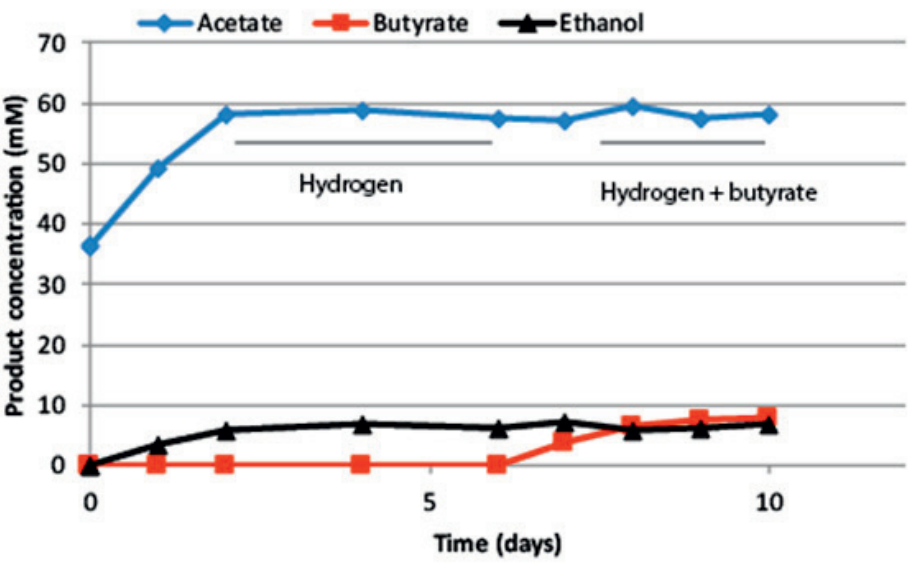

Figure S1. Production spectrum of *C. autoethanogenum* exposed to hydrogen or hydrogen and butyrate. Lines labelled 'Hydrogen' or 'Hydrogen + butyrate' indicate the time frame where transcriptomics samples were taken (at least 3 samples) Butyrate was introduced after day 6.

Chapter 7

A flexible alcohol metabolism in *C. autoethanogenum* allows for additional energy conservation

Authors: Martijn Diender, Ivette Parera Olm, Alfons J.M. Stams & Diana. Z. Sousa

Abstract

Carbon monoxide can act as substrate for the Wood-Ljungdahl pathway (WLP) in *Clostridium autoethanogenum*, resulting in the production of acetate and ethanol. Ethanol production in acetogens is often found to be positively correlated with low pH values (4-5). Here we show that the CO/CO_2 ratio directly influences the alcohol production patterns in *Clostridium autoethanogenum*. Alcohol production is enhanced when CO levels dissolved in the liquid rise (and thus CO/CO_2 rises), while their oxidation occurs at low CO dissolved concentrations. Alcohol oxidation to its respective acid requires co-oxidation of CO and appears to result in an increase in energy yield of 1.5-2 times per CO consumed. We hypothesize alcohol oxidation takes place via acetaldehyde and acetyl-CoA to acetate, allowing for additional energy generation in the form of direct substrate level phosphorylation. In chemostats, ethanol formation and consumption could be steered by changing the CO dissolved in the liquid. During these runs a higher biomass yield (per mol acetate consumed) was observed when cells were exposed to higher dissolved CO levels. Our results suggest that *C. autoethanogenum* employs an unexpected novel mode of energy conservation during gas fermentation in presence of higher CO dissolved concentrations.

Introduction

Microbial conversion of carbon monoxide has gained renewed interest due to the potential application of syngas and industrial off-gases for bio-based industries (Bengelsdorf et al., 2013; Daniell et al., 2012; Redl et al., 2017). Three physiological groups of microorganisms are identified to ferment this strongly reduced substrate: hydrogenogens, methanogens and acetogens (Diender et al., 2015, Chapter 2; Oelgeschläger and Rother, 2008). The physiology of carboxydotrophic acetogens has over the last years been extensively explored. Mainly the involvement of the RnF complex (Müller et al., 2008; Tremblay et al., 2012) and several bifurcation mechanisms (Buckel and Thauer, 2013), have led to a better understanding of the carboxydotrophic acetogenic metabolism. Also genome scale models, of especially model organisms such as *Clostridium autoethanogenum* or *Clostridium ljungdahlii,* gave insight in the carboxydotrophic metabolism of acetogens (Valgepea et al., 2017, 2018).

Alcohol production by acetogens (solventogenesis) was previously shown to be strongly dependent on pH; producing more alcohols at relatively lower pH (4-5) (Abubackar et al., 2012). While formation of alcohols with varying chain length has been shown to be possible from their respective acids during CO fermentation (Liu et al., 2014b), ethanol metabolism is by far the most studied. It is theorised that the production of ethanol from acetate is regulated by thermodynamics, and is suggested to serve as detoxification mechanism of acetic-acid inside the cell (Richter et al.,

2016b; Valgepea et al., 2017). During CO fermentation, ethanol can be formed via two routes, the indirect route via acetate and the direct route from acetyl-CoA (Köpke et al., 2010). Knockout studies and metabolomics analysis in *C. autoethanogenum* showed that the indirect pathway is the main route for alcohol production (Liew et al., 2017; Valgepea et al., 2017). Via this route, utilizing acetate kinase, additional ATP is conserved via substrate level phosphorylation. The role of the direct pathway via acetaldehyde dehydrogenase remains unknown as it appears to not be involved in ethanol formation and knockout of the gene even resulted in increase of ethanol production, but growth decreased significantly (Liew et al., 2017).

In some studies, the re-oxidation of alcohols to their respective acids near end-growth was observed in cultures using CO (Diender et al., 2016b, Chapter 5; Köpke et al., 2010) or H2 (Mock et al., 2015) as substrate. This suggests that the alcohol production pathway in these organisms is reversible, and the alcohol is potentially acting as electron donor in acetogenesis, similar to what was shown in *Acetobacterium. woodii* (Bertsch et al., 2016). This study aimed to further elucidate on the control and direction of the alcohol metabolism in *C. autoethanogenum* when it is grown on CO. We hypothesize that alcohol production relates to the CO dissolved levels in the liquid and in combination with acetic acid and alcohol levels determines alcohol production or oxidation.

Material and methods

Strains and cultivation

Clostridium autoethanogenum (DSM10061) was purchased from the DSMZ strain collection (Braunschweig, Germany). *C. autoethanogenum* was initially cultivated in DSM-640 medium. Unless stated otherwise, experiments were conducted in medium containing (per liter of medium): 0.9 g NH_4CL, 0.9 g NaCl, 0.2 g $MgSO_4$ * $7H_2O$, 0.75 g KH_2PO_4, 1.94 g K_2HPO_4 * 3 H_2O, 0.02 g $CaCl_2$ and 0.5 mg resazurin. The medium was supplemented with the following trace-elements (per liter of medium): 1.5 mg $FeCl_2$ * 4 H_2O, 0.025 mg $FeCl_3$ * 6 H_2O, 0.070 mg $ZnCl_2$, 0.1 mg MnCl * 4 H_2O, 0.006 mg H_3BO_3, 0.190 mg $CoCl_2$ * $6H_2O$, 0.002 mg $CuCl_2$ * 2 H_2O, 0.024 mg $NiCl_2$ * 6 H_2O and 0.056 mg Na_2MoO_4 * 2 H_2O, 0.0035 mg, Na_2SeO_3 and 0.2 mg Na_2WO_4. The medium was boiled and cooled on ice under N_2 flow, after which 0.75 g L-cysteine was added per liter of medium as reducing agent. Unless stated otherwise the pH was set to 6 using NaOH and HCl. Medium was dispensed under N_2 flow, into glass serum bottles that were immediately capped with rubber stoppers and aluminium caps. The headspace was filled with the desired gas (e.g., CO, H_2/CO_2) to a final pressure ranging from of 150 kPa. Bottles were autoclaved immediately after preparation. Before inoculation, the medium was further supplemented with a vitamin solution in a 1:50 dilution, containing per liter: 1 mg biotin, 10 mg nicotinamid, 5 mg

p-aminobenzoic acid, 10 mg thiamin, 5 mg panthothenic acid, 25 mg pyridoxamine, 5 mg cyanocobalamine and 5 mg riboflavine. Other additives, such as: yeast extract (0.5 g/l), ethanol and acetate were added from sterile stock solutions. Unless stated otherwise, cultivation was done at 37 °C while shaking at 150 rpm.

Bioreactor operation

Cultivation of *C. autoethanogenum* in continuous conditions, was performed in a 1.5 liter bioreactor (Applikon, Delft, the Netherlands). CO was supplied using mass flow controllers (Brooks Instruments BV, Ede, the Netherlands). The liquid volume in the reactor was set to 750 ml. Stirring was performed by two rushton stirrers on a single shaft, stirrers were placed at 33% and 66% of the liquid height. The pH was controlled using 3 M KOH. Gas outflow rates were determined using a bubble counter. After sterilization, reactors were connected to the control tower, initiating temperature (37 °C) and pH control. Reactors were flushed for 3 hours with N_2 at a rate of 20 ml/min, to create anaerobic conditions. Right before inoculation the N_2 flow was changed for a CO/N_2 flow. Additionally, vitamins, yeast extract, and L-Cysteine were introduced in the reactor in the same concentration as described for bottle cultivation. After reduction of the medium below -300 mV the reactor was inoculated with the culture in a 1:20 ratio. For continuous operation a peristaltic pump (Masterflex, Gelsenkirchen, Germany) was used, applying a HRT of 1.5 days. The medium tank contained fully prepared medium and was acidified using 30 ml 37% HCl per 10 L medium to ensure sterile conditions of the inflowing medium. The medium vessel was continuously sparged with nitrogen (5 l/h) to ensure anaerobic conditions of the inflow medium. All mentions of gas-volumes in supply or production rates throughout the text are considered to be at 1 atm pressure and 298 °K.

Active cell tests

The metabolic shift between acid and alcohol production was studied in more detail in 16-mL screw-cap Hungate-tubes that permitted 24-hour experiments under different conditions. Tubes were made anoxic with N_2 and filled with 15 mL of active culture from a *C. autoethanogenum* bioreactor operated in steady state and were centrifuged for 20 minutes at 3000 g. The supernatant was replaced by 5 mL fresh medium free of yeast extract and vitamins. Acetate, ethanol and butanol were added in concentrations ranging from 0 mM to 50 mM. CO was introduced in the headspace to a desired final proportion ranging from 0 to 40%. The tubes were incubated horizontally in a shaker at an agitation speed of 60 rpm and at 37 °C. Depending on the metabolic activity of each test, sampling was done every one or every two hours until depletion of CO. At the end of the experiment, final pH was measured. All sets of experiments were performed in triplicates.

Analytical techniques

Liquid phase composition was analysed via high pressure liquid chromatography equipped with a MetaCarb 67H column (Agilent Technologies, Santa Clara, CA). The column was operated at a temperature of 45 °C with a flow rate of 0.9 ml/min. Detection was done via a RI and UV detector. 0.01 N H_2SO_4 was used as eluent. In all cases, samples of 0.5 ml were taken and immediately centrifuged at 13000g. Subsequently 0.4 ml supernatant was added to 0.6 ml 10 mM DMSO in 0.1 N H_2SO_4 solution. Concentrations below 0.1 mM could not be accurately be quantified and are further referred to as trace amounts.

In order to more accurately determine lower amounts of alcohols (<1 mM) samples were analysed on GC-2010 (Shimazu, Tokio, Japan). The column (DB wax UI of 30 m, 0.53 µm diameter) was operated at a temperature gradient of 40 °C for 5 minutes, subsequently ramping to 200 °C over 5 minutes and remaining at the higher temperature for 5 minutes. A flame ionization detector was used.

Acetaldehyde concentrations in the liquid were determined using GC-M. GC-MS was performed using a Trace GC Ultra coupled to a DSQ mass spectrometer installed with quadrupole mass filter (Shimadzu, Tokyo, Japan). The GC was installed with a RT Q-bond column. Initial oven temperature was 50 °C and was after 2 minutes ramped to 200 °C over 5 minutes and kept at this level for 5 minutes. Liquid samples were stored in air tight rubber stopped vials of 1 ml, and allowed to equilibrate with the gas phase for 1 hour. Gas samples of 1 ml for injection in GC-MS taken using a 1 ml syringe.

For gas analysis of CO, H_2 and CO_2, gas samples of 0.2 ml were taken with a 1 ml syringe and analysed in a Compact GC 4.0 (Global Analyser Solutions, The Netherlands). CO and H_2 was measured using a molsieve 5A column operated at 100 °C coupled to a Carboxen 1010 pre-column. CO_2 was measured using a Rt-Q-BOND column operated at 80 ºC. Detection was in all cases done via a thermal conductivity detector.

In order to determine CO concentrations in the liquid, samples of 5 ml liquid broth were taken an injected in a gas tight, glass rubber stoppered vial of 7 ml. Samples were instantly put at 4 °C and left overnight to equilibrate the gas- and liquid phase. Oxygen present in the vial combined with the low temperature caused instant inactivation of the microbes. CO present in the headspace of the vials was determined using GC. Total CO present in the vial was recalculated from the headspace value using Henrys-law.

Dry weight was determined by centrifuging a predetermined volume of culture broth (of at least 10 ml) and washing the pellet in ultrapure water two times. Cells were then dried at 120 °C in pre-weighed aluminium baskets, before re-weighing.

Results

C. autoethanogenum is capable of alcohol oxidation in the presence of CO

When growing on CO as sole carbon and energy source, *C. autoethanogenum* initially shows a typical solventogenic metabolism with the formation of ethanol and acetate (figure 1A). However, when CO concentration drops to 5-10 kPa and CO_2 levels rise to 20 kPa (around day 3 of incubation), ethanol is oxidized and acetate concentration increases. Ethanol oxidation appears to provide additional electrons to the metabolism of *C. autoethanogenum*, allowing for more acetate production at the expense of less CO (Eq. 1) compared to carboxydotrophic acetogenesis (Eq. 2).

$$2\ CO + Ethanol + H_2O \rightarrow 2\ Acetate^- + 2\ H^+ \quad (1)$$

$$4\ CO + 2\ H_2O \rightarrow Acetate^- + 2\ CO_2 + H^+ \quad (2)$$

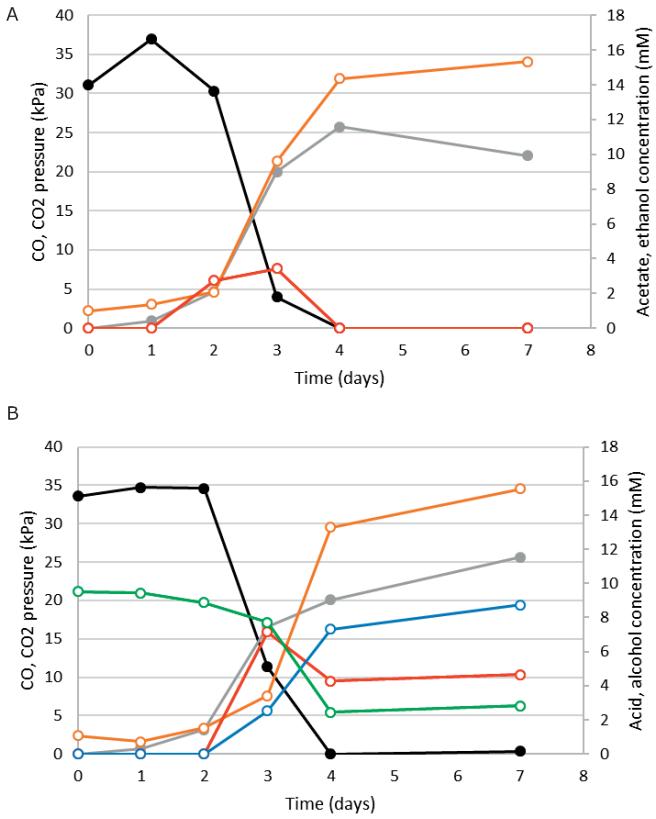

Figure 1. Alcohol production and subsequent oxidation by *C. autoethanogenum* in closed bottle tests. Closed and open symbols indicate left and right axis respectively. A) production and consumption of ethanol during growth of *C. autoethanogenum*. CO: black circles, CO_2 grey circles, Acetate: orange circles, Ethanol: red circles B) oxidation of butanol by *C. autoethanogenum*, CO: black circles, CO_2 grey circles, Acetate: orange circles, Ethanol: red circles, Butanol: green circles, Butyrate: blue circles.

Oxidation was also observed when other alcohols were supplemented to the cultures. In figure 1B, conversion of butanol to butyrate by *C. autoethanogenum* is illustrated. Interestingly, ethanol was produced during butanol oxidation, showing that both alcohol production and oxidation can take place at the same time. Alcohols were not further converted when CO was depleted (figure 1B), suggesting CO is required for the conversion of alcohols back to acids. Alcohol oxidation alone did not sustain growth of *C. autoethanogenum*, as incubation with only alcohols as electron donor did not result in growth or show oxidation activity after two weeks of incubation.

CO/CO_2 ratio affects alcohol oxidation metabolism

To get a more accurate view on the switch between alcohol oxidation and production, concentrated cell suspensions of *C. autoethanogenum*, harvested from a chemostat, were used. Harvested active cells were tested over a course of several hours for ethanol production or oxidation activity with different initial CO pressures, acetate and ethanol concentrations. Similar to observations in bottle experiments, high ratios of CO/CO_2 at the start of all experiments (irrespective of total CO pressure) caused formation of alcohols, while near the end of the experiments at lower CO/CO_2 ratios oxidation of alcohols was observed (figure 2). Additionally, initial higher levels of acetate promoted solventogenesis while initial higher levels of alcohols promoted alcohol oxidation under similar gas compositions. The starting pH during these experiments was in all cases 5.8, while the end pH ranged between 4.8 and 5.2. When plotting the data displaying either alcohol oxidation or alcohol production against the CO/CO_2 ratio, a clear separation between alcohol oxidizing and alcohol producing samples was observed (figure 2). As expected, alcohol oxidizing cultures are located in the lower CO/CO_2 regions. In addition, the thermodynamic thresholds for activity of the acetaldehyde oxidoreductase (Aor) were plotted for an external pH of 4.8, 5.5 and 5.8 (figure 2A). For calculations we assumed an intracellular pH of 6.8, acetaldehyde concentrations of 50 μM, a direct relation of CO/CO_2 ratio with the ferredoxin redox potential in the cell and a direct relation of CO and CO_2 pressure with their dissolved concentrations. Points localized above the line should theoretically be in Aor active state (thus enabling ethanol production), while points below should be in Aor inactive state (allowing ethanol oxidation). With increasing length of incubation all points move towards the alcohol consumption phase, due to a combination of lower pH and lower CO/CO_2 ratios.

Chemostats were used to further study the effect of CO dissolved on the alcohol metabolism of *C. autoethanogenum* under more controlled conditions. Chemostat runs of *C. autoethanogenum* at pH 6 with relatively low CO inflow rates (1 ml/min) showed mainly production of acetate (about 20 mM) and trace amounts of ethanol (around 0.2 mM). The CO concentration in the liquid was determined to

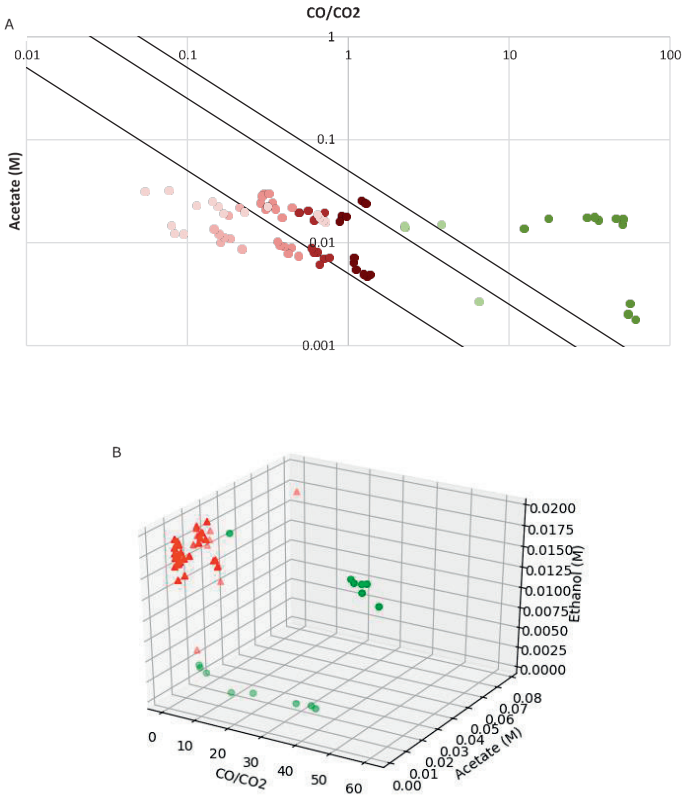

Figure 2. Validation of alcohol production and oxidation in Hungate tubes using active cells. Black lines indicate the theoretical threshold for alcohol oxidation at different external pH (up to down: pH 5.8, 5.5, 4.8). Points in red are experimental points validated to be in oxidation stage and green points are experimental points validated to be in alcohol production stage. Colour intensity indicates length of incubation, higher intensity being earlier in the incubation (and thus higher pH). B) Same points plotted in a 3-D graph including the alcohol exposure levels. Green points indicate alcohol producing while red points indicate alcohol consumption.

be very low (in the range of 1-10 µmol/L). A sudden increase of the CO inflow to 3 ml/min, caused a peak in CO dissolved (figure 3). After 2 minutes acetaldehyde formation is observed, followed by ethanol production after 10-15 minutes (figure 3B). During the CO spike ethanol concentration increased, but remained below 1 mM (figure 3A). When ending the CO spike and reverting the CO flux back to 1 ml/min, ethanol was quickly consumed till depletion, resulting in a sudden increase in acetate concentration. This shows that alcohol production and consumption can be quickly reverted.

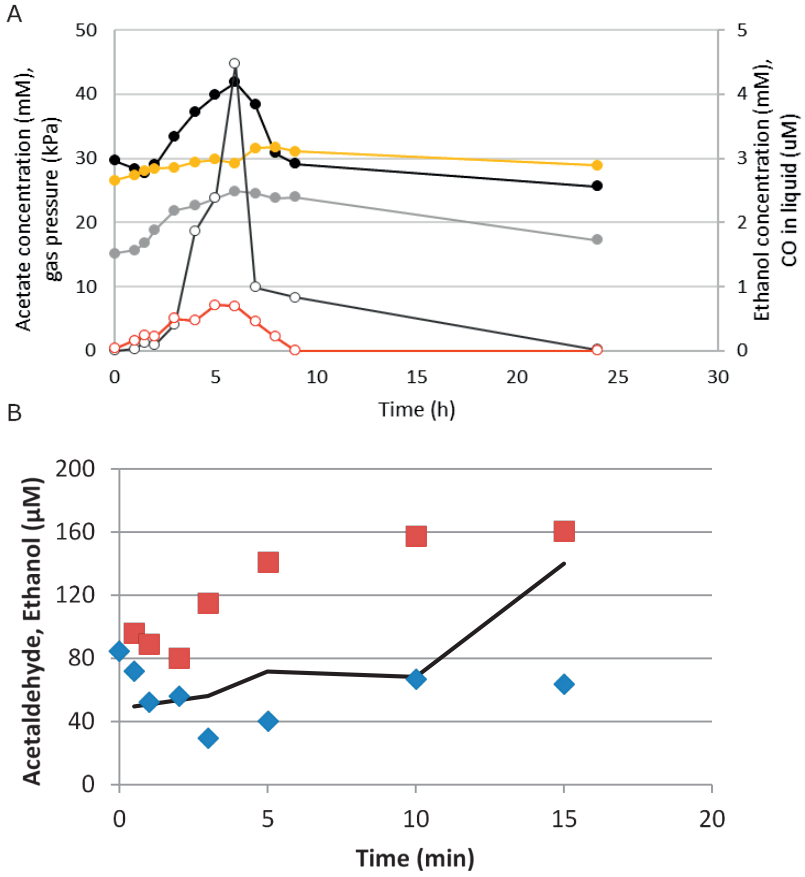

Figure 3. Alcohol production and consumption by *C. autoethanogenum* in a chemostat. A) physiological profile of the reactor run operated at pH 6 with CO spike. Spike was initiated at t = 0 and stopped at t = 6. CO headspace (black dots), CO_2 headspace (grey dots), CO dissolved (dark grey dots), Acetate (yellow dots), Ethanol (red dots). Open and closed symbols indicate left and right axis respectively. B) profile of the first 15 minutes after CO spike, showing acetaldehyde levels with CO spike (red) and without spike (blue). Black line indicates ethanol levels during in the CO spike conditions. During the non-spike condition no ethanol was detected.

Biomass yield of *C. autoethanogenum* growing on alcohol and CO is higher than on CO alone

During growth tests with 10 mM ethanol starting concentration and varying CO headspace pressure (30, 50 and 100 kPa) ethanol oxidation was observed at 30 and 50 kPa starting pressures. In these incubations 1.5-2 times more biomass was formed per CO consumed when compared to the conditions lacking ethanol (figure 4). The CO/CO_2 ratios in the bottles incubated with ethanol show a value of 3 while a value

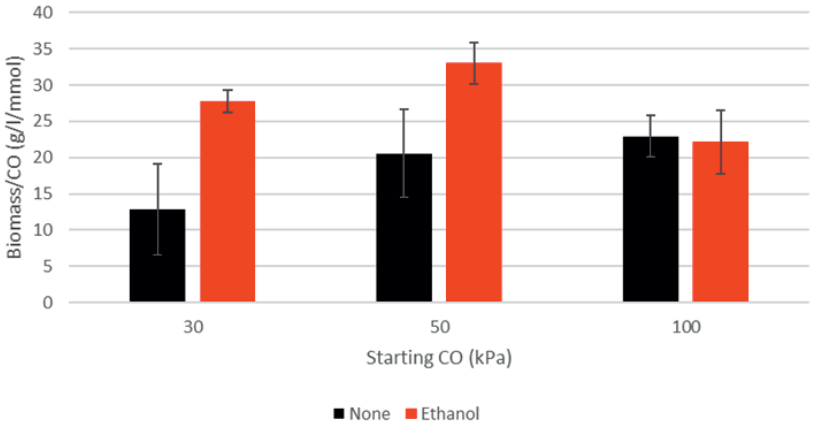

Figure 4. Biomass yields per CO consumed in *C. autoethanogenum* in presence or absence of ethanol. Cells were grown on 30, 50 or 100 kPa CO in closed bottles. Standard deviations are shown over triplicate experiments.

of 2 is found in the control condition, indicating less CO_2 release in the former. Ethanol addition appears to solely have effect at lower CO starting pressures, as in presence of 100 kPa initial CO pressure biomass yields are the same for the tested conditions. In these 100 kPa bottles a net production of ethanol was found, indicating no net ethanol oxidation had taken place.

To further study the effect of ethanol consumption on biomass yields of *C. autoethanogenum*, growth was performed in a chemostat at a CO inflow rate of 1 ml/min at pH 6. In steady state, 20 mM acetate was formed with traces of ethanol (~0.2 mM) and biomass accumulated to 0,1 g/l dry weight. After steady state was reached CO inflow was increased to 3 ml/min, after which the dissolved CO rapidly increased (figure 5). CO increase was followed by ethanol production, increase in acetate concentration and a rapid increase of biomass. Within 6 h the biomass concentration in the reactor doubled from 0.1 to 0.2 g/l. Due to the fast formation of biomass and products, the dissolved CO levels dropped quickly, additionally resulting in lower CO pressure in the liquid and subsequently in ethanol to be consumed again. When after 3 days steady state was reached at 3 ml/min CO inflow, formation of 48 ± 0.7 mM acetate, 0,24 ± 0.02 g/l dry weight biomass and traces of ethanol were observed. The ratios of biomass formed per acetate produced are ~0.005 g biomass/mmol acetate in both, 1 and 3 ml/min, steady-state conditions. Interestingly, during the non-steady state period, biomass reaches the steady value much faster (6-24h) than the acetate concentrations (~3 days). This suggests that when the high CO regime

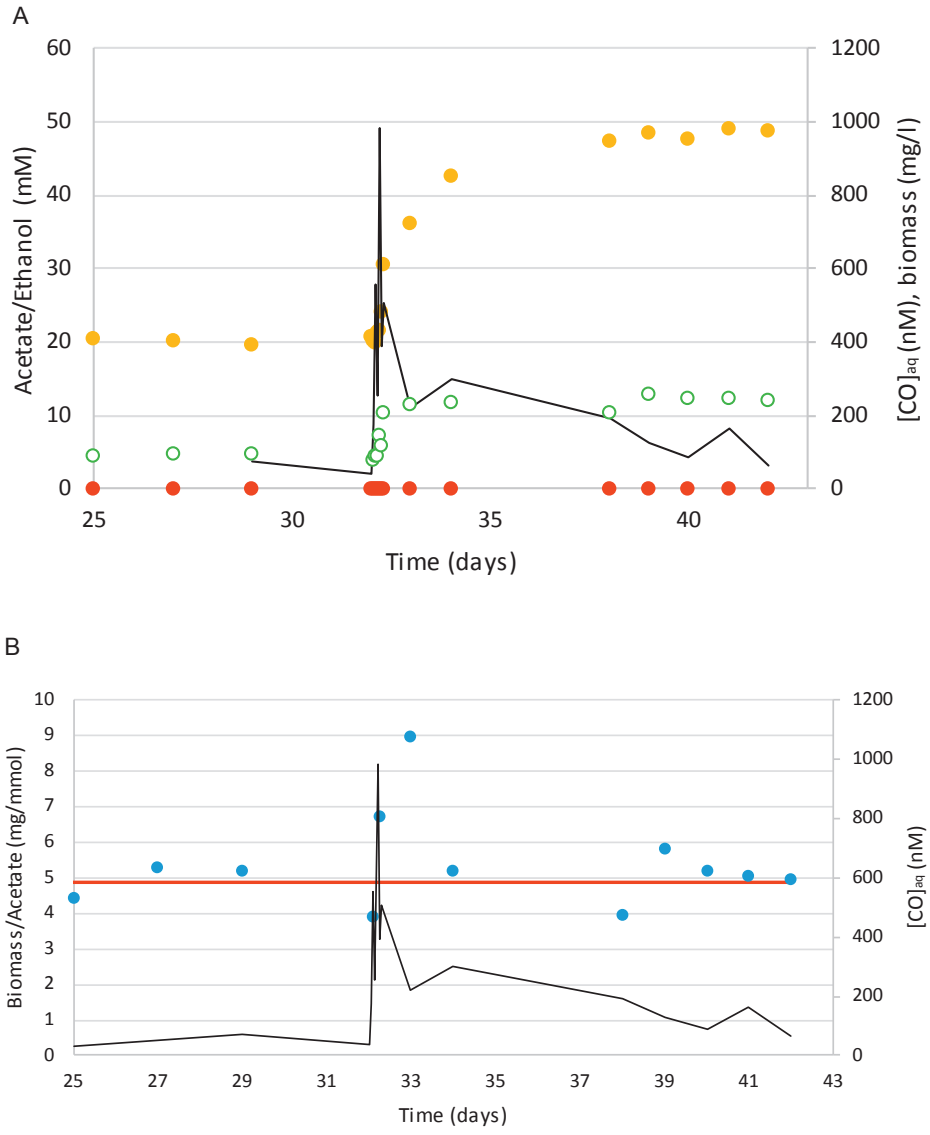

Figure 5. Physiological profile of *C. autoethanogenum* grown in a chemostat reactor at pH 6, during sudden CO increase from 1 ml/min to 3 ml/min (at t = 32). Acetate (yellow dots), ethanol (red dots) are displayed on the left axis (closed symbols), CO dissolved (black line) and biomass (green dots) are displayed on the right axis (open symbols). B) Acetate production per biomass formed during the CO ramp. Biomass yield per acetate (blue dots) and average biomass in steady state (red line) is displayed on the left axis while CO dissolved (black line) is displayed on the right axis.

has just been initiated, less acetate formation is required to sustain the formation of the same amount of cell mass. Over the first 6 h after CO increase, ~0.1 g/l biomass is formed while ~10 mM acetate is produced. In steady state 0.1 g/l biomass requires production of ~20 mM of acetate, which is double the amount as required during the CO-burst phase. As CO dissolved levels drop towards the steady state, biomass remains stable while the amount of acetate keeps increasing bringing the biomass/acetate ratio back to the value found for the original steady state (figure 5B).

The same experiment was performed at a pH of 5 to see if similar behaviour would occur. The initial phase with low CO feeding resulted in similar conditions as at pH 6. Before increasing the CO flow 0.11 ± 0.03 g/l biomass, 22 ± 0.8 mM acetate and traces of ethanol were found. CO was increased to 3 ml/min and biomass increased over 6 h to 0.2 ± 0.01 g/l dry weight doubling the original biomass. Instead of acetate formation, observed in the pH 6 condition, larger amounts of ethanol were formed, decreasing acetate values to 15 mM while ethanol increased up to 8 mM (figure 6). This response at pH 5 is clearly more solventogenic as at pH 6 as acetate is taken up from the environment to produce ethanol (figure 6). Biomass generated per acetate produced is only for a short time altered after the spike, and appears to stabilize at a value slightly above the value found in the original steady state (figure 6B).

Discussion

Alcohol production or oxidation in *C. autoethanogenum* appears to be determined by three factors: CO/CO_2 ratio, acetic acid concentration and ethanol concentration. In cultures of *C. autoethanogenum*, oxidation of alcohols to acids was preferred in presence of relatively low CO/CO_2 ratio, low acetic acid or high alcohol concentrations (figure 2). As suggested by Richter et al., 2016, activity of the Aor enzyme determines if the pathway towards alcohol production is activated, depending on undissociated acid concentrations (Richter et al., 2016b). For alcohols to be oxidized, the Aor preferably has to be switched off. The other way around, alcohols are the preferred product under high acetic-acid concentrations and high CO/CO_2 ratios, where Aor is active.

Similar to alcohol production, their oxidation can occur via two pathways: via acetaldehyde to acetate or via acetaldehyde and acetyl-CoA to acetate (figure 7). Both pathways generate reduction equivalents, however the pathway via Aor is expected to yield ferredoxin and/or NAD(P)H whereas the pathway via acetaldehyde dehydrogenase generates only NAD(P)H equivalents. The latter pathway is however expected to yield one ATP via acetate kinase (Ack). Judging from the biomass yields, alcohol consumption appears to be linked to significant energy conservation, as the relative biomass yield per CO increased by 1.5-2 fold when ethanol is oxidized compared to solely carboxydotrophic acetogenic cultivation of *C. autoethanogenum*

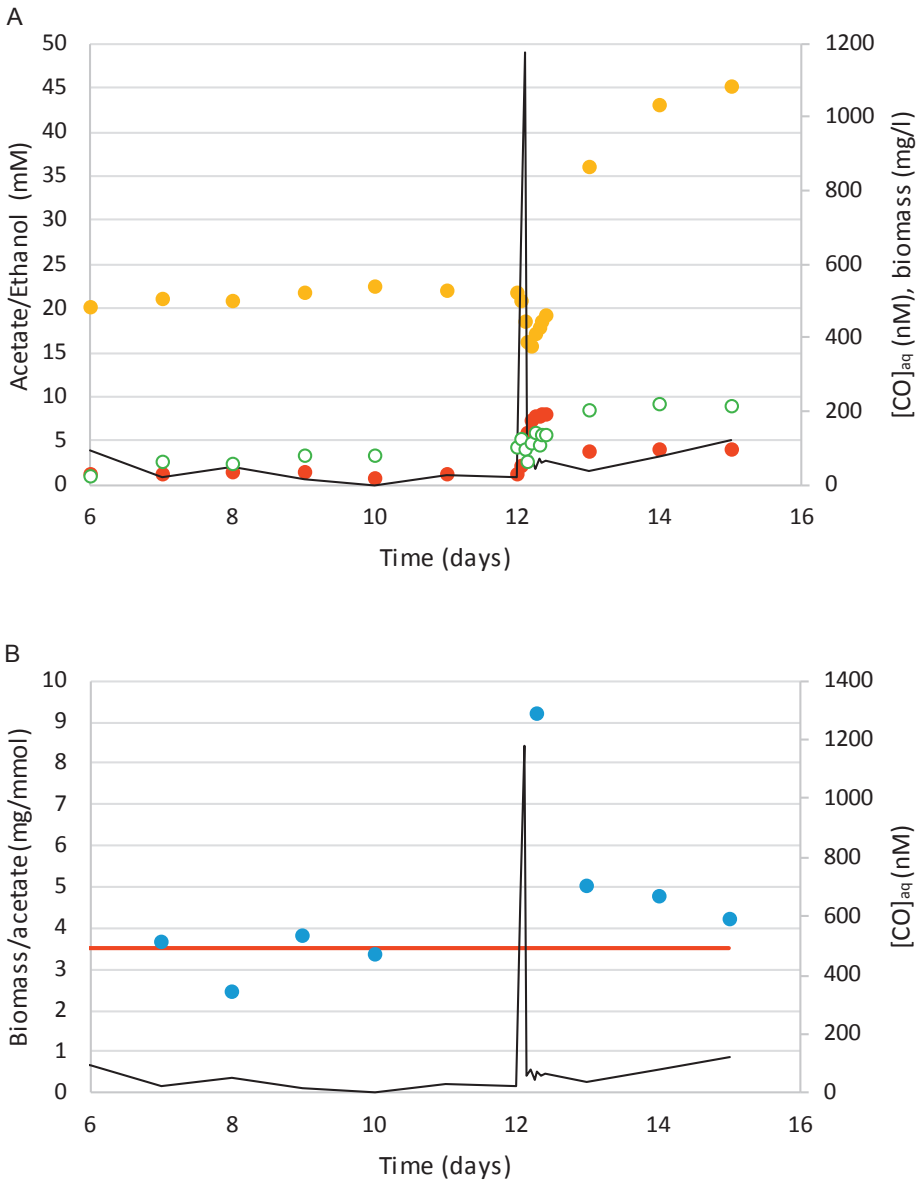

Figure 6. Physiological profile of *C. autoethanogenum* grown in a chemostat reactor at pH 5, during sudden CO increase from 1 ml/min to 3 ml/min (at t = 12). Acetate (yellow dots) and ethanol (red dots) are displayed on the left axis (closed symbols) while CO dissolved (black line) and biomass (green dots) are displayed on the right axis (open symbols). B) Acetate production per biomass formed during the CO ramp. Biomass yield per acetate (blue dots) and average biomass in steady state (black line) is displayed on the left axis while CO dissolved (red line) is displayed on the right axis.

(figure 4). Assuming a bifurcational methylene-THF reductase, as suggested by modelling studies done on *C. autoethanogenum* (Valgepea et al., 2018), an estimate can be made of the ATP gain of *C. autoethanogenum* per CO consumed. The energy yield per CO for acetogenesis from both ethanol and CO (Eq. 1) compared to acetogenesis from solely CO (Eq. 2) increases ~1.7 times if alcohol oxidation runs via the Adh pathway (assuming NADH as involved cofactor), while a 1.3 times decrease is expected if this runs via the reverse Aor (assuming ferredoxin and NADH are released by this pathway).

A 1.5-2 times increase in biomass per CO consumed was found during ethanol oxidation (figure 4), suggesting that the Adh pathway is taken when ethanol is oxidized. Addition of ethanol only promotes the biomass yield at lower starting pCO, being absent at 100 kPa starting pressure (figure 4). This is likely due to the unfavourable conditions for alcohol oxidation at higher CO/CO_2 ratios, causing initial alcohol production. In the 100 kPa bottles net ethanol production was found, not benefiting from the energy gain of alcohol oxidation. At lower pCO starting pressure, ethanol is oxidized earlier due to faster decrease in CO/CO_2 ratios, gaining sooner access to ethanol as a substrate. It is unlikely that the observed increase in energy yield is caused by ethanol as biomass precursor, as for acetogens growing on CO this is more costly compared to fixation of CO_2 via the Wood-Ljungdahl pathway due to net ATP generation when acetyl-CoA is formed from CO (Diender et al., 2015, **Chapter 2**). Additionally, if ethanol acted as biomass precursor allowing for lower energy investment on biomass formation, the same yield increase would likely be observed at 100 kPa CO pressure as well.

Alcohol oxidation in gas fermenting acetogens has been observed before (Bertsch et al., 2016; Köpke et al., 2010), but has not been elaborately described for *C. autoethanogenum*. Additionally, the observation of co-consumption is interesting as ethanol can in theory supply enough electrons to reduce 2 CO_2 to acetate and conserve net energy, similar to what is observed in *Acetobacterium woodii* (Bertsch et al., 2016). For *C. autoethanogenum* we do not observe significant alcohol consumption in the absence of CO (figure 1B), suggesting that there is interference in the metabolism of *C. autoethanogenum* during solely alcohol oxidation. Reduction equivalents such as NADPH or NADH could in theory supply higher potential electrons, as ferredoxin, via bifurcation mechanisms in *C. autoethanogenum* such as the bifurcating methylene-THF reductase or the RnF complex. It was suggested that during growth of *A. woodii* on ethanol the RnF operates in reverse at the expense of ATP.

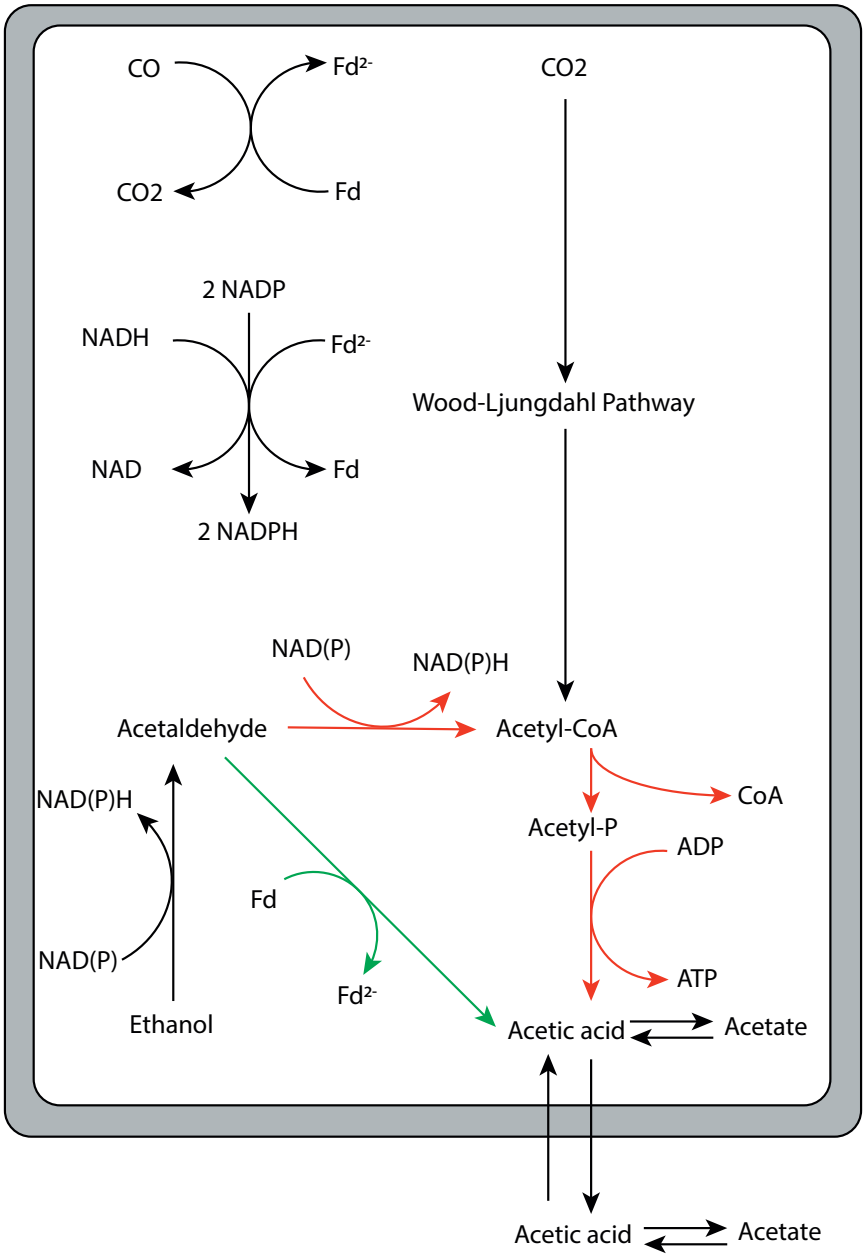

Figure 7. Simplified schematic representation of the proposed alcohol oxidation pathways in *C. autoethanogenum*. Pathway shown in red indicates the oxidation of ethanol via acetyl-CoA while the pathway shown in red indicates the oxidation via the Aor reverse reaction. Fd: Ferredoxin. Reactions shown with NAD(P)H are either unknown for their exact energy acceptor/donor or can occur with both NADH or NADPH.

Alcohol oxidation in gas fermenting acetogens has been observed before (Bertsch et al., 2016; Köpke et al., 2010), but has not been elaborately described for *C. autoethanogenum*. Additionally, the observation of co-consumption is interesting as ethanol can in theory supply enough electrons to reduce 2 CO_2 to acetate and conserve net energy, similar to what is observed in *Acetobacterium woodii* (Bertsch et al., 2016). For *C. autoethanogenum* we do not observe significant alcohol consumption in the absence of CO (figure 1B), suggesting that there is interference in the metabolism of *C. autoethanogenum* during solely alcohol oxidation. Reduction equivalents such as NADPH or NADH could in theory supply higher potential electrons, as ferredoxin, via bifurcation mechanisms in *C. autoethanogenum* such as the bifurcating methylene-THF reductase or the RnF complex. It was suggested that during growth of *A. woodii* on ethanol the RnF operates in reverse at the expense of ATP. The formed proton gradient is used to drive ferredoxin reduction, which allows redox balancing via the Wood-Ljungdahl pathway. In theory *C. autoethanogenum* is able to perform a similar type of metabolism. However, for *C. autoethanogenum* it remains unknown which exact redox equivalents are generated during alcohol oxidation, making it difficult to assess why no growth on solely alcohols is observed. Potentially the origin of this lies in the utilization of the bifurcating methylene-THF reductase in *C. autoethanogenum*. If alcohol oxidation would only generate NAD(P)H reducing equivalents, the RnF complex is needed to make additional reduced ferredoxin (figure 8). However, in contrast to *A. woodii*, *C. autoethanogenum* is suggested to contain a bifurcating methylene-THF reductase complex generating ferredoxin from NADH during operation of the methyl-branch of the Wood-Ljungdahl pathway (Bertsch et al., 2016; Valgepea et al., 2017). The ferredoxin generated from the methylene-THF reductase potentially drives the RnF to form a proton gradient, potentially causing interference in the redox metabolism during utilization of ethanol as sole substrate (figure 8). *A. woodii* lacks the bifurcational methylene-THF reductase allowing the generated ATP to generate the required proton gradient without interference. Besides the acetic acid concentration in the cell, ethanol production or consumption appears related with the exposure to higher or lower CO/CO_2 ratios (figure 2). This was shown in batch bottle experiments as well as reactor runs where a clear relation was observed between CO dissolved and ethanol production/consumption (figure 2/3/5/6). Spiking CO resulted in short term ethanol production, going down upon decreasing CO flow or after increasing biomass concentration (figure 3,5,6). The stimulatory effect of CO dissolved on alcohol production potentially also explains why limiting growth of CO fermenting acetogens by other factors (e.g. temperature, medium supplements) is observed (Kundiyana et al., 2011; Ramió-Pujol et al., 2015; Richter et al., 2013). Such conditions potentially cause CO to accumulate in the liquid, resulting in more ethanol formation.

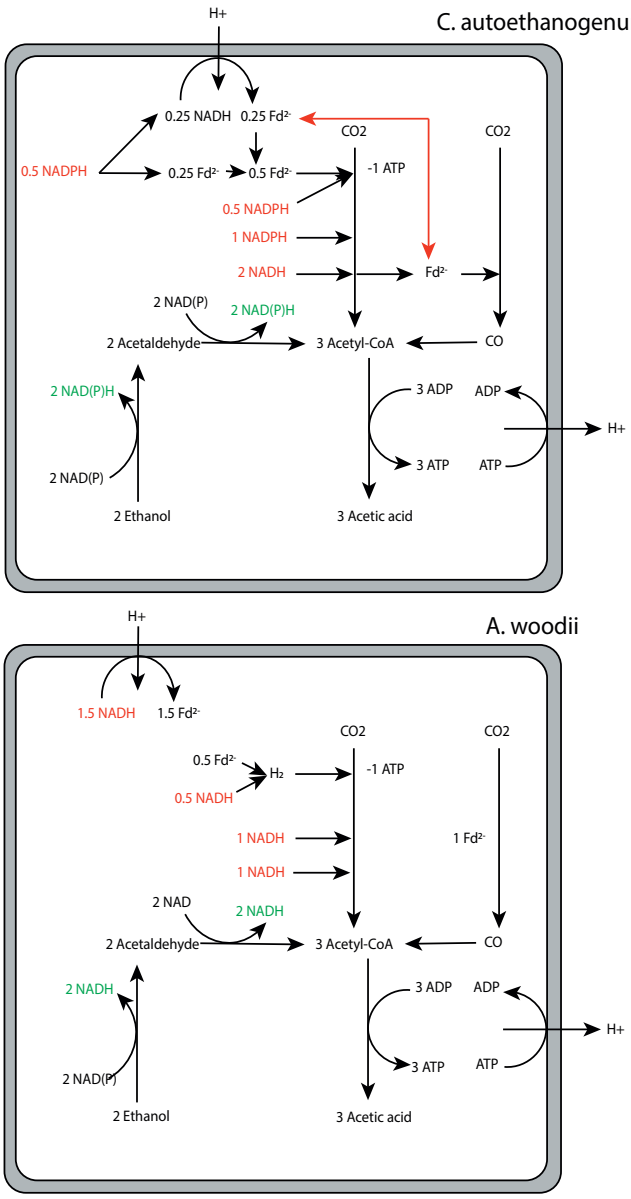

Figure 8. Schematic representation of potential electron flow in *C. autoethanogenum* (above) vs. *A. woodii* (below) when grown on ethanol as sole substrate. Cofactors indicated in green are derived from ethanol oxidation, while cofactors indicated in red are the ones moved into the metabolism for reduction of CO_2. The red arrow in the schematic of *C. autoethanogenum* indicates the potential hampering factor in ethanol oxidation. The ATP/H+ yield of the ATPase and Rnf complex is not displayed stoichiometrically.

The control of the alcohol/acid metabolism of *C. autoethanogenum* can be explained by the activity of two enzymes: Aor and Adh. Aor is dependent on the redox pressure of ferredoxin, intracellular pH, and concentrations of acetaldehyde and acetic-acid (Eq. 3). Adh is dependent on the redox pressure of NAD(P)H, intracellular pH, and concentrations of acetaldehyde and ethanol (Eq. 4). Together, activity of both enzymes control the size of the acetaldehyde pool, balancing out based on the concentrations of acetic acid and ethanol. The external pH indirectly influences the internal acetic-acid concentration, influencing Aor activity.

$$Fd^{2-} + 2\ H^{+} + CH_3COOH \leftrightarrow Acetaldehyde + Fd + H_2O \quad (3)$$

$$Acetaldehyde + NAD(P)H \leftrightarrow Ethanol + NAD(P) + H_2O \quad (4)$$

As intracellular metabolite concentrations and pH for *C. autoethanogenum* are largely unknown and likely are variable during growth, it is difficult to predict the shift point where solventogenesis goes over into alcohol oxidation. However, based on the thermodynamics of the Aor enzyme a prediction can be made as depicted in figure 2. All points situated at the top side of the line are expected to be in state of alcohol formation, while points below the line are expected in state of alcohol oxidation for the specific external pH. In addition to Aor activity, alcohol oxidation also depends on the direction of the Adh enzyme. Gibbs free energy change calculations, assuming intracellular pH of 6.8, 10 μM acetaldehyde and ratio for NAD/NAD(P)H of 10 (E_0' = -0.320 V), suggest ethanol can accumulate to 10 mM before oxidation becomes more favourable. Alcohol oxidation or production is thus not solely linked with Aor activity, but is likely also affected by the thermodynamics of the Adh enzyme. This independence of alcohol oxidation and production processes is highlighted by the simultaneous oxidation and production of alcohols, as is observed for the case where butanol is present (figure 1B). If butyraldehyde concentrations are low in the cell due to the absence of butyraldehyde formation by the Aor complex, butanol is oxidized, subsequently causing formation of butyrate. Acetaldehyde concentrations might simultaneously not be low enough for ethanol oxidation, causing ethanol to be formed. This causes that with the same CO/CO_2 ratio and pH, alcohol oxidation and production for different alcohols/acid pairs can take place at the same time.

Based on the observation that co-consumption of ethanol and CO result in a significant increase in energy yield, we theorise that the alcohol oxidation takes place via Adh/Ack route. Therefore, if Aor and the Adh indeed operate independently, a scenario where acetaldehyde is formed, but not further reduced to ethanol is possible. Similar to what is expected to happen during alcohol oxidation, acetaldehyde could be converted to acetyl-CoA and subsequently acetate (figure 9). Activity of this pathway would result in no net change of the overall metabolism, remaining stoichiometrically the same as acetogenesis (Eq. 2). However, due to additional energy gain via acetate

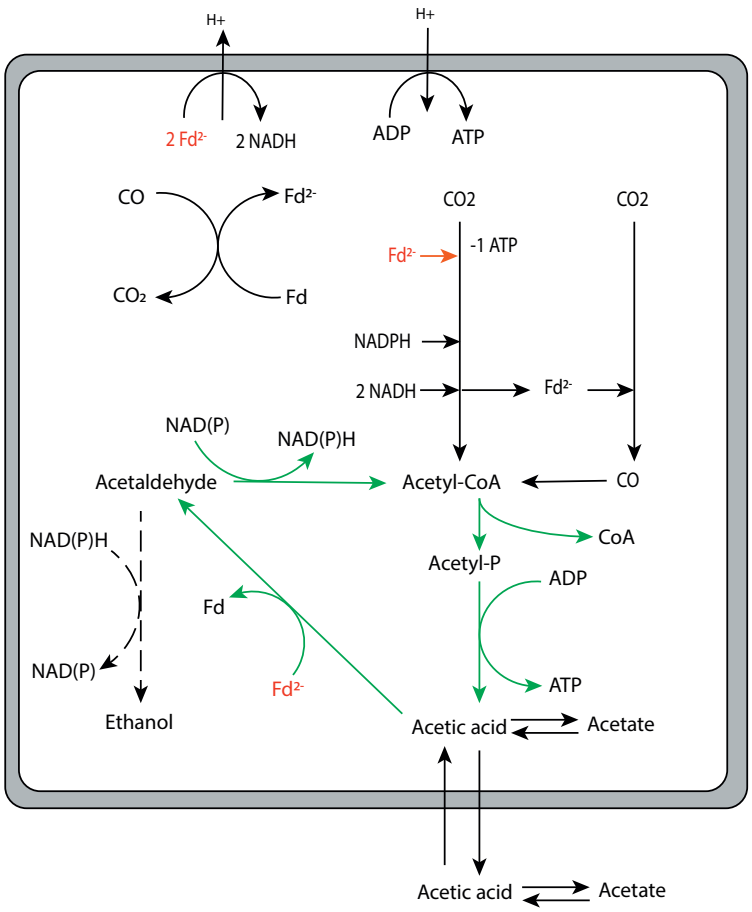

Figure 9. Schematic representation of the potential acetate cycling pathway (in green) in *C. autoethanogenum*, contributing to increased energy yield under increased CO/CO_2 ratios. Dashed lines indicate the ethanol oxidation step, which might also be active in the direction of ethanol production if acetaldehyde levels are sufficient enough. Ferredoxin (Fd) indicated in red shows where the reduction equivalents formed from CO oxidation first enter the metabolism. The reduction of CO_2 to formate via the bifurcating formate dehydrogenase (orange arrow) is comprised of multiple reactions but is here displayed as a single reaction. The ATP/H^+ yield of the ATPase and Rnf complex is not displayed stoichiometrically.

kinase, this would increase the overall ATP yield of the Wood-Ljungdahl pathway by a factor of two. This ATP increase is similar to the biomass yield increase that is found in the chemostat experiments at pH 5 and 6 (figure 5b/6b). As long as the pressure provided by the CO/CO_2 pair is enough to drive sufficient acetaldehyde production and NAD(P) redox levels are suitable (Eq. 5), production of acetyl-CoA from acetaldehyde could become favourable. Hence, acetyl-CoA concentrations

have to be in a range where both acetaldehyde conversion to acetyl-CoA and ATP production from its conversion to acetate are still feasible. It is possible that during ethanol production the pathway from acetaldehyde to acetyl-CoA is also active as long as the thermodynamics and kinetics of the pathway allow it. Indications that such activity is occurring, is the slightly higher biomass/acetate yield observed in the second steady state (3 ml/min CO), where a visible background of ethanol is formed, compared to the first steady state (1 ml/min CO) at the pH 5 reactor (figure 6b).

$$\text{Acetaldehyde} + \text{NAD(P)}^{-} + \text{H}^{+} + \text{CoA} + \text{H}_2\text{O} \leftrightarrow \text{AcetylCoA} + \text{NAD(P)H} \qquad (5)$$

Earlier reports of acetaldehyde dehydrogenase (AdhE) knock-out strains of *C. autoethanogenum* showed increased ethanol formation (Liew et al., 2017), suggesting that AdhE of *C. autoethanogenum* potentially has a role in the oxidation of ethanol. Additionally, the same study showed growth deficiencies of *C. autoethanogenum* with an AdhE knockout, which was suggested to be due to disturbance of the redox metabolism. An alternative explanation would be that less energy is conserved due to

Conclusions

Next to alcohol production, *C. autoethanogenum* appears to be able to oxidize alcohols to their respective acids as well. This however only appears possible in presence of CO, acting as co-substrate for the production of acetate. Next to pH, the CO/CO_2 ratio (and thus the reduction state of ferredoxin) appears essential for determining if alcohol production or oxidation takes place. Due to the apparent thermodynamic control of the system also acetic-acid and alcohol concentrations strongly influence the direction of the alcohol metabolism. Alcohol oxidation seems to be linked to additional energy conservation, suggesting that the pathway via acetate kinase is taken for the oxidation of alcohols. In addition we observe a significant biomass yield increase during exposure of the cells to higher CO dissolved concentrations. Potentially, production and subsequent oxidation of acetaldehyde in the cells back to acetate via acetyl-CoA occurs, cycling acetate at the expense of CO oxidation, driving additional energy conservation via substrate level phosphorylation.

Chapter 8

General Discussion

Chapter 8: General discussion

In the past four years that this project was conducted, fundamental and applied aspects of syngas fermentation got much attention. Research efforts by industry and establishment of gas-fermentation projects by companies as Lanzatech, AcelorMittal and Evonik (AcelorMittal and Lanzatech, 2015; Haas et al., 2018), indicate the increasing interest for synthesis gas fermentation technology. Work described in this thesis contributes to gain insight into the physiology of gas fermenting microbes (**Chapter 2, Chapter 3, Chapter 6 & Chapter 7**). Additionally, this work pioneers in applying synthetic mixed cultures in syngas conversion processes (**Chapter 4, Chapter 5 & Chapter 6**). This approach opens-up new opportunities for syngas fermentation compared to current strategies based on pure- or undefined mixed cultures. Next to the proof of concept of co-cultivation, fundamental knowledge was obtained on the mechanisms underlying the interaction between the two organisms in such synthetic cultures (**Chapter 6**). This gives a broader insight in how thermodynamics affects microbial interactions, not only considering the typical syntrophic examples, but also within microorganisms that do not strictly depend on the activity of each other to live. Insight was gained in the energy conserving mechanisms of *Clostridium autoethanogenum*, highlighting an energy conserving strategy based on co-utilization of CO and alcohols. This resulted in a hypothesis for a new energy conservation mechanism based on cycling of acetate at increased CO exposure in the liquid (**Chapter 7**). This chapter will discuss the current developments in the field of syngas fermentation and will place those in the light of this thesis.

Future application potential of gas fermentation

Synthesis gas fermentation has the potential to become an important sustainable route for the production of chemicals and fuels from waste streams. Gas utilized in the fermentation process can be derived from multiple sources, such as off-gases from industry (Molitor et al., 2016), gasification of carbon wastes from both biomass or municipal sources (Daniell et al., 2016; Drzyzga et al., 2015) or thermo-chemical/electrochemical reduction of CO_2/H_2O streams (Dubois and Dubois, 2009; Furler et al., 2012; Redissi and Bouallou, 2013). This makes gas fermentation highly flexible in its starting materials compared to other bio-based approaches (table 1) and allows for utilization of carbon normally not available for biological fermentation processes, such as recalcitrant municipal wastes (e.g. plastics or rubber). This flexibility allows for the integration of multiple waste streams into a single fermentation process. Additionally, contrary to sugar fermentation, waste products from gas fermentation, mainly CO_2 and biomass, can be reused by introducing them to the incoming waste stream. In this way, low carbon emissions can be reached by introducing additional hydrogen to the incoming gas stream, lowering the CO_2 output of the fermentation while increasing product formation (**Chapter 6**). These features of syngas

Table 1: Biomass conversion to chemicals – conversion technology comparison, adapted from Daniell et al,. 2012.

	Biochemical (pretreat + enzyme + fermentation)	Thermochemical (gasification + catalysis)	Hybrid (gasification + fermentation)
Catalysts	Enzymes and Microorganisms	Metal catalyst	Microorganisms
Feedstock	**Specific** Lignocellulosic biomass, such as forestry crops, perennial grasses and agricultural residues. Pre-treatment steps are usually biomass type-specific.	**Flexible** Gasification process allows a wide range and mixture of feedstock to be used (coal, lignocellulosic biomass, municipal wastes).	**Flexible** Gasification process allows a wide range and mixture of feedstock to be used (coal, lignocellulosic biomass, municipal wastes).
Syngas composition		**Specific** Catalysts require specific syngas composition to obtain good product yields. Extensive pre-treatment steps are needed to minimise contaminants.	**Flexible** Microbial catalyst can utilise a wide range of syngas H_2:CO composition while retaining product specificity. Pre-treatment steps are needed to reduce contaminants.
Tolerance to inhibitors	**Low** Pre-treatment process releases and creates inhibitors potentially toxic to enzymes used in the saccharification, and bacteria used in fermentation.	**Low** Catalysts can be irreversibly inactivated when exposed to low concentrations of contaminants (e.g. ppm range for sulfide)	**Medium** Tolerant to many impurities such as sulphur-containing compounds. Consequently, fewer clean-up steps are required than for thermochemical route. However, still more research is required to define the exact toxicity of bio-catalysts to specific syngas impurities (e.g. tars).
Tolerance to microbial contamination	**Poor** Risk for contamination as microorganisms growing on sugars are abundant in nature.	-	**Medium** As CO and H_2 are the only substrates the opportunity for microbial contamination is reduced.

fermentation might in the future proof valuable. Especially when fossil sources become scarce, biomass and carbon waste-streams are potentially the main carbon sources for production processes.

Irrespective of composition, conversion of the starting material via gasification would allow for most of the material to become available as a mixture of H_2, CO and CO_2, becoming accessible for subsequent conversion processes. Different gasification setups can be employed, each having advantages or disadvantages for conversion of specific types of starting material (Heidenreich and Foscolo, 2015). Drawbacks of traditional gasification processes are the requirements for relatively dry starting material and the highly variable gas composition, depending on gasification technique and the parameters used (Drzyzga et al., 2015; Piccolo and Bezzo, 2009; Ptasinski, 2008). Additionally, energy efficiencies of commonly used gasification processes are highly variable and often have energetic efficiencies between 20-70% depending on technique used (Heidenreich and Foscolo, 2015). However, recent developments aim to improve the overall process and minimize drawbacks. Such developments include plasma gasification, using the high temperature of plasma to efficiently decompose biomass or municipal wastes into syngas (Tang et al., 2013). Plasma gasification has high reaction rates enabling production of syngas with high H_2 and CO content containing less CO_2. Additionally, due to the high reaction rate, less tar contaminants are present in the final gas (Heidenreich and Foscolo, 2015). Disadvantages are however the high energy consumption for plasma heating, lowering the energy efficiency of the process. Another interesting development is supercritical water gasification, which enables the gasification of organics in liquid streams (Heidenreich and Foscolo, 2015). This however also requires high energy investment in order to reach supercritical state of water, which lowers the overall efficiency. Due to these relatively large energy investments of gasification, recycling of heat/energy is thus of utmost importance to keep the process energy- and cost-efficient. Commonly employed gasification processes are currently mainly applied to convert well defined substrates, relatively low in moisture content (e.g. coal), and processes are designed to be integrated with subsequent chemical catalysis or combustion processes to make optimal use of energy streams. With the use of more undefined streams such as biomass and municipal waste the gasification process needs to be redesigned to become efficient. The integration of the gasification and fermentation processes in a single process design is required to reach optimal efficiency and economics of the overall process. Likely the cost price of energy will play a major role here due to the large energy investment required for gasification of undefined (often moist) waste streams.

Besides biological gas fermentation as addressed in this thesis, syngas can also be converted via chemical catalysis, applying metal catalysts to form fuels or commodity chemicals. Examples are Fischer-Tropsch processes converting syngas to liquid hydrocarbons (de Klerk, 2013) or the Sabatier process forming synthetic natural gas (SNG) from syngas (Kopyscinski et al., 2010). Due to the metal catalysts applied in these processes, chemical catalysis is highly sensitive to contaminants in the syngas (e.g. sulfide), and products formed from these processes depend strongly on the syngas composition, possibly resulting in formation of undesired side products (Kopyscinski et al., 2010). This makes the highly variable composition of syngas a complicating factor to deal with and therefore requires strong gas purification and composition tuning before it can be applied in chemical catalysis. While biological fermentation processes are slower compared to chemical catalysis, they are less sensitive to contaminants and composition of the syngas and in some cases contaminants might even act as supplements for growth (e.g. sulfur-compounds, ammonia). This potentially allows for less stringent syngas cleaning prior to use. More elaborate research is however required to exactly determine the sensitivity of the bio-catalysts to specific contaminants that are often present in syngas such as tars (e.g. phenolic- or aromatic compounds). An additional advantage of bio-catalysis is the high specificity towards a single end-product, allowing for higher yield of a single product irrespective of gas composition (Daniell et al., 2012). Currently, main products from syngas fermentation processes include hydrogen, acetate and ethanol (figure 1) (Bengelsdorf et al., 2013; Diender et al., 2018, **Chapter 4**; Redl et al., 2017). Products less often observed are short and medium-chain fatty acids and alcohols (**Chapter 5, 6**), lactic acid and diols (Bengelsdorf et al., 2013; Köpke et al., 2011b; Redl & Diender et al., 2017). Production of higher-value products, such as medicine or food additives, is likely not feasible to perform directly from syngas fermentation due to the relatively low energy yield of gas fermentation metabolism (Diender et al., 2015, **Chapter 2**; Molitor et al., 2017). However, from the perspective of waste recycling it is interesting to consider the coupling of syngas fermentation and subsequent biological processes utilizing the simple organic carbon products (e.g. acetate, ethanol) formed from syngas fermentation process for aerobic production of biomass with purpose of food/feed protein production. This might be an indirect way to convert a diverse spectrum of waste streams (or even pure CO_2 streams) to products for feed/food application. The CO_2 released in the aerobic part of the process can be recycled in the gas fermentation process, limiting the CO_2 exhaust. While appealing from a waste utilization perspective, the question remains if such a process is feasible from an energetic and cost point of view compared to other production processes. Therefore, industrial bulk chemicals will likely remain the main product focus of syngas fermentation in the near future.

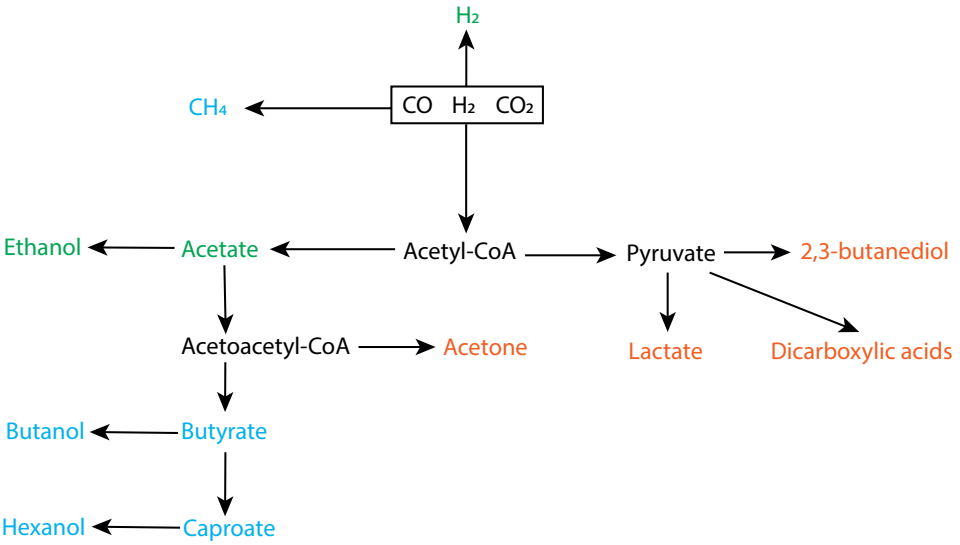

Figure 1. Potential products from syngas fermentation using microbial fermentation. Products generated naturally from syngas fermenting strains as major end-products are shown in green, other products can be observed but are often found as side products in the fermentation process (orange/blue). Products shown in blue are produced via co-cultures described in this thesis. Figure adapted from Redl & Diender et al., 2017.

Because of their flexibility and strong recycling capacity, integration of gas fermentation processes will likely play an important role in the future circular economy. However, this should be done in parallel with development of other technologies in order make optimal use of value of each waste stream. While gasification of a broad range of carbon materials is possible, this does not mean it is always valuable to do so. Gasification of easily fermentable material or products with higher economic value (e.g. sugar rich streams, recyclable plastics, hard wood) should be prevented as they can either be processed more easily or have higher application value in other processes. Therefore society should not aim for a single dominant technology to replace fossil driven processes, but should rather focus on building a diverse chain of technologies capable of closing the carbon cycle in our economy.

New opportunities for syngas fermentation: synthetic mixed cultures

In this thesis we showed that application of synthetic mixed cultures can contribute to the expansion of the product spectrum of syngas fermentation. Chain elongated products were observed before from syngas fermentation by Clostridium carboxydivorans (Ramió-Pujol et al., 2015) and was recently also shown to be produced by undefined mixed cultures with CO as substrate (He et al., 2018), but

in both studies at relatively low yield and low final concentrations of products were reached. In this thesis we showed production of chain elongated acids and alcohols with relatively high product/substrate yields (**Chapter 5 & 6**). We also showed that CO sensitive processes, such as methanogenesis, become more efficient when applying the co-cultivation strategy (**Chapter 4**). In order to enhance biological fermentation processes, the main research focus is usually directed towards genetic engineering approaches, where advantages can be gained from introducing or removing crucial genes of pathways to boost production or produce non-native products. However, as many gas fermentation pathways, such as the Wood-Ljungdahl pathway, operate at the thermodynamic limit to sustain energy production, there is little room for introducing, removing or altering major metabolic pathways (Molitor et al., 2017). The observation that gas fermentation pathways, such as solventogenesis, appear to be controlled by thermodynamics rather than by gene expression (Richter et al., 2016b) leaves the question if pathways can actually be controlled well via genetic engineering without significantly impairing the metabolism of the microorganism. Constructing synthetic communities of different bacterial partners, forming a food chain, is a possible alternative way to broaden the product spectrum of syngas fermentation.

In the methanogenic co-cultures, the CO removal by *Carboxydothermus hydrogenoformans* improved rates of methanogenesis significantly. Rates of the co-culture were higher than rates of complex communities on syngas and less by-products were formed (**Chapter 4**). Despite not reaching 100% pure methane gas, due to a non-optimal ratio of CO and H_2 (1:2) of the incoming gas, the culture should be capable of reaching such composition. Why a CO:H_2 ratio of 1:3 in the gas inflow did not sustain a functional culture remains unknown, but potentially is related to redox stress or light sensitivity in the methanogen. Interestingly, the co-culture reactor system was found to be sensitive to light in the stage where a 5:2 ratio of H_2:CO was fed (**Chapter 4**), whereas there was no clear sign of light inhibition in earlier stages of operation using a lower ratio of H_2:CO. Fluorescent tube lighting was used in the laboratory where reactors were operated, which have a peak spectrum around 430 nm (Khazova and O'Hagan, 2008). This potentially interacts with the F420 co-factors of methanogens (Olson et al., 1991), potentially giving additional stress under strongly reduced conditions. In addition to shielding from light, more biomass build-up (e.g. by increasing HRT) could allow a better performance at higher CO:H_2 ratios. The higher biomass density will result in even higher volumetric methane production rates. The, thus far, highest volumetric production rate reported for methane in a biological system is 288 l/l/day, in a pure culture of *M. thermoautotrophicus* grown on H_2:CO_2. This is significantly higher than the rates obtained in the syngas fermenting culture of 4 l/l/day (**Chapter 4**). However, biomass levels were 7 times higher in

the reported mono-culture and gas feed rates were 62 l/l/h while the co-culture was merely fed with 0.36 l/l/h. Correcting for the biomass concentration a rate of 28 l/l/day can be achieved by the co-culture, which is 10 % of the reported methanogenic system with H_2/CO_2. Additionally, biomass yields of 0.3-0.5 g/mol were reported for the monoculture of *M. thermoautotrophicus* on CO_2:H_2 while in the co-culture on syngas we obtain 2.2 g/mol methane. The higher yield might be explained by the presence of *C. hydrogenoformans* causing additional biomass formation from CO to hydrogen conversion. Production rates of methane from the syngas fermenting co-culture can likely be improved by additional gas feeding, better biomass retention and tuning for optimal gas composition. Ideally, an overflow chemostat setting is used, only supplying concentrated medium while letting the water formation of methanogenesis (eq. 1) determine the outflow rate. Assuming all water consuming reactions and evaporation can be neglected during process operation, 1 mole of methane production would result in 1 mole of water (18.01 g or ~18 ml).

$$CO + 3\ H_2 \rightarrow CH_4 + H_2O \qquad (1)$$

Such setup allows for a slow turnover of the liquid in the system, resulting in high biomass concentrations. Gas transfer has to remain the limiting factor though due to sensitivity of the methanogen to CO. Eventually an equilibrium will be reached between the rate of methanogenesis (determining the outflow rate) and biomass growth (determining the rate of methanogenesis). Such system might achieve high rates of methanogenesis and might be applied to convert CO rich gas streams to methane.

The co-culture of *C. autoethanogenum* and *C. kluyveri* that converts syngas or CO to chain elongated acids and alcohols demonstrates that it is possible to extend the product spectrum of syngas fermentation to products rarely observed from gas fermentation (**Chapter 5**). One of the more fundamental observations in this culture was the metabolic shift of C. autoethanogenum towards ethanol production (**Chapter 6**). Attempts to improve ethanol production in *C. autoethanogenum* via genetic engineering resulted in stressed cells and subsequent low biomass yields (Liew et al., 2017). This suggests that genetic engineering to improve industrial strains for ethanol production by altering its central metabolism might be difficult due to impairing biomass formation. Instead, continuous extraction of ethanol or instant conversion to other products during cultivation might significantly contribute to the overall product yield. Compared to the co-culture (**Chapter 5, 6**), systems fed with ethanol as substrate, or two stage systems perform better for chain elongation in terms of rate and product concentrations (Grootscholten et al., 2013; Richter et al., 2013; Vasudevan et al., 2014). The lower production rates of the co-culture can likely be explained by two factors, the non-optimal pH for both organisms (**Chapter**

5, Richter et al., 2016a) and the relatively low gas feed rate used in the applied reactor systems (keeping ethanol production the limiting factor). Continuation of the chemostat experiments, performed in **Chapter 6**, feeding additional acetate and hydrogen, was done in order to further assess the effect of higher pH on the co-culture and the combined effect of hydrogen and acetate feeding (table 2). We observed that at pH 6.6 chain elongation becomes more favourable and that ethanol again becomes the limiting factor in the system. This likely is the result of more optimal conditions for *C. kluyveri* combined with the lower toxicity towards chain elongated products at higher pH. Further increasing the pH to 6.8 resulted in rapid decrease in gas utilization followed by culture crash indicating an inactivation of *C. autoethanogenum*. Ramping the gas flow in the acetate reactor resulted in further build-up of chain elongated products, reaching 10 mM caproate (1.16 g/l) at a rate of 7 mmol/l/day. Vasudevan et al., (2014) reported on a two-phase system, using syngas effluent, able to achieve 1 g/l caproate with a mixed culture performing chain elongation at pH 5.44. A similar two-phase system applying a pure culture of *C. kluyveri* at pH 7 was able to reach production rates of 40 mmol/l/day of caproate using syngas fermentation effluent containing acetate and ethanol (Gildemyn et al., 2017). Application of two-stage systems using syngas fermentation effluent is likely hampered by the relatively large pH difference between the optimal pH for chain elongation (7-8) and the pH around 5 for solventogenesis. Thus, to efficiently perform reverse β-oxidation from syngas effluent in a two-phase system, large amounts of caustics are required to alter the pH to favourable levels in the second fermentation process. In the co-culture described here, using a combination of CO_2 limitation (by applying hydrogen), a pH ~6.5-6.8 and a high gas influx will likely result in the optimal production conditions. However, higher concentration of products might be achieved by designing a new co-culture, capable of performing the process at higher pH (7-8), omitting toxicity of the chain elongation products and allowing for *C. kluyveri* to grow more optimally. It is important to note that acetogens produce ethanol usually at lower pH (~5) However, by using the co-culture concept (**Chapter 6**), ethanol production might be boosted by presence of *C. kluyveri*, potentially stimulating ethanol production even at higher pH. A potential strain to test this with is *Alkalibaculum bacchi* (Allen et al., 2010), known to produce slight amounts of ethanol from CO at pH >7. Assuming the metabolism of *A. bacchi* is also thermodynamically regulated, the co-culture interaction combined with acetate pressure can cause a larger flux towards ethanol and subsequently chain elongation, potentially resulting in chain elongation in a co-culture from syngas at high pH. Further diversification of products by the described co-culture can be done by addition of a propionate producer (e.g. *Anaerotignum neopropionicum*) allowing for production of uneven chain elongated acids such as valerate (C5) and heptanoate (C7), and their respective alcohols.

Table 2. Data from the continuation of chemostat experiments performed in **Chapter 6**. Acetate and gas inflow are displayed, as well as the pH and found product concentrations in steady state.

	Acetate feed (mmol/l/day)	inflow (ml/min)			Concentration (mM)				
		H_2	CO	pH	acetate	butyrate	caproate	ethanol	butanol
H_2 reactor (**Chapter 6**)	0	3.2	2	6.2	48	12.6	7.1	5.5	4
H_2 reactor	0	3.2	2	6.6	48	15.2	9.6	0	0
Acetate reactor (**Chapter 6**)	60	0	2	6.2	68	14	5.5	0	0
Acetate reactor	60	0	3	6.2	67	14	8	0	0
Acetate reactor	60	1	3	6.2	69	15.9	10	0	0

Production of chain elongated alcohols such as butanol, hexanol and octanol was observed during cultivation of a chain elongating co-culture on syngas or CO (**Chapter 5**) (Haas et al., 2018; Richter et al., 2016a). The formation of these alcohols is likely due to use of excess reducing equivalents by the syngas fermenter, using the respective acids as electron acceptor. Alcohol production is also observed when hydrogen is fed in excess, limiting CO_2 availability, resulting in ethanol and butanol production (table 2, **Chapter 6**). The observation that alcohols are oxidized at lower CO pressure (**Chapter 7**) explains why during most of the, gas transfer limited, chemostat cultivation runs alcohols are not formed (**Chapter 6**). Chemostat cultivation of a co-culture of *C. ljungdahlii* and *C. kluyveri* did result in alcohol formation (Richter et al., 2016a), but the co-culture was fed with a larger amount of gas (30-80 ml/l/min) compared to the co-culture study described here (3-5 ml/l/min), likely causing more reduction equivalents to enter the cells. Initially, the production of both alcohols and acids appears as a negative aspect, due to dilution of the product of interest. However, the mechanism shown for alcohol oxidation (**Chapter 7**) suggests that exposing the culture to lower CO influx before the broth is down-stream processed allows for full re-oxidation of the alcohols to their respective acids. This would yield solely chain elongated acids as end product. The other way around, supplying with excess gas feed just before downstream processing, potentially combined with lowering pH, can result in production of mainly alcohols. Production of both acids and alcohols might be an advantage during fermentation due to distribution of toxicity over multiple products. One of the mechanisms to counter acetate toxicity during syngas fermentation is thought to be conversion of acetate to ethanol (Richter et al., 2016b). Similarly caproate conversion to hexanol might allow for an overall higher concentration of C6 molecules in the broth, eventually resulting in a higher end-product concentrations when the mix of acids and alcohols is converted to either acids or alcohols just before down-stream processing.

Overall the co-cultures performing syngas fermentation are able to fulfil a niche function in the conversion of CO-rich gases directly to products other than acetate and ethanol in a single fermentation set-up. Before such technology might become competitive, advances have to be made in rates and concentrations of the products, but the novelty and potential of these synthetic cultures is relevant. Computational biology might offer additional insights in pairing of strains and design of synthetic communities. Also a combination of community- and genetic-engineering can result in interesting production capabilities as modifications can be spread over two or more strains, lowering the potential impact on the growth potential of each of the strains. A drawback of the co-culture approach that remains is the requirement for a sterile system to function as a defined system. Similar to monocultures, the defined co-cultures might lose efficiency due to contamination by external microbes. In the

experiments performed in this thesis we did not observe any contamination on longer term (>3 months) chemostat reactor runs for both co-cultures. This might have to do with the specific function of each of the microbes in the system and the difficulty for other microbes to grow competitively in the specifically designed environment. Experiments where contamination is done on purpose might be performed to study the stability and resistance of these synthetic cultures further. In order to make the co-cultures even more robust to environmental changes and potential contamination, the application of multiple strains with similar function (e.g. two syngas utilizers) might strengthen the robustness of the culture. With expansion of the defined synthetic cultures, addition of yeast extract and vitamins might become obsolete due to the more diverse production pathways in a larger synthetic community.

Gas fermentation metabolism and its thermodynamic properties

Research efforts on the metabolism syngas fermenting microorganisms, especially acetogens, have resulted in new insights on their physiology. Since publication of **Chapter 2**, reviewing the metabolism of syngas fermenting microorganisms, two main insights in acetogenic metabolism have been gained, the thermodynamic regulation of solventogenesis in *C. autoethanogenum* (which likely also occurs in other gas fermenting acetogens), and the further confirmation of a potential bifurcating nature of the methylene-THF reductase. While not yet proven, it is suggested the methylene-THF reductase is a bifurcational enzyme that oxidizes two NADH while reducing one methylene-THF and one ferredoxin (Huang et al., 2012). This bifurcating process is suggested to be required to explain the observed growth rates of cells on syngas mixtures (Valgepea et al., 2018). However, direct experimental proof of such activity by this enzyme is still required to further confirm and understand the metabolism of acetogenic syngas fermenting acetogens.

All microbial processes are affected, and to certain extend controlled by thermodynamics, but usually it is assumed that pathways are switched on or off via genetic control. This appears not to be the case for *C. autoethanogenum* and *C. ljungdahlii* during gas fermentation, keeping expression of their acetogenic and solventogenic pathways continuously active during gas fermentation (Richter et al., 2016b; Valgepea et al., 2018). Additionally, the product spectrum of *C. autoethanogenum* could be steered by applying external electrons during growth, resulting in more lactate and 2,3-butanediol production (Kracke et al., 2016). The study concluded that changes in redox metabolism were caused by the shift in the potential at which electrons were supplied. This points towards a thermodynamics based origin for the shift. Indications for thermodynamic regulation were also observed in this thesis: I) we observed a shift of the metabolism of *C. autoethanogenum* towards ethanol production in co-culture without change in the transcriptome of the central carbon or redox metabolism (**Chapter 6**) and II) rapid switches between

the production/oxidation of alcohols depending on the CO concentration in the liquid (**Chapter 7**). Continuous expression of both the acetogenic and solventogenic pathways is potentially related the CO metabolism of these microbes. Sudden exposure to high levels of CO can quickly inhibit the metabolism (**Chapter 2**) and this might result in cell death. Direct inhibition of metallo-enzymes (e.g. hydrogenases) by CO can be problematic, and redox inhibition might occur as well as theorized for some methanogens (**Chapter 3**). Thermodynamic control of the CO metabolism enables a rapid metabolic shift. As can be seen from data during CO spike experiments (**Chapter 7**), *C. autoethanogenum* responds within < 2 minutes to the increased CO inflow. Having to wait on expression changes and subsequent translation of all the required pathways for CO removal would take time and increases the chance of inhibition of the metabolism before good activity can be reached. Controlling pathway activity based on thermodynamics might thus be essential for survival of carboxydotrophic metabolism, and the continuous expression of pathways aiding in CO-utilization could contribute to survival of the microbes and the community they live in. Due to the requirement of CO as intermediate in the Wood-Ljungdahl pathway, acetogens are ideal for the role as CO-scavenging in their natural environment, similar to the proposed role of hydrogenogenic carboxydotrophs in thermophilic hot springs (Techtmann et al., 2011). Additional support for CO scavenging role of acetogens is found in the high turnover of the CODH enzyme (**Chapter 2**), and the high affinity towards CO as a substrate in order to reach low CO concentrations. *C. autoethanogenum* was capable of removing CO during cultivation till below the detection limit of the GC (1-10 ppm), showing the ability to cleanse the environment of CO. The potential high affinity of these microbes to CO as substrate might obscure the production of such gases in their natural environments and the importance of CO metabolism in many environments might therefore be currently underestimated.

In addition to recent discoveries mentioned above, the observation done in this thesis that the energy yield of *C. autoethanogenum* appears to vary with the CO concentration in the liquid (**Chapter 7**) indicates that the metabolism of gas fermenting acetogens is not yet fully understood. As suggested in **Chapter 7** a possible mechanism for flexible ATP yield would be the cycling of acetate through acetaldehyde and acetyl-CoA resulting in a net ATP gain. Direct proof for this is however missing, but preliminary experiments were performed to get support for this theory. A chemostat setup with similar settings as used in the experiment performed in **Chapter 7** was used to assess if 1-^{13}C labelled acetate could be traced into the acetyl-CoA pool of *C. autoethanogenum* during fermentation of CO. Preliminary experiments were initiated during steady state conditions and executed over a range of 6 steps (table 3).

In samples t = 1-3 ^{13}C-acetyl-CoA was difficult to detect, and quantification was not possible due to the too low concentration in the extraction samples. If this inability

Table 3. Sampling scheme of ^{13}C tracking in the acetyl-CoA pool of *C. autoethanogenum*

Phase	Time after start (min)	pH	CO inflow (ml/min)	Remarks
0	0	6	1	inject ^{13}C label (10 mM)
1	0.5	6	1	sample t = 1
2	5	6	1	sample t = 2, ramp gas to 3 ml/min CO
3	5.5	6	3	sample t = 3
4	11	6	3	sample t = 4, pH lowered to 5.5 after this point
5	16	5.5	3	sample t = 5
6	50	5.5	3	sample t = 6

of detection was due to small size of the acetyl-CoA pool or due to experimental procedures remains unknown (all samples were extracted simultaneously). For samples 4-6 ^{13}C acetyl-CoA detection was possible, and ratios higher than the natural abundance for 1-^{13}C acetyl-CoA and monoisotopic acetyl-CoA were detected (figure 2). Acetyl-CoA contains 23 carbon molecules and, assuming 1.1% natural abundance of ^{13}C, one expects ~77% (0.989^{23}) of all acetyl-CoA to be monoisotopic and only contain ^{12}C carbons. For samples 4, 5, and 6 we observed a clear enrichment of the acetyl-CoA pool with label (figure 2) compared to the control sample (pure acetyl-CoA in extraction buffer). This suggests that the label is indeed taken up from externally provided acetate into acetyl-CoA. If this is the result of the acetate cycling mechanism proposed is not clear yet due to the difficulty of detection of acetyl-CoA in the first three samples. The observed ratios of 1-^{13}C and monoisotopic acetyl-CoA match with the expectations of how the pool should be saturated: 10 mM of labelled acetate was added on top of 20 mM acetate of natural composition (already present in the chemostat). This means that label abundance in external acetate would be roughly 34%. This will result in about 1/3th of acetyl-CoA to be additionally labelled in addition to the ~23% that is already naturally labelled, making up about a bit more than half of the pool during saturation.

In **Chapter 7** a short comparison of data obtained in other studies was made to support the acetate cycling theory that can explain the lower biomass yields in adhE knockout strains of *C. autoethanogenum*. However, when comparing with co-culture data (**Chapter 6**) there are some potential contradicting observations with the acetate-cycling theory. In co-culture, *C. autoethanogenum* becomes more solventogenically active, having a very active conversion of acetate to ethanol. This suggests that acetate cycling should also be possible during this time due to activity of Aor, potentially allowing for increased energy and growth yields. However, lower biomass yields were observed in the co-culture, contradicting with this hypothesis.

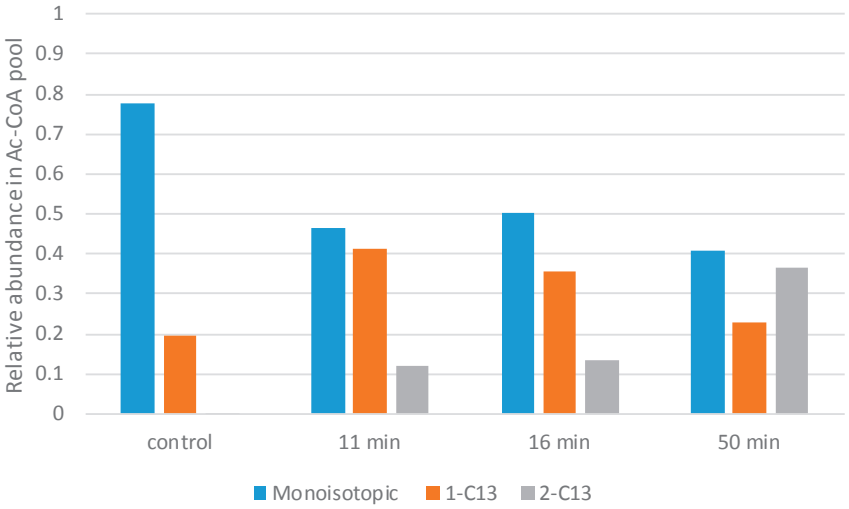

Figure 2. Relative abundance in time of labelled acetyl-CoA in 1-^{13}C acetate spiked cultures of *C. autoethanogenum* cultivated in chemostat. Numbers on the x-axis indicate the amount of minutes after sampling. Acetyl-CoA was detected via FT-ICR.

A potential explanation for this is the thermodynamics of the system, favouring ethanol production over acetaldehyde conversion to acetyl-CoA. Low background levels of ethanol were always observed in *C. autoethanogenum* cultures (~0.2 mM) and are likely the maximum concentration allowed by thermodynamics under these conditions. In general, accumulation of acetaldehyde via Aor activity would result in enhancing both: ethanol and acetyl-CoA production. However, removal of ethanol subsequently drains the acetaldehyde pool, potentially limiting the flux towards acetyl-CoA (or even making it thermodynamically unfavourable). Unfortunately, modelling this interaction is difficult due to the unknown size of the pools of many of the intermediates and redox shuttles. In addition, pool size and redox shuttles potentially also fluctuate making the whole system very dynamic. More experimental data is thus required to get full evidence for this acetate cycle theory.

Conclusion

It is clear that gas fermentation is gaining increased interest from both academic and industrial partners. Syngas fermentation will likely play an important role in our future production chains due to the broad spectrum of starting materials and waste converting potential. To reach this state, it is important to further optimize both the gasification and fermentation process, and preferably integrate them together in a single process design. Furthermore, future research has to deepen our fundamental understanding of both the physiology of gas fermenting biocatalysts and their interactions in community structures. As shown in this thesis, synthetic cultures have

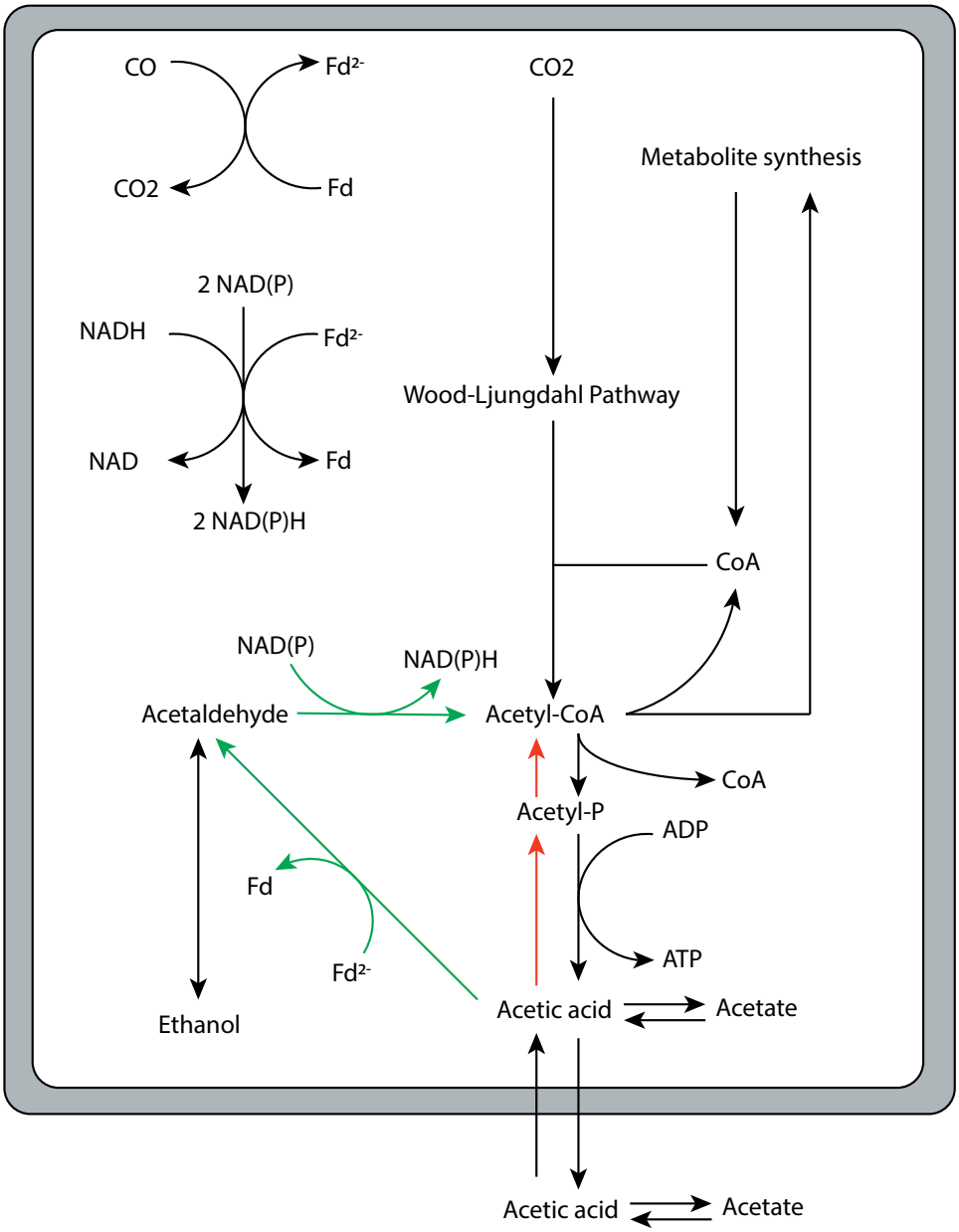

Figure 3. Schematic representation of acetate cycling metabolism and the potential flow of the isotopic acetate label. Green arrows represent the acetate cycling whereas red arrows indicate acetate take-up via reverse acetate kinase.

the potential to improve gas fermentation processes and has shown that microbial interactions can result in further improvement of the overall fermentation process. In the end, the syngas route might be the ultimate route to produce fuels and chemicals, allowing for establishment of a complete circular economy.

Appendices

References
English Summary
Dutch Summary
Co-author affiliations
Acknowledgements
About the Author
List of Publications
SENSE Dimploma

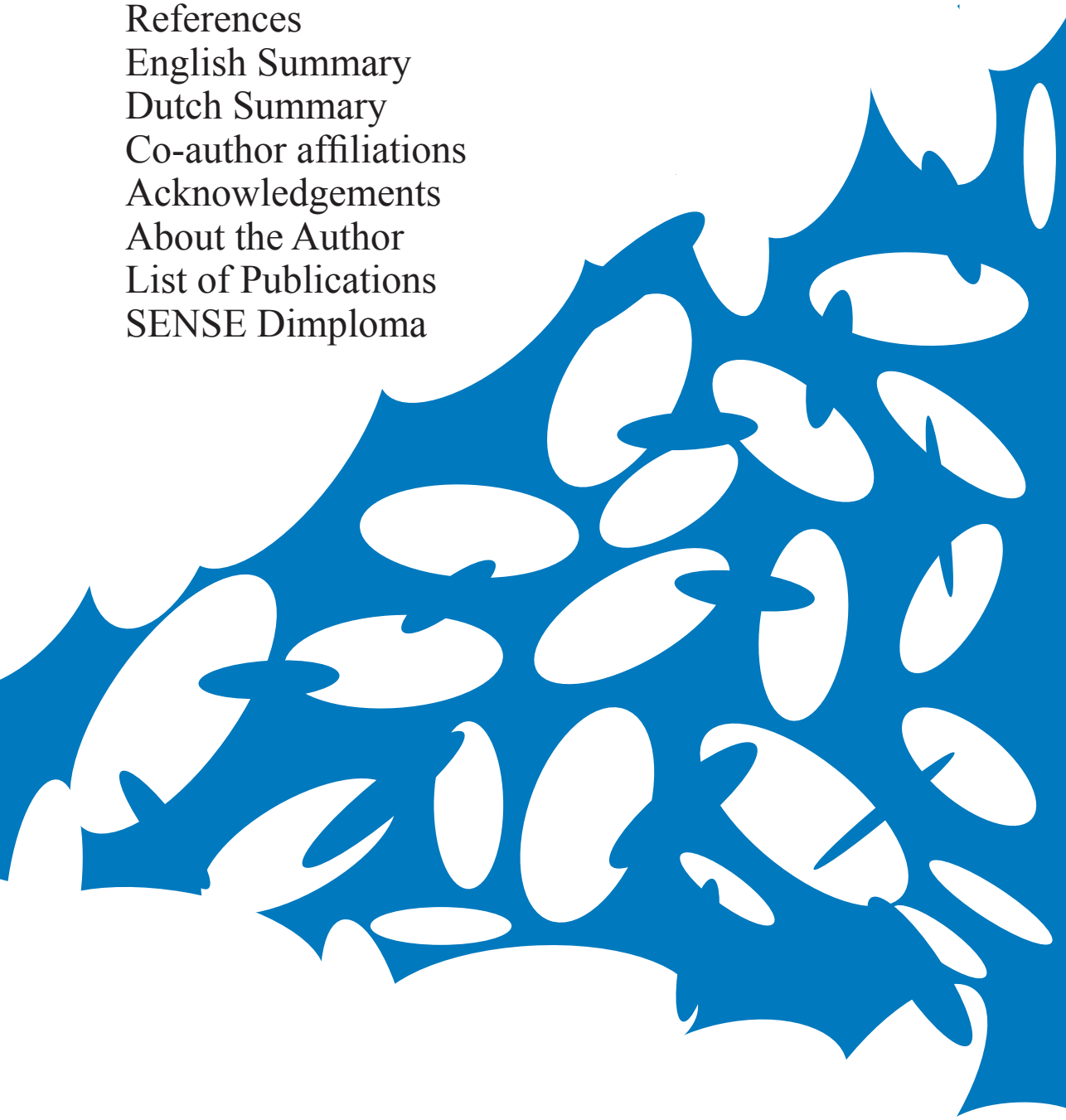

References

Abbanat, D. R., and Ferry, J. G. (1991). Resolution of component proteins in an enzyme complex from *Methanosarcina thermophila* catalyzing the synthesis or cleavage of acetyl-CoA. *Proc. Natl. Acad. Sci.* 88, 3272–3276. doi:10.1073/pnas.88.8.3272.

Abee, T., and Wouters, J. A. (1999). Microbial stress response in minimal processing. I*nt. J. Food Microbiol*. 50, 65–91. doi:10.1016/S0168-1605(99)00078-1.

Abrini, J., Naveau, H., and Nyns, E.-J. (1994). *Clostridium autoethanogenum*, sp. nov., an anaerobic bacterium that produces ethanol from carbon monoxide. *Arch. Microbiol*. 161, 345–351. doi:10.1007/bf00303591.

Abubackar, H. N., Fernández-Naveira, Á., Veiga, M. C., and Kennes, C. (2016). Impact of cyclic pH shifts on carbon monoxide fermentation to ethanol by *Clostridium autoethanogenum*. *Fuel* 178, 56–62. doi:10.1016/j.fuel.2016.03.048.

Abubackar, H. N., Veiga, M. C., and Kennes, C. (2012). Biological conversion of carbon monoxide to ethanol: Effect of pH, gas pressure, reducing agent and yeast extract. *Bioresour. Technol.* doi:10.1016/j.biortech.2012.03.027.

Abubackar, H. N., Veiga, M. C., and Kennes, C. (2015). Carbon monoxide fermentation to ethanol by *Clostridium autoethanogenum* in a bioreactor with no accumulation of acetic acid. *Bioresour. Technol.* 186, 122–127. doi:10.1016/j.biortech.2015.02.113.

AcelorMittal, and Lanzatech (2015). ArcelorMittal, LanzaTech and Primetals Technologies announce partnership to construct breakthrough €87m biofuel production facility. News Release. Available at: http://www.lanzatech.com/arcelormittal-lanzatech-primetals-technologies-announce-partnership-construct-breakthrough-e87m-biofuel-production-facility/ [Accessed August 27, 2018].

Adams, M. W. W. (1990a). The metabolism of hydrogen by extremely thermophilic, sulfur-dependent bacteria. *FEMS Microbiol. Lett.* 75, 219–237. doi:10.1111/j.1574-6968.1990.tb04096.x.

Adams, M. W. W. (1990b). The structure and mechanism of iron-hydrogenases. *Biochim. Biophys. Acta - Bioenerg.* 1020, 115–145. doi:10.1016/0005-2728(90)90044-5.

Adlunger, K., Dziekan, K., Lange, M., and Mönch, L. (2016). Climate Neutral Mobility: Natural Gas and Methane as Part of the Solution.

Afting, C., Hochheimer, A., and Thauer, R. K. (1998). Function of H_2-forming methylenetetrahydromethanopterin dehydrogenase from *Methanobacterium thermoautotrophicum* in coenzyme F420 reduction with H_2. *Arch. Microbiol.* 169, 206–210. doi:10.1007/s002030050562.

Afting, C., Kremmer, E., Brucker, C., Hochheimer, A., and Thauer, R. K. (2000). Regulation of the synthesis of H_2-forming methylenetetrahydromethanopterin dehydrogenase (Hmd) and of HmdII and HmdIII in *Methanothermobacter marburgensis*. *Arch. Microbiol.* 174, 225–232. doi:10.1007/s002030000197.

Agler, M. T., Wrenn, B. A., Zinder, S. H., and Angenent, L. T. (2011). Waste to bioproduct conversion with undefined mixed cultures: The carboxylate platform. *Trends Biotechnol.* 29, 70–78. doi:10.1016/j.tibtech.2010.11.006.

Allen, T. D., Caldwell, M. E., Lawson, P. A., Huhnke, R. L., and Tanner, R. S. (2010). *Alkalibaculum bacchi* gen. nov., sp. nov., a CO-oxidizing, ethanol-producing acetogen isolated from livestock-impacted soil. Int. *J. Syst. Evol. Microbiol.* 60, 2483–2489. doi:10.1099/ijs.0.018507-0.

Alves, J. I., van Gelder, A. H., Alves, M. M., Sousa, D. Z., and Plugge, C. M. (2013). *Moorella stamsii* sp. nov., a new anaerobic thermophilic hydrogenogenic carboxydotroph isolated from digester sludge. *Int. J. Syst. Evol. Microbiol*. 63, 4072–4076. doi:10.1099/ijs.0.050369-0.

Asimakopoulos, K., Gavala, H. N., and Skiadas, I. V. (2018). Reactor systems for syngas fermentation processes: A review. *Chem. Eng. J.* 348, 732–744. doi:10.1016/J.CEJ.2018.05.003.

Bae, S. S., Kim, T. W., Lee, H. S., Kwon, K. K., Kim, Y. J., Kim, M.-S., et al. (2012). H_2 production from CO, formate or starch using the hyperthermophilic archaeon, *Thermococcus onnurineus*. *Biotechnol. Lett.* 34, 75–79. doi:10.1007/s10529-011-0732-3.

Bae, S. S., Kim, Y. J., Yang, S. H., Lim, J. K., Jeon, J. H., Lee, H. S., et al. (2006). *Thermococcus*

onnurineus sp. nov., a hyperthermophilic archaeon isolated from a deep-sea hydrothermal vent area at the PACMANUS field. *J. Microbiol. Biotechnol.*

Balch, W. E., Schoberth, S., Tanner, R. S., and Wolfe, R. S. (1977). Acetobacterium, a new genus of hydrogen-oxidizing, carbon dioxide-reducing, anaerobic bacteria. *Int. J. Syst. Bacteriol.* 27, 355–361. doi:10.1099/00207713-27-4-355.

Balk, M., Heilig, H. G. H. J., van Eekert, M. H. A., van Stams, A. J. M., van Rijpstra, I. C., van Sinninghe-Damsté, J. S., et al. (2009). Isolation and characterization of a new CO-utilizing strain, t*hermoanaerobacter thermohydrosulfuricus* subsp. carboxydovorans, isolated from a geothermal spring in Turkey. *Extremophiles*. doi:10.1007/s00792-009-0276-9.

Barker, H. A., and Taha, M. (1941). *Clostridium kluyverii*, an organism concerned in the formation of caproic acid from ethyl alcohol. *J. Bacteriol.* 43, 347–363.

Bengelsdorf, F. R., Straub, M., and Dürre, P. (2013). Bacterial synthesis gas (syngas) fermentation. *Environ. Technol. (United Kingdom)* 34, 1639–1651. doi:10.1080/09593330.2013.827747.

Berg, I. A., Kockelkorn, D., Ramos-Vera, W. H., Say, R. F., Zarzycki, J., Hügler, M., et al. (2010). Autotrophic carbon fixation in archaea. *Nat. Rev. Microbiol.* 8, 447–460. doi:10.1038/nrmicro2365.

Bertsch, J., and Müller, V. (2015a). Bioenergetic constraints for conversion of syngas to biofuels in acetogenic bacteria. *Biotechnol. Biofuels* 8, 1–12. doi:10.1186/s13068-015-0393-x.

Bertsch, J., and Müller, V. (2015b). CO metabolism in the acetogen *Acetobacterium woodii*. *Appl. Environ. Microbiol.* 81, 5949–5956. doi:10.1128/AEM.01772-15.

Bertsch, J., Siemund, A. L., Kremp, F., and Müller, V. (2016). A novel route for ethanol oxidation in the acetogenic bacterium *Acetobacterium woodii*: the acetaldehyde/ethanol dehydrogenase pathway. *Environ. Microbiol.* 18, 2913–2922. doi:10.1111/1462-2920.13082.

Berzin, V., Tyurin, M., and Kiriukhin, M. (2013). Selective n-butanol production by clostridium sp. MTButOH1365 during continuous synthesis gas fermentation due to expression of synthetic thiolase, 3-hydroxy butyryl-CoA dehydrogenase, crotonase, butyryl-CoA dehydrogenase, butyraldehyde dehydrogenase. *Appl. Biochem. Biotechnol*. 169, 950–959. doi:10.1007/s12010-012-0060-7.

Biegel, E., Schmidt, S., González, J. M., and Müller, V. (2011). Biochemistry, evolution and physiological function of the Rnf complex, a novel ion-motive electron transport complex in prokaryotes. *Cell. Mol. Life Sci.* 68, 613–634. doi:10.1007/s00018-010-0555-8.

Bonam, D., Lehman, L., Roberts, G. P., and Ludden, P. W. (1989). Regulation of carbon monoxide dehydrogenase and hydrogenase in *Rhodospirillum rubrum*: Effects of CO and oxygen on synthesis and activity. *J. Bacteriol.* 171, 3102–3107. doi:10.1128/jb.171.6.3102-3107.1989.

Bonam, D., and Ludden, P. W. (1987). Purification and characterization of carbon monoxide dehydrogenase, a nickel, zinc, iron-sulfur protein, from *Rhodospirillum rubrum*. *J. Biol. Chem.* 262, 2980–2987.

Bornstein, B. T., and Barker, H. A. (1948). The nutrition of *Clostridium kluyveri.* J. Bacteriol. 55, 223–230. doi:10.1016/B978-1-4160-4047-7.50058-0.

Bott, M., Eikmanns, B., and Thauer, R. K. (1986). Coupling of carbon monoxide oxidation to CO_2 and H_2 with the phosphorylation of ADP in acetate grown *Methanosarcina barkeri. Eur. J. Biochem*. 159, 393–398. doi:10.1111/j.1432-1033.1986.tb09881.x.

Bott, M., and Thauer, R. K. (1989). Proton translocation coupled to the oxidation of carbon monoxide to CO_2 and H_2 in *Methanosarcina barkeri. Eur. J. Biochem.* 179, 469–472. doi:10.1111/j.1432-1033.1989.tb14576.x.

Braun, M., Mayer, F., and Gottschalk, G. (1981). *Clostridium aceticum* (Wieringa), a microorganism producing acetic acid from molecular hydrogen and carbon dioxide. *Arch. Microbiol.* 128, 288–293. doi:10.1007/BF00422532.

Braun, V., and Killmann, H. (1999). Bacterial solutions to the iron-supply problem. *Trends Biochem.* Sci. 24, 104–109. doi:10.1016/S0968-0004(99)01359-6.

Brüggemann, H., Falinski, F., and Deppenmeier, U. (2000). Structure of the $F420H_2$:quinone oxidoreductase of *Archaeoglobus fulgidus* identification and overproduction of the $F420H_2$-oxidizing

subunit. *Eur. J. Biochem*. 267, 5810–5814. doi:10.1046/j.1432-1327.2000.01657.x.

Buckel, W., and Thauer, R. K. (2013). Energy conservation via electron bifurcating ferredoxin reduction and proton/Na^+ translocating ferredoxin oxidation. *Biochim. Biophys. Acta - Bioenerg.* 1827, 94–113. doi:10.1016/j.bbabio.2012.07.002.

Byrne-Bailey, K. G., Wrighton, K. C., Melnyk, R. A., Agbo, P., Hazen, T. C., and Coates, J. D. (2010). Complete genome sequence of the electricity-producing *Thermincola potens* strain JR. *J. Bacteriol.* 192, 4078–4079. doi:10.1128/JB.00044-10.

Chin, B. Y., and Otterbein, L. E. (2009). Carbon monoxide is a poison to microbes! CO as a bactericidal molecule. *Curr. Opin. Pharmacol.* 9, 490–500. doi:10.1016/j.coph.2009.06.025.

Cho, C., Jang, Y. S., Moon, H. G., Lee, J., and Lee, S. Y. (2015). Metabolic engineering of clostridia for the production of chemicals. *Biofuels, Bioprod. Biorefining* 9, 211–225. doi:10.1002/bbb.1531.

Claassens, N. J., Sousa, D. Z., dos Santos, V. A. P. M., de Vos, W. M., and van der Oost, J. (2016). Harnessing the power of microbial autotrophy. *Nat. Rev. Microbiol.* 14, 692–706. doi:10.1038/nrmicro.2016.130.

Clark, J. E., and Ljungdahl, L. G. (1986). Purification and Properties of 5,10-Methylenetetrahydrofolate Reductase from *Clostridium formicoaceticum*. *Methods Enzymol*. 259, 10845–10849. doi:10.1016/0076-6879(86)22199-0.

Clomburg, J. M., Crumbley, A. M., and Gonzalez, R. (2017). Industrial biomanufacturing: The future of chemical production. *Science* (80-.). 355. doi:10.1126/science.aag0804.

Collins, M. D., Lawson, P. A., Willems, A., Cordoba, J. J., Fernandez-garauzabal, J., Garcia, P., et al. (1994). The phylogeny of the genus clostridium: proposal of five new genera and eleven new species combinations. *Int. J. Syst. Bacteriol.* 44, 812–826. doi:10.1099/00207713-44-4-812.

Cotter, J. L., Chinn, M. S., and Grunden, A. M. (2009). Influence of process parameters on growth of *Clostridium ljungdahlii* and *Clostridium autoethanogenum* on synthesis gas. *Enzyme Microb. Technol.* 44, 281–288. doi:10.1016/j.enzmictec.2008.11.002.

Cox, J., and Mann, M. (2008). MaxQuant enables high peptide identification rates, individualized p.p.b.-range mass accuracies and proteome-wide protein quantification. *Nat. Biotechnol.* doi:10.1038/nbt.1511.

Czekaj, I., Struis, R., Wambach, J., and Biollaz, S. (2011). Sulphur poisoning of Ni catalysts used in the SNG production from biomass: Computational studies. *Catal. Today* 176, 429–432. doi:10.1016/j.cattod.2010.10.078.

Daniel, S. L., Hsu, T., Dean, S. I., and Drake, H. L. (1990). Characterization of the H_2- and CO-dependent chemolithotrophic potentials of the acetogens *Clostridium thermoaceticum* and *Acetogenium kivui*. *J. Bacteriol.* 172, 4464–71. doi:10.1128/JB.172.8.4464-4471.1990.

Daniell, J., Köpke, M., and Simpson, S. D. (2012). Commercial biomass syngas fermentation. *Energies* 5, 5372–5417. doi:10.3390/en5125372.

Daniell, J., Nagaraju, S., Burton, F., Köpke, M., and Simpson, S. D. (2016). "Low-carbon fuel and chemical production by anaerobic gas fermentation," in *Advances in Biochemical Engineering/Biotechnology* (Springer, Cham), 293–321. doi:10.1007/10_2015_5005.

Daniels, L., Fuchs, G., Thauer, R. K., and Zeikus, J. G. (1977). Carbon Monoxide Oxidation by Methanogenic Bacteria. *J. Bacteriol.*132, 118–126.

Darnault, C., Volbeda, A., Kim, E. J., Legrand, P., Vernède, X., Lindahl, P. A., et al. (2003). Ni-Zn-[Fe4-S4] and Ni-Ni-[Fe4-S4] clusters in closed and open α subunits of acetyl-CoA synthase/carbon monoxide dehydrogenase. *Nat. Struct. Mol. Biol.* 10, 271–279. doi:10.1038/nsb912.

Dashekvicz, M. P., and Uffen, R. L. (1979). Identification of a Carbon Monoxide-Metabolizing Bacterium as a Strain of *Rhodopseudomonas gelatinosa* (Molisch) van Nielt. *Int. J. Syst. Bacteriol.* 29, 145–148. doi:10.1099/00207713-29-2-145.

de Klerk, A. (2013). "Fischer-Tropsch Process," in *Kirk-Othmer Encyclopedia of Chemical Technology* (Hoboken, NJ, USA: John Wiley & Sons, Inc.), 1–20. doi:10.1002/0471238961.fiscdekl.a01.

De Lacey, A. L., Fernández, V. M., Rousset, M., and Cammack, R. (2007). Activation and inactivation of hydrogenase function and the catalytic cycle: spectroelectrochemical studies. *Chem. Rev.* 107, 4304–4330. doi:10.1021/cr0501947.

de Mes, T. Z. D., Stams, A. J. M., Reith, J. H., and Zeeman, G. (2003). Methane production by anaerobic digestion of wastewater and solid wastes. Bio-methane Bio-hydrogen, Status Perspect. *Biol. methane Hydrog. Prod.* doi:10.1016/j.biortech.2010.08.032.

Deppenmeier, U., Müller, V., and Gottschalk, G. (1996). Pathways of energy conservation in methanogenic archaea. *Arch. Microbiol.* 165, 149–163. doi:10.1007/BF01692856.

Diender, M., Pereira, R., Wessels, H. J. C. T., Stams, A. J. M., and Sousa, D. Z. (2016a). Proteomic Analysis of the Hydrogen and Carbon Monoxide Metabolism of *Methanothermobacter marburgensis*. *Front. Microbiol.* 7. doi:10.3389/fmicb.2016.01049.

Diender, M., Stams, A. J. M., and Sousa, D. Z. (2015). Pathways and bioenergetics of anaerobic carbon monoxide fermentation. *Front. Microbiol.* 6. doi:10.3389/fmicb.2015.01275.

Diender, M., Stams, A. J. M., and Sousa, D. Z. (2016b). Production of medium-chain fatty acids and higher alcohols by a synthetic co-culture grown on carbon monoxide or syngas. *Biotechnol. Biofuels* 9. doi:10.1186/s13068-016-0495-0.

Diender, M., Uhl, P. S., Bitter, J. H., Stams, A. J. M., and Sousa, D. Z. (2018). High rate biomethanation of carbon monoxide-rich gases via a thermophilic synthetic coculture. *ACS Sustain. Chem. Eng.* 6, 2169–2176. doi:10.1021/acssuschemeng.7b03601.

Dobbek, H., Svetlitchnyi, V., Gremer, L., Huber, R., and Meyer, O. (2001). Crystal structure of a carbon monoxide dehydrogenase reveals a [Ni-4Fe-5S] cluster. *Science* (80-.). 293, 1281–1285. doi:10.1126/science.1061500.

Doukov, T. I. (2002). A Ni-Fe-Cu center in a bifunctional carbon monoxide dehydrogenase/ Acetyl-CoA synthase. *Science* (80-.). 298, 567–572. doi:10.1126/science.1075843.

Drake, H. L., and Daniel, S. L. (2004). Physiology of the thermophilic acetogen *Moorella thermoacetica*. *Res. Microbiol.* 155, 869–883. doi:10.1016/j.resmic.2004.10.002.

Drake, H. L., Hu, S., and Wood, H. G. (1980). Purification of carbon monoxide dehydrogenase, a nickel enzyme from *Clostridium thermocaceticum*. *J. Biol. Chem.* 255, 7174–7180.

Drennan, C. L., Heo, J., Sintchak, M. D., Schreiter, E., and Ludden, P. W. (2001). Life on carbon monoxide: X-ray structure of *Rhodospirillum rubrum* Ni-Fe-S carbon monoxide dehydrogenase. *Proc. Natl. Acad. Sci.* 98, 11973–11978. doi:10.1073/pnas.211429998.

Drzyzga, O., Revelles, O., Durante-Rodríguez, G., Díaz, E., García, J. L., and Prieto, A. (2015). New challenges for syngas fermentation: towards production of biopolymers. *J. Chem. Technol. Biotechnol.* 90, 1735–1751. doi:10.1002/jctb.4721.

Dubois, M. R., and Dubois, D. L. (2009). Development of molecular electrocatalysts for CO_2 reduction and H_2 production/oxidation. *Acc. Chem. Res.* 42, 1974–1982. doi:10.1021/ar900110c.

Dunn, S. (2002). Hydrogen futures: Toward a sustainable energy system. *Int. J. Hydrogen Energy* 27, 235–264. doi:10.1016/S0360-3199(01)00131-8.

Duret, A., Friedli, C., and Maréchal, F. (2005). Process design of Synthetic Natural Gas (SNG) production using wood gasification. *J. Clean. Prod.* 13, 1434–1446. doi:10.1016/j.jclepro.2005.04.009.

Dürre, P., and Eikmanns, B. J. (2015). C1-carbon sources for chemical and fuel production by microbial gas fermentation. *Curr. Opin. Biotechnol.* 35, 63–72. doi:10.1016/j.copbio.2015.03.008.

Edwards, R., Larive, J.-F., Mahieu, V., and Rounveirolles, P. (2004). Well-to-Wheels analysis of future automotive fuels and powertrains in the european context. *SAE Tech. Pap.* doi:10.2788/79018.

Eikmanns, B., Fuchs, G., and Thauer, R. K. (1985). Formation of carbon monoxide from CO_2 and H_2 by *Methanobacterium thermoautotrophicum*. *Eur. J. Biochem.* 146, 149–154. doi:10.1111/j.1432-1033.1985.tb08631.x.

Ensign, S. A., and Ludden, P. W. (1991). Characterization of the CO oxidation/H_2 evolution system of *Rhodospirillum rubrum*: Role of a 22-kDa iron-sulfur protein in mediating electron transfer between

carbon monoxide dehydrogenase and hydrogenase. *J. Biol. Chem.* 266, 18395–18403.

Fardeau, M.-L. (2004). Isolation from oil reservoirs of novel thermophilic anaerobes phylogenetically related to *Thermoanaerobacter subterraneus*: reassignment of *T. subterraneus, Thermoanaerobacter yonseiensis, Thermoanaerobacter tengcongensis* and *Carboxydibrachium pacificum* to *Caldanaerobacter subterraneus* gen. nov., sp. nov., comb. nov. as four novel subspecies. *Int. J. Syst. Evol. Microbiol.* 54, 467–474. doi:10.1099/ijs.0.02711-0.

Fernández-Naveira, Á., Abubackar, H. N., Veiga, M. C., and Kennes, C. (2016). Efficient butanol-ethanol (B-E) production from carbon monoxide fermentation by *Clostridium carboxidivorans. Appl. Microbiol. Biotechnol.* 100, 3361–3370. doi:10.1007/s00253-015-7238-1.

Fischer, F., Lieske, R., and Winzer, K. (1931). Die umsetzungen des kohlenoxyds. *Biochem. Z.*, 247–267.

Fischer, R., and Thauer, R. K. (1990). Ferredoxin-dependent methane formation from acetate in cell extracts of *Methanosarcina barkeri* (strain MS). *FEBS Lett.* 269, 368–372. doi:10.1016/0014-5793(90)81195-T.

Fox, J. D., Kerby, R. L., Roberts, G. P., and Ludden, P. W. (1996a). Characterization of the CO-induced, CO-tolerant hydrogenase from *Rhodospirillum rubrum* and the gene encoding the large subunit of the enzyme. *J. Bacteriol.* 178, 1515–1524. doi:10.1128/jb.178.6.1515-1524.1996.

Fox, J. D., Yiping, H. E., Shelver, D., Roberts, G. P., and Ludden, P. W. (1996b). Characterization of the region encoding the CO-induced hydrogenase of *Rhodospirillum rubrum. J. Bacteriol*. 178, 6200–6208. doi:10.1128/jb.178.21.6200-6208.1996.

Frost, Hartvigsen, and Elangovan (2010). Formation of synthesis gas using solar concentrator photovoltaics (SCPV) and high temperature co-electrolysis (HTCE) of CO_2 and H_2O. Offshore Technol. Conf. Proc. doi:10.2523/20408-MS.

Fuchs, G. (2010). Alternative pathways of carbon dioxide fixation: insights into the early evolution of life? *Annu. Rev. Microbiol.* 65, 631–658. doi:10.1146/annurev-micro-090110-102801.

Furler, P., Scheffe, J. R., and Steinfeld, A. (2012). Syngas production by simultaneous splitting of H_2O and CO_2 via ceria redox reactions in a high-temperature solar reactor. *Energy Environ. Sci.* 5, 6098–6103. doi:10.1039/c1ee02620h.

Galagan, J. E., Nusbaum, C., Roy, A., Endrizzi, M. G., Macdonald, P., Fitzhugh, W., et al. (2002). The genome of *M. acetivorans* reveals extensive metabolic and physiological diversity. *Genome Res.* 12, 532–542. doi:10.1101/gr.223902.

Geerligs, G., Schönheit, P., and Diekert, G. (1989). Sodium dependent acetate formation from CO2 in *Peptostreptococcus productus* (strain Marburg). *FEMS Microbiol. Lett.* 57, 353–357. doi:10.1111/j.1574-6968.1989.tb03363.x.

Genthner, B. R. S., and Bryant, M. P. (1982). Growth of *Eubacterium limosum* with carbon monoxide as the energy source. *Appl. Environ. Microbiol*. 43, 70–74. doi:10.1016/0016-2361(79)90017-6.

Genthner, B. R. S., and Bryant, M. P. (1987). Additional characteristics of one-carbon-compound utilization by *Eubacterium limosum* and *Acetobacterium woodii. Appl. Environ. Microbiol*. 53, 471–476.

Gildemyn, S., Molitor, B., Usack, J. G., Nguyen, M., Rabaey, K., and Angenent, L. T. (2017). Upgrading syngas fermentation effluent using *Clostridium kluyveri* in a continuous fermentation. *Biotechnol. Biofuels* 10, 83. doi:10.1186/s13068-017-0764-6.

Gottwald, M., Andreesen, J. R., LeGall, J., and Ljungdahl, L. G. (1975). Presence of cytochrome and menaquinone in *Clostridium formicoaceticum* and *Clostridium thermoaceticum*. *J. Bacteriol*. 122, 325–328.

Grahame, D. A. (2003). Acetate C–C bond formation and decomposition in the anaerobic world: the structure of a central enzyme and its key active-site metal cluster. *Trends Biochem. Sci.* 28, 221–224. doi:10.1016/S0968-0004(03)00063-X.

Grootscholten, T. I. M., Steinbusch, K. J. J., Hamelers, H. V. M., and Buisman, C. J. N. (2013). Chain elongation of acetate and ethanol in an upflow anaerobic filter for high rate MCFA production. *Bioresour. Technol.* 135, 440–445. doi:10.1016/j.biortech.2012.10.165.

Guiot, S. R., Cimpoia, R., and Carayon, G. (2011). Potential of wastewater-treating anaerobic granules for biomethanation of synthesis gas. *Environ. Sci. Technol.* 45, 2006–2012. doi:10.1021/es102728m.

Haas, T., Krause, R., Weber, R., Demler, M., and Schmid, G. (2018). Technical photosynthesis involving CO_2 electrolysis and fermentation. *Nat. Catal.* 1, 32–39. doi:10.1038/s41929-017-0005-1.

Hamelinck, C. N., Hooijdonk, G. van, and Faaij, A. P. (2005). Ethanol from lignocellulosic biomass: techno-economic performance in short-, middle- and long-term. *Biomass and Bioenergy* 28, 384–410. doi:10.1016/j.biombioe.2004.09.002.

Hammel, K. E., Cornwell, K. L., Diekert, G. B., and Thauer, R. K. (1984). Evidence for a nickel-containing carbon monoxide dehydrogenase in *Methanobrevibacter arboriphilicus*. *J. Bacteriol.* 157, 975–978.

He, P., Han, W., Shao, L., and Lü, F. (2018). One-step production of C6-C8 carboxylates by mixed culture solely grown on CO. *Biotechnol. Biofuels* 11. doi:10.1186/s13068-017-1005-8.

Hedderich, R., and Forzi, L. (2006). Energy-converting [NiFe] hydrogenases: More than just H_2 activation. *J. Mol. Microbiol. Biotechnol.* 10, 92–104. doi:10.1159/000091557.

Heidenreich, S., and Foscolo, P. U. (2015). New concepts in biomass gasification. P*rog. Energy Combust. Sci.* 46, 72–95. doi:10.1016/J.PECS.2014.06.002.

Heiskanen, H., Virkajärvi, I., and Viikari, L. (2007). The effect of syngas composition on the growth and product formation of *Butyribacterium methylotrophicum*. *Enzyme Microb. Technol.* 41, 362–367. doi:10.1016/j.enzmictec.2007.03.004.

Henstra, A. M., Dijkema, C., and Stams, A. J. M. (2007a). *Archaeoglobus fulgidus* couples CO oxidation to sulfate reduction and acetogenesis with transient formate accumulation. *Environ. Microbiol.* 9, 1836–1841. doi:10.1111/j.1462-2920.2007.01306.x.

Henstra, A. M., Sipma, J., Rinzema, A., and Stams, A. J. (2007b). Microbiology of synthesis gas fermentation for biofuel production. *Curr. Opin. Biotechnol.* 18, 200–206. doi:10.1016/j.copbio.2007.03.008.

Henstra, A. M., and Stams, A. J. M. (2004). Novel physiological features of *Carboxydothermus hydrogenoformans* and *Thermoterrabacterium ferrireducens*. *Appl. Environ. Microbiol.* 70, 7236–7240. doi:10.1128/AEM.70.12.7236-7240.2004.

Henstra, A. M., and Stams, A. J. M. (2011). Deep conversion of carbon monoxide to hydrogen and formation of acetate by the anaerobic thermophile *Carboxydothermus hydrogenoformans*. *Int. J. Microbiol.* 2011, 1–4. doi:10.1155/2011/641582.

Herrmann, G., Jayamani, E., Mai, G., and Buckel, W. (2008). Energy conservation via electron-transferring flavoprotein in anaerobic bacteria. *J. Bacteriol.* 190, 784–791. doi:10.1128/JB.01422-07.

Hess, V., Schuchmann, K., and Müller, V. (2013). The ferredoxin: NAD^+ Oxidoreductase (Rnf) from the acetogen *Acetobacterium woodii* requires Na^+ and is reversibly coupled to the membrane potential. *J. Biol. Chem.* 288, 31496–31502. doi:10.1074/jbc.M113.510255.

Hickey, R. F., and Switzenbaum, M. S. (1990). Behavior of carbon monoxide as a trace component of anaerobic digester gases and methanogenesis from acetate. *Environ. Sci. Technol.* 24, 1642–1648. doi:10.1021/es00081a003.

Hippler, B., and Thauer, R. K. (1999). The energy conserving methyltetrahydromethanopterin:coenzyme M methyltransferase complex from methanogenic archaea: Function of the subunit MtrH. *FEBS Lett.* 449, 165–168. doi:10.1016/S0014-5793(99)00429-9.

Hocking, W. P., Stokke, R., Roalkvam, I., and Steen, I. H. (2014). Identification of key components in the energy metabolism of the hyperthermophilic sulfate-reducing archaeon *Archaeoglobus fulgidus* by transcriptome analyses. *Front. Microbiol.* 5, 1–20. doi:10.3389/fmicb.2014.00095.

Hu, Z., Spangler, N. J., Anderson, M. E., Xia, J., Ludden, P. W., Lindahl, P. A., et al. (1996). Nature of the C-cluster in Ni-containing carbon monoxide dehydrogenases. *J. Am. Chem. Soc.* 118, 830–845. doi:10.1021/ja9528386.

Huang, H., Chai, C., Li, N., Rowe, P., Minton, N. P., Yang, S., et al. (2016). CRISPR/Cas9-based efficient genome editing in *Clostridium ljungdahlii*, an autotrophic gas-fermenting bacterium. *ACS*

Synth. Biol. 5, 1355–1361. doi:10.1021/acssynbio.6b00044.

Huang, H., Wang, S., Moll, J., and Thauer, R. K. (2012). Electron bifurcation involved in the energy metabolism of the acetogenic bacterium *Moorella thermoacetica* growing on glucose or H_2 plus CO_2. *J. Bacteriol.* 194, 3689–3699. doi:10.1128/JB.00385-12.

Hugenholtz, J., and Ljungdahl, L. G. (1989). Electron transport and electrochemical proton gradient in membrane vesicles of *Clostridium thermoautotrophicum*. *J. Bacteriol*. 171, 2873–2875. doi:10.1128/jb.171.5.2873-2875.1989.

Humphreys, C. M., and Minton, N. P. (2018). Advances in metabolic engineering in the microbial production of fuels and chemicals from C1 gas. *Curr. Opin. Biotechnol.* 50, 174–181. doi:10.1016/J.COPBIO.2017.12.023.

Hurst, K. M., and Lewis, R. S. (2010). Carbon monoxide partial pressure effects on the metabolic process of syngas fermentation. *Biochem. Eng. J.* 48, 159–165. doi:10.1016/j.bej.2009.09.004.

IPCC (2014). Climate Change 2014: Synthesis Report. Contribution of Working Groups I, II and III to the Fifth Assessment Report of the Intergovernmental Panel on Climate Change. doi:10.1017/CBO9781107415324.004.

Jeon, W. B., Singer, S. W., Ludden, P. W., and Rubio, L. M. (2005). New insights into the mechanism of nickel insertion into carbon monoxide dehydrogenase: Analysis of *Rhodospirillum rubrum* carbon monoxide dehydrogenase variants with substituted ligands to the $[Fe_3S_4]$ portion of the active-site C-cluster. *J. Biol. Inorg. Chem.* 10, 903–912. doi:10.1007/s00775-005-0043-z.

Jeong, J., Bertsch, J., Hess, V., Choi, S., Choi, I. G., Chang, I. S., et al. (2015). Energy conservation model based on genomic and experimental analyses of a carbon monoxide-utilizing, butyrate-forming acetogen, *Eubacterium limosum* KIST612. Appl. *Environ. Microbiol.* 81, 4782–4790. doi:10.1128/AEM.00675-15.

Jeoung, J. H., Fesseler, J., Goetzl, S., and Dobbek, H. (2014). Carbon monoxide. Toxic gas and fuel for anaerobes and aerobes: Carbon monoxide dehydrogenases. doi:10.1007/978-94-017-9269-1-3.

Jetten, M. S. M., Stams, A. J. M., and Zehnder, A. J. B. (1989). Purification and characterization of an oxygen stable carbon monoxide dehydrogenase of *Methanothrix soehngenii*. *Eur. J. Biochem.* 181, 437–441. doi:10.1111/j.1432-1033.1989.tb14744.x.

Jing, Y., Campanaro, S., Kougias, P., Treu, L., Angelidaki, I., Zhang, S., et al. (2017). Anaerobic granular sludge for simultaneous biomethanation of synthetic wastewater and CO with focus on the identification of CO-converting microorganisms. *Water Res.* 126, 19–28. doi:10.1016/j.watres.2017.09.018.

Jönsson, L. J., and Martín, C. (2016). Pretreatment of lignocellulose: Formation of inhibitory by-products and strategies for minimizing their effects. *Bioresour. Technol.* 199, 103–112. doi:10.1016/j.biortech.2015.10.009.

Jung, G. Y., Jung, H. O., Kim, J. R., Ahn, Y., and Park, S. (1999). Isolation and characterization of *Rhodopseudomonas palustris* P4 which utilizes CO with the production of H_2. *Biotechnol. Lett.* 21, 525–529. doi:10.1023/A:1005560630351.

Kaster, A.-K., Moll, J., Parey, K., and Thauer, R. K. (2011). Coupling of ferredoxin and heterodisulfide reduction via electron bifurcation in hydrogenotrophic methanogenic archaea. *Proc. Natl. Acad. Sci.* 108, 2981–2986. doi:10.1073/pnas.1016761108.

Kerby, R. L., Ludden, P. W., and Roberts, G. P. (1995). Carbon monoxide-dependent growth of *Rhodospirillum rubrum*. *J. Bacteriol.* 199, 2241–2244. doi:10.1128/jb.177.8.2241-2244.1995.

Kerby, R. L., Ludden, P. W., and Roberts, G. P. (1997). In vivo nickel insertion into the carbon monoxide dehydrogenase of *Rhodospirillum rubrum*: Molecular and physiological characterization of cooCTJ. *J. Bacteriol.* 179, 2259–2266. doi:10.1128/jb.179.7.2259-2266.1997.

Khalil, M. A. K., and Rasmussen, R. A. (1990). The global cycle of carbon monoxide: Trends and mass balance. *Chemosphere* 20, 227–242. doi:10.1016/0045-6535(90)90098-E.

Khazova, M., and O'Hagan, J. B. (2008). Optical radiation emissions from compact fluorescent lamps. *Radiat. Prot. Dosimetry* 131, 521–525. doi:10.1093/rpd/ncn234.

Kluyver, A. J., and Schnellen, C. G. T. P. (1947). On the fermentation of carbon monoxide by pure

cultures of methane bacteria. *Arch. Biochem.* 14, 57–70.

Kochetkova, T. V., Rusanov, I. I., Pimenov, N. V., Kolganova, T. V., Lebedinsky, A. V., Bonch-Osmolovskaya, E. A., et al. (2011). Anaerobic transformation of carbon monoxide by microbial communities of Kamchatka hot springs. *Extremophiles* 15, 319–325. doi:10.1007/s00792-011-0362-7.

Koehorst, J. J., Van Dam, J. C. J., Saccenti, E., Martins Dos Santos, V. A. P., Suarez-Diez, M., and Schaap, P. J. (2018). SAPP: Functional genome annotation and analysis through a semantic framework using FAIR principles. *Bioinformatics* 34, 1401–1403. doi:10.1093/bioinformatics/btx767.

Köpke, M., Gerth, M. L., Maddock, D. J., Mueller, A. P., Liew, F. M., Simpson, S. D., et al. (2014). Reconstruction of an acetogenic 2,3-butanediol pathway involving a novel NADPH-dependent primary-secondary alcohol dehydrogenase. *Appl. Environ. Microbiol.* 80, 3394–3303. doi:10.1128/AEM.00301-14.

Köpke, M., Held, C., Hujer, S., Liesegang, H., Wiezer, A., Wollherr, A., et al. (2010). *Clostridium ljungdahlii* represents a microbial production platform based on syngas. *Proc. Natl. Acad. Sci.* 107, 15305–15305. doi:10.1073/pnas.1011320107.

Köpke, M., Mihalcea, C., Bromley, J. C., and Simpson, S. D. (2011a). Fermentative production of ethanol from carbon monoxide. *Curr. Opin. Biotechnol.* 22, 320–325. doi:10.1016/j.copbio.2011.01.005.

Köpke, M., Mihalcea, C., Liew, F. M., Tizard, J. H., Ali, M. S., Conolly, J. J., et al. (2011b). 2,3-Butanediol production by acetogenic bacteria, an alternative route to chemical synthesis, using industrial waste gas. *Appl. Environ. Microbiol.* 77, 5467–5475. doi:10.1128/AEM.00355-11.

Kopyscinski, J., Schildhauer, T. J., and Biollaz, S. M. A. (2010). Production of synthetic natural gas (SNG) from coal and dry biomass – A technology review from 1950 to 2009. *Fuel* 89, 1763–1783. doi:10.1016/J.FUEL.2010.01.027.

Kracke, F., Virdis, B., Bernhardt, P. V., Rabaey, K., and Krömer, J. O. (2016). Redox dependent metabolic shift in *Clostridium autoethanogenum* by extracellular electron supply. *Biotechnol. Biofuels* 9. doi:10.1186/s13068-016-0663-2.

Krumholz, L. R., and Bryant, M. P. (1985). *Clostridium pfennigii* sp. nov. Uses Methoxyl Groups of Monobenzenoids and Produces Butyrate. *Int. J. Syst. Bacteriol*. 35, 454–456. doi:10.1099/00207713-35-4-454.

Kundiyana, D. K., Huhnke, R. L., and Wilkins, M. R. (2011). Effect of nutrient limitation and two-stage continuous fermentor design on productivities during *Clostridium ragsdalei* syngas fermentation. *Bioresour. Technol.* 102, 6058–6064. doi:10.1016/j.biortech.2011.03.020.

Kusel, K., Dorsch, T., Acker, G., Stackebrandt, E., and Drake, H. L. (2000). *Clostridium scatologenes* strain SL1 isolated as an acetogenic bacterium from acidic sediments. *Int. J. Syst. Evol. Microbiol.* 50, 537–546. doi:10.1099/00207713-50-2-537.

Latif, H., Zeidan, A. A., Nielsen, A. T., and Zengler, K. (2014). Trash to treasure: Production of biofuels and commodity chemicals via syngas fermenting microorganisms. *Curr. Opin. Biotechnol.* 27, 79–87. doi:10.1016/j.copbio.2013.12.001.

Lessner, D. J., Li, L., Li, Q., Rejtar, T., Andreev, V. P., Reichlen, M., et al. (2006). An unconventional pathway for reduction of CO_2 to methane in CO-grown *Methanosarcina acetivorans* revealed by proteomics. *Proc. Natl. Acad. Sci.* 103, 17921–17926. doi:10.1073/pnas.0608833103.

Li, L., Li, Q., Rohlin, L., Kim, U., Salmon, K., Rejtar, T., et al. (2007). quantitative proteomic and microarray analysis of the archaeon *Methanosarcina acetivorans* grown with acetate versus methanol. *J. Proteome Res.* 6, 759–771. doi:10.1021/pr060383l.

Liesegang, H., Kaster, A. K., Wiezer, A., Goenrich, M., Wollherr, A., Seedorf, H., et al. (2010). Complete genome sequence of *Methanothermobacter marburgensis*, a methanoarchaeon model organism. *J. Bacteriol.* 192, 5850–5851. doi:10.1128/JB.00844-10.

Liew, F., Henstra, A. M., Köpke, M., Winzer, K., Simpson, S. D., and Minton, N. P. (2017). Metabolic engineering of *Clostridium autoethanogenum* for selective alcohol production. *Metab. Eng.* 40, 104–114. doi:10.1016/j.ymben.2017.01.007.

Lindahl, P. A. (2002). The Ni-containing carbon monoxide dehydrogenase family: Light at the end of the tunnel? *Biochemistry* 41, 209–2105. doi:10.1021/bi015932+.

Liou, J. S.-C. (2005). *Clostridium carboxidivorans* sp. nov., a solvent-producing clostridium isolated from an agricultural settling lagoon, and reclassification of the acetogen *Clostridium scatologenes* strain SL1 as *Clostridium drakei* sp. nov. *Int. J. Syst. Evol. Microbiol*. 55, 2085–2091. doi:10.1099/ijs.0.63482-0.

Liu, K., Atiyeh, H. K., Stevenson, B. S., Tanner, R. S., Wilkins, M. R., and Huhnke, R. L. (2014a). Continuous syngas fermentation for the production of ethanol, n-propanol and n-butanol. *Bioresour. Technol.* 151, 69–77. doi:10.1016/j.biortech.2013.10.059.

Liu, K., Atiyeh, H. K., Stevenson, B. S., Tanner, R. S., Wilkins, M. R., and Huhnke, R. L. (2014b). Mixed culture syngas fermentation and conversion of carboxylic acids into alcohols. *Bioresour. Technol.* 152, 337–346. doi:10.1016/j.biortech.2013.11.015.

Liu, K., Atiyeh, H. K., Tanner, R. S., Wilkins, M. R., and Huhnke, R. L. (2012a). Fermentative production of ethanol from syngas using novel moderately alkaliphilic strains of *Alkalibaculum bacchi*. *Bioresour. Technol.* 104, 336–341. doi:10.1016/j.biortech.2011.10.054.

Liu, Z., Chu, B., Zhai, X., Jin, Y., and Cheng, Y. (2012b). Total methanation of syngas to synthetic natural gas over Ni catalyst in a micro-channel reactor. *Fuel* 95, 599–605. doi:10.1016/j.fuel.2011.12.045.

Lorowitz, W. H., and Bryant, M. P. (1984). *Peptostreptococcus productus* strain that grows rapidly with CO as the energy source. *Appl. Environ. Microbiol.* 47, 961–964.

Lux, M. F., and Drake, H. L. (1992). Reexamination of the metabolic potentials of the acetogens *Clostridium aceticum* and *Clostridium formicoaceticum* - chemolithoautotrophic and aromatic-dependent growth. *Fems Microbiol. Lett.* 95, 49–56. doi:10.1111/j.1574-6968.1992.tb05341.x.

Lynd, L. H., and Zeikus, J. G. (1983). Metabolism of H_2-CO_2, methanol, and glucose by *Butyribacterium methylotrophicum*. *J. Bacteriol.* 153, 1415–1423.

Lynd, L., Kerby, R., and Zeikus, J. G. (1982). Carbon monoxide metabolism of the methylotrophic acidogen *Butyribacterium methylotrophicum*. *J. Bacteriol.* 149, 255–263.

Lyon, E. J., Shima, S., Boecher, R., Thauer, R. K., Grevels, F. W., Bill, E., et al. (2004). Carbon monoxide as an intrinsic ligand to iron in the active site of the iron-sulfur-cluster-free hydrogenase H_2-forming methylenetetrahydromethanopterin dehydrogenase as revealed by infrared spectroscopy. *J. Am. Chem. Soc.* 126, 14239–14248. doi:10.1021/ja046818s.

Maness, P. C., Huang, J., Smolinski, S., Tek, V., and Vanzin, G. (2005). Energy generation from the CO oxidation-hydrogen production pathway in *Rubrivivax gelatinosus*. *Appl. Environ. Microbiol.* 71, 2870–2874. doi:10.1128/AEM.71.6.2870-2874.2005.

Martin, M. E., Richter, H., Saha, S., and Angenent, L. T. (2016). Traits of selected Clostridium strains for syngas fermentation to ethanol. *Biotechnol. Bioeng*. 113, 531–539. doi:10.1002/bit.25827.

Matschiavelli, N., Oelgeschläger, E., Cocchiararo, B., Finke, J., and Rother, M. (2012). Function and regulation of isoforms of carbon monoxide dehydrogenase/acetyl coenzyme A synthase in *Methanosarcina acetivorans*. *J. Bacteriol.* 194, 5377–5387. doi:10.1128/JB.00881-12.

Matschiavelli, N., and Rother, M. (2015). Role of a putative tungsten-dependent formylmethanofuran dehydrogenase in *Methanosarcina acetivorans*. *Arch. Microbiol.* 197, 379–388. doi:10.1007/s00203-014-1070-3.

Maynard, E. L., and Lindahl, P. A. (1999). Evidence of a molecular tunnel connecting the active sites for CO_2 reduction and acetyl-CoA synthesis in acetyl-CoA synthase from *Clostridium thermoaceticum*. *J. Am. Chem. Soc.* 121, 9221–9222. doi:10.1021/ja992120g.

McKendry, P. (2002). Energy production from biomass (part 2): Conversion technologies. *Bioresour. Technol.* 83, 47–54. doi:10.1016/S0960-8524(01)00119-5.

Meyer, O., Jacobitz, S., and Krüger, B. (1986). Biochemistry and physiology of aerobic carbon monoxide-oxidizing bacteria. *FEMS Microbiol. Rev.* 39, 161–179. doi:10.1111/j.1574-6968.1986.tb01858.x.

Meyer, O., and Schlegel, H. G. (1983). Biology of aerobic carbon monoxide-oxidizing bacteria. *Annu. Rev. Microbiol.* 37, 277–310. doi:10.1146/annurev.mi.37.100183.001425.

Miyakawa, S., Yamanashi, H., Kobayashi, K., Cleaves, H. J., and Miller, S. L. (2002). Prebiotic

synthesis from CO atmospheres: Implications for the origins of life. *Proc. Natl. Acad. Sci*. 99, 14628–14631. doi:10.1073/pnas.192568299.

Mock, J., Zheng, Y., Mueller, A. P., Ly, S., Tran, L., Segovia, S., et al. (2015). Energy conservation associated with ethanol formation from H_2 and CO_2 in *Clostridium autoethanogenum* involving electron bifurcation. *J. Bacteriol.* doi:10.1128/JB.00399-15.

Molitor, B., Marcellin, E., and Angenent, L. T. (2017). Overcoming the energetic limitations of syngas fermentation. *Curr. Opin. Chem. Biol*. 41, 84–92. doi:10.1016/j.cbpa.2017.10.003.

Molitor, B., Richter, H., Martin, M. E., Jensen, R. O., Juminaga, A., Mihalcea, C., et al. (2016). Carbon recovery by fermentation of CO-rich off gases - Turning steel mills into biorefineries. *Bioresour. Technol.* 215, 386–396. doi:10.1016/j.biortech.2016.03.094.

Müller, V. (2003). Energy conservation in acetogenic bacteria. *Appl. Environ. Microbiol.* 69, 6345–6353. doi:10.1128/AEM.69.11.6345-6353.2003.

Müller, V., Imkamp, F., Biegel, E., Schmidt, S., and Dilling, S. (2008). Discovery of a ferredoxin: NAD^+-oxidoreductase (Rnf) in *Acetobacterium woodii*: A novel potential coupling site in acetogens. Ann. N. Y. Acad. Sci. 1125, 137–146. doi:10.1196/annals.1419.011.

Muñoz, R., Meier, L., Diaz, I., and Jeison, D. (2015). A review on the state-of-the-art of physical/chemical and biological technologies for biogas upgrading. *Rev. Environ. Sci. Biotechnol.* 14, 727–759. doi:10.1007/s11157-015-9379-1.

Naik, S. N., Goud, V. V., Rout, P. K., and Dalai, A. K. (2010). Production of first and second generation biofuels: A comprehensive review. *Renew. Sustain. Energy Rev.* 14, 578–597. doi:10.1016/J.RSER.2009.10.003.

Navarro, S. S., Cimpoia, R., Bruant, G., and Guiot, S. R. (2016). Biomethanation of syngas using anaerobic sludge: Shift in the catabolic routes with the CO partial pressure increase. *Front. Microbiol.* doi:10.3389/fmicb.2016.01188.

Nitschke, W., and Russell, M. J. (2012). Redox bifurcations: Mechanisms and importance to life now, and at its origin. *BioEssays* 34, 106–109. doi:10.1002/bies.201100134.

Nitschke, W., and Russell, M. J. (2013). Beating the acetyl coenzyme a-pathway to the origin of life. Philos. *Trans. R. Soc. B Biol. Sci.* doi:10.1098/rstb.2012.0258.

Novikov, A. A., Sokolova, T. G., Lebedinsky, A. V., Kolganova, T. V., and Bonch-Osmolovskaya, E. A. (2011). *Carboxydothermus islandicus* sp. nov., a thermophilic, hydrogenogenic, carboxydotrophic bacterium isolated from a hot spring. *Int. J. Syst. Evol. Microbiol.* 61, 2532–2537. doi:10.1099/ijs.0.030288-0.

O'Brien, J. M., Wolkin, R. H., Moench, T. T., Morgan, J. B., and Zeikus, J. G. (1984). Association of hydrogen metabolism with unitrophic or mixotrophic growth of *Methanosarcina barkeri* on carbon monoxide. *J. Bacteriol.* 158, 373–375.

Oelgeschläger, E., and Rother, M. (2008). Carbon monoxide-dependent energy metabolism in anaerobic bacteria and archaea. *Arch. Microbiol*. 190, 257–269. doi:10.1007/s00203-008-0382-6.

Oelgeschläger, E., and Rother, M. (2009). In vivo role of three fused corrinoid/methyl transfer proteins in *Methanosarcina acetivorans*. *Mol. Microbiol.* 72, 1260–1272. doi:10.1111/j.1365-2958.2009.06723.x.

Olson, K. D., McMahon, C. W., and Wolfe, R. S. (1991). Light sensitivity of methanogenic archaebacteria. *Appl. Environ. Microbiol.* 57, 2683–2686.

Oswald, F., Dörsam, S., Veith, N., Zwick, M., Neumann, A., Ochsenreither, K., et al. (2016). Sequential mixed cultures: From syngas to malic acid. *Front. Microbiol.* doi:10.3389/fmicb.2016.00891.

Parshina, S. N., Kijlstra, S., Henstra, A. M., Sipma, J., Plugge, C. M., and Stams, A. J. M. (2005). Carbon monoxide conversion by thermophilic sulfate-reducing bacteria in pure culture and in co-culture with *Carboxydothermus hydrogenoformans*. *Appl. Microbiol. Biotechnol.* 68, 390–396. doi:10.1007/s00253-004-1878-x.

Parshina, S. N., Sipma, J., Henstra, A. M., and Stams, A. J. M. (2010). Carbon monoxide as an electron donor for the biological reduction of sulphate. *Int. J. Microbiol.* 2010. doi:10.1155/2010/319527.

Perec, L., Krasna, A. I., and Rittenberg, D. (1962). The inhibition of hydrogenase by carbon monoxide and the reversal of this inhibition by light. *Biochemistry* 1, 270–275. doi:10.1021/bi00908a013.

Perez, J. M., Richter, H., Loftus, S. E., and Angenent, L. T. (2013). Biocatalytic reduction of short-chain carboxylic acids into their corresponding alcohols with syngas fermentation. *Biotechnol. Bioeng.* 110, 1066–1077. doi:10.1002/bit.24786.

Phillips, J. R., Atiyeh, H. K., Tanner, R. S., Torres, J. R., Saxena, J., Wilkins, M. R., et al. (2015). Butanol and hexanol production in *Clostridium carboxidivorans* syngas fermentation: Medium development and culture techniques. *Bioresour. Technol.* 190, 114–121. doi:10.1016/j.biortech.2015.04.043.

Phillips, J. R., Clausen, E. C., and Gaddy, J. L. (1994). Synthesis gas as substrate for the biological production of fuels and chemicals. *Appl. Biochem. Biotechnol.* 45–46, 145–157. doi:10.1007/BF02941794.

Piccolo, C., and Bezzo, F. (2009). A techno-economic comparison between two technologies for bioethanol production from lignocellulose. *Biomass and Bioenergy* 33, 478–491. doi:10.1016/J.BIOMBIOE.2008.08.008.

Pierce, E., Xie, G., Barabote, R. D., Saunders, E., Han, C. S., Detter, J. C., et al. (2008). The complete genome sequence of *Moorella thermoacetica (f. Clostridium thermoaceticum*). *Environ. Microbiol.* 10, 2550–2573. doi:10.1111/j.1462-2920.2008.01679.x.

Poehlein, A., Schmidt, S., Kaster, A. K., Goenrich, M., Vollmers, J., Thürmer, A., et al. (2012). An ancient pathway combining carbon dioxide fixation with the generation and utilization of a sodium ion gradient for ATP synthesis. *PLoS One* 7, e33439. doi:10.1371/journal.pone.0033439.

Ptasinski, K. J. (2008). Thermodynamic efficiency of biomass gasification and biofuels conversion. *Biofuels, Bioprod. Biorefining* 2, 239–253. doi:10.1002/bbb.65.

Ragsdale, S. W., and Pierce, E. (2008). Acetogenesis and the Wood–Ljungdahl pathway of CO_2 fixation. *Biochim. Biophys. Acta - Proteins Proteomics* 1784, 1873–1898. doi:10.1016/j.bbapap.2008.08.012.

Rajagopalan, S., P. Datar, R., and Lewis, R. S. (2002). Formation of ethanol from carbon monoxide via a new microbial catalyst. *Biomass and Bioenergy* 23, 487–493. doi:10.1016/S0961-9534(02)00071-5.

Ramió-Pujol, S., Ganigué, R., Bañeras, L., and Colprim, J. (2015). Incubation at 25°C prevents acid crash and enhances alcohol production in *Clostridium carboxidivorans* P7. *Bioresour. Technol.* 192, 296–303. doi:10.1016/j.biortech.2015.05.077.

Rao, Y., Wan, J., Liu, Y., Angelidaki, I., Zhang, S., Zhang, Y., et al. (2018). A novel process for volatile fatty acids production from syngas by integrating with mesophilic alkaline fermentation of waste activated sludge. *Water Res.* 139, 372–380. doi:10.1016/j.watres.2018.04.026.

Raybuck, S. A., Bastian, N. R., Orme-Johnson, W. H., and Walsh, C. T. (1988). Kinetic characterization of the carbon monoxide-acetyl-CoA (carbonyl group) exchange activity of the acetyl-CoA synthesizing carbon monoxide dehydrogenase from *Clostridium thermoaceticum*. *Biochemistry* 27, 7698–7702. doi:10.1021/bi00420a019.

Redissi, Y., and Bouallou, C. (2013). Valorization of carbon dioxide by co-electrolysis of CO_2/H_2O at high temperature for syngas production. in *Energy Procedia* (Elsevier), 6667–6678. doi:10.1016/j.egypro.2013.06.599.

Redl, S., Diender, M., Jensen, T. Ø., Sousa, D. Z., and Nielsen, A. T. (2017). Exploiting the potential of gas fermentation. *Ind. Crops Prod.* 106, 21–30. doi:10.1016/j.indcrop.2016.11.015.

Richter, H., Martin, M. E., and Angenent, L. T. (2013). A two-stage continuous fermentation system for conversion of syngas into ethanol. *Energies* 6, 3987–4000. doi:10.3390/en6083987.

Richter, H., Molitor, B., Diender, M., Sousa, D. Z., and Angenent, L. T. (2016a). A narrow pH range supports butanol, hexanol, and octanol production from syngas in a continuous co-culture of *Clostridium ljungdahlii* and *Clostridium kluyveri* with in-line product extraction. *Front. Microbiol.* 7. doi:10.3389/fmicb.2016.01773.

Richter, H., Molitor, B., Wei, H., Chen, W., Aristilde, L., and Angenent, L. T. (2016b). Ethanol production in syngas-fermenting: *Clostridium ljungdahlii* is controlled by thermodynamics rather than by enzyme expression. *Energy Environ. Sci.* 9, 2392–2399. doi:10.1039/c6ee01108j.

Roberts, G. P., Thorsteinsson, M. V., Kerby, R. L., Lanzilotta, W. N., and Poulos, T. (2001). CooA: a heme-containing regulatory protein that serves as a specific sensor of both carbon monoxide and redox state. *Prog. Nucleic Acid Res. Mol. Biol.* 67, 35–63. doi:10.1016/S0079-6603(01)67024-7.

Rother, M., and Metcalf, W. W. (2004). Anaerobic growth of *Methanosarcina acetivorans* C2A on carbon monoxide: An unusual way of life for a methanogenic archaeon. *Proc. Natl. Acad. Sci.* 101, 16929–16934. doi:10.1073/pnas.0407486101.

Rother, M., Oelgeschläger, E., and Metcalf, W. W. (2007). Genetic and proteomic analyses of CO utilization by *Methanosarcina acetivorans*. *Arch. Microbiol.* 188, 463–472. doi:10.1007/s00203-007-0266-1.

Ryter, S. W., and Otterbein, L. E. (2004). Carbon monoxide in biology and medicine. *Bioessays* 26, 270–280. doi:10.1002/bies.20005.

Sant'Anna, F. H., Lebedinsky, A. V., Sokolova, T. G., Robb, F. T., and Gonzalez, J. M. (2015). Analysis of three genomes within the thermophilic bacterial species *Caldanaerobacter subterraneus* with a focus on carbon monoxide dehydrogenase evolution and hydrolase diversity. *BMC Genomics* 16. doi:10.1186/s12864-015-1955-9.

Santala, S., Karp, M., and Santala, V. (2014). Rationally engineered synthetic coculture for improved biomass and product formation. *PLoS One* 9, e113786. doi:10.1371/journal.pone.0113786.

Sapra, R., Bagramyan, K., and Adams, M. W. W. (2003). A simple energy-conserving system: proton reduction coupled to proton translocation. *Proc. Natl. Acad. Sci. U. S. A.* 100, 7545–7550. doi:10.1073/pnas.1331436100.

Savage, M. D., and Drake, H. L. (1986). Adapation of the acetogen *Clostridium thermoautotrophicum* to minimal medium. *J. Bacteriol.* 165, 315–318. doi:10.1128/jb.165.1.315-318.1986.

Savage, M. D., Wu, Z. G., Daniel, S. L., Lundie, L. L., and Drake, H. L. (1987). Carbon monoxide-dependent chemolithotrophic growth of *Clostridium thermoautotrophicum*. *Appl. Environ. Microbiol.* 53, 1902–1906.

Schlegel, K., Welte, C., Deppenmeier, U., and Müller, V. (2012). Electron transport during aceticlastic methanogenesis by *Methanosarcina acetivorans* involves a sodium-translocating Rnf complex. *FEBS* J. 279, 4444–4452. doi:10.1111/febs.12031.

Schuchmann, K., and Müller, V. (2013). Direct and reversible hydrogenation of CO_2 to formate by a bacterial carbon dioxide reductase. *Science* (80-.). 342, 1382–1385. doi:10.1126/science.1244758.

Schuchmann, K., and Müller, V. (2014). Autotrophy at the thermodynamic limit of life: A model for energy conservation in acetogenic bacteria. *Nat. Rev. Microbiol.* 12, 809–821. doi:10.1038/nrmicro3365.

Schwede, S., Bruchmann, F., Thorin, E., and Gerber, M. (2017). Biological syngas methanation via immobilized methanogenic archaea on biochar. *Energy Procedia* 105, 823–829. doi:10.1016/j.egypro.2017.03.396.

Seravalli, J., and Ragsdale, S. W. (2008). ^{13}C NMR characterization of an exchange reaction between CO and CO_2 catalyzed by carbon monoxide dehydrogenase. *Biochemistry* 47, 6770–6781. doi:10.1021/bi8004522.

Shanmugasundaram, T., and Wood, H. G. (1992). Interaction of ferredoxin with carbon monoxide dehydrogenase from *Clostridium thermoaceticum*. *J. Biol. Chem.* 267, 897–900.

Sim, J. H., Kamaruddin, A. H., Long, W. S., and Najafpour, G. (2007). *Clostridium aceticum*-A potential organism in catalyzing carbon monoxide to acetic acid: Application of response surface methodology. *Enzyme Microb. Technol*. 40, 1234–1243. doi:10.1016/j.enzmictec.2006.09.017.

Singer, S. W., Hirst, M. B., and Ludden, P. W. (2006). CO-dependent H_2 evolution by *Rhodospirillum rubrum*: Role of CODH:CooF complex. *Biochim. Biophys. Acta - Bioenerg.* 1757, 1582–1591. doi:10.1016/j.bbabio.2006.10.003.

Slepova, T. V., Sokolova, T. G., Kolganova, T. V., Tourova, T. P., and Bonch-Osmolovskaya, E. A. (2009). *Carboxydothermus siderophilus* sp. nov., a thermophilic, hydrogenogenic, carboxydotrophic, dissimilatory Fe(III)-reducing bacterium from a Kamchatka hot spring. *Int. J. Syst. Evol. Microbiol.* 59, 213–217. doi:10.1099/ijs.0.000620-0.

Slepova, T. V., Sokolova, T. G., Lysenko, A. M., Tourova, T. P., Kolganova, T. V., Kamzolkina, O. V., et al. (2006). *Carboxydocella sporoproducens* sp. nov., a novel anaerobic CO-utilizing/H_2-producing thermophilic bacterium from a Kamchatka hot spring. *Int. J. Syst. Evol. Microbiol.* 56, 797–800. doi:10.1099/ijs.0.63961-0.

Slobodkin, A. I., Sokolova, T. G., Lysenko, A. M., and Wiegel, J. (2006). Reclassification of *Thermoterrabacterium ferrireducens* as *Carboxydothermus ferrireducens* comb. nov., and emended description of the genus Carboxydothermus. *Int. J. Syst. Evol. Microbiol.* 56, 2349–2351. doi:10.1099/ijs.0.64503-0.

Smith, D. R., Doucette-Stamm, L. A., Deloughery, C., Lee, H., Dubois, J., Aldredge, T., et al. (1997). Complete genome sequence of *Methanobacterium thermoautotrophicum* deltaH: functional analysis and comparative genomics. *J. Bacteriol.* 179, 7135–7155. doi:10.1128/jb.179.22.7135-7155.1997.

Smith, K. S., and Ingram-Smith, C. (2007). Methanosaeta, the forgotten methanogen? *Trends Microbiol.* 15, 150–155. doi:10.1016/j.tim.2007.02.002.

Soboh, B., Linder, D., and Hedderich, R. (2002). Purification and catalytic properties of a CO-oxidizing:H_2-evolving enzyme complex from *Carboxydothermus hydrogenoformans*. *Eur. J. Biochem.* 269, 5712–5721. doi:10.1046/j.1432-1033.2002.03282.x.

Sokolova, T. G., González, J. M., Kostrikina, N. A., Chernyh, N. A., Slepova, T. V., Bonch-Osmolovskaya, E. A., et al. (2004a). *Thermosinus carboxydivorans* gen. nov., sp. nov., a new anaerobic, thermophilic, carbon-monoxide-oxidizing, hydrogenogenic bacterium from a hot pool of Yellowstone National Park. Int. *J. Syst. Evol. Microbiol.* 54, 2353–2359. doi:10.1099/ijs.0.63186-0.

Sokolova, T. G., González, J. M., Kostrikina, N. A., Chernyh, N. A., Tourova, T. P., Kato, C., et al. (2001). *Carboxydobrachium pacificum* gen. nov., sp. nov., a new anaerobic, thermophilic, CO-utilizing marine bacterium from Okinawa Trough. *Int. J. Syst. Evol. Microbiol.* 51, 141–149. doi:10.1099/00207713-51-1-141.

Sokolova, T. G., Jeanthon, C., Kostrikina, N. A., Chernyh, N. A., Lebedinsky, A. V., Stackebrandt, E., et al. (2004b). The first evidence of anaerobic CO oxidation coupled with H_2 production by a hyperthermophilic archaeon isolated from a deep-sea hydrothermal vent. *Extremophiles* 8, 317–323. doi:10.1007/s00792-004-0389-0.

Sokolova, T. G., Kostrikina, N. A., Chernyh, N. A., Kolganova, T. V., Tourova, T. P., and Bonch-Osmolovskaya, E. A. (2005). *Thermincola carboxydiphila* gen. nov., sp. nov., a novel anaerobic, carboxydotrophic, hydrogenogenic bacterium from a hot spring of the Kae Baikal area. *Int. J. Syst. Evol. Microbiol.* 55, 2069–2073. doi:10.1099/ijs.0.63299-0.

Sokolova, T. G., Kostrikina, N. A., Chernyh, N. A., Tourova, T. P., Kolganova, T. V., and Bonch-Osmolovskaya, E. A. (2002). *Carboxydocella thermautotrophica* gen. nov., sp. nov., a novel anaerobic, CO-utilizing thermophile from a kamchatkan hot spring. *Int. J. Syst. Evol. Microbiol.* 52, 1961–1967. doi:10.1099/ijs.0.02173-0.

Sokolova, T., Hanel, J., Onyenwoke, R. U., Reysenbach, A. L., Banta, A., Geyer, R., et al. (2007). Novel chemolithotrophic, thermophilic, anaerobic bacteria *Thermolithobacter ferrireducens* gen. nov., sp. nov. and *Thermolithobacter carboxydivorans* sp. nov. *Extremophiles* 11, 145–157. doi:10.1007/s00792-006-0022-5.

Sokolova, T., and Lebedinsky, A. (2013). "CO-Oxidizing anaerobic thermophilic prokaryotes," in Thermophilic Microbes in Environmental and Industrial Biotechnology: Biotechnology of Thermophiles doi:10.1007/978-94-007-5899-5_7.

Sowers, K. R., Baron, S. F., and Ferry, J. G. (1984). *Methanosarcina acetivorans* sp. nov., an Acetotrophic Methane-Producing Bacterium Isolated from Marine Sediments. *Appl Env. Microbiol* 47, 971–978.

Steinbusch, K. J. J., Hamelers, H. V. M., Plugge, C. M., and Buisman, C. J. N. (2011). Biological formation of caproate and caprylate from acetate: fuel and chemical production from low grade biomass. *Energy Environ. Sci.* 4, 216–224. doi:10.1039/C0EE00282H.

Stoots, C. M., O'Brien, J. E., Herring, J. S., and Hartvigsen, J. J. (2009). Syngas production via high-temperature coelectrolysis of steam and carbon dioxide. *J. Fuel Cell Sci. Technol.* 6. doi:10.1115/1.2971061.

Struis, R. P. W. J., Schildhauer, T. J., Czekaj, I., Janousch, M., Biollaz, S. M. A., and Ludwig, C. (2009).

Sulphur poisoning of Ni catalysts in the SNG production from biomass: A TPO/XPS/XAS study. *Appl. Catal. A Gen.* 362, 121–128. doi:10.1016/j.apcata.2009.04.030.

Stupperich, E., Hammel, K. E., Fuchs, G., and Thauer, R. K. (1983). Carbon monoxide fixation into the carboxyl group of acetyl coenzyme A during autotrophic growth of Methanobacterium. *FEBS Lett.* 152, 21–23. doi:10.1016/0014-5793(83)80473-6.

Sutton, D., Kelleher, B., and Ross, J. R. H. (2001). Review of literature on catalysts for biomass gasification. *Fuel Process. Technol*. 73, 155–173. doi:10.1016/S0378-3820(01)00208-9.

Svetlichny, V. A., Sokolova, T. G., Gerhardt, M., Ringpfeil, M., Kostrikina, N. A., and Zavarzin, G. A. (1991). *Carboxydothermus hydrogenoformans* gen. nov., sp. nov., a CO-utilizing Thermophilic Anaerobic Bacterium from Hydrothermal Environments of Kunashir Island. *Syst. Appl. Microbiol*. 14, 254–260. doi:10.1016/S0723-2020(11)80377-2.

Svetlichnyi, V. A., Peschel, C., Acker, G., and Meyer, O. (2001). Two membrane-associated NiFeS-carbon monoxide dehydrogenases from the anaerobic carbon-monoxide-utilizing eubacterium *Carboxydothermus hydrogenoformans*. *J. Bacteriol*. 183, 5134–5144. doi:10.1128/JB.183.17.5134-5144.2001.

Tagawa, K., and Arnon, D. I. (1968). Oxidation-reduction potentials and stoichiometry of electron transfer in ferredoxins. *BBA - Bioenerg*. 153, 602–613. doi:10.1016/0005-2728(68)90188-6.

Tang, L., Huang, H., Hao, H., and Zhao, K. (2013). Development of plasma pyrolysis/gasification systems for energy efficient and environmentally sound waste disposal. *J. Electrostat.* 71, 839–847. doi:10.1016/J.ELSTAT.2013.06.007.

Tanner, R. S., Miller, L. M., and Yang, D. (1993). *Clostridium ljungdahlii* sp-Nov, an Acetogenic Species in Clostridial Ribosomal-RNA Homology Group-I. *Int. J. Syst. Bacteriol.* 43, 232–236. doi:10.1099/00207713-43-2-232.

Techtmann, S. M., Colman, A. S., Murphy, M. B., Schackwitz, W. S., Goodwin, L. A., and Robb, F. T. (2011). Regulation of multiple carbon monoxide consumption pathways in anaerobic bacteria. *Front. Microbiol.* 2, 1–12. doi:10.3389/fmicb.2011.00147.

Techtmann, S. M., Colman, A. S., and Robb, F. T. (2009). "That which does not kill us only makes us stronger": The role of carbon monoxide in thermophilic microbial consortia: Minireview. *Environ. Microbiol.* 11, 1027–1037. doi:10.1111/j.1462-2920.2009.01865.x.

Techtmann, S. M., Lebedinsky, A. V., Colman, A. S., Sokolova, T. G., Woyke, T., Goodwin, L., et al. (2012). Evidence for horizontal gene transfer of anaerobic carbon monoxide dehydrogenases. *Front. Microbiol.* 3, 1–16. doi:10.3389/fmicb.2012.00132.

Terlesky, K. C., and Ferry, J. G. (1988). Ferredoxin requirement for electron transport from the carbon monoxide dehydrogenase complex to a membrane-bound hydrogenase in acetate-grown *Methanosarcina thermophila. J. Biol. Chem*. 263, 4075–4079.

Thauer, R. K., Jungermann, K., Henninger, H., Wenning, J., and Decker, K. (1968). The energy metabolism of *Clostridium kluyveri. Eur. J. Biochem.* 4, 173–180. doi:10.1111/j.1432-1033.1968.tb00189.x.

Thauer, R. K., Kaster, A.-K., Goenrich, M., Schick, M., Hiromoto, T., and Shima, S. (2010). Hydrogenases from Methanogenic Archaea, Nickel, a novel cofactor, and H_2 Storage. *Annu. Rev. Biochem*. 79, 507–536. doi:10.1146/annurev.biochem.030508.152103.

Thauer, R. K., Kaster, A. K., Seedorf, H., Buckel, W., and Hedderich, R. (2008). Methanogenic archaea: Ecologically relevant differences in energy conservation. *Nat. Rev. Microbiol.* 6, 579–591. doi:10.1038/nrmicro1931.

Thrän, D., Billig, E., Persson, T., Svensson, M., Daniel-Gromke, J., Ponitka, J., et al. (2014). Biomethane Status and Factors Affecting Market Development and Trade.

Tiquia-Arashiro, S. M. (2014). "CO-oxidizing Microorganisms," in Thermophilic Carboxydotrophs and their Applications in Biotechnology doi:10.1007/978-3-319-11873-4.

Tremblay, P. L., Zhang, T., Dar, S. A., Leang, C., and Lovley, D. R. (2012). The Rnf complex of *Clostridium ljungdahlii* is a proton-translocating ferredoxin:NAD^+ oxidoreductase essential for autotrophic growth. *MBio* 4, e00406-12. doi:10.1128/mBio.00406-12.

Tschech, A., and Pfennig, N. (1984). Growth yield increase linked to caffeate reduction in *Acetobacterium woodii*. *Arch. Microbiol.* 137, 163–167. doi:10.1007/BF00414460.

Uffen, R. L. (1976). Anaerobic growth of a Rhodopseudomonas species in the dark with carbon monoxide as sole carbon and energy substrate. *Proc. Natl. Acad. Sci.* USA 73, 3298–3302. doi:10.1073/pnas.73.9.3298.

Valgepea, K., De Souza Pinto Lemgruber, R., Abdalla, T., Binos, S., Takemori, N., Takemori, A., et al. (2018). H_2 drives metabolic rearrangements in gas-fermenting *Clostridium autoethanogenum*. *Biotechnol. Biofuels* 11. doi:10.1186/s13068-018-1052-9.

Valgepea, K., de Souza Pinto Lemgruber, R., Meaghan, K., Palfreyman, R. W., Abdalla, T., Heijstra, B. D., et al. (2017). Maintenance of ATP Homeostasis Triggers Metabolic Shifts in Gas-Fermenting Acetogens. *Cell Syst.* 4, 505–515.e5. doi:10.1016/j.cels.2017.04.008.

van de Guchte, M., Serror, P., Chervaux, C., Smokvina, T., Ehrlich, S. D., and Maguin, E. (2002). Stress responses in lactic acid bacteria. doi:10.1023/A:1020631532202.

van der Meijden, C. M., Veringa, H. J., and Rabou, L. P. L. M. (2010). The production of synthetic natural gas (SNG): A comparison of three wood gasification systems for energy balance and overall efficiency. *Biomass and Bioenergy* 34, 302–311. doi:10.1016/j.biombioe.2009.11.001.

Varma, S. J., Muchowska, K. B., Chatelain, P., and Moran, J. (2018). Native iron reduces CO_2 to intermediates and end-products of the acetyl-CoA pathway. *Nat. Ecol. Evol*. 2, 1019–1024. doi:10.1038/s41559-018-0542-2.

Vassilev, S. V., Baxter, D., Andersen, L. K., Vassileva, C. G., and Morgan, T. J. (2012). An overview of the organic and inorganic phase composition of biomass. Fuel 94, 1–33. doi:10.1016/J.FUEL.2011.09.030.

Vasudevan, D., Richter, H., and Angenent, L. T. (2014). Upgrading dilute ethanol from syngas fermentation to n-caproate with reactor microbiomes. *Bioresour. Technol.* 151, 378–382. doi:10.1016/j.biortech.2013.09.105.

Vermeij, P., Pennings, J. L. A., Maassen, S. M., Keltjens, J. T., and Vogels, G. D. (1997). Cellular levels of factor 390 and methanogenic enzymes during growth of *Methanobacterium thermoautotrophicum* δH. *J. Bacteriol*. 179, 6640–6648.

Vizcaíno, J. A., Csordas, A., Del-Toro, N., Dianes, J. A., Griss, J., Lavidas, I., et al. (2016). 2016 update of the PRIDE database and its related tools. *Nucleic Acids Res.* 4, 447–456. doi:10.1093/nar/gkv1145.

Wagner, R. (2001). The regulation of ribosomal RNA synthesis and bacterial cell growth. *Curr. Opin. Biotechnol.* 161, 100–107. doi:10.1007/BF00276469.

Wang, S., Huang, H., Kahnt, H. H., Mueller, A. P., Köpke, M., and Thauer, R. K. (2013). NADP-Specific electron-bifurcating [FeFe]-hydrogenase in a functional complex with formate dehydrogenase in *Clostridium autoethanogenum* grown on CO. *J. Bacteriol.* 195, 4373–4386. doi:10.1128/JB.00678-13.

Wasserfallen, A., Nölling, J., Pfister, P., Reeve, J., and De Macario, E. C. (2000). Phylogenetic analysis of 18 thermophilic Methanobacterium isolates supports the proposals to create a new genus, Methanothermobacter gen. nov., and to reclassify several isolates in three species, *Methanothermobacter thermautotrophicus* comb. nov.,. *Int. J. Syst. Evol. Microbiol*. 50, 43–53. doi:10.1099/00207713-50-1-43.

Weiland, P. (2010). Biogas production: Current state and perspectives. *Appl. Microbiol. Biotechnol*. 85, 849–860. doi:10.1007/s00253-009-2246-7.

Weimer, P. J., Nerdahl, M., and Brandl, D. J. (2015). Production of medium-chain volatile fatty acids by mixed ruminal microorganisms is enhanced by ethanol in co-culture with *Clostridium kluyveri*. *Bioresour. Technol*. 175, 97–101. doi:10.1016/j.biortech.2014.10.054.

Weimer, P. J., and Stevenson, D. M. (2012). Isolation, characterization, and quantification of *Clostridium kluyveri* from the bovine rumen. *Appl. Microbiol. Biotechnol.* 94, 461–466. doi:10.1007/s00253-011-3751-z.

Weinstock, B., and Niki, H. (1972). Carbon monoxide balance in nature. *Science* (80-.). 176, 290–292. doi:10.1126/science.176.4032.290.

Welte, C., and Deppenmeier, U. (2011). Re-evaluation of the function of the F420 dehydrogenase in electron transport of *Methanosarcina mazei. FEBS J.* 278, 1277–1287. doi:10.1111/j.1742-4658.2011.08048.x.

Wessels, H. J. C. T., Gloerich, J., van der Biezen, E., Jetten, M. S. M., and Kartal, B. (2011). Liquid chromatography-mass spectrometry-based proteomics of Nitrosomonas. *Methods Enzymol.* 486, 465–482. doi:10.1016/B978-0-12-381294-0.00021-3.

Westman, S., Chandolias, K., and Taherzadeh, M. (2016). Syngas Biomethanation in a Semi-Continuous Reverse Membrane Bioreactor (RMBR). *Fermentation* 2, 8. doi:10.3390/fermentation2020008.

Wiedinmyer, C., Yokelson, R. J., and Gullett, B. K. (2014). Global Emissions of Trace Gases, Particulate Matter, and Hazardous Air Pollutants from Open Burning of Domestic Waste. *Environ. Sci. Technol.* 48, 9523–9530. doi:10.1021/es502250z.

Wohlfarth, G., Geerligs, G., and Diekert, G. (1990). Purification and properties of a NADH-dependent 5,10-methylenetetrahydrofolate reductase from *Peptostreptococcus productus. Eur. J. Biochem.* 192, 411–417. doi:10.1111/j.1432-1033.1990.tb19242.x.

Woolston, B. M., Emerson, D. F., Currie, D. H., and Stephanopoulos, G. (2018). Rediverting carbon flux in *Clostridium ljungdahlii* using CRISPR Interference (CRISPRi). *Metab. Eng.* 48, 243–253. doi:10.1016/j.ymben.2018.06.006.

Worden, R. M., Grethlein, A. J., Zeikus, J. G., and Datta, R. (1989). Butyrate production from carbon monoxide by *Butyribacterium methylotrophicum*. *Appl. Biochem. Biotechnol*. 20, 687–699.

Wu, M., Ren, Q., Durkin, A. S., Daugherty, S. C., Brinkac, L. M., Dodson, R. J., et al. (2005). Life in Hot Carbon Monoxide: The Complete Genome Sequence of *Carboxydothermus hydrogenoformans* Z-2901. *PLoS Genet* 1, e65. doi:10.1371/journal.pgen.0010065.

Xie, B. T., Liu, Z. Y., Tian, L., Li, F. L., and Chen, X. H. (2015). Physiological response of *Clostridium ljungdahlii* DSM 13528 of ethanol production under different fermentation conditions. *Bioresour. Technol.* 177, 302–307. doi:10.1016/j.biortech.2014.11.101.

Yoneda, Y., Yoshida, T., Kawaichi, S., Daifuku, T., Takabe, K., and Sako, Y. (2012). *Carboxydothermus pertinax* sp. nov., a thermophilic, hydrogenogenic, Fe(III)-reducing, sulfur-reducing carboxydotrophic bacterium from an acidic hot spring. *Int. J. Syst. Evol. Microbiol.* 62, 1692–1697. doi:10.1099/ijs.0.031583-0.

Younesi, H., Najafpour, G., and Mohamed, A. R. (2005). Ethanol and acetate production from synthesis gas via fermentation processes using anaerobic bacterium, *Clostridium ljungdahlii*. *Biochem. Eng. J.* 27, 110–119. doi:10.1016/j.bej.2005.08.015.

Youngsukkasem, S., Chandolias, K., and Taherzadeh, M. J. (2015). Rapid bio-methanation of syngas in a reverse membrane bioreactor: Membrane encased microorganisms. *Bioresour. Technol.* 178, 334–340. doi:10.1016/j.biortech.2014.07.071.

Zavarzina, D. G., Sokolova, T. G., Tourova, T. P., Chernyh, N. A., Kostrikina, N. A., and Bonch-Osmolovskaya, E. A. (2007). *Thermincola ferriacetica* sp. nov., a new anaerobic, thermophilic, facultatively chemolithoautotrophic bacterium capable of dissimilatory Fe(III) reduction. Extremophiles 55, 2069–2073. doi:10.1007/s00792-006-0004-7.

Zhang, F., Ding, J., Zhang, Y., Chen, M., Ding, Z. W., van Loosdrecht, M. C. M., et al. (2013). Fatty acids production from hydrogen and carbon dioxide by mixed culture in the membrane biofilm reactor. *Water Res*. 47, 6122–6129. doi:10.1016/j.watres.2013.07.033.

Zhou, Y., Dorchak, A. E., and Ragsdale, S. W. (2013). In vivo activation of methyl-coenzyme M reductase by carbon monoxide. F*ront. Microbiol*. 4. doi:10.3389/fmicb.2013.00069.

Zhu, J., Zheng, H., Ai, G., Zhang, G., Liu, D., Liu, X., et al. (2012). The genome characteristics and predicted function of methyl-group oxidation pathway in the obligate aceticlastic methanogens, methanosaeta spp. *PLoS One* 7, e36756. doi:10.1371/journal.pone.0036756.

Zinder, S. H., and Anguish, T. (1992). Carbon monoxide, hydrogen, and formate metabolism during methanogenesis from acetate by thermophilic cultures of Methanosarcina and Methanothrix strains. *Appl. Environ. Microbiol.* 58, 3323–3329.

Zirngibl, C., Hedderich, R., and Thauer, R. K. (1990). N5,N10-Methylenetetrahydromethanopterin

dehydrogenase from *Methanobacterium thermoautotrophicum* has hydrogenase activity. *FEBS Lett.* 261, 112–116. doi:10.1016/0014-5793(90)80649-4.

Zwietering, M. H., Jongenburger, I., Rombouts, F. M., and Van't Riet, K. (1990). Modeling of the bacterial growth curve. *Appl. Environ. Microbiol.* 56, 1875–1881. doi:10.1111/j.1472-765X.2008.02537.x.

English Summary

Synthesis gas (syngas) fermentation is a process capable of processing a gaseous substrate via bacterial fermentation into commodity chemicals and fuels. Gas (mainly consisting of hydrogen, carbon monoxide and carbon dioxide) fed to the fermentation process can be obtained from a wide variety of sources, including off-gases from industry, gasification of solid carbon wastes (e.g. municipal waste, lignocellulosic biomass) or gas derived from electrochemical reduction/physicochemical reduction processes.

Current limitations of the fermentation process are the relatively poorly understood physiology and genetics of the biocatalysts involved. Therefore the work in this thesis aimed at unravelling of the syngas metabolism of acetogenic and methanogenic strains, with main focus on carbon monoxide metabolism. In addition, the application of synthetic co-cultures for syngas fermentation was explored to assess if such cultivation approach could be interesting for application. Co-cultivation studies provided a proof-of-concept for broadening syngas-derived products spectrum, but resulted as well in new fundamental insights in the metabolism of the involved strains.

As in the last 30 years much research has been conducted on the metabolism of CO fermentation, this was reviewed, and compared to recent developments in the last 5-10 years, in **Chapter 2**. Here we studied the general CO metabolism of hydrogenogenic, acetogenic and methanogenic strains, and highlight their similarities and differences. Main focus is given to the Wood-Ljungdahl pathway, playing a role in all these three metabolisms. In addition, the effect of the strong reduction power of CO on the end-product spectrum and its potential toxicity effects on microbial catalysts is discussed.

In **Chapter 3** we explored the carboxydotrophic metabolism of *Methanothermobacter marburgensis*. Here we observe a poor ability of CO-conversion and attribute this to redox stress caused by the CO molecule. This was supported by the observation of upregulation of redox stress factors in the proteome. Additionally, it was found that presence of hydrogen on the background was required before methanogenesis on CO could take place. This is likely needed to drive the bifurcating heterodisulfide reductase against the redox pressure generated from CO oxidation.

Based on findings in **Chapter 3** and the general reports of methanogens growing poorly in presence of CO as substrate, a co-culture was constructed in order to facilitate methane production from CO, this is described in **Chapter 4**. The co-culture consisted of *Carboxydothermus hydrogenoformans* and *Methanothermobacter thermoautotrophicus*, and together formed an efficient system to generate methane from CO containing gas. The culture was able to achieve 4 l/l_{iquid}/day of methane

production in a proof of principal setup, reaching 90% substrate conversion efficiency and 73% methane content in the outflow gas (max. yield 75%, at this inflow composition). This showed that this culture is highly efficient in biological conversion of CO-rich gas to methane and might compete with or work in parallel to other methane production processes such as the Sabatier process, or anaerobic digestion.

As the product spectrum from syngas fermentation is currently still relatively narrow, often resulting in acetate and ethanol, co-cultivation approaches can be used to enhance this product range. **Chapter 5** describes a defined co-culture capable of converting CO or syngas mixtures to chain elongated acids (butyrate and caproate) and their respective alcohols (butanol and hexanol). These products are rarely generated by a single microbe from syngas and if so, are usually low in concentration and production rate. The co-culture consists of *Clostridium autoethanogenum* and *Clostridium kluyveri* allowing the former to convert the syngas/CO to acetate and ethanol, subsequently resulting in conversion of these products by *C. kluyveri* into chain elongated acids. The observed alcohols are subsequently formed by reduction steps performed by *C. autoethanogenum*. This shows the strength of the co-culture approach in the expanding of product range from syngas.

As follow-up to **Chapter 5**, the co-culture and interactions taking place are studied in more detail in **Chapter 6**. Here we conducted a transcriptomic and physiological analysis on the *C. autoethanogenum* strain in mono- and co-culture. During chemostat cultivation we observed a clear shift in the product spectrum of *C. autoethanogenum* towards solventogenesis, under the same reactor conditions, in co-culture compared to the monoculture. Interestingly, no major changes were found in the transcriptome of *C. autoethanogenum* in the central carbon or redox metabolism when comparing mono- and co-culture conditions, suggesting no changes take place on genetic level. Therefore we believe the product shift is caused by the removal of ethanol from the medium by *C. kluyveri*, resulting in thermodynamically more favourable conditions for solventogenesis by *C. autoethanogenum*.

Over several experiments conducted for the clostridial co-culture we observed the oxidation of alcohols by *C. autoethanogenum* at lower CO pressure exposure. We investigated this behaviour further, which is described in **Chapter 7**. Alcohols appear to act as electron donor when the cells are exposed to low CO levels, co-oxidizing them with CO as a substrate. Oxidation of alcohols was observed to result in a significant energy gain per CO consumed, suggesting oxidation takes place via acetyl-CoA as intermediate, allowing conservation of energy via the acetate kinase enzyme. Furthermore data shows that during exposure to increased CO concentrations in the liquid, *C. autoethanogenum* conserves more energy per acetate

formed. We hypothesize that this increased energy conservation can be explained by the cycling of acetate, via acetaldehyde and acetyl-CoA back to acetate, resulting in CO-driven ATP conservation.

Overall we see quick developments in the field of syngas fermentation, both from a fundamental and applied perspective. The recent developments in the field are described in **Chapter 8** and placed in the light of this thesis. From the bio-catalyst point of view, most important developments include the establishment of genetic systems for model gas fermenting clostridia and insight in the thermodynamic regulation of the metabolism by these organisms. Additionally, we highlight recent findings in preliminary studies on the acetate cycling hypothesis (**Chapter 7/8**). Here we show that ^{13}C labelled acetate is incorporated into acetyl-CoA during exposure to high levels of CO, confirming part of the acetate cycling puzzle. Also the efficiency of the synthetic co-culture approach is discussed (**Chapter 4-6, 8**) and advantages and downsides of the co-culture strategy are highlighted, overall indicating it as a suitable strategy for improving the syngas process in the future.

Nederlandse samenvatting

Synthesegas (syngas) fermentatie is een proces waarmee het mogelijk is om gas-substraat om te zetten naar bruikbare chemicaliën en brandstoffen. Gas (vnl. bestaand uit koolmonoxide, waterstof en kooldioxide) dat gebruikt wordt voor deze toepassing kan verkregen worden vanuit meerdere bronnen, dit omvat: afvalgassen vanuit de industrie, gas afkomstig uit gassificatie van vast koolstof-rijk afval (bijv. huishoudelijk afval of biomassa), of gas afkomstig uit elektrochemische of chemische reductie processen.

Huidige limitaties van dit fermentatie proces zijn de slecht begrepen fysiologie en genetica van de betrokken microbiële katalysatoren. Om deze reden richt het onderzoek beschreven in dit proefschrift zich op het ontrafelen van het syngas metabolisme van acetogene en methanogene micro-organismen, en focust met name op de omzetting van koolstofmonoxide. Ook is in deze thesis de werking van synthetische co-cultures voor de omzetting van syngas getest. Hierbij is een concept studie gedaan waarin het eindproduct spectrum, en productie efficiëntie van het fermentatie process zijn getest. Dit deel van het onderzoek heeft daarnaast geleid tot nieuwe fundamentele inzichten in de rol organismen in deze co-cultures.

In de afgelopen 30 jaar is er uitgebreid onderzoek gedaan naar het metabolisme van koolmonoxide fermentatie. Beschikbare literatuur over dit onderwerp wordt besproken in **Hoofdstuk 2**. Voornamelijk de CO metabolismen van hydrogene, acetogene en methanogene micro-organismen wordt hier besproken, met focus op de gelijkenissen en verschillen. De focus ligt hier op de werking van de Wood-Ljungdahl route, die een centrale rol speelt in alle 3 van deze metabolismen. Daarnaast wordt de sterk reducerende eigenschap van koolmonoxide op het fermentatie product spectrum, en potentiele toxische effecten op verscheidene micro-organismen besproken.

In **Hoofdstuk 3** wordt het koolmonoxide metabolisme van *Methanothermobacter marburgensis* besproken. Dit micro-organisme is in staat koolmonoxide te gebruiken als substraat, maar doet dit niet efficiënt. Dit kan waarschijnlijk worden verklaard door redox stress, geïnduceerd door koolmonoxide. Deze theorie wordt ondersteund door de toename in productie van redox stress eiwitten in het proteoom. Een andere belangrijke bevinding was dat waterstof nodig is voor de omzetting van koolmonoxide door deze methanogeen. Waterstof is waarschijnlijk nodig om de reductiekracht te leveren voor activiteit van het heterodisulfide reductase enzym, wat essentieel is voor het functioneren van het centrale redox metabolisme van deze methanogeen.

Gebaseerd op bevindingen in **Hoofdstuk 3**, en op algemene bevindingen dat methanogenen slecht groeien op CO als substraat, is de co-cultuur techniek toegepast

om de omzetting van koolmonoxide naar methaan te faciliteren. Dit werk is beschreven in **Hoofdstuk 4**. De co-cultuur, bestaande uit *Carboxydothermus hydorgenoformans* en *Methanothermobacter thermoautotrophicus*, vormde samen een efficiënt systeem waarin CO-rijk gas werd omgezet naar methaan. Het was mogelijk om een efficiëntie te behalen van 90% substraat omzetting met een 73% methaan gehalte (maximaal 75% mogelijk bij de compositie van de gebruikte inkomende gas stroom). Dit toont aan dat deze co-cultuur in staat is om met hoge efficiëntie het koolmonoxide rijke gas om te zetten naar methaan. Dit systeem kan mogelijk in parallel opereren of competeren met andere methaan producerende processen zoals het Sabatier proces of anaerobe vergisting.

Het product spectrum van syngas fermentatie is gelimiteerd, vaak resulterend in productie van acetaat en ethanol. De co-cultuur techniek kan gebruikt worden om andere producten te produceren. In **Hoofdstuk 5** wordt een co-cultuur besproken die in staat is om koolmonoxide of syngas mengsels om te zetten naar keten verlengde producten (butyraat, carpoaat) en de respectieve alcoholen (butanol en hexanol). Deze producten worden zelden gevormd door één microbe alleen, en in de gevallen waar dat wel zo is zijn de product concentraties en productie snelheden laag. De co-cultuur bestaat uit *Clostridium autoethanogenum* en *Clostridium kluyveri,* waarin eerstgenoemde de koolmonoxide omzet naar acetaat en ethanol, wat gevolgd wordt door ketenverlenging door laatstgenoemde microbe. De gevormde alcoholen ontstaan door reductie van de organische-zuren door *C. autoethanogenum*. Dit laat zien dat het mogelijk is om het product spectrum van syngas fermentatie uit te breiden met de co-cultuur techniek.

Als vervolg op **Hoofdstuk 5**, zijn de interacties in de co-cultuur verder bestudeerd, dit is beschreven in **Hoofdstuk 6**. Hier is gebruikgemaakt van een combinatie van transcriptoom analyse en fysiologische experimenten op *C. autoethanogenum* in mono- en co-cultuur. Gedurende chemostaat cultivatie werd een duidelijke verschuiving waargenomen in het product spectrum van *C. autoethanogenum*, waarbij meer ethanol werd gevormd in de co-cultuur conditie ten opzichte van de monocultuur bij gelijkblijvende omgevingscondities. Opmerkelijk was dat er geen duidelijke veranderingen plaatsvonden in het transcriptoom van *C. autoethanogenum*, wat suggereert dat de verandering in eind product spectrum niet het gevolg zijn van veranderingen in genexpressie. Daarom hypothetiseren we dat de verschuiving in product spectrum komt door de verwijdering van ethanol door *C. kluyveri*. Dit veroorzaakt dat het voor *C. autoethanogenum* thermodynamisch meer voordelig wordt om ethanol te maken, resulterende in de geobserveerde verschuiving.

Tijdens de co-cultuur experimenten werd meerdere keren geobserveerd dat *C. autoethanogenum* in staat is om alcoholen te oxideren bij lagere opgeloste

koolmonoxide concentratie. Deze eigenschap is verder onderzocht, en beschreven in **Hoofdstuk 7**. Alcoholen lijken te dienen als elektron donor op het moment dat de cellen blootgesteld worden aan lagere koolmonoxide concentraties, resulterend in co-oxidatie van koolmonoxide en de alcoholen. Oxidatie van alcoholen lijkt gekoppeld aan een significante toename in energie conservatie per koolmonoxide molecuul verbruikt. Dit suggereert dat oxidatie van de alcoholen plaatsvind via acetyl-CoA as tussenstap, wat extra energie conservatie toelaat via het enzym acetaat kinase. Verder laat data zien dat bij blootstelling aan hogere koolmonoxide concentratie in de vloeistof meer energie conservatie plaatsvind per acetaat gevormd. We hypothetiseren dat dit komt door het rondpompen van acetaat via acetaldehyde en acetyl-CoA terug naar acetaat, wat resulteert in koolmonoxide gedreven ATP conservatie.

Over het gehele veld van syngas fermentatie zien we snelle ontwikkelingen, zowel op fundamenteel als toegepast gebied. Recente ontwikkelingen worden beschreven in **Hoofdstuk 8**, waar deze geplaats worden in de context van deze thesis. Vanuit het gebied van microbiologie zijn de belangrijkste ontwikkelingen: het tot stand brengen van genetische systemen voor Clostrida, en het verkrijgen van inzicht in de thermodynamische regulatie van syngas metabolisme. Ook worden recente bevindingen omtrent de acetaat cyclus hypothese (**Hoofdstuk 7/8**) besproken. Hier tonen we aan dat ^{13}C-gelabeld acetaat teruggevonden wordt in acetyl-CoA gedurende blootstelling aan hogere opgeloste koolmonoxide concentraties, wat een deel van de acetaat cyclus hypothese bevestigd. Verder wordt ook de efficiëntie van synthetische co-cultivatie in syngas fermentatie besproken (**Hoofdstuk 4-6,8**), en voor- en nadelen van deze strategie uitgelicht. Hieruit concluderen we dat de co-cultuur strategie een geschikte aanpak is voor het verbeteren van syngas fermentatie processen in de toekomst.

Co-author affiliations

Diana. Z. Sousa [1]

Alfons J.M. Stams [1, 2]

Hans J.C.T Wessels [3]

Ricardo Pereira [1]

Philipp S. Uhl [1]

Johannes H. Bitter [4]

Jasper J. Koehorst [5]

Peter J. Schaap [5]

Ivette Parera Olm [1]

Marten Gelderloos [1]

[1] Laboratory of Microbiology, Wageningen University and Research, Stippeneng 4, 6708 WE Wageningen, The Netherlands

[2] Centre of Biological Engineering, University of Minho, Campus de Gualtar, 4710-057, Braga, Portugal

[3] Radboud Proteomics Center, Translational Metabolic Laboratory, Department of Laboratory Medicine, Radboud UMC Nijmegen, Nijmegen, The Netherlands

[4] Bio based chemistry & technology, Wageningen University and Research, Bornse Weilanden 9, 6708 WG, Wageningen, The Netherlands.

[5] Laboratory of Systems and Synthetic Biology, Wageningen University, Stippeneng 4, 6708 WE, Wageningen, the Netherlands

List of Publications

Diender, M., Stams, A. J. M., and Sousa, D. Z. (2015). Pathways and bioenergetics of anaerobic carbon monoxide fermentation. Front. Microbiol. 6. doi:10.3389/fmicb.2015.01275.

Diender, M., Pereira, R., Wessels, H. J. C. T., Stams, A. J. M., and Sousa, D. Z. (2016). Proteomic Analysis of the Hydrogen and Carbon Monoxide Metabolism of *Methanothermobacter marburgensis*. Front. Microbiol. 7. doi:10.3389/fmicb.2016.01049.

Diender, M., Stams, A. J. M., and Sousa, D. Z. (2016). Production of medium-chain fatty acids and higher alcohols by a synthetic co-culture grown on carbon monoxide or syngas. Biotechnol. Biofuels 9. doi:10.1186/s13068-016-0495-0.\

Timmers H.A.P, Suarez-Zuluaga A.D., van Rossem M., **Diender M.**, Stams A.J.M, Plugge C.M. (2016). Anaerobic oxidation of methane associated with sulfate reduction in a natural freshwater gas source. ISME 10, 1400-1412. doi: https://doi.org/10.1038/ismej.2015.213

Richter, H., Molitor, B., **Diender, M.**, Sousa, D. Z., and Angenent, L. T. (2016). A narrow pH range supports butanol, hexanol, and octanol production from syngas in a continuous co-culture of *Clostridium ljungdahlii* and *Clostridium kluyveri* with in-line product extraction. Front. Microbiol. 7. doi:10.3389/fmicb.2016.01773.

Redl, S.*, **Diender, M.***, Jensen, T. Ø., Sousa, D. Z., and Nielsen, A. T. (2017). Exploiting the potential of gas fermentation. Ind. Crops Prod. 106, 21–30. doi:10.1016/j.indcrop.2016.11.015.

Diender, M., Uhl, P. S., Bitter, J. H., Stams, A. J. M., and Sousa, D. Z. (2018). High rate biomethanation of carbon monoxide-rich gases via a thermophilic synthetic coculture. ACS Sustain. Chem. Eng. 6, 2169–2176. doi:10.1021/acssuschemeng.7b03601.

* authors contributed equally

Acknowledgements

‘If I have seen further it is by standing on the shoulders of Giants’

– Isaac Newton

Completing a PhD is not something done alone. Along the way there are many teachers, supporters and idols. Some were there already before things started, others just showed up yesterday. Without the help of many I would not have been able to complete this work, and I am grateful to have learned from all of you and will keep doing so in the future.

Diana, as co-promoter you have been a great guide for me in the past four years. Next to learning from your extensive scientific knowledge/experience, I think I might have learned most from your ability to flexibly deal with work in a relaxed way. You have given me great support over the years for doing research and have given me all the freedom I needed to also test my own ideas/hypothesises. For this I am very grateful. I have enjoyed the many discussions we had over the past few years and I am sure many good ones will follow in the future.

Fons, I think you are the most true and honest scientist I have met and I hope to one day live up to that status. It was great having you as promotor and I enjoyed being part of your research group in the past years. Next to motivation and support, your extensive scientific knowledge and experience has been very valuable for my personal and scientific development.

Caroline, Serve & Gosse, you have been very important catalysts for developing my interest and knowledge in the field of microbiology during my BSc.,MSc. and PhD studies. You caused the spark that gave me an exceptional interest for the physiology of microbes. Also I want to thank you for the scientific input and good discussions we had over the years, which have contributed to this thesis.

This work could never have been completed without the help of the microbiology staff, you all make working at microbiology a very enjoyable experience. **Anja, Heidi, Carolien**: Thank you for all the support over the years, especially on the administrative side. **Ton** thank you for all the help in the lab, many analytical problems would not have been solved without your help. Also thank you for teaching me the background for all analytical equipment we run in the lab, these analytical tips & tricks are valuable knowledge to have. T**om v/d W,** your technical help was essential for all the reactor work performed in this thesis, without you, the Applikon reactor systems would still be catching dust. Also to the rest of the technician team: **Tom S, Ineke, Merlijn, Steven, Iame, Monika, Philippe, Sjon, Rob** and of course **Wim**: thank you for all the help, big or small, it has been very valuable.

Ivette, I am very happy to have had you as a student and I am very proud to now have you as a colleague. I have really enjoyed working with you on the syngas topic over the last few years and I hope to enjoy your happy company and friendship for many more years to come. **Daan**, I have enjoyed all our conversations, meetings, drinks and labwork moments we have shared together. I learned a lot from you on both the scientific and personal field and I hope we can share many more good moments in the future. **Lot,** you are an amazing officemate, thank you for the many interesting scientific (and non-scientific) conversations. **Anna**, as office mate I enjoyed many good moments with you, thank you for all the support and friendship over the years. Also the rest of the Micfys family: I**rene, Nam, Susakul, Nicolas, Nikolaos, Yuan, Nohemi, Sara, Anna, Roy, Sudarshan, Monir, Lara, Jueeli, Peter, James, Catalina, Dandan, Marjet, Rik, Vicente, Samet, Michael, Bruna, Connal, Ryan, Cristina, Denny**: you all have been great company over the last years, making MicFys a great place to work. **Ivonne, Florin** and **Oliver**: I enjoy our collaboration on further uncovering the acetate cycle described in chapter 7. I hope our future collaborations will result in its definitive confirmation. Also **Stephanie, Torbjørn** it was great writing the syngas review together and I hope to be able to collaborate with both of you in the future. Also **Lars, Bastian** and **Hanno**, we had some fruitful scientific discussions on syngas fermentation and on the applicability of the co-culture systems. I enjoyed working together and hope to keep doing so in the future.

Of course, none of this would have been fully completed without the help of the great team of students that have helped me throughout the years. I could not have wished for better help. As I state in one of my propositions, I have gained more thorough understanding of the syngas topic with your help. You all have contributed significantly to this work either in a direct or indirect way. All of you have worked hard and that has payed-off as all of you have landed good jobs or will certainly do so in the future. So therefore: **Philipp, Sonja, Ivette, Sierd, Jordy, Timo, Marten, Sophie** and **Timon**, thank you for all your help, without you this would have been impossible. Also, **João** and **Ricardo**: while I did not supervise you as main supervisor I did enjoy working with you on the syngas topic a lot, and in both cases this resulted in fruitful results.

I also want to thank all **colleagues** working at the Laboratory of Microbiology for all the great times in the past years, I enjoyed all our conversations, discussions and events. Special thanks goes to the organizers of the PhD-trip, which was truly a great experience. **Peer, João, Elleke**, next to your colleague I have also been your student at some point and I am grateful for all the things I have learned from you. **Jorrit** I enjoyed being member of the daily board together, making strategy day presentations, drinking a beer or eating surströming in the middle of the night on a

beach in Kopenhagen, always 'gezellig'. Also **Hugo, Marnix, Jeroen, Carrie, Tijn** I enjoyed our conversations on a wide variety of topics over lunch or over a few beers. **Emmy, Linde, Joyshree:** next to many good moments during lab events or lunch, I enjoyed a lot organizing the lab trip with you in 2017. **Laura, Jules, Michiel, Francisca, Cornelia, Melvin, Saara, Marissa, Leonor, Sigrid**: I enjoyed the SIAM events over the past four years and thanks for all the important scientific discussions and fun events. Also thanks to the SSB people: **Emma, Nung, Maarten, Ruben, Bastian, Jasper, Erika, Lotte, Benoit, Bart** for both the scientific collaborations and the fun times. **Lieke, Ricardo, Mengru, Tommy, Lucie** and **Guusje**, being in the WIMEK PhD council with you was very enjoyable and fruitful.

To all old residents of the Veenderweg 34a, my home base during my studies, and first year of the PhD, thank you for all the fun over the years. **Rob**, next to our regular squash games, I have in the past years enjoyed all our chats on a wide variety of topics, including latest technological inventions or where to put the money in the stock market (even though financial profits are not yet through the roof). **Femmy**, I have enjoyed all the time we spend together during our studies. The conversations we had have given me good reflections on life and helped me make the right decisions. **Geronda**, you have been a great example for me since we met, and you still are. While still on the drawing table, I am sure our 'sheep rumen microbiota driven motorcycle' concept will one day become integrated technology. Also **Maarten, Leontien, Bas**, **Tineke**: I have enjoyed all our lunches, dinners, parties and discussions we have had over the years and I hope to have many more in the future.

Stefan, our friendship goes already back more than 16 years, thanks for all the good moments and fun in the past years. I enjoyed all our moments of running, weightlifing, Warhammer and (computer) games. But above all I enjoy our amazing conversations. I think that there has not been a single time since high school that we did not have discussions that go way too far, long, complicated or the combination of all three, but all of them are great. **Tom, Ilona, Sebastien, Lineke, Roxanne, Lennard, Simone, Marco, Claire, Marcus, Laura & Merijn,** no year is ever boring with all the lunches, dinners, events, parties etc. thanks for all these amazing moments I hope to share many more with you in the future.

Beste familie, aan zowel de **Diender** als aan de **Verlaan** kant van de familie. Jullie hebben mijn gehele leven een grote rol gespeeld. Jullie zijn naast familie ook voorbeelden, leraren, luisteraars, critici en vrienden geweest. Bedankt voor alle leuke en gezellige momenten in de afgelopen jaren. Ook **Jan, Yvonne** en **Ilse**, bedankt voor alle leuke momenten die we hebben gedeeld.

Bernadette, Ruud en **Natanja**, jullie zijn altijd een belangrijke steun geweest de afgelopen jaren. Bedankt voor alle mooie momenten tot nu toe en ik hoop dat we er nog veel meer mogen meemaken.

Mam & Pap: bedankt voor alles, jullie zijn er altijd voor mij geweest en hebben altijd achter al mijn keuzes gestaan. Jullie hebben altijd maximale interesse getoond voor alles wat ik doe en ik kan altijd blind op jullie vertrouwen. Ik zie in mijn werkstijl en karakter steeds meer een reflectie van jullie en daar ben ik trots op. Jullie zijn mijn grootste voorbeelden en zullen dat altijd blijven. **Remco**: je betekent ontzettend veel voor me. Ik heb me altijd enorm gefascineerd door je drive en ongelofelijke durf, waar ik je ooit op een dag in hoop te evenaren. Je bent een van mijn grootste voorbeelden en ik weet zeker dat ik nog veel van je kan leren in de toekomst. **Isolde**, ik bewonder je kracht en doorzettingsvermogen, je bent voor mij een grote inspiratiebron. Bedankt de afgelopen jaren voor alle gezellige momenten waarvan ik hoop er nog veel mee te mogen maken.

Manon, voor al meer dan 10 jaar ben jij essentieel in mijn leven. Ik kan altijd op je rekenen en zonder jou steun was het voltooien van deze thesis een stuk moeilijker geweest. Jij kan me laten reflecteren en houdt me met beide benen op de grond. Je bent altijd een van de eerste die mijn meest recente theorieën (wetenschappelijk of niet) hoort, maar je bent altijd geïnteresseerd of het nou ‘s ochtends vroeg is of ’s avonds laat. Het is onmogelijk om in woorden te vatten wat je voor mij betekent, en ik ben blij dat we het leven samen kunnen delen.

About the author

Martijn Diender was born on February 22, 1991 in Lelystad, the Netherlands.

He obtained a Bachelors degree in Biology at the Wageningen University, specializing in cellular and molecular biology. During his bachelor Thesis he researched the process of anaerobic respiration of methane coupled to sulfate reduction, in the group of Alfons J.M. Stams.

He continued his studies with a Masters in Biotechnology at Wageningen University focussing on biotechnological processes for bio-based economy. His Master Thesis was perfomed in the group of John van der Oost on the genetic engineering of a thermophilic Bacillus strain for succinic acid production. After this he worked for a short time as an intern at Wetsus, centre of sustainable water technology, where he researched the possibility utilize carbon monoxide rich feed gas as electron donor for treating a bleed stream of the ThioPaq gas desulfurization process (Paques, Shell).

In 2014 he started his PhD at the Wageningen University in the group of Alfons J.M. Stams on the topic of synthesis gas fermentation, which has resulted in this thesis.

Netherlands Research School for the
Socio-Economic and Natural Sciences of the Environment

D I P L O M A

For specialised PhD training

The Netherlands Research School for the
Socio-Economic and Natural Sciences of the Environment
(SENSE) declares that

Martijn Diender

born on 22 February 1991 in Lelystad, The Netherlands

has successfully fulfilled all requirements of the
Educational Programme of SENSE.

Wageningen, 8 February 2019

The Chairman of the SENSE board

Prof. dr. Martin Wassen

the SENSE Director of Education

Dr. Ad van Dommelen

The SENSE Research School has been accredited by the Royal Netherlands Academy of Arts and Sciences (KNAW)

KONINKLIJKE NEDERLANDSE
AKADEMIE VAN WETENSCHAPPEN

The SENSE Research School declares that **Martijn Diender** has successfully fulfilled all requirements of the Educational PhD Programme of SENSE with a work load of 45.2 EC, including the following activities:

SENSE PhD Courses

- Environmental research in context (2015)
- Research in context activity: 'Co-organizing workshop on "Personal bias and scientific research: the biomass – bioenergy case" (18 June 2015, Wageningen)'
- Laser and optics in fluid research (2014)

Other PhD and Advanced MSc Courses

- Soehngen Institute of Anaerobic Microbiology (SIAM) thermodynamics workshop, Nijmegen (2016)
- SIAM PhD summer school on anaerobic microbiology, Royal Netherlands Institute for Sea research-NIOZ (2016)
- Scientific writing, Wageningen Graduate Schools (2016)
- SIAM PhD retreat, Wageningen University and Research (2017)
- Scientific artwork with Photoshop and illustrator, Wageningen University Library (2017)
- SIAM pitching course, Delft (2018)

Didactic Skills Training

- Supervising of 4 BSC students and 5 MSc students (2014-2018)
- Teaching in the BSc course 'Microbial physiology' (2015-2018)

Management skills Training

- Member of the Microbiology chair group's daily board (2014-2018)
- Co-organizing SENSE summer symposium "Make a change! - Successful interaction with society" (2015)
- Chair of WIMEK PhD council (2015-2017)

Oral Presentations

- *Conversion of carbon monoxide or syngas into chain elongated products and higher alcohols by using a synthetic co-culture*. 6th International Bielefeld-CeBiTec Research Conference, 26-28 September 2016, Bielefeld, Germany
- *Methanogenesis on carbon monoxide, a harsh way of life.* Royal Dutch Society of Microbiology (KNVM) spring meeting, 12 April 2017, Arnhem, the Netherlands
- *High rate biomethanation of carbon monoxide rich gases via a thermophilic synthetic co-culture.* 3rd International Conference on Biogas Microbiology, 1-3 May 2017, Wageningen, The Netherlands

SENSE Coordinator PhD Education

Dr. Peter Vermeulen

Research described in this Thesis was supported by a SIAM Gravitation Grant (024.002.002) from the Netherlands organization for Scientific Research.

Cover design: Martijn Diender

Thesis layout: Martijn Diender
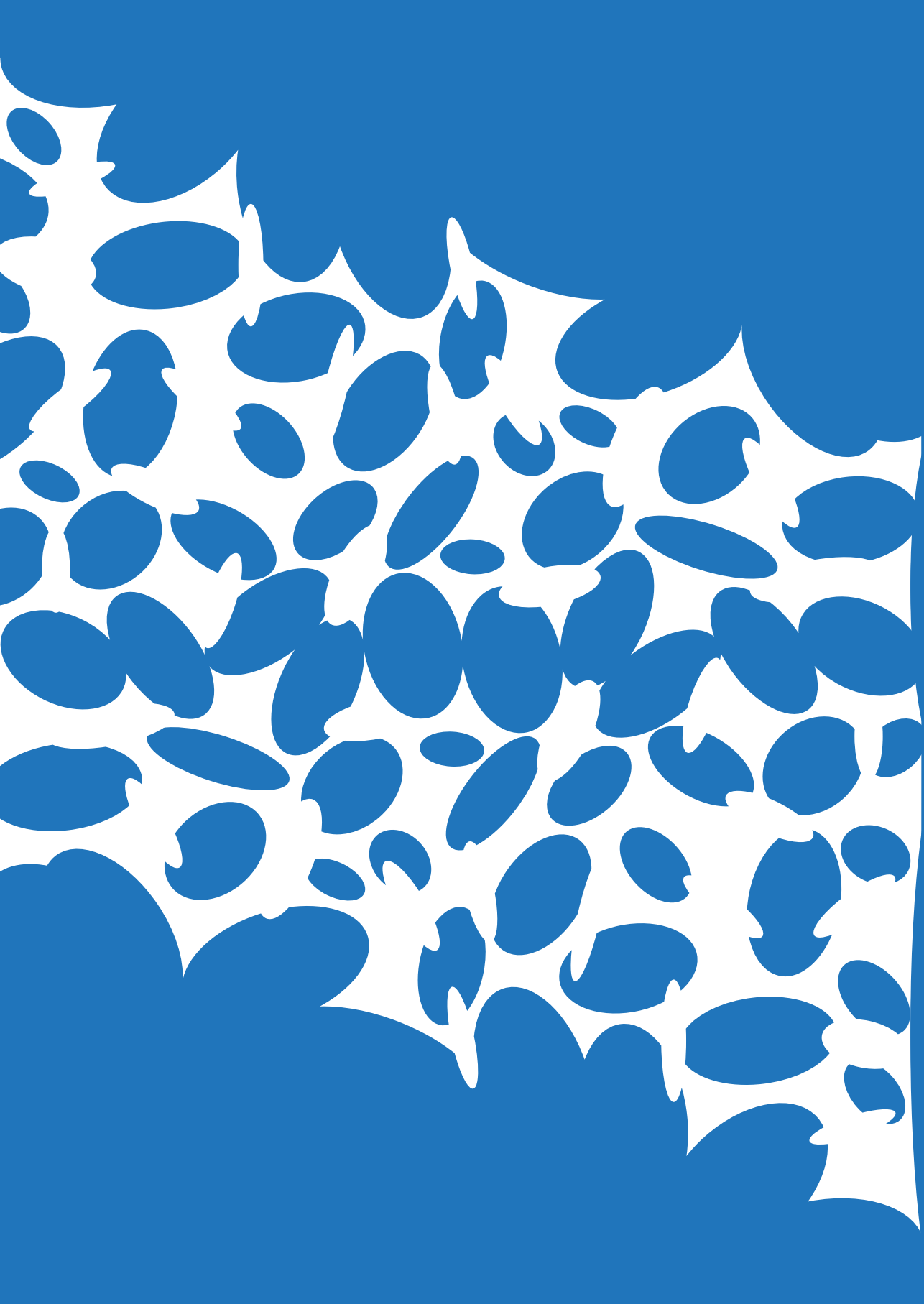
Printed by: Proefschriftmaken.nl | Digiforce Vianen